NASA-CR-132350) ANALYSIS AND DESIGN OF THREE DIMENSIONAL SUPERSONIC NOZZLES. VOLUME 1: NOZZLE-EXHAUST FLOW (Advanced Technology Labs., Inc., Westbury, N.Y.)

N74-11113

CSCL 20D G3/12

Unclas 22581

ADVANCED TECHNOLOGY LABORATORIES, INC.

CR 132350

OCTOBER 1972

ANALYSIS AND DESIGN OF THREE DIMENSIONAL SUPERSONIC NOZZLES

ATL TR 166 - VOLUME I
NOZZLE-EXHAUST FLOW FIELD ANALYSIS BY A REFERENCE PLANE CHARACTERISTICS TECHNIQUE

By

S. Dash and P. DelGuidice

PREPARED FOR

NATIONAL AERONAUTICS AND SPACE ADMINISTRATION

HAMPTON, VIRGINIA

UNDER

CONTRACT NO. NAS1-10327

BY

ADVANCED TECHNOLOGY LABORATORIES, INC.
Merrick and Stewart Avenues
Westbury, New York 11590

INDEX

INDEX (Continued)

LIST OF FIGURES

LIST OF FIGURES (Continued)

LIST OF FIGURES (Continued)

LIST OF FIGURES (Continued)

LIST OF SYMBOLS

P	-	pressure (lbs./ft.^{2})
ρ	-	density (slugs/ft.^{3})
$\bar{V}$	-	velocity (ft./sec.)
h	-	static enthalpy (ft.^{2}/sec.^{2})
H	-	stagnation enthalpy (ft.^{2}/sec.^{2})
a	-	local equilibrium sound speed (ft./sec.)
T	-	static temperature (^oR)
Γ	-	equilibrium isentropic exponent
Φ	-	fuel to air equivalence ratio
u,v,w	-	velocity components (ft./sec.)
x,y,z	-	Cartesian coordinates (ft.)
R,θ,z	-	line source coordinates (ft., radians, ft.)
r,θ,z	-	cylindrical coordinates (ft., radians, ft.)
q	-	velocity component in reference plane (ft./sec.)
ϕ,ψ	-	flow deflection angles (radians)
β	-	Mach number function
$\lambda^{\pm}$	-	projections of characteristic directions onto reference plane
$F^{\pm}$	-	forcing functions in characteristic compatability relation

LIST OF SYMBOLS (Continued)

β, c - cosine directions defining discontinuity surfaces

T - thrust (lbs.)

L - lift (lbs.)

M_y - pitching moment (ft.-lbs.)

$\tilde{\alpha}, \tilde{\beta}$ - second order averaging coefficients

ABSTRACT

A second order numerical method employing reference plane characteristics has been developed for the calculation of geometrically complex three dimensional nozzle-exhaust flow fields, heretofore uncalculable by existing methods. The nozzles may have irregular cross sections with swept throats and may be stacked in modules using the vehicle undersurface for additional expansion. The nozzles may have highly non-uniform entrance conditions, the medium considered being an equilibrium hydrogen-air mixture. The program calculates and carries along the underexpansion shock and contact as discrete discontinuity surfaces, for a nonuniform vehicle external flow. Additionally, shock formation due to coalescence is detected. A wide variety of geometric problems may be considered since the reference plane method has been developed for three separate coordinate systems, all incorporated into a single program.

ACKNOWLEDGEMENTS

The authors are pleased to acknowledge the advice, assistance and guidance of Dr. Antonio Ferri of Advanced Technology Laboratories, Inc., in many aspects of this work. This work was supported by the National Aeronautics and Space Administration Langley, Virginia under Contract No. NAS1-10327. The technical aspects of this contract were monitored by Mr. Walter Vahl of the NASA Langley facility.

I. INTRODUCTION

The propulsion system of a scramjet powered hypersonic aircraft is one of the dominant portions of the vehicle structure, and requires a high degree of vehicle-propulsion system integration to achieve optimum performance. The engine exhaust flow, because of physical area limitations, may be underexpanded at the nozzle exit and, in order to obtain maximum propulsive efficiency, the vehicle afterbody under-surface is used to provide additional expansion. This results in a three dimensional nozzle flow whose boundaries are defined by the solid walls of the nozzle and the vehicle surface and by the stream surface separating the nozzle flow from the external flow field of the vehicle. The effect of this complex interaction of the nozzle flow with the external flow, in terms of the forces and moments produced on the vehicle, can greatly influence the vehicle stability and aerodynamic performance, as well as the engine performance and must be considered in design studies of hypersonic airbreathing aircraft.

While much effort has been expended on developing numerical techniques for the solution of three dimensional supersonic flow fields, only a few working computer programs have evolved from these efforts. The numerical schemes generally fall into one of the following categories: (1) finite difference methods; (2) bi-characteristic methods; and (3) reference plane methods.

The reference plane method has been selected for this effort due to the geometric complexity of the flow field and the occurence of both embedded and external shock waves. The finite difference approach becomes difficult to apply when the boundaries cannot be represented by simple analytic functions and the accuracy of shock calculations tends to be very poor if the shocks are not steeply inclined with respect to the marching direction. A bi-characteristic approach may lead to problems of complex grid ordering and interpolation procedures and the calculation of internal discontinuities can be a formidable task. The reference plane method can alleviate these difficulties provided that a coordinate system is chosen which is suitably aligned with the flow field. Additionally, in the local reference planes, there is a strong analogy to a two dimensional flow field, hence the logic and numerical grid ordering appropriate to a two dimensional system can be applied. This is particularly important for the geometrically complex flow fields being considered, since the reference planes can be locally oriented to conform to the vehicle geometry, thus leading to excellent flow visualization.

Under this contract two families of exhaust nozzles will be analyzed. The first family (Vehicle I) will be characterized as having nozzle modules with cross-sections which are rectangular in shape. These nozzles may be arranged in multiples and discharge into a common nozzle, as is the case, for example, of

several engine exhaust nozzles using a vehicle undersurface for additional expansion area. This arrangement is shown in Figure (1). The second family (Vehicle II) is characterized as having a throat of curvilinear shape with one dimension much larger than the other. The throat may be sweptback in the downstream direction. This configuration is depicted in Figure (2).

The reference plane method was first proposed by Ferrari in 1949 (Reference 1) and further discussed by Ferri in (1954) (Reference 2). More recently, the method was used by Moretti (References 3 and 4) and Rakich (References 5, 6 and 7) for the analysis of external flow fields about inclined bodies of revolution.

The choice of the reference plane system to be employed for external flow fields around inclined bodies of revolution is quite clear, namely an r, θ, z system where z coincides with the body or wind axis and the cross flow is in the θ direction. For the analysis of scramjet exhaust nozzle flow fields the choice depends on the specific nozzle geometry; different configurations require different reference plane systems.

In addition, for a given configuration different reference systems may be used in different regions of the flow field so that

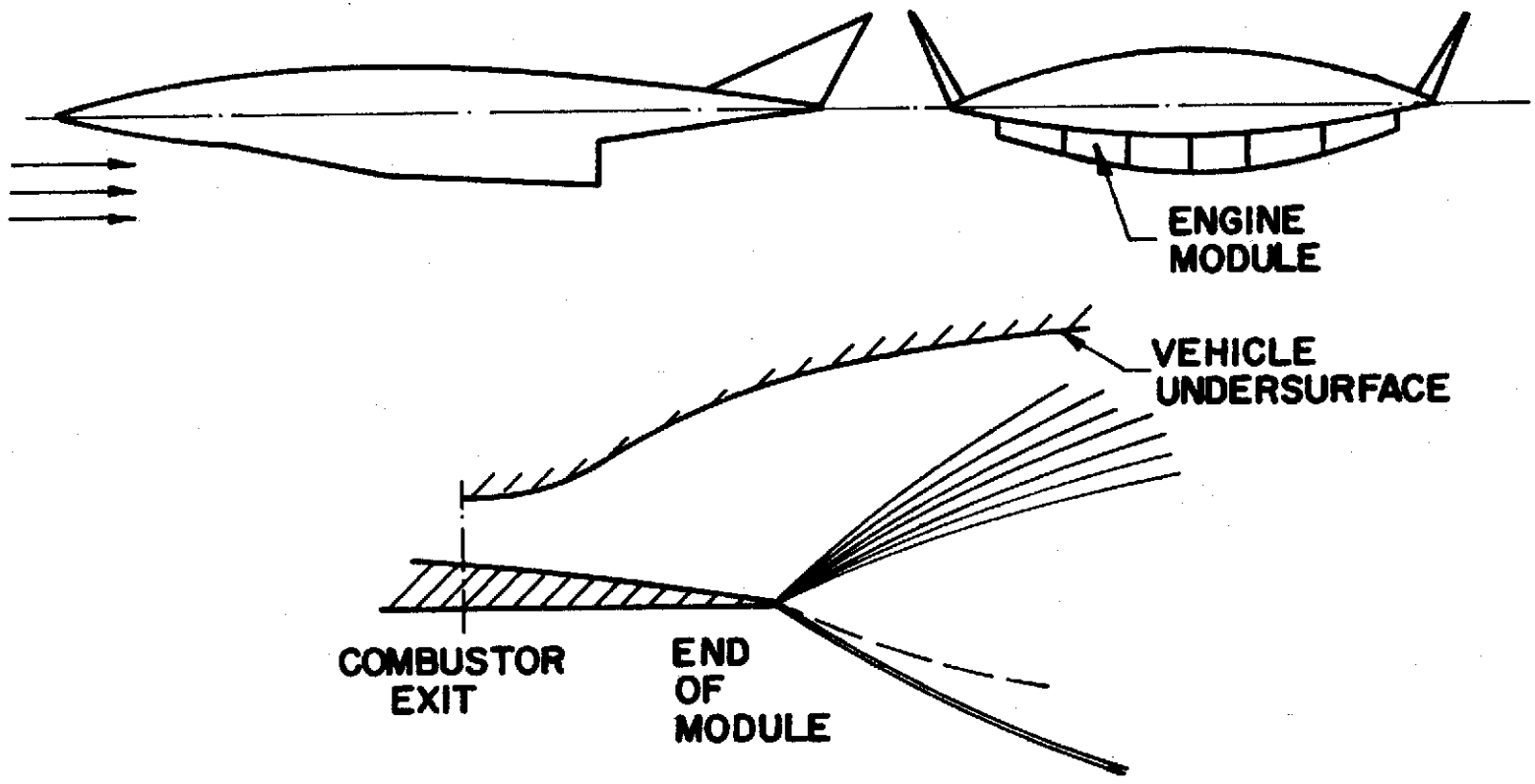

FIGURE 1. VEHICLE I, CONFIGURATION

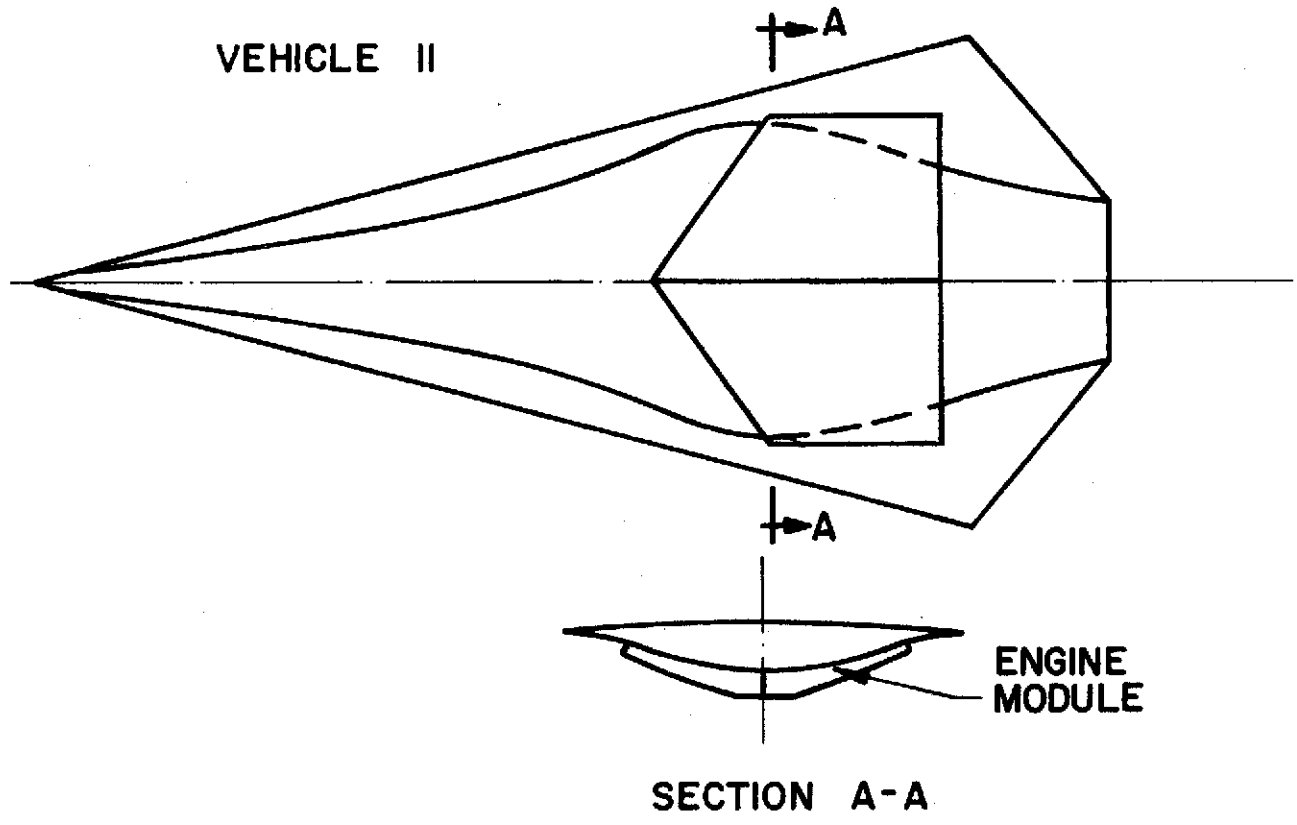

FIGURE 2. VEHICLE II, CONFIGURATION

each system is locally aligned with the flow field and the boundary conditions can be properly satisfied.

In the reference plane method, the configuration of the reference planes is chosen such that the primary flow variations occur within the reference planes while the coordinate normal to them describes the local cross flow. The governing equations are written in this reference coordinate system with the terms representing derivatives normal to the reference planes treated as forcing functions. The characteristic directions are those of the two dimensional system in the reference plane while the compatibility relations differ from those of the two dimensional system by the inclusion of the cross derivative terms, which are evaluated on the initial surface at each marching step. Note that flow variations must be continuous with respect to the cross flow direction, while wave-like discontinuous flow is permissible in the reference planes.

The gas mixture considered consists of air and combustion products (with hydrogen as the fuel) and is assumed to be inviscid and in chemical equilibrium. Three parameter curve fits (p, Φ, h) have been developed from the data of Reference (8) for the necessary thermodynamic properties, as described in Appendix I. The flow may be rotational and nonhomentropic.

The numerical procedure in a given reference plane employs a

Hartree type numerical grid, the streamline projections being traced in the individual reference planes. This approach affords excellent flow visualization through the tracing of these quasi streamlines, and provides a self enforced mesh tightening in regions of flow compression, since the quasi streamlines converge in these areas, thereby decreasing the axial step size. This also provides an aid in the detection of embedded shock waves.

The overall numerical approach is second order both with respect to reference plane characteristic calculations and the evaluation of derivatives. That is difference coefficients appearing in the compatability relations as well as derivative functions are averaged during a global second order computation. The program, however, does provide for a purely first order computation as well as local second order characteristic calculations using only the initial value derivatives. During global calculations shock and contact surface cross angles are updated in addition to cross derivatives.

All interpolations are linear since this always led to stable numerical results as well as ensuring convergence of the difference solution to the exact solution. However, care must be exercised in using an extremely course grid spacing in the reference planes since excessive numerical diffusion of the solution will result.

II. GOVERNING EQUATIONS

The equations governing the steady three-dimensional flow of an inviscid gas mixture in chemical equilibrium are as follows:

Continuity

$$\nabla \cdot (\rho \bar{v}) = 0 \tag{1}$$

Momentum

$$\rho(\bar{v} \cdot \nabla)\bar{v} + \nabla p = 0 \tag{2}$$

Conservation of Stagnation Enthalpy

$$\bar{v} \cdot \nabla(H) = 0 \tag{3}$$

Conservation of Entropy

$$\bar{v} \cdot \nabla s = 0 \tag{4}$$

Equation of State

$$\left(\frac{\partial p}{\partial \rho}\right)_s = \frac{\Gamma p}{\rho} = a^2 \tag{5}$$

Constancy of Equivalence Ratio Along Streamline

$$\bar{v} \cdot \nabla \Phi = 0 \tag{6}$$

Curve Fit For Isentropic Exponent

$$\Gamma = f(h, p, \Phi)^* \tag{7}$$

*Fits for Γ have been expressed in polynomial form from properties tabulated in Reference (8) as described in Appendix I.

Combining Equations (4) and (5) yields the relation

$$\bar{v} \cdot \nabla p = a^2 \nabla p$$

and hence the continuity equation may be written in the form

$$\bar{v} \cdot \nabla p + a^2 \rho \nabla \cdot \bar{v} = 0 \qquad (8)$$

The analysis of the nozzle-exhaust flow fields for Vehicles I and II has required the use of three types of coordinate systems.

(1) Line Source System: This is an r-θ-z system with the flow predominantly aligned with the r direction as depicted in Figure (3). The reference planes are the planes θ=constant and the marching direction is r. The velocity vector in this system is depicted in Figure (4).

(2) Cartesian System: This is an x-y-z system with the flow predominantly aligned with the x direction as depicted in Figure (5). The reference planes are the planes y-constant and the marching direction is x. The velocity vector in this system is depicted in Figure (6).

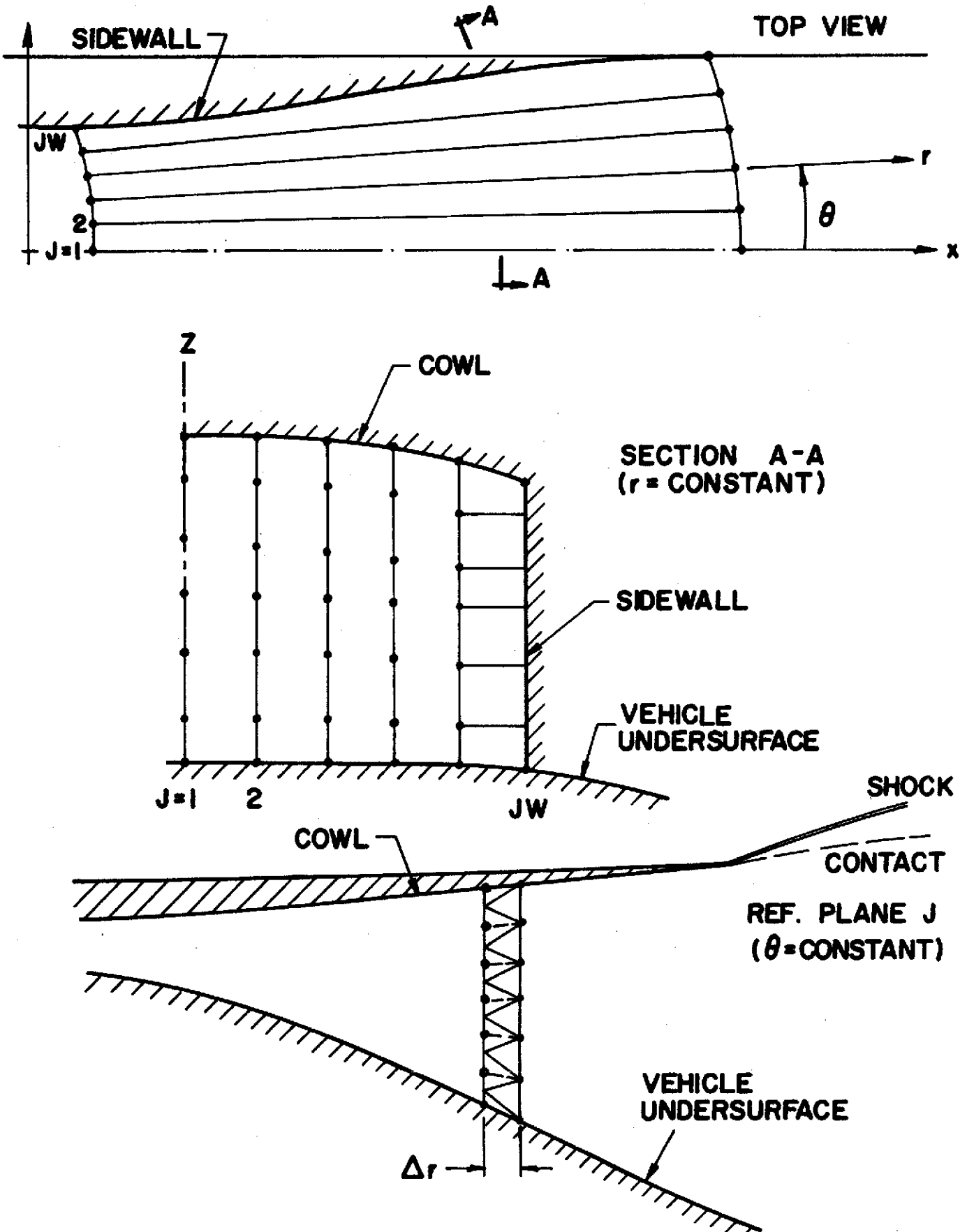

FIGURE 3. LINE SOURCE SYSTEM

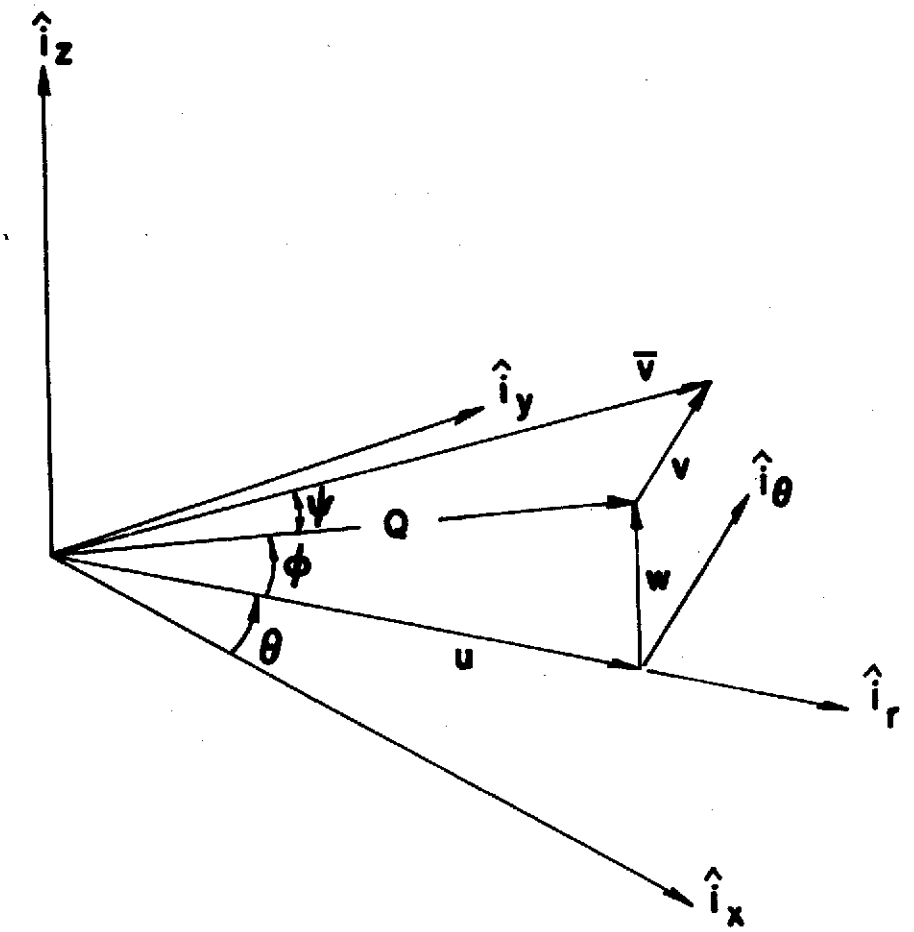

$$V = u\,\hat{i}_r + v\,\hat{i}_\theta + w\,\hat{i}_z$$

$$Q = V\cos\psi \qquad Q = (u^2+w^2)^{\frac{1}{2}}$$

$$u = Q\cos\phi \qquad \phi = \tan^{-1}(w/u)$$

$$v = Q\tan\psi \qquad \psi = \tan^{-1}(v/Q)$$

$$w = Q\sin\phi$$

FIGURE 4. VELOCITY VECTOR IN LINE SOURCE SYSTEM

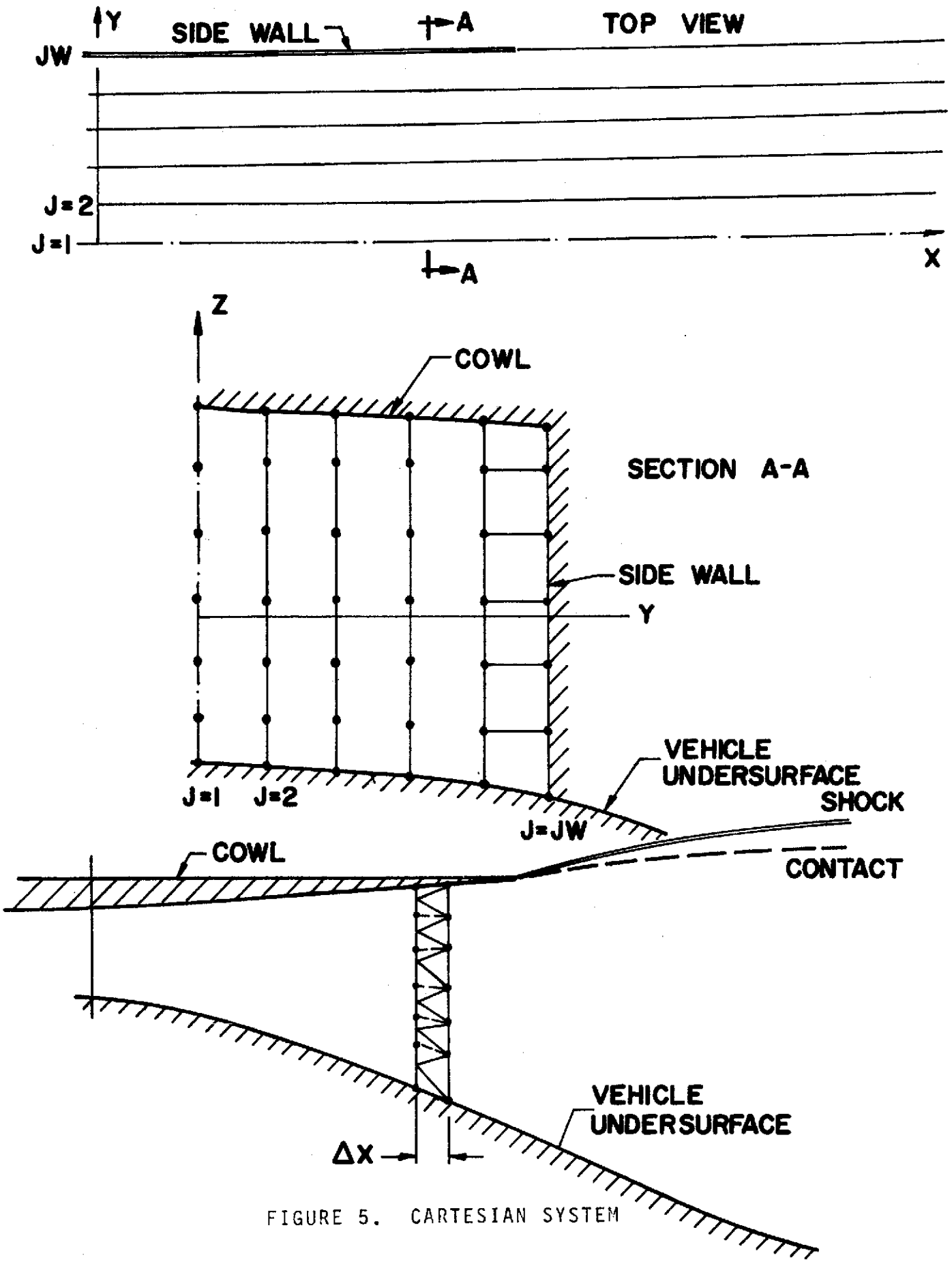

FIGURE 5. CARTESIAN SYSTEM

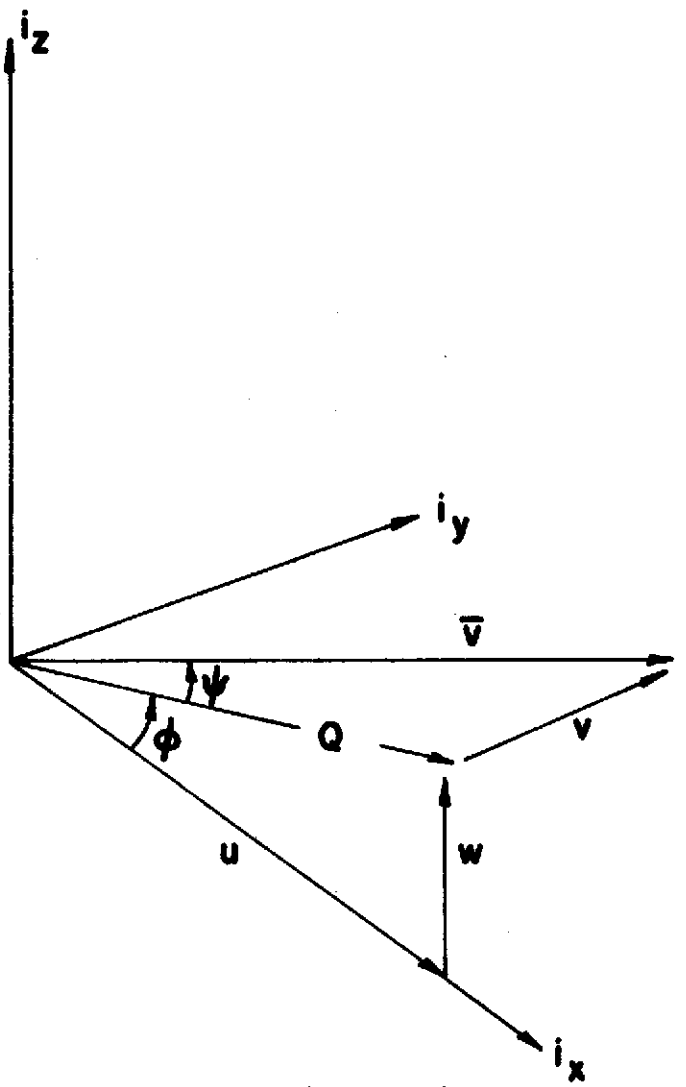

$$\bar{V} = u\,\hat{i}_x + v\,\hat{i}_y + w\,\hat{i}_z$$

$$Q = V\cos\psi \qquad Q = (u^2+w^2)^{\frac{1}{2}}$$

$$u = Q\cos\phi \qquad \phi = \tan^{-1}(w/u)$$

$$v = Q\tan\psi \qquad \psi = \tan^{-1}(v/Q)$$

$$w = Q\sin\phi$$

FIGURE 6. VELOCITY VECTOR IN CARTESIAN SYSTEM

(3) Cylindrical System: This is an r-θ-x system with the flow predominantly aligned with the x direction as depicted in Figure (7).

The reference planes are the planes θ=constant and the marching direction is x. The velocity vector in this system is depicted in Figure (8).

In the overall nozzle-exhaust analysis, let us define the internal flow as that portion of the flow field bounded by the vehicle undersurface, cowl and sidewalls (or planes of symmetry), and the external flow as that portion of the flow field bounded by the vehicle undersurface and an outer prescribed stream surface (or planes of symmetry).

In analyzing the internal flow field for Vehicle I, a line source system would be employed if the sidewalls were curved or aligned with a ray other than one parallel to the x direction as shown in Figure (3), while a Cartesian system would be employed if the sidewalls are parallel to the x-z plane, as in Figure (5). For the internal flow portion of Vehicle II, a cylindrical system is employed as shown in Figure (7).

If a central module of Vehicle I is being analyzed, the sidewalls are replaced by planes of symmetry in the external flow and the Cartesian system shown in Figure (9a) is employed while

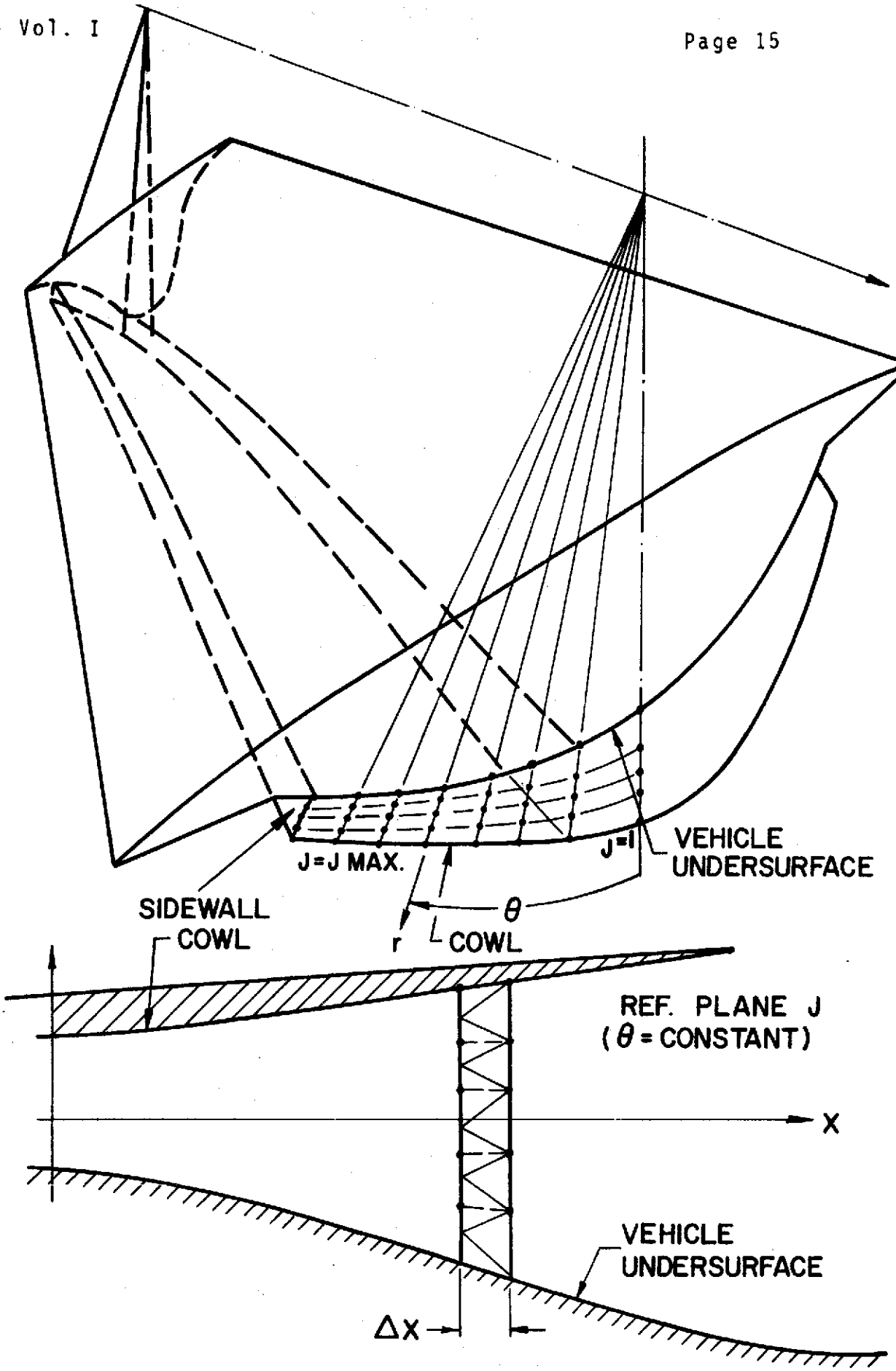

FIGURE 7. CYLINDRICAL SYSTEM

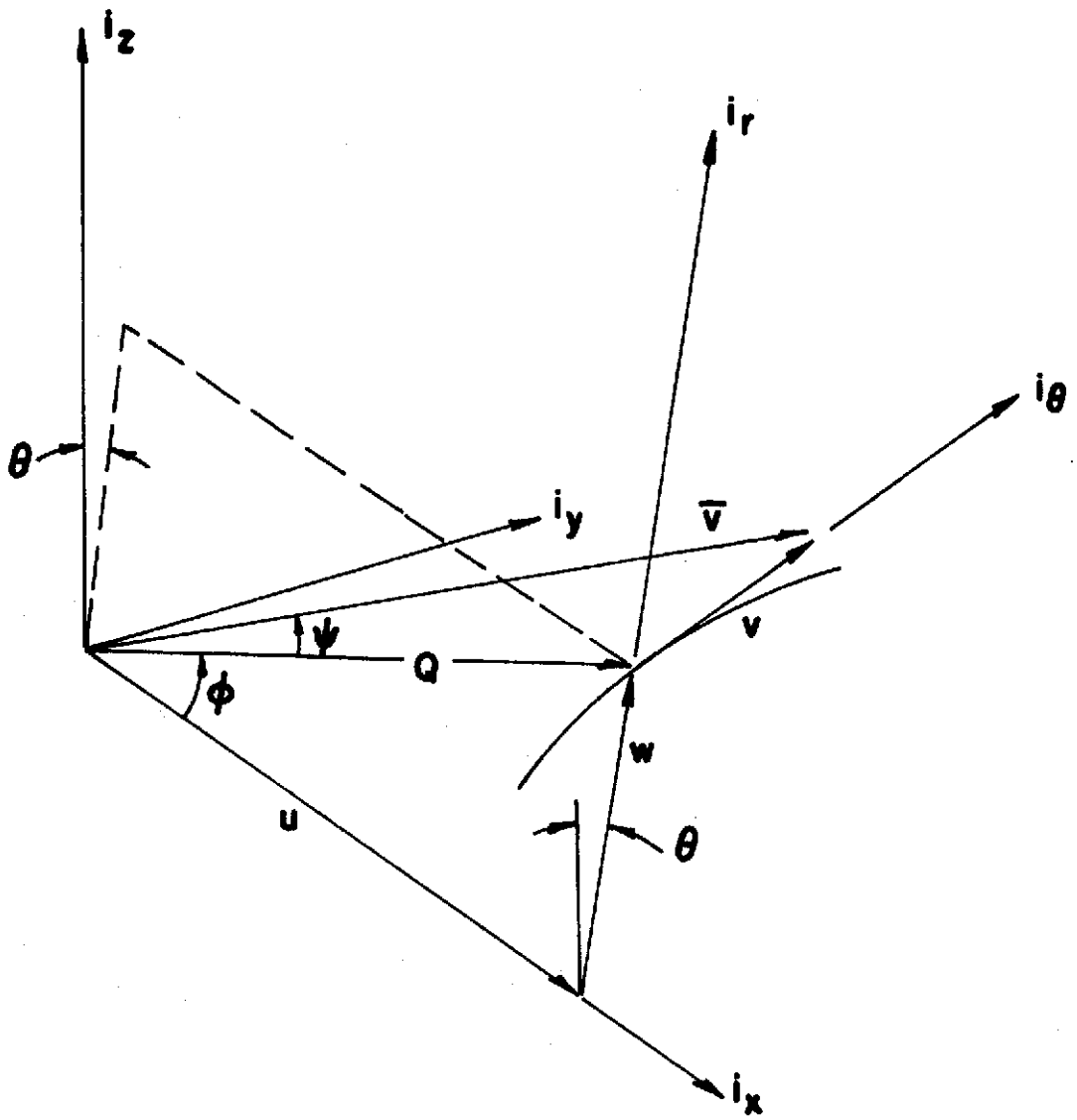

$$V = u\,\hat{i}_x + v\,\hat{i}_\theta + w\,\hat{i}_r$$

$$Q = V\cos\psi \qquad Q = (u^2+w^2)^{\frac{1}{2}}$$

$$u = Q\cos\phi \qquad \phi = \tan^{-1}(w/u)$$

$$v = Q\tan\psi \qquad \psi = \tan^{-1}(v/Q)$$

$$w = Q\sin\phi$$

FIGURE 8. VELOCITY VECTOR IN CYLINDRICAL SYSTEM

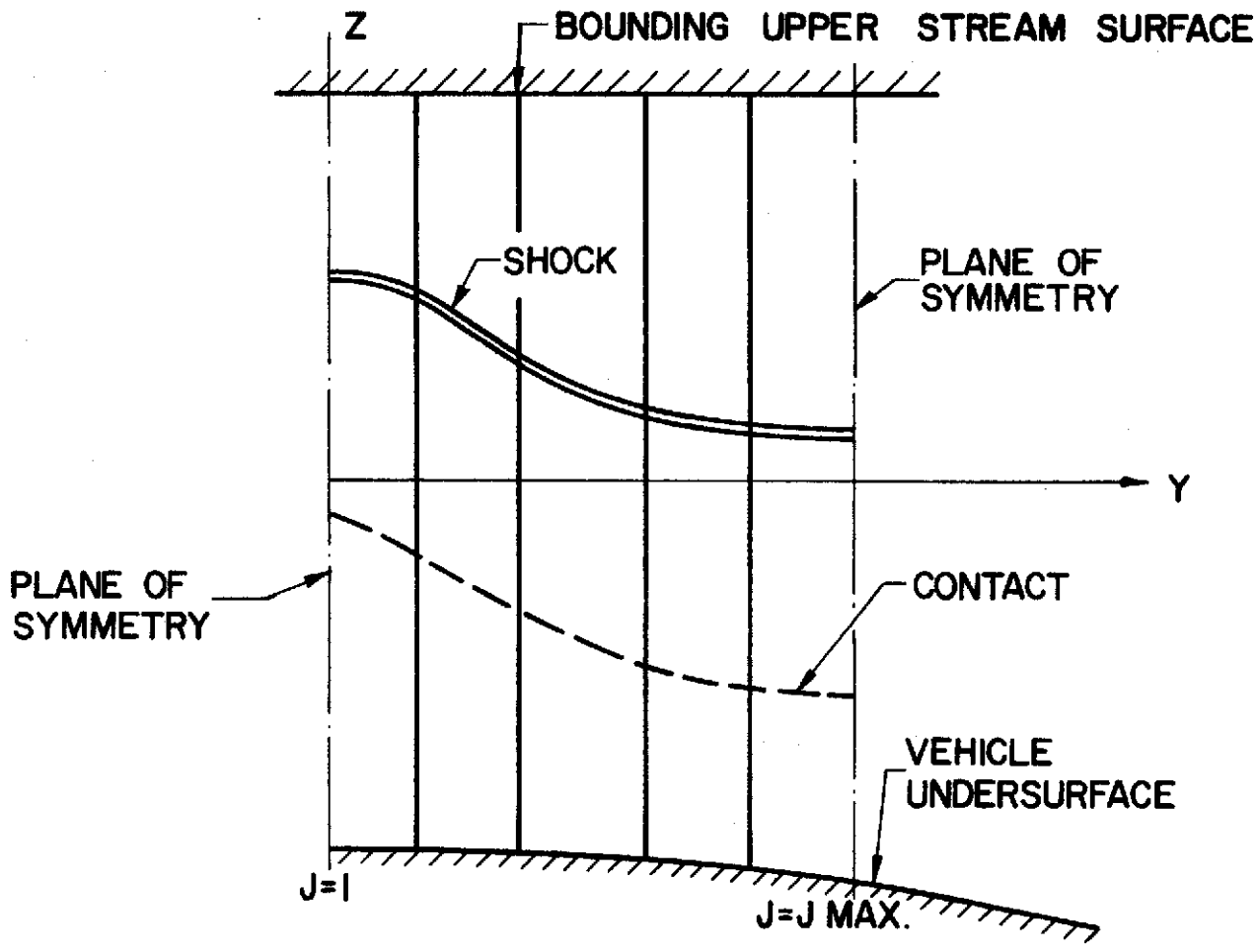

FIGURE 9a. EXTERNAL FLOW-VEHICLE I CENTRAL MODULE

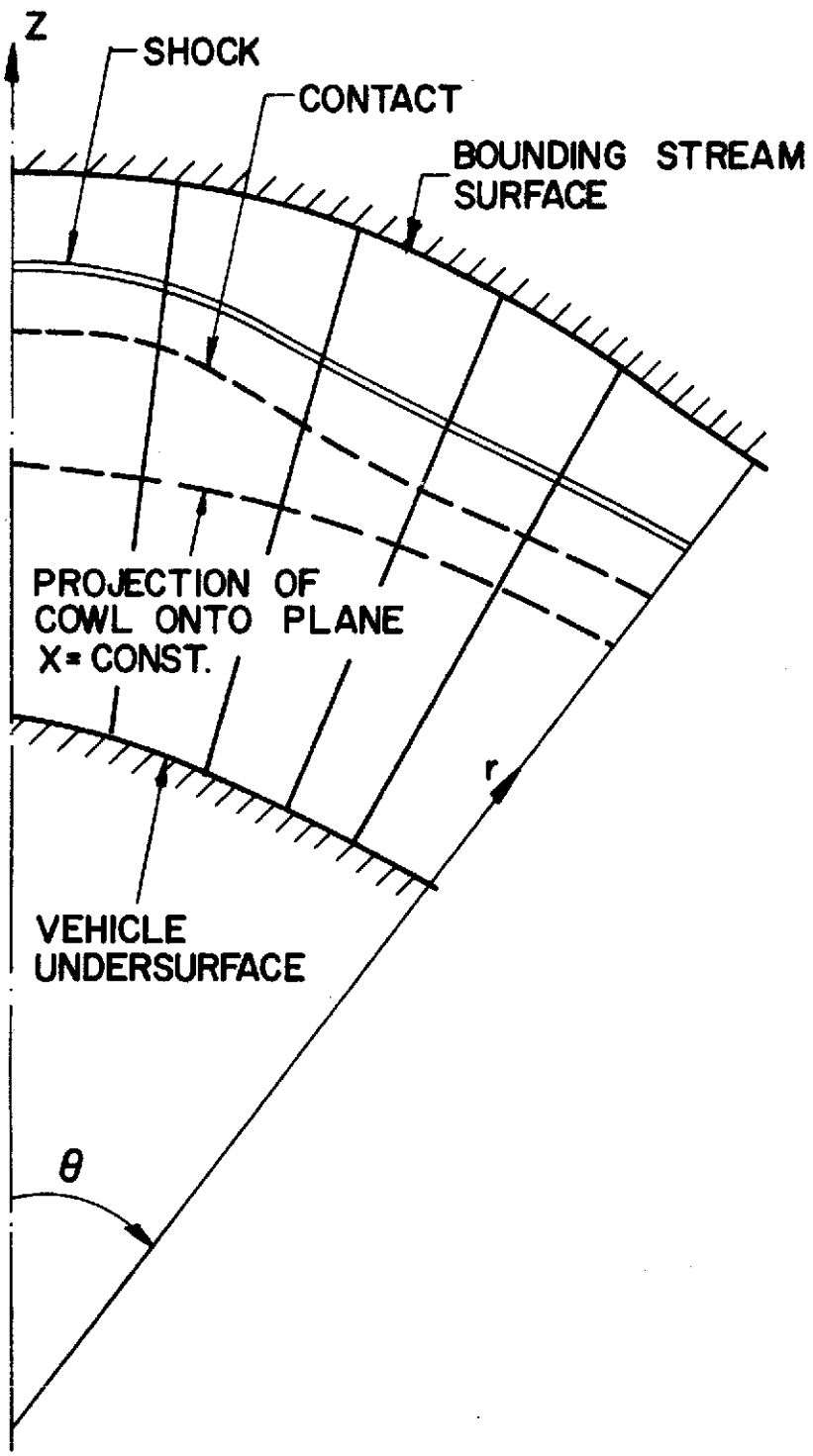

FIGURE 9b. EXTERNAL FLOW-VEHICLE II

for Vehicle II the external flow is computed as indicated in Figure (9b). The end modules are analyzed only for Vehicle I and are computed separately in a locally Cartesian system as depicted in Figure (10).

A. Line Source System In this system, the reference planes are the planes θ = constant and variations in these planes are expressed by differentiation in the r and z directions. The primary criterion in selecting a reference plane system is that the reference planes be aligned such that the velocity component normal to them is as small as possible in order to obtain the maximum axial step size in the difference scheme.

The scalar equations of motion are:

Continuity

$$\rho a^2\left(u_r + \frac{u}{r} + \frac{v_\theta}{r} + w_z\right) + up_r + \frac{vp_\theta}{r} + wp_z = 0 \qquad (9)$$

r - momentum

$$\rho\left(uu_r - \frac{v^2}{r} + \frac{vu_\theta}{r} + wu_z\right) + p_r = 0 \qquad (10)$$

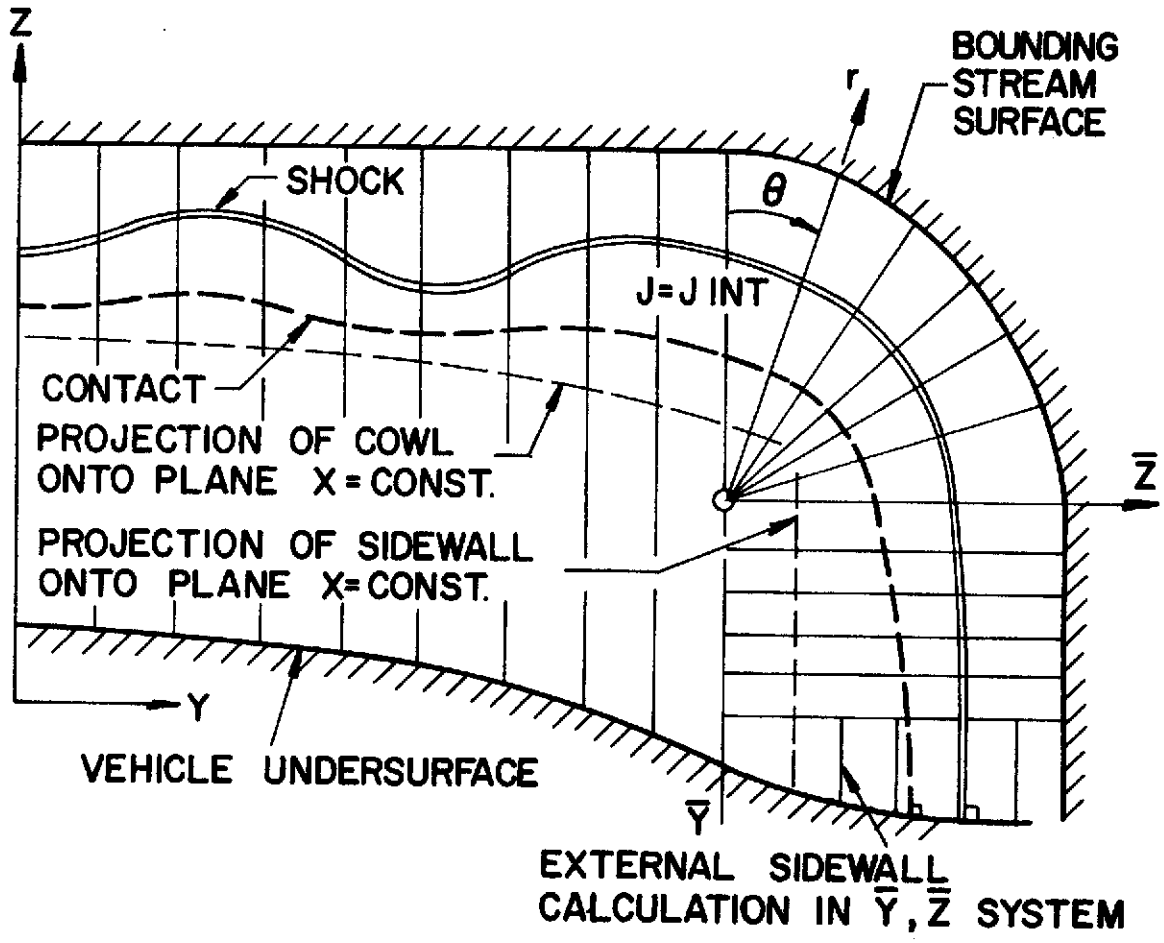

FIGURE 10. EXTERNAL FLOW END MODULE

θ-momentum

$$\rho(v\frac{v_\theta}{r} + wv_z + uv_r + \frac{uv}{r}) + \frac{p_\theta}{r} = 0 \tag{11}$$

z-momentum

$$\rho(ww_z + uw_r + \frac{vw_\theta}{r}) + p_z = 0 \tag{12}$$

The following relations are valid along streamlines

$$\frac{dp}{p} = \Gamma\frac{d\rho}{\rho} \tag{13}$$

$$H = \text{constant} \tag{14}$$

$$\Phi = \text{constant} \tag{15}$$

$$a^2 = \frac{\Gamma p}{\rho} \tag{16}$$

The system of Equations (9) - (16) constitutes a system of quasi-linear partial differential equations in the variables u, v, w, p, ρ, H, Φ and a. The system can be solved numerically by an ordinary finite difference formulation based on arbitrary coordinate directions or by a finite difference scheme based on characteristic directions. The ordinary finite difference formulation leads to a great simplification of the problem if the flow is everywhere continuous and the boundaries are smooth. However, major problems in accuracy are encountered

in devising means of satisfying boundary conditions on surfaces not corresponding to coordinate planes, which then necessitates interpolation or extrapolation. Also, even on boundaries corresponding to coordinate planes, the derivatives at the boundaries can only be approximated by one-sided differences.

A true three-dimensional characteristic calculation is quite complex from a computational point of view. The usefulness of the characteristic method is weakened when three independent variables are considered, since the system of equations no longer reduces to a system of ordinary differential equations but rather to a system of partial differential equations in two independent variables on characteristic surfaces. The complexities involved in analyzing nonuniform flow fields with embedded shocks and complicated geometries, makes the use of a three-dimensional characteristic approach numerically complex and far less attractive than the present method.

The method employed to numerically solve the system of Equations (9) - (16) in this analysis uses a finite difference grid consisting of the characteristic directions obtained by considering the momentum equations in the r and z directions and the continuity equation. These characteristics are not the bicharacteristics of the three-dimensional system, but rather represent the projection of the bi-characteristics onto the reference planes.

The r-momentum, z-momentum and modified continuity equation are rewritten by putting the terms involving derivatives in the θ direction onto the righthand side. These equations now take the form

$$\rho(uu_r + wu_z) + p_r = \rho\frac{v^2}{r} - \rho\frac{vu_\theta}{r} \tag{17}$$

$$\rho(uw_r + ww_z) + p_z = -\rho\frac{vw_\theta}{r} \tag{18}$$

$$\rho a^2(u_r + w_z) + up_r + wp_z = -a^2\rho(\frac{u}{r} + \frac{v_\theta}{r}) - \frac{vp_\theta}{r} \tag{19}$$

The initial value plane is one of constant r in this coordinate system and the righthand side terms, including the cross derivatives, will be evaluated in this initial plane. Then, the system (17) - (19) is a system of 3 quasi-linear partial differential equations in the variables u, w and p and the lefthand side is equivalent to the corresponding two-dimensional system in the r-z plane. The characteristic directions for this system are those of the two-dimensional system and the compatibility relations differ from the two-dimensional relations by the inclusion of cross derivative terms in the θ direction.

Letting, q, Φ and ψ represent the velocity vector in place of u, v and w (as shown in Figure 4), the velocity vector $\bar{v}$

may be written,

$$\bar{v} = u\,\hat{i}_r + v\,\hat{i}_\theta + w\,\hat{i}_f = \qquad (20)$$

$$q\,(\cos\phi\,\hat{i}_r + \tan\psi\,\hat{i}_\theta + \sin\phi\,\hat{i}_z)$$

where q represents the projection of the velocity $\bar{v}$ onto the reference plane θ=constant.

The characteristic directions are given by the equations

$$\left(\frac{dz}{dr}\right)_{C\pm} = \frac{(q/a)^2 \cos\phi \sin\phi \pm \beta}{(q/a)^2 \cos^2\phi - 1} = \lambda\pm \qquad (21)$$

where $\beta^2 = q^2/a^2 - 1$

and

$$\left(\frac{dz}{dr}\right)_{S.L.} = \tan\phi = \frac{w}{u} \qquad (22)$$

which represents the streamlines projection onto the reference plane.

Along a C± characteristic, the compatibility relation takes the form

$$\rho q^2 \, d\phi \pm \beta \, dp = (F_\pm) \, dr \tag{23}$$

where

$$F_\pm = \frac{\rho q^2}{r} \left[(\sin\phi - \cos\phi \, \lambda_\pm) \left(\frac{\psi_\theta}{\cos^2\psi} + \frac{\tan\psi}{\rho a^2} p_\theta + \cos\phi \right) - \tan\psi \, (\phi_\theta) \right. \tag{24}$$

$$\left. (\sin\phi \, \lambda_\pm + \cos\phi) - \lambda_\pm \tan^2\psi \right]$$

B. Cartesian System In this system, the reference planes are the planes y-constant and variations in these planes are expressed by differentiation in the x and z directions. Analogous to Equations (9) - (12) for the line source system, the scalar equations in the Cartesian system take the form:

Continuity

$$\rho a^2 (u_x + v_y + w_z) + up_x + vp_y + wp_z = 0 \tag{25}$$

x-momentum

$$\rho (uu_x + vu_y + wu_z) + p_x = 0 \tag{26}$$

y-momentum

$$\rho(uv_x+vv_y+wv_z) + p_y=0 \tag{27}$$

z-momentum

$$\rho(uw_x+vw_y+ww_z) + p_z=0 \tag{28}$$

The streamline relations (Equations 13 - 16) are valid for all coordinate systems. The x-momentum, z-momentum and continuity equations are rewritten by putting the terms involving derivatives in the y direction onto the right hand side. The initial value plane is one of constant x and the terms on the right hand side are evaluated on this plane.

Letting q, ϕ and ψ represent the velocity vector as depicted in Figure (6), the characteristic directions are given by the equations

$$\left(\frac{dz}{dx}\right)_{C_\pm} = \frac{(q/a)^2 \cos\phi \sin\phi \mp \beta}{(q/a)^2 \cos^2\phi - 1} = \lambda^\pm \tag{29}$$

where

$$\beta^2 = q^2/a^2 - 1$$

and

$$\left(\frac{dz}{dx}\right)_{S.L} = \tan\phi = \frac{w}{u} \tag{30}$$

Along a $C_\pm$ characteristic, the compatibility relation takes the

form

$$\rho q^2 \, d\phi \pm \beta \, dp = (F_{\pm}) \, dx \tag{31}$$

where

$$F_{\pm} = \rho q^2 \left[(\sin \phi - \lambda^{\pm} \cos \phi) \left(\frac{\psi_y}{\cos^2 \psi} + \frac{\tan \psi}{\rho a^2} py \right) - \tan \psi (\phi_y) (\cos \phi + \lambda^{\pm} \sin \phi) \right] \tag{32}$$

C. Cylindrical System In this system, the reference planes are the planes θ=constant and variations in these planes are expressed by differentiation in the x and r directions. Analogous to Equations (9) - (12) for the line source system, the scalar Equations in the cylindrical system take the form:

Continuity

$$\rho a^2 (u_x + \frac{v_\theta}{r} + w_r + \frac{w}{r}) + up_x + \frac{v}{r} p_\theta + wp_r = 0 \tag{33}$$

x-momentum

$$\rho (uu_x + \frac{v}{r} u_\theta + wu_r) + p_x = 0 \tag{34}$$

θ-momentum

$$\rho (uv_x + \frac{v}{r} v_\theta + \frac{wv}{r} + wv_r) + \frac{p_\theta}{r} = 0 \tag{35}$$

r-momentum

$$\rho(uw_r + \frac{v}{r} w_\theta - \frac{v^2}{r} + ww_z) + p_r = 0 \tag{36}$$

The x-momentum, r-momentum and continuity equations may be re-written with the terms involving derivatives in the θ direction being put on the right hand side. Letting q, ϕ and ψ represent the velocity vector as depicted in Figure (8), the characteristic directions are given by the equations

$$\left(\frac{dr}{dx}\right)_{C_\pm} = \frac{(q/a)^2 \sin\phi \cos\phi \pm \beta}{(q/a)^2 \cos^2\phi - 1} = \lambda^\pm \tag{37}$$

where $\beta^2 = \frac{q^2}{a^2} - 1$

and

$$\left(\frac{dr}{dx}\right)_{S.L.} = \tan\phi = \frac{w}{u} \tag{38}$$

Along a $C_\pm$ characteristic, the compatibility relation takes the form

$$\rho q^2 \, d\phi \pm \beta \, dp = F^\pm \, dx \tag{39}$$

where

$$F^\pm = \frac{\rho}{r}\left[q(\sin\phi - \lambda^\pm \cos\phi) \left(v_\theta - \frac{vq_\theta}{q} + \frac{vp_\theta}{\rho a^2} + q \sin\phi \right) - qv\,\phi_\theta\,(\lambda^\pm \sin\phi + \cos\phi) + v^2 \right] \tag{40}$$

III. NUMERICAL SCHEME

Consider the numerical grids depicted in Figures **(12a)**, **(12b)** and **(12c)** for the line-source, Cartesian and cylindrical systems respectively. The reference planes are the planes J= constant and in a given reference plane, the index I goes from 1 (lower wall) to IMAX(J) (cowl or boundary stream surface). The reference plane J=1 is always a plane of symmetry.

The variables p, q, ϕ, ψ, ρ, h and Φ are specified at all the mesh points I, J in the initial surface ($r=r_1$ for line-source system in Figure **(12a)**; $x=x_1$ for both the Cartesian and cylindrical systems in Figures **(12b)** and **(12c)** respectively). It is desired to calculate properties at the station r_2 (for the line-source system) or x_2 (for the Cartesian and cylindrical systems) where the step-size Δr or Δx is constrained by stability considerations to be discussed in a subsequent section. Note that a uniform step-size is **taken** for all grid points since the evaluation of cross derivatives on the surface r or x=constant is required.

A. Cross Derivatives at Interior Points Before proceeding with the calculation, cross derivatives must be evaluated and stored at all mesh points I, J on the initial surface. This is complicated by the fact that the spacing of the grid points is arbitrary in each reference plane J and that the

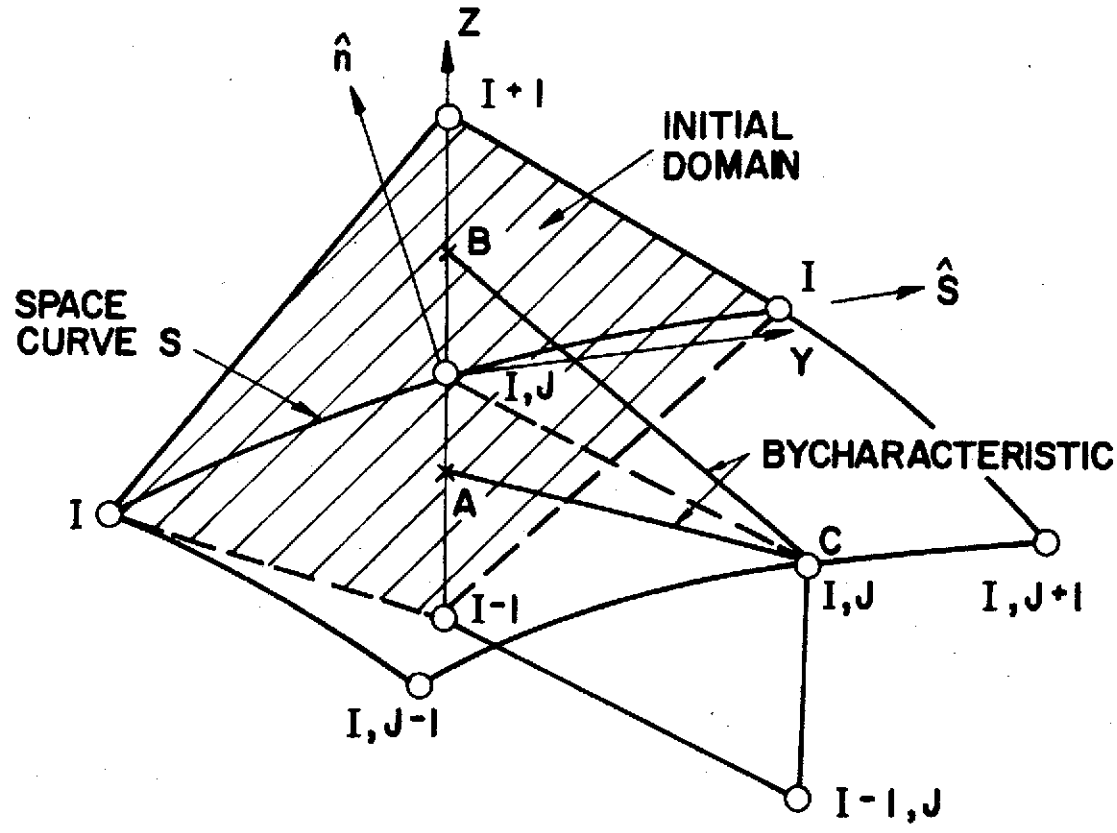

FIGURE 11. INTERIOR GRID FOR CROSS DERIVATIVE

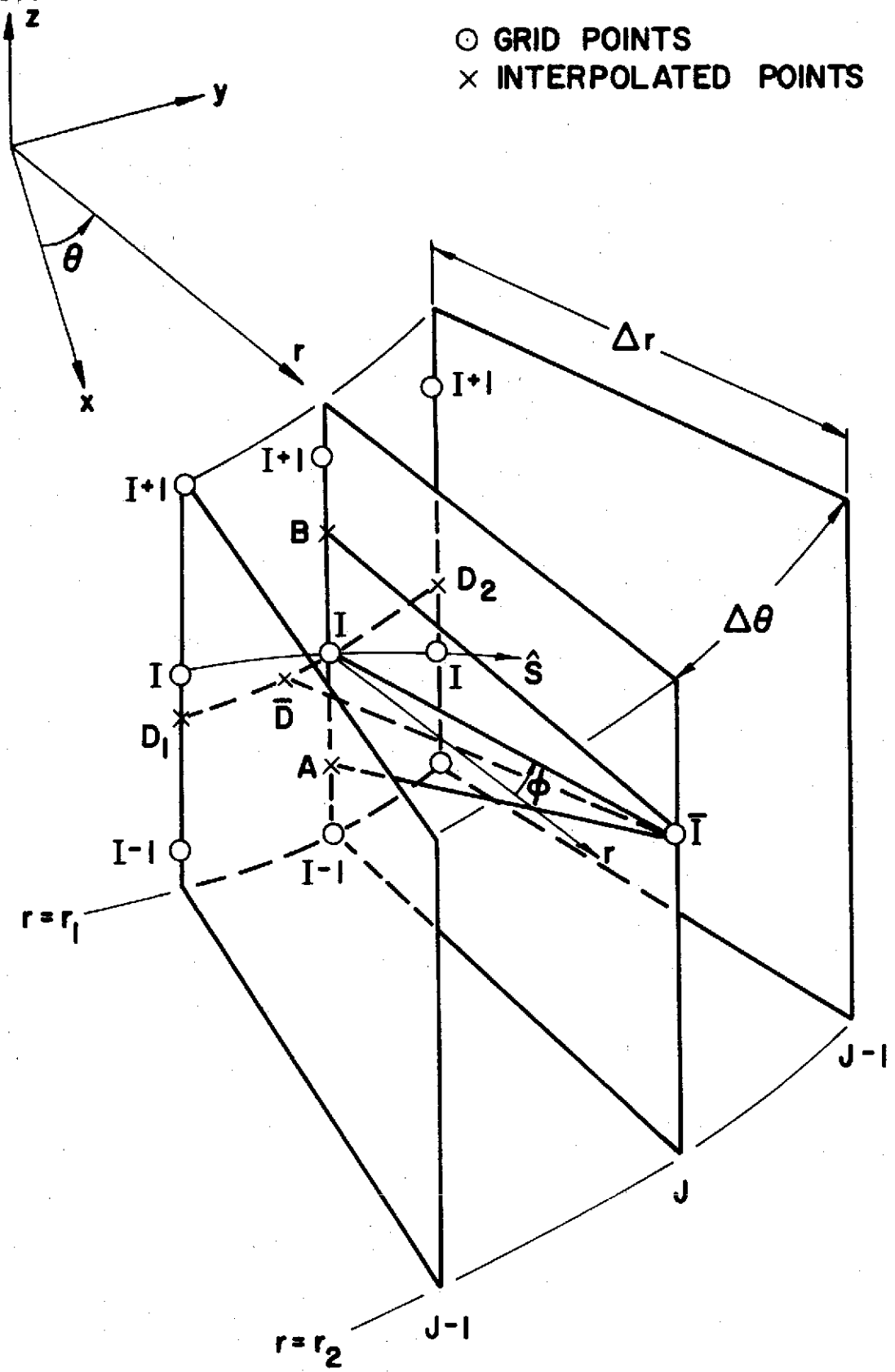

FIGURE 12a. NUMERICAL GRID FOR LINE-SOURCE SYSTEM

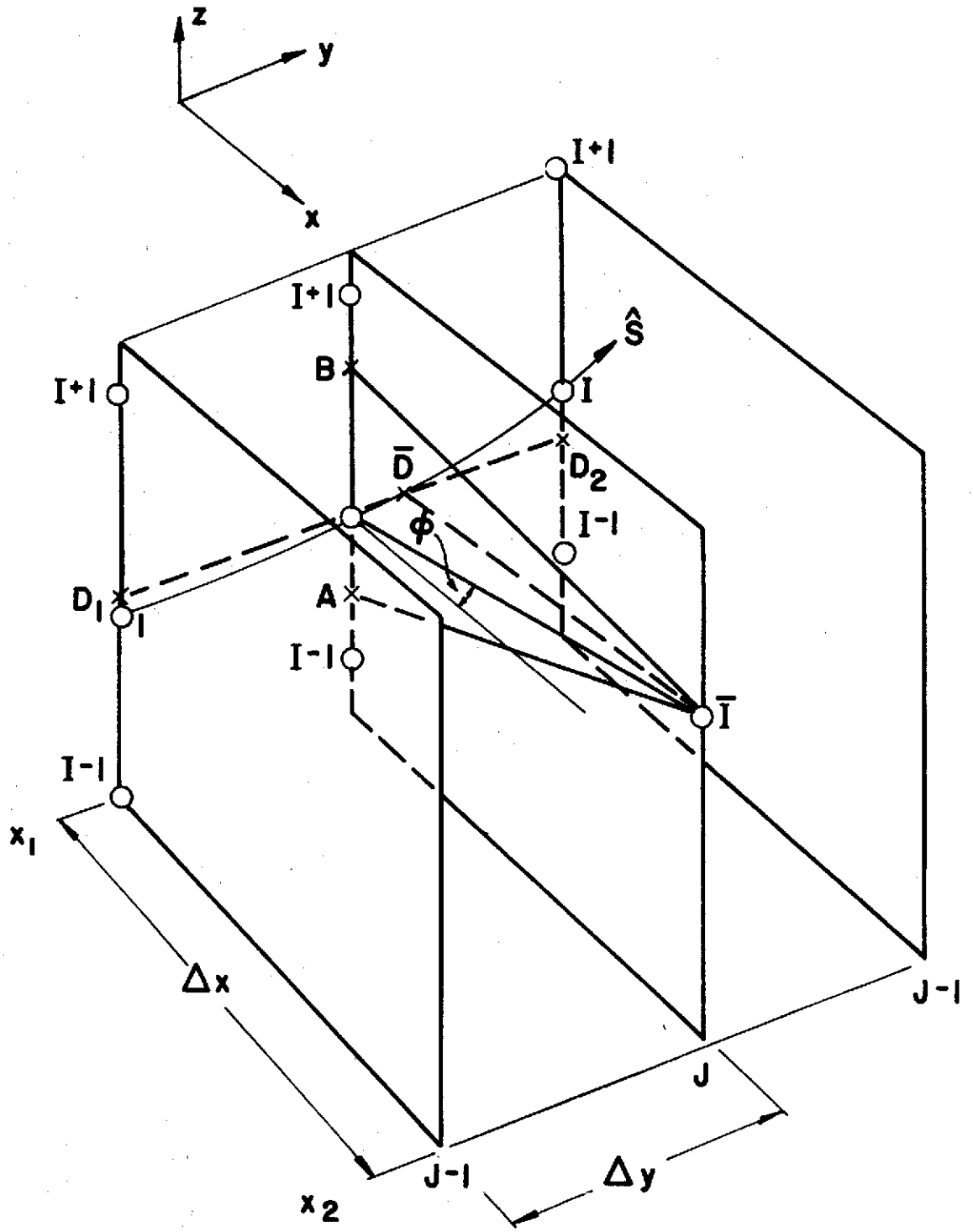

FIGURE 12b. NUMERICAL GRID FOR CARTESIAN SYSTEM

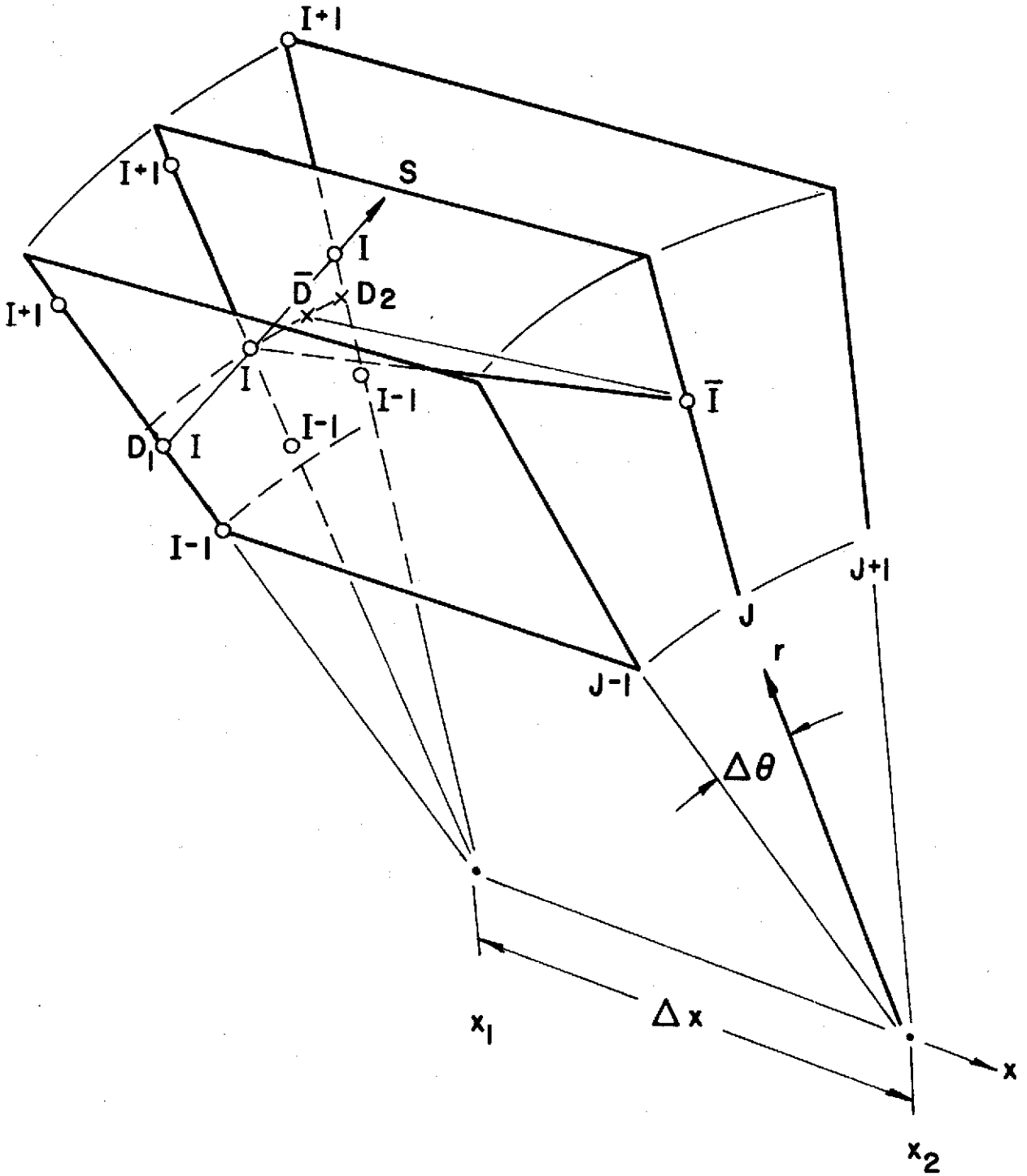

FIGURE 12c. NUMERICAL GRID FOR CYLINDRICAL SYSTEM

spacing ($\Delta\theta$ or Δy) of the reference planes is arbitrary. It is required that each reference plane contain an identical number of points. Referring to Figure (11) all cross derivatives ($\partial f/\partial y$) are computed by combining derivatives ($\partial f/\partial z$) and derivatives ($\partial f/\partial s$). This requires that there be a one to one correspondence between points (I,J-1), (I,J) and (I,J+1) which form the arbitrary surface n = constant. This approach has the advantage of eliminating unnecessary interpolation of initial data. In addition, derivatives at discontinuities, fixed boundaries and interior points are computed in a consistent manner.

The relation that exists between derivatives in the z,s and y(or θ) directions on the initial surface is:

$$\left(\frac{\partial f}{\partial s}\right)_n = \left(\frac{\partial f}{\partial y}\right)_z \left(\frac{\partial y}{\partial s}\right)_n + \left(\frac{\partial f}{\partial z}\right)_y \left(\frac{\partial z}{\partial s}\right)_n \tag{41}$$

where Δs is defined as

$$\Delta s = [(\Delta y)^2 + (\Delta z)^2]^{\frac{1}{2}}$$

Thus, knowing the derivatives ($\partial f/\partial s$), and ($\partial f/\partial z$), as well as the direction angles ($\partial y/\partial s$) and ($\partial z/\partial s$) allows us to compute the cross derivative ($\partial f/\partial y$) at every point (I,J) of flow field.

(1) Line Source System: At all interior mesh points (I,J) the derivative $(\partial f/\partial \theta)$ is required for the property f. Referring to Figure (12a) the n = constant surface is formed by points (I,J-1), (I,J) and (I,J+1). Then

$$\Delta s_1 = [(z_{I,J} - z_{I,J-1})^2 + r^2(\theta_J - \theta_{J-1})^2]^{\frac{1}{2}}$$
$$\Delta s_2 = [(z_{I,J+1} - z_{I,J})^2 + r^2(\theta_{J+1} - \theta_J)^2]^{\frac{1}{2}} \quad (42)$$

using the standard centered difference formula for nonuniform spacing

$$\frac{\partial \theta}{\partial s} = \frac{\theta^{J+1}\left(\frac{\Delta s_1}{\Delta s_2}\right) - \theta^J\left(\frac{\Delta s_1}{\Delta s_2} - \frac{\Delta s_2}{\Delta s_1}\right) - \theta^{J-1}\left(\frac{\Delta s_2}{\Delta s_1}\right)}{(\Delta s_1 + \Delta s_2)}$$

$$\frac{\partial f}{\partial s} = \frac{z_I^{J+1}\left(\frac{\Delta s_1}{\Delta s_2}\right) - z_I^J\left(\frac{\Delta s_1}{\Delta s_2} - \frac{\Delta s_2}{\Delta s_1}\right) - z_I^{J-1}\left(\frac{\Delta s_2}{\Delta s_1}\right)}{(\Delta s_1 + \Delta s_2)} \quad (43)$$

and for any property f

$$\frac{\partial f}{\partial s} = \frac{f_I^{J+1}\left(\frac{\Delta s_1}{\Delta s_2}\right) - f_I^J\left(\frac{\Delta s_1}{\Delta s_2} - \frac{\Delta s_2}{\Delta s_1}\right) - f_I^{J-1}\left(\frac{\Delta s_2}{\Delta s_1}\right)}{(\Delta s_1 + \Delta s_2)} \quad (44)$$

using

$$\Delta z_1 = z_{I,J} - z_{I-1,J}$$

$$\Delta z_2 = z_{I+1,J} - z_{I,J}$$

then

$$\frac{\partial f}{\partial z} = \frac{f^J_{I+1}\left(\frac{\Delta z_1}{\Delta z_2}\right) - f^J_I\left(\frac{\Delta z_1}{\Delta z_2} - \frac{\Delta z_2}{\Delta z_1}\right) - f^J_{I-1}\left(\frac{\Delta z_2}{\Delta z_1}\right)}{(\Delta z_1 + \Delta z_2)} \tag{45}$$

the cross derivative can thus be determined from Equation (41)

$$\left(\frac{\partial f}{\partial \theta}\right) = \left[\frac{\partial f}{\partial s} - \left(\frac{\partial f}{\partial z}\right)\frac{\partial z}{\partial s}\right] / \frac{\partial \theta}{\partial s} \tag{46}$$

2. Cartesian System: The derivative $(\partial f/\partial y)$ for all properties f are required. The procedure is analogous to that described for the line source system except that referring to Figure (12b)

$$\Delta s_1 = \left[(z_{I,J} - z_{I,J-1})^2 + (y_J - y_{J-1})^2\right]^{\frac{1}{2}} \tag{47}$$

$$\Delta s_2 = \left[(z_{I,J+1} - z_{I,J})^2 + (y_{J+1} - y_J)^2\right]^{\frac{1}{2}}$$

The cross derivative is then determined from Equation (41)

$$\left(\frac{\partial f}{\partial y}\right) = \left[\frac{\partial f}{\partial s} - \left(\frac{\partial f}{\partial z}\right)\frac{\partial z}{\partial s}\right] / \frac{\partial y}{\partial s} \tag{48}$$

3. Cylindrical System: The derivative $(\partial f/\partial \theta)$ is required at all interior mesh points (I,J) for the properties f. The procedure is analogous to the line source system except that referring to Figure (12c)

$$\Delta s_1 = [(r_{I,J} - r_{I,J-1})^2 + \bar{r}^2(\theta_J - \theta_{J-1})^2]^{\frac{1}{2}}$$
$$\Delta s_2 = [(r_{I,J+1} - r_{I,J})^2 + \bar{r}^2(\theta_{J+1} - \theta_J)^2]^{\frac{1}{2}} \quad (49)$$

and the cross derivative is from Equation (41)

$$(\frac{\partial f}{\partial \theta}) = [\frac{\partial f}{\partial s} - (\frac{\partial f}{\partial r})\frac{\partial r}{\partial s}]/\frac{\partial \theta}{\partial s} \quad (50)$$

B. Cross Derivatives At Boundary Points - The calculation of cross derivatives at discontinuity surfaces and walls are formally similar to the calculation of cross derivatives at interior points of the flow field. The arbitrary n = constant surfaces are replaced by physical walls, shock or contact surfaces. However, care must be exercised in the computation of $(\partial f/\partial z)$ derivatives. Due to stability considerations, forward and backward differencing for these derivatives replaces the usual centered differences.

As shown in Figure (13) no distinction is made between an upper wall boundary or the lower surface of a shock or contact discontinuity. Similarly, no distinction is made between a lower wall boundary and the upper surface of a shock or contact discontinuity.

For example, in a Carteisan system $(\partial f/\partial y)$ the required cross derivative at the boundary is defined by

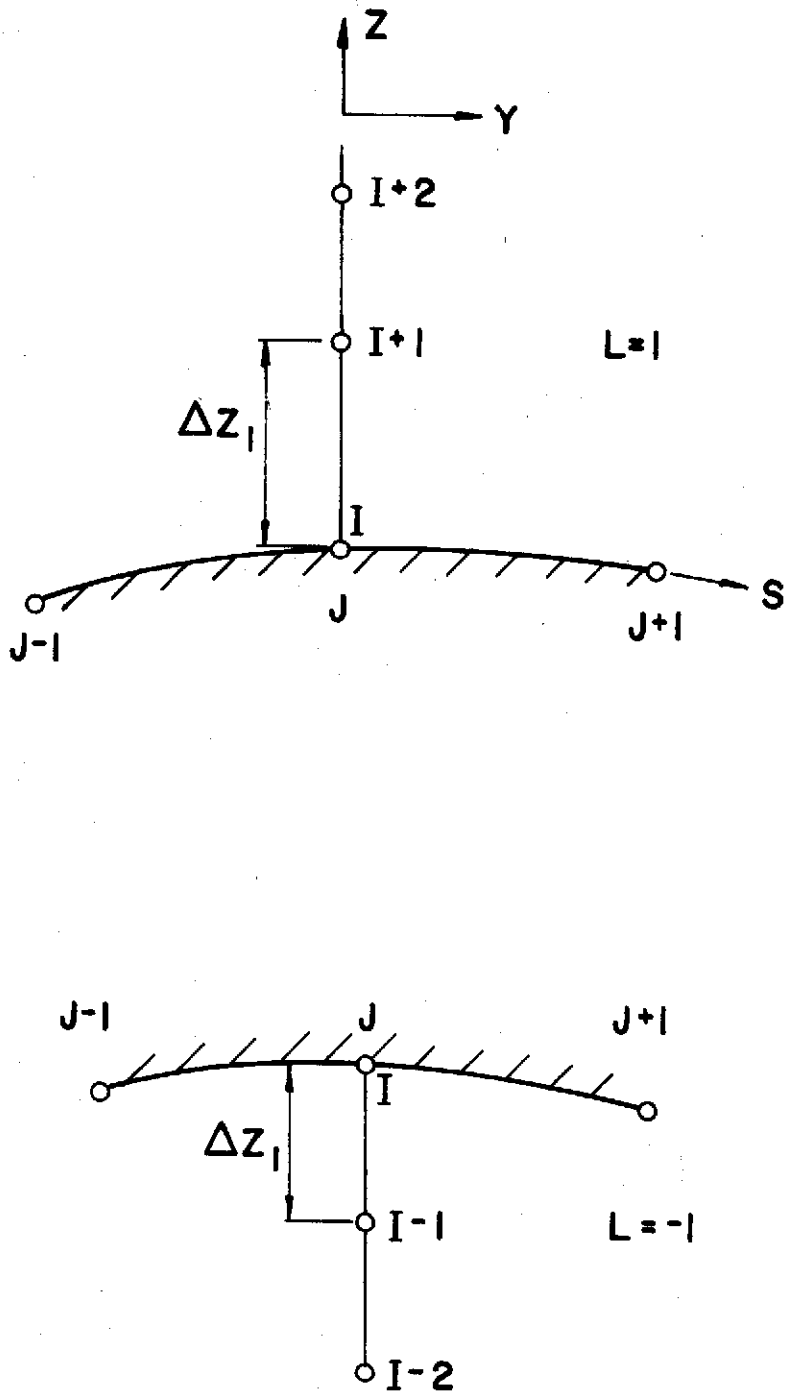

FIGURE 13. UPPER BOUNDARY OR LOWER SURFACE OF DISCONTINUITY

$$\frac{\partial f}{\partial y} = \left[\frac{\partial f}{\partial s} - \left(\frac{\partial f}{\partial z}\right) \frac{\partial z}{\partial s} \right] / \frac{\partial y}{\partial s} \tag{51}$$

where $(\partial f/\partial z)$ is replaced by the appropriate forward or backward difference formula.

Referring to Figure (13) a combined differencing scheme for $(\partial f/\partial z)$ on either a lower type boundary (L=1) or an upper type boundary (L=-1) is

$$\left(\frac{\partial f}{\partial z}\right) = \frac{\Delta^2 f^J_{I+2L} - (1+\Delta)^2 f^J_{I+L} + (1+2\Delta) f^J_I}{\Delta z_1 (1+\Delta)} \tag{52}$$

where

$$\Delta z_1 = z_I - z_{I+L}$$

and

$$\Delta = (\Delta z_1)/(z_{I+L} - z_{I+2L})$$

C. Step Size Criterion - The step size is limited by the Courant-Friedrichs-Lewy (C-F-L) stability criterion which states in geometric terms that the domain of dependence of the differential equations must be embedded within the domain of dependence of the difference scheme. Referring to Figure (14) for the (I,J) point depicted, the domain of the difference scheme is enclosed by the points (I,J-1), (I+1,J), (I,J+1) and (I-1,J).

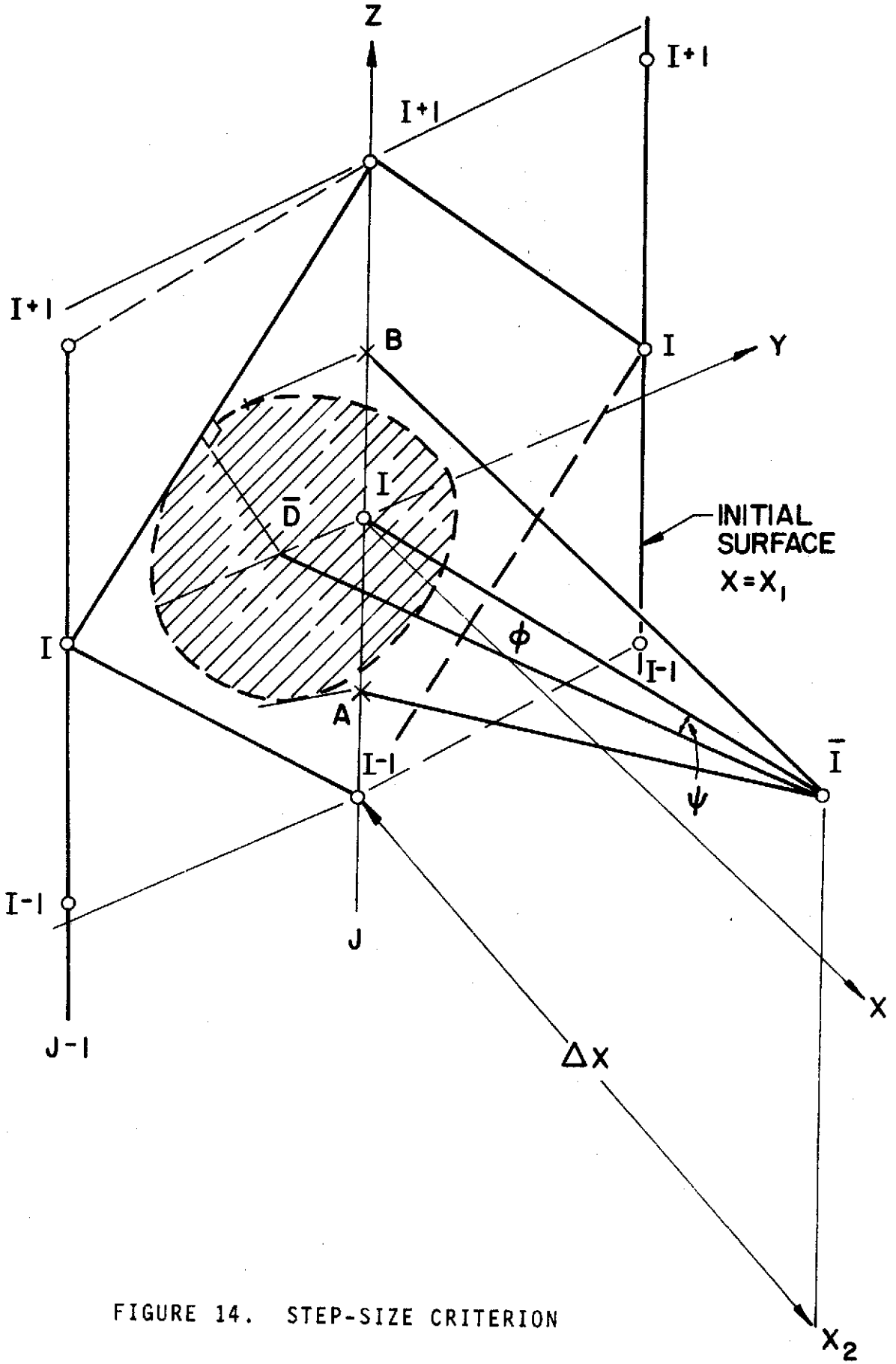

FIGURE 14. STEP-SIZE CRITERION

Then, the C-F-L stability criterion states that the region formed by the intersection of the Mach fore cone through $\bar{I}$ with the plane $x=x_1$ (the shaded ellipsoidal area in Figure 14) must be enclosed by the domain of the difference scheme. This criterion then allows one to determine the maximum marching step ($\Delta x_{I,J} = x_{I,J} - x_{I,J}$) for each mesh point I,J and hence select the overall marching step Δx_{1-2} as the minimum of all the $\Delta x_{I,J}$.

When discontinuities are present in the flow, the step-size is restricted by the consideration that no derivatives may be made by crossing a discontinuity. Referring to Figure (15) derivatives in the z direction at point I cannot be made by the usual centered difference formula since this would entail crossing a discontinuity and hence violate the C-F-L stability criteria. Thus, as previously described in Section B above, the appropriate forward or backward difference is used in making the z derivative. The domain of dependence in this case is given by the ellipsoid of shaded area of Figure (15). Thus, the C-F-L condition at a boundary is applied in a formally analogous fashion to that of an interior point.

D. Interior Point Calculation* - Referring to Figure (11), a typical interior point calculation for the line source system in the reference plane J is performed as follows.

---

*Let C refer to the point ($\bar{I}$,J) and D refer to the point (I,J) in Figures (11), (12) and (13).

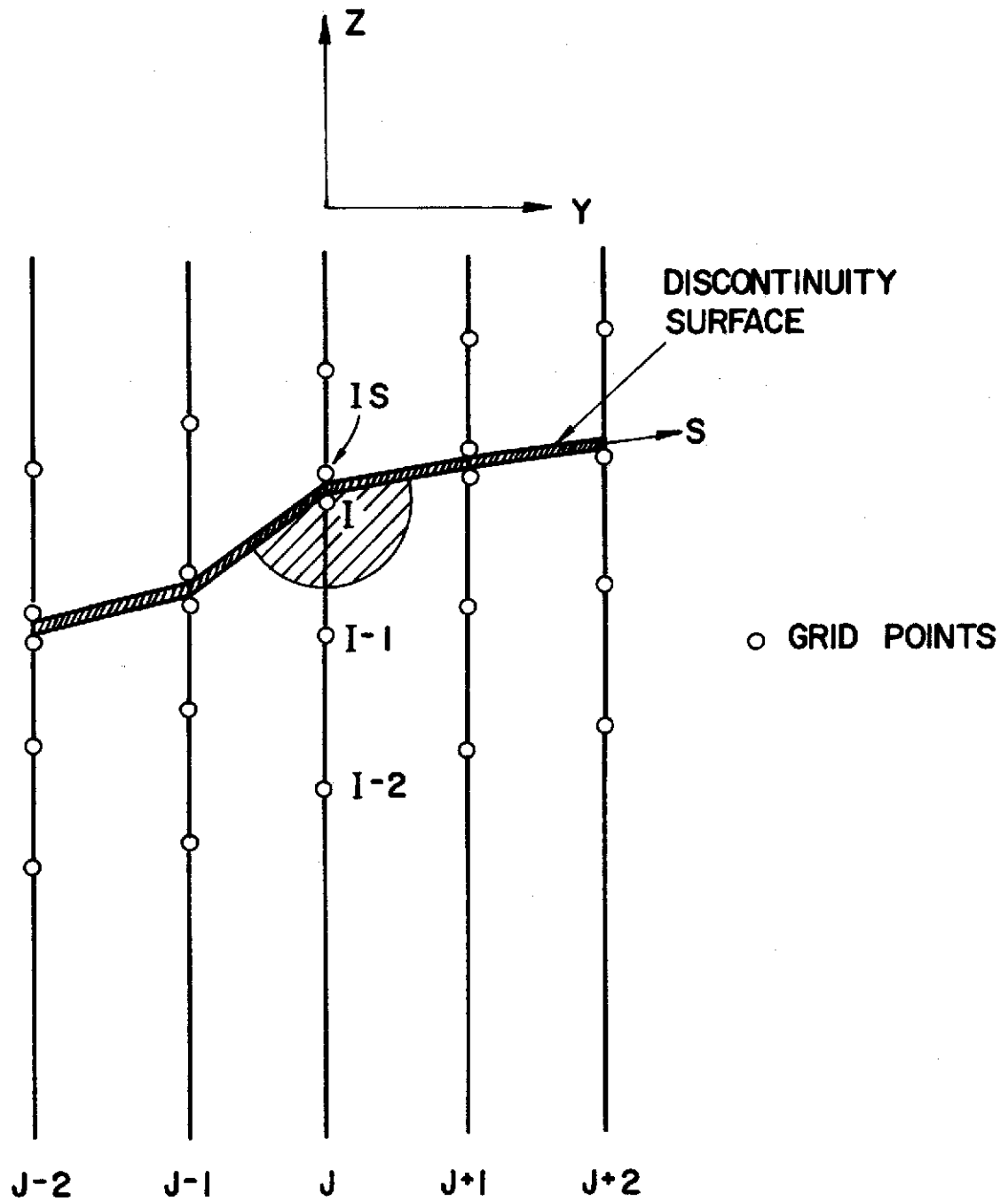

FIGURE 15. DERIVATIVE AND DOMAIN OF DEPENDENCE A+A DISCONTINUITY SURFACE

The point C is located by projecting a quasi-streamline from D a distance Δr downstream (Δr being the overall marching step). Using Equation (22) in difference form

$$z_C = z_D + \tan \phi_D \, \Delta r \tag{53}$$

Points A and B are located by shooting back characteristic projections from point C, locating these points between the mesh points I-1 and I, and I and I+1 respectively, by an iteration procedure, using Equation (21) in difference form:

$$\begin{matrix} z_A \\ B \end{matrix} = z_C - (\lambda)^{\pm}_{\substack{A \\ B}} \Delta r \tag{54}$$

All required properties can be obtained at A and B by a linear interpolation, including cross derivatives which are stored at the grid point locations.

The pressure p_C and flow deflection angle in the reference plane ϕ_C can be determined by solving the linear relations along AC and BC.

$$(\rho q^2)_A \, (\phi_C - \phi_A) + \beta_A \, (p_C - p_A) = F_A^+ \, \Delta r \tag{55}$$

$$(\rho q^2)_B \, (\phi_C - \phi_B) - \beta_B \, (p_C - p_B) = F_B^- \, \Delta r \tag{56}$$

The θ-momentum equation (Equation 11) may be rewritten in the form

$$\rho u \, (v_r + \frac{w}{u} \, v_z) = - \frac{p_\theta}{r} - \frac{\rho v v_\theta}{r} - \frac{\rho u v}{r} \tag{57}$$

since

$$u \frac{\partial}{\partial r} + w \frac{\partial}{\partial z} = q \frac{\partial}{\partial s} \tag{58}$$

(where $\frac{\partial}{\partial s}$ represents the change along the direction CD, a streamline projection), we obtain the difference equation:

$$v_C = v_D - \frac{1}{r \cos \phi_D} \left[\frac{p_\theta}{\rho q} + \tan \psi \left(\tan \psi \, (q_\theta) + \frac{q \psi_\theta}{\cos^2 \psi} + q \cos \phi \right) \right]_D \Delta r \tag{59}$$

All streamline relations are valid along the actual streamline $\bar{D}C$. Properties at $\bar{D}^*$ may be obtained to first order by the relation

$$f_{\bar{D}^*} = f_D - (f_\theta)_D \, \Delta\theta \tag{60}$$

which upon incorporating streamline geometry reduces to

$$f_{\bar{D}^*} = f_D - (f_\theta)_D \left[\frac{\tan \psi}{r \cos \phi} \right]_D \Delta r \tag{61}$$

The pressure density relation, expressed in differential form along a streamline in Equation (13) may be integrated holding Γ constant for the small integration step $C\bar{D}^*$, yielding

$$\rho_C = \rho_{\bar{D}^*} \left(\frac{p_C}{p_{\bar{D}^*}} \right)^{1/\Gamma_{\bar{D}^*}} \tag{62}$$

The Bernoulli relation

$$\frac{dp}{\rho} + \frac{dV^2}{2} = 0 \tag{63}$$

may be integrated along D*C, making use of Equation (56), yielding

$$v_C = \left[v_{D*}^2 + \frac{2\Gamma}{\Gamma-1}_{D*} \left(\frac{p}{\rho}_{D*} - \frac{p}{\rho}_{C} \right) \right]^{\frac{1}{2}} \tag{64}$$

The conservation of total enthalpy states that $h_C = h_{D*}$ and hence,

$$h_C = h_{D*} + \frac{1}{2} (v_{D*}^2 - v_C^2) \tag{65}$$

For inviscid flows, the equivalence ratio remains constant along a streamline, hence,

$$\Phi_C = \Phi_{D*} \tag{66}$$

The isentropic exponent Γ_C may now be obtained from the polynomial fit

$$\Gamma_C = \Gamma (h_C, p_C, \Phi_C) \tag{67}$$

and the equilibrium sound speed obtained from the relation

$$a_C = \left[\frac{\Gamma_C p_C}{\rho_C} \right]^{\frac{1}{2}} \tag{68}$$

For a Cartesian system, Δr in Equations (53), (54), (55) and (56) is replaced by Δx. The y momentum equation replaces Equation (57) and takes the form

$$\rho u \left(v_x + \frac{w}{u} v_z\right) = - \rho v v_y - p_y \tag{69}$$

Noting that,

$$u \frac{\partial}{\partial x} + w \frac{\partial}{\partial z} = q \frac{\partial}{\partial s} \tag{70}$$

the expression for the change in cross flow velocity along the streamline projection CD takes the form

$$v_C = v_D - \frac{1}{\cos \phi_D} \left[\frac{p_y}{\rho q} + \tan \psi \left(\tan \psi \, q_y + \frac{q \psi_y}{\cos^2 \psi} \right) \right]_D \Delta x \tag{71}$$

Properties at $\overline{D}$ are obtained using the relation

$$f_{\overline{D}} = f_D - (f_y)_D \left(\frac{\tan \psi}{\cos \phi} \right)_D \Delta x \tag{72}$$

All other equations and remarks pertinent to the line source system also apply to the Cartesian system.

For the cylindrical system, the C point is located using Equation (73)

$$r_C = r_D + \tan \phi_D \, (\Delta x) \tag{73}$$

Points A and B are located using the relation

$$r_{\substack{A \\ B}} = r_C - (\lambda \pm)_{\substack{A \\ B}} \quad \Delta x \tag{74}$$

The pressure p_C and flow deflection angle ϕ_C in the reference plane are determined by solving the linear relations along AC and BC with Δr replaced by Δx.

The θ-momentum equation may be written along the streamline projection in the reference plane, yielding

$$v_C = v_D - \frac{1}{\rho_D \, r_D \, q_D \cos \phi_D} [p_\theta + \rho v v_\theta + \rho v q \sin \phi] \, \Delta x \tag{75}$$

All streamline relations are valid along the actual streamline D*C, where properties at D* are obtained using the relation

$$f_{D*} = f_D - (f_\theta)_D \left[\frac{v}{rq \cos \phi} \right] \Delta x \tag{76}$$

The streamline relations (Equations 62-68) described for the line source system are also valid for this system.

E. Upper or Lower Boundary Point Calculation For a line source system*, the upper or lower boundaries are prescribed by equations of the form

$$z = f(r,\theta) \tag{77}$$

where f is everywhere continuous and differentiable. Referring to Figure (16), which depicts an upper wall calculation, the appropriate boundary condition at point C is

$$\bar{v} \cdot \hat{n} = 0 \tag{78}$$

where

$$\bar{v} = u\,\hat{i}_r + v\,\hat{i}_\theta + w\,\hat{i}_z$$

and

$$\bar{n} = f_r\,\hat{i}_r + \frac{f_\theta}{r}\,\hat{i}_\theta - \hat{i}_z$$

which yields

$$\left(\frac{w}{u}\right)_C = f_r + \left(\frac{v}{u}\right)_C \frac{f_\theta}{r} \tag{79}$$

where

$$\left(\frac{w}{u}\right)_C = \tan \phi_C \tag{80}$$

*C is the grid point IMAX(J), J at station $r=r_2$ and D is the grid point IMAX(J),J at station $r=r_1$ for an upper wall calculation. For a lower wall calculation the corresponding points would be the I,J points at the stations r_2 and r_1.

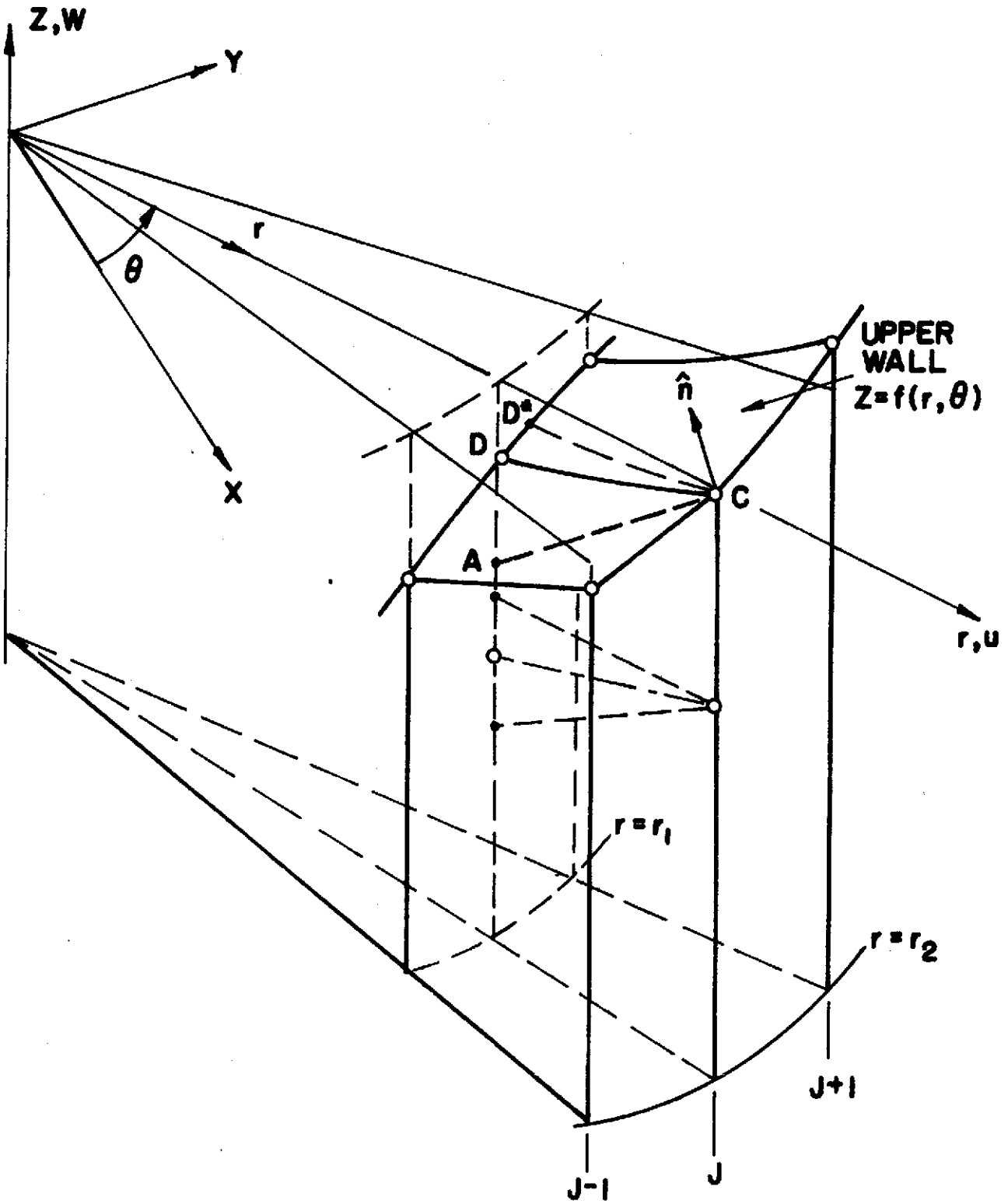

FIGURE 16. UPPER WALL POINT CALCULATION IN LINE SOURCE SYSTEM

ϕ_C being the flow deflection required for the characteristic calculation. The wall calculation requires the following iterative procedure:

(1) A value for $(\frac{v}{u})_C$ is assumed, for example the value at point D.

(2) A value for ϕ_C is obtained from Equation (80) and hence p_C can then be obtained using the compatibility relation along AC, (Equation 55) with ϕ_C prescribed.*

(3) The normal momentum equation (Equation 59) is applied along C-D yielding the cross velocity v_C.

(4) The actual streamline passing through C is traced back locating the point D* on the vehicle wall and application of the pressure-density relation (Equation 62) (holding Γ constant) and the Bernoulli relation (Equation 64) yields the total velocity v at C

$$v^2 = u^2 \left[\frac{v^2}{u} + \frac{w^2}{u} \right] \rightarrow u_C \rightarrow v_C^* \qquad (81)$$

*For a lower wall calculation the compatibility relation along BC (Equation 56) would be employed.

(5) v_C and v_C^* are checked for consistency and if they differ by more than a specified tolerance a new value of $(\frac{v}{u})_C$ is assumed and the process repeated until convergence is obtained. After two values of $(\frac{v}{u})_C$ have been assumed, further values may be obtained by a standard linear error extrapolation procedure.

For a Cartesian system, the upper or lower boundaries are prescribed by equations of the form

$$z = f(x,y) \tag{82}$$

the velocity $\bar{v}$ is expressed by

$$\bar{v} = u\, i_x + v\, i_y + w\, i_z \tag{83}$$

and the normal to the boundary is given by

$$\hat{n} = f_x\, \hat{i}_x + f_y\, \hat{i}_y - \hat{i}_z \tag{84}$$

Hence the boundary condition $\bar{v}.\hat{n} = 0$ yields

$$(\frac{v}{u})_{\hat{C}} = f_x + (\frac{v}{u})_C f_y \tag{85}$$

The iterative procedure is the same as that described for the line source system.

For a cylindrical system, the upper or lower boundaries are prescribed by equations of the form

$$r = f(\theta, x) \tag{86}$$

The velocity $\bar{V}$ is expressed by

$$\bar{V} = u\,\hat{i}_x + v\,\hat{i}_\theta + w\,\hat{i}_r \tag{87}$$

and the normal to the boundary is given by

$$\hat{n} = f_x\,\hat{i}_x + \frac{f_\theta}{r}\,\hat{i}_\theta - \hat{i}_r \tag{88}$$

Hence the boundary condition $\bar{V}\,n = 0$ yields

$$\left(\frac{w}{u}\right)_C = f_x + \left(\frac{v}{u}\right)_C \frac{f_\theta}{r} \tag{89}$$

The iterative procedure is again the same as that for the line source system.

F. Sidewall Calculation For the internal flow analysis of Vehicle I, the sidewalls are calculated using a local cartesian reference plane system, the reference planes being the planes z = constant, as indicated in Figures (5) and (6). Additionally, for all external flow calculations a portion of

the vehicle undersurface can be interpretted as a sidewall in a local cartesian $(\bar{y},\bar{z})$ system as indicated in Figure (10).

The sidewall calculation is geometrically complicated when a line source system is employed for the calculation of the other reference planes since local transformations must be made between the cartesian and line source systems. This situation is depicted in Figure (17). For the internal flow sidewall calculation of Vehicle II, a local reference plane system is used where the reference planes are the surfaces r = constant, as indicated in Figure (7). The sidewall calculation is performed after all interior mesh points have already been calculated. In performing this calculation it would be expeditous to use reference planes normal to the wall, but this is ruled out by the geometric complexities involved in obtaining cross derivatives for arbitrarily oriented planes.

(1) Line Source or Cartesian System: Referring to Figure (17), point C is located as the intersection of the sidewall with the plane z = constant at the station being calculated. The sidewall is specified by an equation of the form

$$y - f(x,z) = \text{constant} \tag{99}$$

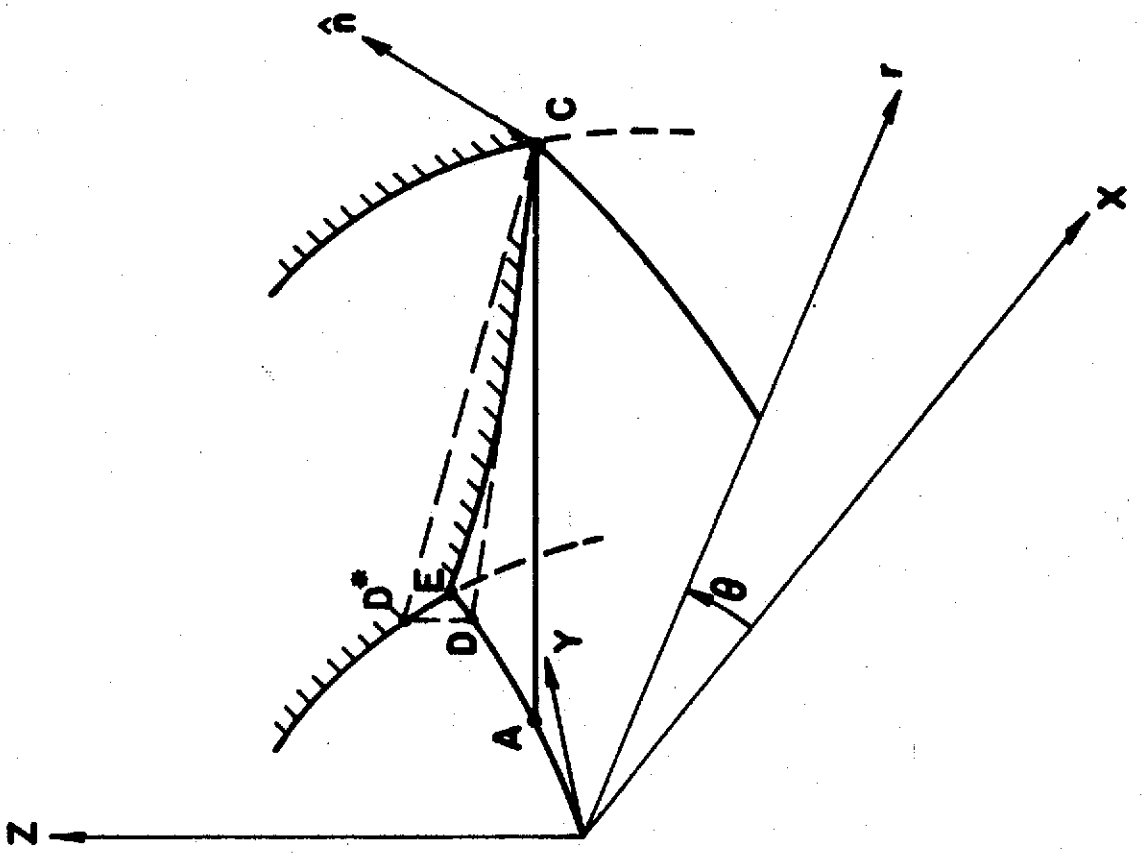

FIGURE 17. SIDEWALL CALCULATION, LINE SOURCE OR CARTESIAN SYSTEM

The normal is then given by

$$\hat{n} = [-f_x \hat{i} + \hat{j} - f_z \hat{k}] / (1 + f_x^2 + f_z^2)^{\frac{1}{2}} \tag{91}$$

At point C, the wall boundary conditions is

$$(\bar{v} \cdot \hat{n})_C = 0 \tag{92}$$

which may be written

$$\left(\frac{v}{u}\right)_C = f_{x_C} + \left(\frac{w}{u}\right)_C f_{z_C} \tag{93}$$

The streamline differential equations are

$$\frac{dx}{u} = \frac{dy}{v} = \frac{dz}{w} \tag{94}$$

Which in differential form become

$$\frac{y_C - y_D^*}{x_C - x_D^*} = \tfrac{1}{2}\left[\left(\frac{v}{u}\right)_{D^*} + \left(\frac{w}{u}\right)_C\right] \tag{95}$$

and

$$\frac{z_C - z_D^*}{x_C - x_D^*} = \tfrac{1}{2}\left[\left(\frac{w}{u}\right)_{D^*} + \left(\frac{w}{u}\right)_C\right] \tag{96}$$

The z momentum equation, written along CD, takes the form

$$w_C = w_D - \left[\frac{pz}{\rho q} + \frac{w w_z}{q} \right] \Delta S_{CD} \tag{97}$$

The characteristic compatibility relation (in the plane z=const) takes the form

$$\rho u^2 \, d\left(\frac{v}{u}\right) \pm \beta \, dp = F^{\pm} \, dr \tag{98}$$

where

$$F^{\pm} = \lambda^{\pm} (\rho w \, u_z) - \rho w v_z + [\lambda^{\pm} - \frac{v}{u}] \tag{99}$$

$$\frac{u}{a^2} \, (-w \, p_z - a^2 \rho w_z)$$

The properties at C are obtained by the following iterative procedure:

Assume a value for $(w/u)_c$; for example, the value at the previous wall point E. Since f_x and f_z are known at C, Equation (93) yields $\left(\frac{v}{u}\right)_c$ for this guess. The location of the D* point may be obtained using Equations (95), (96) and the fact that this point has a radius r (or x is specified) and lies on the sidewall. It is obtained by interpolating between sidewall grid points. The D point (projection of D* onto plane z=constant) is then obtained by setting $z_D = z_C$, $y_D = y_D^*$ and $x_D = x_D^*$.

The A point is located using the characteristic equation on the plane $z = z_C$

$$\frac{y_C - y_A}{x_C - x_A} = \left[\frac{uv \pm a^2\beta}{u^2 - a^2}\right]_A = \lambda_A^+ \tag{100}$$

and knowledge that $r_A = r = (x_A^2 + x_A^2)^{\frac{1}{2}}$ (or that x_A is specified for a Cartesian system) and $z_A = z_C$, by interpolating between grid points on the plane $z = z_C$. Obtaining properties at A, the compatibility relation (98) can be applied to yield p_C for the assumed value $(v/u)_C$. Streamline relations applied along D*C yield ρ_C and v_C. The system can be checked for consistency as follows:

$$v_C, \left(\frac{w}{u}\right)_C \text{ and } \left(\frac{v}{u}\right)_C \neq u_C \neq w_C^* \tag{101}$$

Test if $w_C^* = w_C$ to within a specified tolerance. If not, perturb the value of $(w/u)_C$ assumed, repeat the above calculations and once two values of $(w/u)_C$ and the corresponding errors $(w_C - w_C^*)$ have been obtained, convergence can be obtained by a linear extrapolation of the error to zero.

Upon convergence, the remaining properties (h_C, Φ_C, Γ_C and a_C) can be obtained as described previously.

(2) Cylindrical System: The sidewall network for Vehicle II is depicted in Figure (18). This requires working in reference planes r = constant. The sidewall is specified by the equation

$$\theta = f(r,z) \tag{102}$$

The normal is then given by

$$\hat{n} = (-f_z \hat{i}_z + \frac{1}{r} \hat{i}_\theta - f_r \hat{i}_r)/(f_z^2 + \frac{1}{r^2} + f_r^2)^{\frac{1}{2}} \tag{103}$$

hence at point C, the boundary condition $\overline{v}\cdot\hat{n}=0$ yields

$$(\frac{v}{u})_C = r_C f_z + (\frac{w}{u}) f_{r\ C} \tag{104}$$

The streamline differential equations are

$$\frac{dr}{w} = \frac{rd\theta}{v} = \frac{dx}{u}$$

which in differential form become

$$\frac{\theta_C - \theta_D}{\Delta x} = \left[(\frac{v}{u})_{D^*} + (\frac{v}{u})_C\right]/(r_D^* + r_C) \tag{105}$$

$$\frac{r_C - r_D^*}{\Delta x} = \frac{1}{2}\left[(\frac{w}{u})_{D^*} + (\frac{w}{u})_C\right] \tag{106}$$

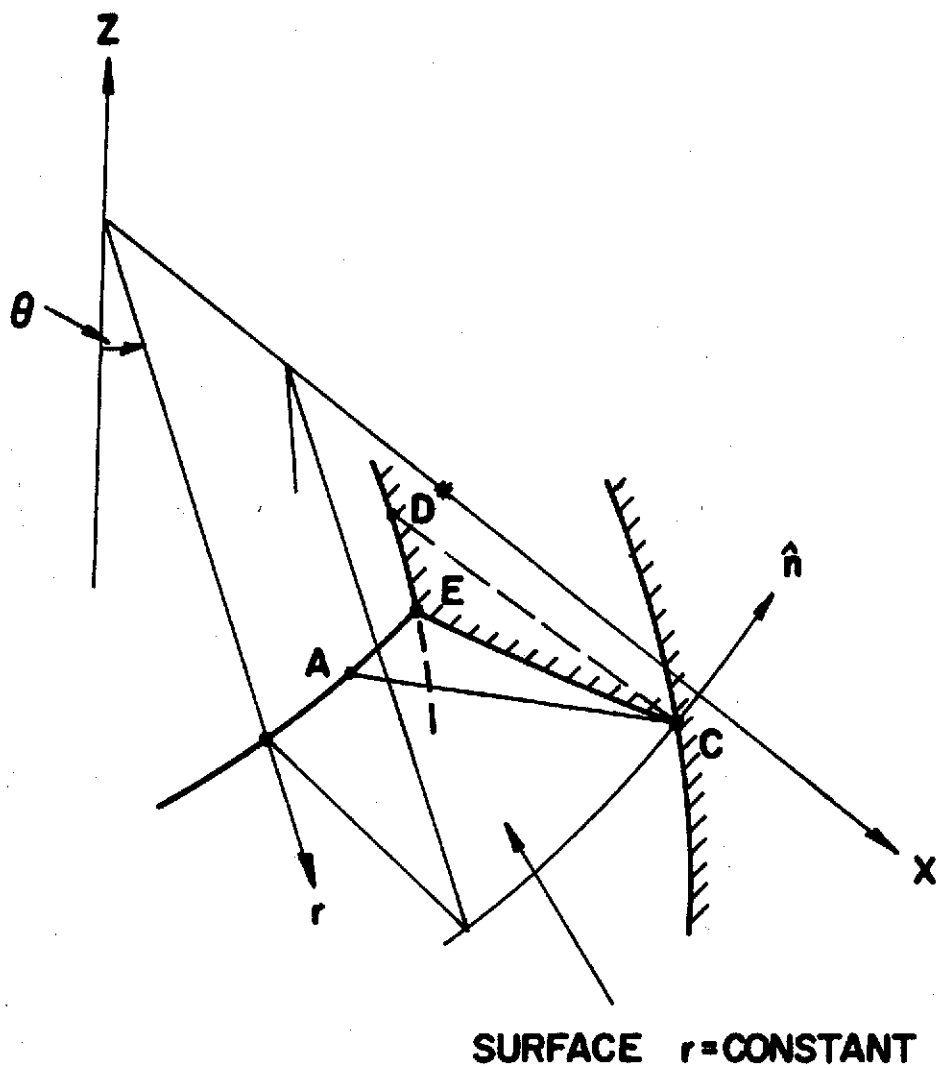

FIGURE 18. SIDEWALL CALCULATION, CYLINDRICAL SYSTEM

The characteristic directions, on the surface r = constant, are given by

$$\frac{d\theta}{dx} = \frac{1}{r}\left[\frac{qv\cos\phi/a^2 \pm \beta}{(q/a)^2\cos^2\phi - 1}\right] \tag{107}$$

where

$$q^2 = v^2 + u^2$$

and

$$\beta^2 = (q/a)^2 - 1$$

Along these characteristics, the compatibility relations take the form

$$u^2\, d\left(\frac{v}{u}\right) \pm \beta\, dp = F^{\pm}\, dx \tag{108}$$

where $F^{\pm}$ is given by

$$F^{\pm} = \rho(-w\, v_r + \lambda^{\pm}\, w\, u_r) - (\lambda^{\pm} u - v)$$
$$(\rho w_r + \frac{w}{a^2}\, p_r) \tag{109}$$

The normal or w-momentum equation may be written along a streamline projection in the reference surface r = constant.

$$w_C = w_D - \frac{1}{q_D}\left[\frac{p_r}{\rho} + w\, w_r - \frac{v^2}{r}\right]_D \Delta S \tag{110}$$

where

$$\Delta S = (r^2 (\theta_C - \theta_D) + \Delta x^2)^{\frac{1}{2}}$$

The logic for the sidewall calculations proceeds as follows: assume a value for $(u/u)_C$. Using Equation (104), yields $(v/u)_C$. The streamline point D* may be located by Equations (105) and (106) in an iterative manner. Using Equation (107) to locate the A point, we may apply Equation (108) along AC yielding p_C, and then apply Equation (110) to determine w_C. Using streamline relations along D*C yields ρ_C and v_C. The system is then checked for consistency; since v_C, $(w/u)_C$ and $(v/u)_C$ yield an independent value w_C^* which is compared with the value of w_C obtained from the normal momentum equation. The same extrapolation method can be used for convergence and the remaining properties (h_C, Φ_C, Γ_C and a_C) may be obtained.

G. Internal Corner Flow Calculation

(1) Line Source System: The corners are defined by the intersection of the upper or lower nozzle walls with the sidewalls. The upper or lower wall is specified by an equation of the form

$$z = f(r,\theta) \qquad (111)$$

while the sidewall is specified by

$$y = g(x,z) \tag{112}$$

The transformation from a Cartesian to a line source system is simply

$$\begin{aligned} x &= r \cos \theta \\ y &= r \sin \theta \\ z &= z \end{aligned} \tag{113}$$

With u, v and w being the velocity components in the line source system (in the r, θ and z directions respectively) and $\bar{u}$, $\bar{v}$ and $\bar{w}$ being the components in the Cartesian system the velocity transformation is

$$\begin{aligned} \bar{u} &= u \cos \theta - v \sin \theta \\ \bar{v} &= u \sin \theta + v \cos \theta \\ \bar{w} &= w \end{aligned} \tag{114}$$

At the corner (point C of Figure 19) the boundary condition $\bar{v} \cdot \hat{n} = 0$ applied to the upper (or lower) surface yields

$$\left(\frac{w}{u}\right) = f_r + \left(\frac{v}{u}\right) \frac{f_\theta}{r} \tag{115}$$

Applying this to the sidewalls yields

$$\left(\frac{\bar{v}}{\bar{u}}\right) = g_x + \left(\frac{\bar{w}}{\bar{u}}\right) g_z \tag{116}$$

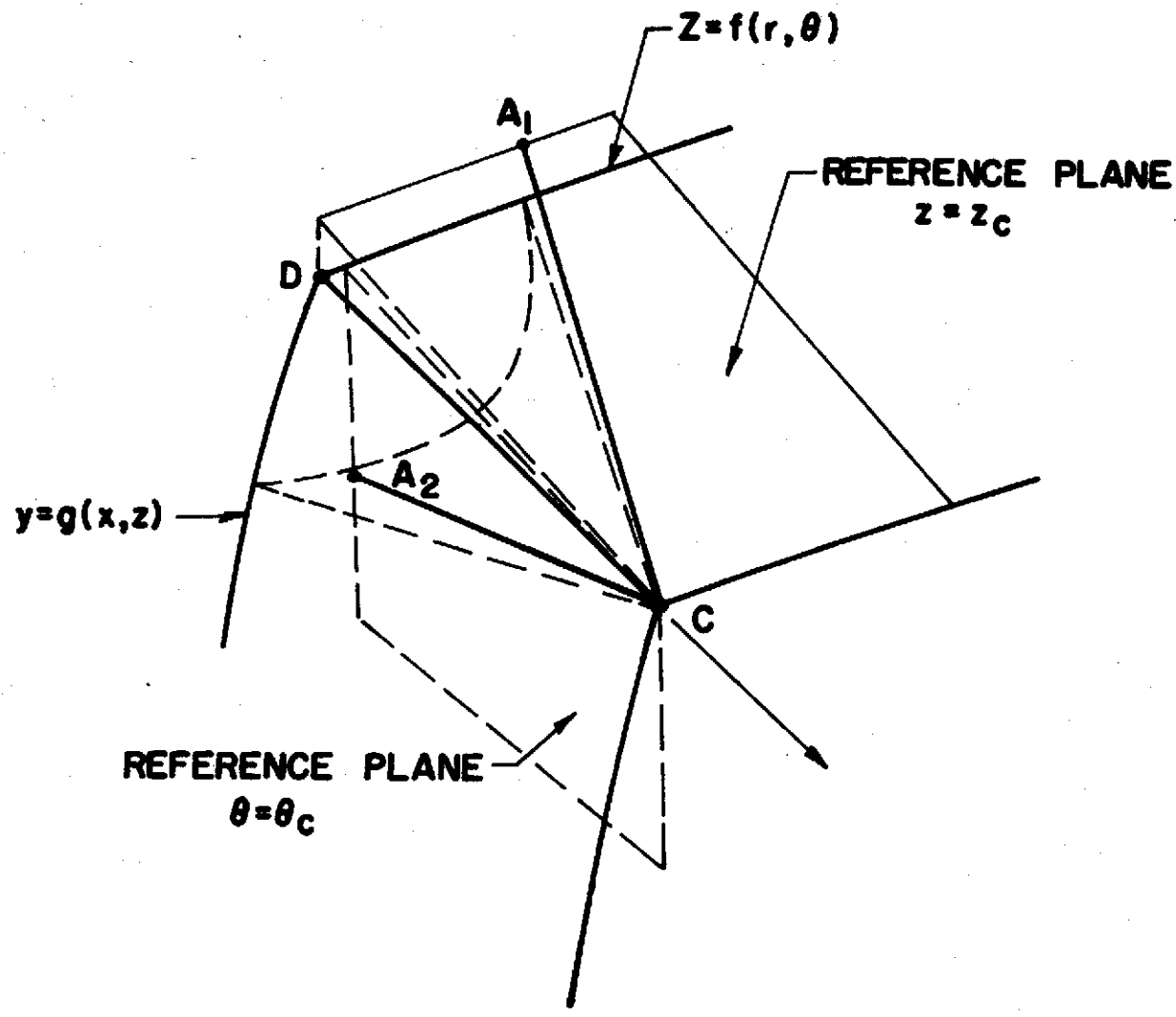

FIGURE 19. INTERNAL CORNER CALCULATION, LINE SOURCE SYSTEM

The vertical reference plane $\theta=\theta_C$ may be intersected with the initial plane as shown in Figure (18).

Applying the velocity transformation (Equation 114) to Equation (116) we obtain

$$\left(\frac{v}{u}\right) = \frac{g_x + \left(\frac{w}{u}\right) g_z \tan\theta}{(1 + g_x \tan\theta)} \tag{117}$$

Now, Equations (116) and (117) can be solved for $\left(\frac{w}{u}\right)$ yielding

$$\left(\frac{w}{u}\right) = \frac{f_r (1 + g_x \tan\theta) + \frac{f\theta}{r} (g_x - \tan\theta)}{(1 + g_x \tan\theta - g_z \frac{f\theta}{r})} \tag{118}$$

Then $\phi_C = \tan^{-1}\left(\frac{w}{u}\right)$ and the compatibility relation (Equation 55 or 56) can be applied along the projection of the bi-characteristic onto the vertical reference plane (A_2C) yielding p_{C_2}. The point A_2 is located by a double interpolation.

The horizontal reference plane $z=z_C$ may be intersected with the initial plane as shown in Figure (18). Transforming Equation (115) to the Cartesian system, we obtain

$$\left(\frac{\bar{w}}{\bar{u}}\right) = \cos\theta\, f_r = \sin\theta \frac{f\theta}{r} + \left(\frac{\bar{v}}{\bar{u}}\right) [\sin\theta\, f_r + \cos\theta \frac{f\theta}{r}] \tag{119}$$

Solving Equation (116) and (119) for $\left(\frac{\bar{v}}{\bar{u}}\right)$ we obtain

$$\frac{\bar{v}}{\bar{u}} = \frac{g_x + [\cos\theta\, f_r - \sin\theta\, \frac{f\theta}{r}]\, g_z}{1 - [\sin\theta\, f_r + \cos\theta\, \frac{f\theta}{r}]\, g_z} \tag{120}$$

Applying the compatibility relation (Equation 98) along the projection of the bi-characteristic onto the horizontal reference plane (A_1C), we obtain an alternate value of the pressure p_{C_1}, where the point A_1 is again obtained by a double interpolation. The pressure p_C is then obtained as a weighted average of the two pressures p_{C_1} and p_{C_2}, the weighing function being determined by the relative wave strengths along the two characteristic projections A_1C and A_2C.

Since a sharp corner is a streamline of the flow field, the streamline relations may be directly applied along CD yielding ρ_C, v_C, h_C and Φ_C. Knowing the velocity v_C and the flow angles, we obtain the velocity components u, v and w or $\bar{u}$, $\bar{v}$ and $\bar{w}$.

2. Cartesian System: The upper or lower wall is specified by an equation of the form

$$z = f(x,y) \tag{121}$$

No velocity transformations are required in this calculation. The boundary condition $\bar{v} \cdot \hat{n}$ applied to the upper (or lower) boundary at C yields

$$(\frac{w}{u}) = f_x + (\frac{v}{u})\, f_y \tag{122}$$

while applied to the sidewall yields

$$\left(\frac{v}{u}\right) = g_x \left(\frac{w}{u}\right) g_z \tag{123}$$

Solving for $\left(\frac{w}{u}\right)$ one obtains

$$\left(\frac{w}{u}\right) = \frac{f_x + g_x f_y}{1 - g_z f_y} \tag{124}$$

The vertical reference plane $y=y_c$ is intersected with the initial plane and the characteristic compatibility relation (Equation 55 or 56) is applied along the projection of the bi-characteristic yielding p_{C_2}, since $\phi_C = \tan^{-1}\left(\frac{w}{u}\right)$ is known.

Similarly, the horizontal reference plane $z=z_c$ is intersected with the initial plane and the characteristic compatibility relation (Equation 98) is applied along it yielding an alternate value of p_{C_1} where $\left(\frac{v}{u}\right)$ is given by

$$\left(\frac{v}{u}\right) = \frac{g_x + f_x g_z}{1 - f_y g_z} \tag{125}$$

The pressure is again a weighted average of p_{C_1} and p_{C_2} based on the relative wave strengths along the two characteristic projections.

3. Cylindrical System: The upper or lower wall is specified by an equation of the form

$$r = f(x,\theta) \tag{126}$$

while the sidewall is specified by

$$\theta = g(x,r) \tag{127}$$

At the corner, the boundary condition $\bar{v} \cdot \hat{n}$ applied to the upper (or lower) surface yields

$$\left(\frac{W}{U}\right) = f_x + \left(\frac{V}{U}\right) \frac{f\theta}{r} \tag{128}$$

and applied to the sidewalls yields

$$\left(\frac{V}{U}\right) = g_x + \left(\frac{W}{U}\right) g_r \tag{129}$$

The reference plane $\theta=\theta_C$ passing through the corner point is intersected with the initial plane and the characteristic compatibility equation (Equation 55 or 56) is applied along the projection of the bi-charachteristic onto this reference plane. This yields p_{C_2} since ϕ_{C_2} is known, being obtained from the relation

$$\phi_{C_2} = \tan^{-1}\left(\frac{W}{U}\right) = \tan^{-1}\left(\frac{f_x + g_x \frac{f\theta}{r}}{1 - g_r \frac{f\theta}{r}}\right) \tag{130}$$

Similarly the surface $r=r_C$ passing through the corner is intersected with the initial plane and an alternate value of the

corner pressure p_{C_1} is obtained using the compatibility relation (Equation 108) along the projection of the bi-characteristic onto this reference surface, where (v/u) is given by

$$\left(\frac{v}{u}\right) = \frac{g_x + f_x\, g_r}{1 - \frac{f\theta}{r}\, g_r} \tag{131}$$

The pressure p_C is then again determined by a weighted average.

H. Flow Field Discontinuities

The numerical program developed can perform three dimensional calculations for discontinuity surfaces propagating into a nonuniform stream. The use of the reference plane technique can greatly simplify the logic by using a two dimensional type of procedure in the reference planes. While this procedure resembles its strictly two dimensional counterpart it should be emphasized that the full three dimensional Hugoniot relations are satisfied at a shock surface, and full three dimensional boundary conditions are applied at a contact surface.

Consistent with the problem considered, only discontinuities which propagate essentially in references planes can be analyzed. This implies that discontinuities formed from sidewalls or large cross-wise flow gradients cannot be analyzed. Equilibrium chemistry is assumed to prevail upstream and downstream of a discontinuity.

(1) Shock Surface: A typical local shock surface orientation is shown in Figure (20). The local shock surface is specified by an ortho-normal triad of vectors consisting of the normal to the surface and two tangent vectors to the surface. With respect to the reference axes, a tangent direction $\hat{t}$ with cosine director β is defined by the shock and reference plane intersection. The tangent $\hat{\ell}$ with director (α) is normal to $\hat{t}$ and the normal to the shock $\hat{n}$ is $\hat{n} = \hat{t} \times \hat{\ell}$, or in terms of α and β

$$\hat{n} = -\cos\alpha\sin\beta\ \hat{i}_r - \sin\alpha\ \hat{i}_\theta + \cos\alpha\cos\beta\ i_z \qquad (132)$$

The velocity vector in terms of the shock oriented coordinates is $v = \tilde{u}\,\hat{n} + \tilde{v}_t\,\hat{t} + \tilde{v}_\ell\,\hat{\ell}$. The local Hugoniot relations are:

$$\rho_1\,\tilde{u}_1 = \rho_2\,\tilde{u}_2 \qquad \text{continuity} \qquad (133)$$

$$P_1 + \rho_1\,\tilde{u}_1^2 = P_2 + \rho_2\,\tilde{u}_2^2 \qquad \text{normal momentum} \qquad (134)$$

$$\tilde{v}_{t_1} = \tilde{v}_{t_2} \qquad \hat{t}\ \text{momentum} \qquad (135)$$

$$\tilde{v}_{\ell_1} = \tilde{v}_{\ell_2} \qquad \hat{\ell}\ \text{momentum} \qquad (136)$$

$$H = \text{constant} = h + \tfrac{1}{2} V^2 \qquad \text{energy} \qquad (137)$$

$$\rho = \rho\,(P, h, \Phi) \qquad \text{state} \qquad (138)$$

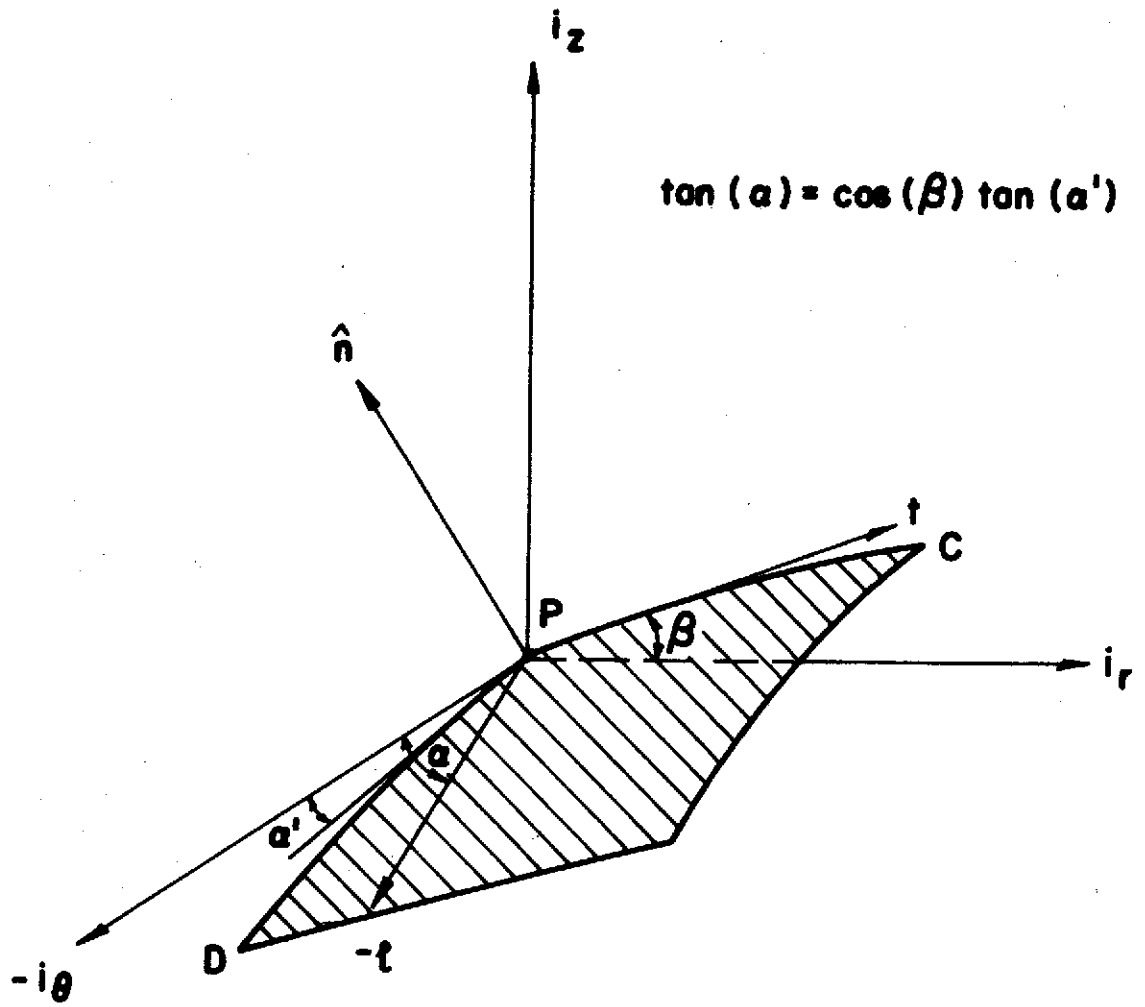

FIGURE 20. ORIENTATION OF DISCONTINUITY SURFACES

Combining and rewriting (133) and (134) in terms of the reference plane parameters we obtain,

$$\rho_1 \tilde{u}_1 (\tilde{u}_1 - \tilde{u}_2) = P_2 - P_1 \qquad \text{continuity \& } \hat{n} \text{ momentum} \qquad (139)$$

$(u = v\sin\alpha + q\cos\alpha\sin(\beta-\phi))$

$$q_1 \cos(\beta-\phi_1) = q_2 \cos(\beta-\phi_2) \qquad \hat{t} \text{ momentum} \qquad (140)$$

$$q_1 (-\sin\alpha\sin(\beta-\phi_1) + \cos\alpha \tan\psi_1) \qquad \hat{\ell} \text{ momentum} \qquad (141)$$

$$= q_2 (-\sin\alpha\sin(\beta-\phi_2) + \cos\alpha \tan\psi_2)$$

$$H_2 = h_2 + \tfrac{1}{2} (q_2/\cos\psi_2)^2 = \text{constant} \qquad \text{energy} \qquad (142)$$

$$\rho_2 = \rho(P_2, h_2, \Phi) \qquad \text{state} \qquad (143)$$

A typical shock wave calculation would be performed as shown in Figure (21). A new shock location (point C) is determined in each reference plane using an assumed value of the cosine director β_c. A new value of the cosine director α_c can now be calculated from geometric considerations using the newly calculated shock locations, and the relation $\tan\alpha = \tan\alpha' \cos\beta$. Since properties are nonuniform upstream of the shock wave, a reference plane characteristic calculation is performed on the upstream side of the wave (A_1C,B_1C) and local flow properties determined at C_1. Using this data and the α and β cosine directors, the Hugoniot relations (Equations 139 through 143) are solved in each reference

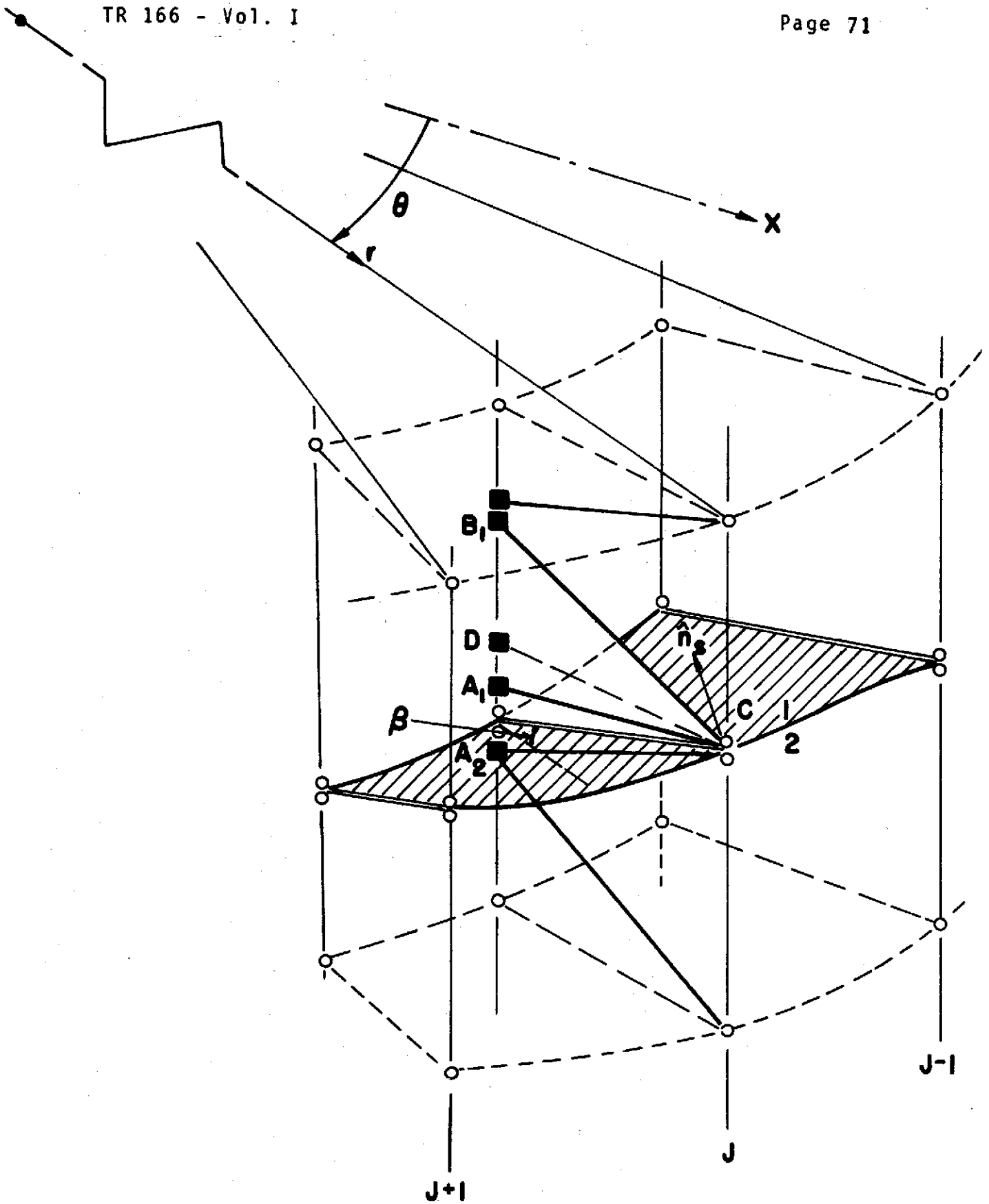

FIGURE 21. TYPICAL SHOCK WAVE CALCULATION

plane for the downstream flow conditions. Satisfying the Hugoniot relations involves an iteration procedure since chemical equilibrium is assumed upstream and downstream of the shock wave. This particular procedure is analogous to that employed in two dimensional flow calculations. Using the calculated Hugoniot flow deflection in each reference plane a value of pressure is calculated on the downstream side of the wave (C_2) using the compatibility relation along (C_2-A_2). This pressure is compared to the value calculated from the jump relations. If the difference in pressures exceeds a specified tolerance, a new shock wave location is computed using a new value of the cosine director β_c for the reference plane being calculated until convergence is achieved. This process is repeated in all reference planes. After convergence is obtained in all planes, improved crosswise directors α_c are computed using the converged shock locations and the procedure may be repeated until two subsequent values of α in a given reference plane agree to within a specified tolerance.

(2) Contact Surface: The numerical grid for the computation of a three dimensional contact surface is depicted in Figure (22). Let (1) and (2) denote conditions below and above the contact surface respectively. Properties are to be determined at the point C in the reference plane θ = constant. The contact surface cuts this reference plane along the line C-D, the local angle of the cut making an angle β with respect to the r direction.

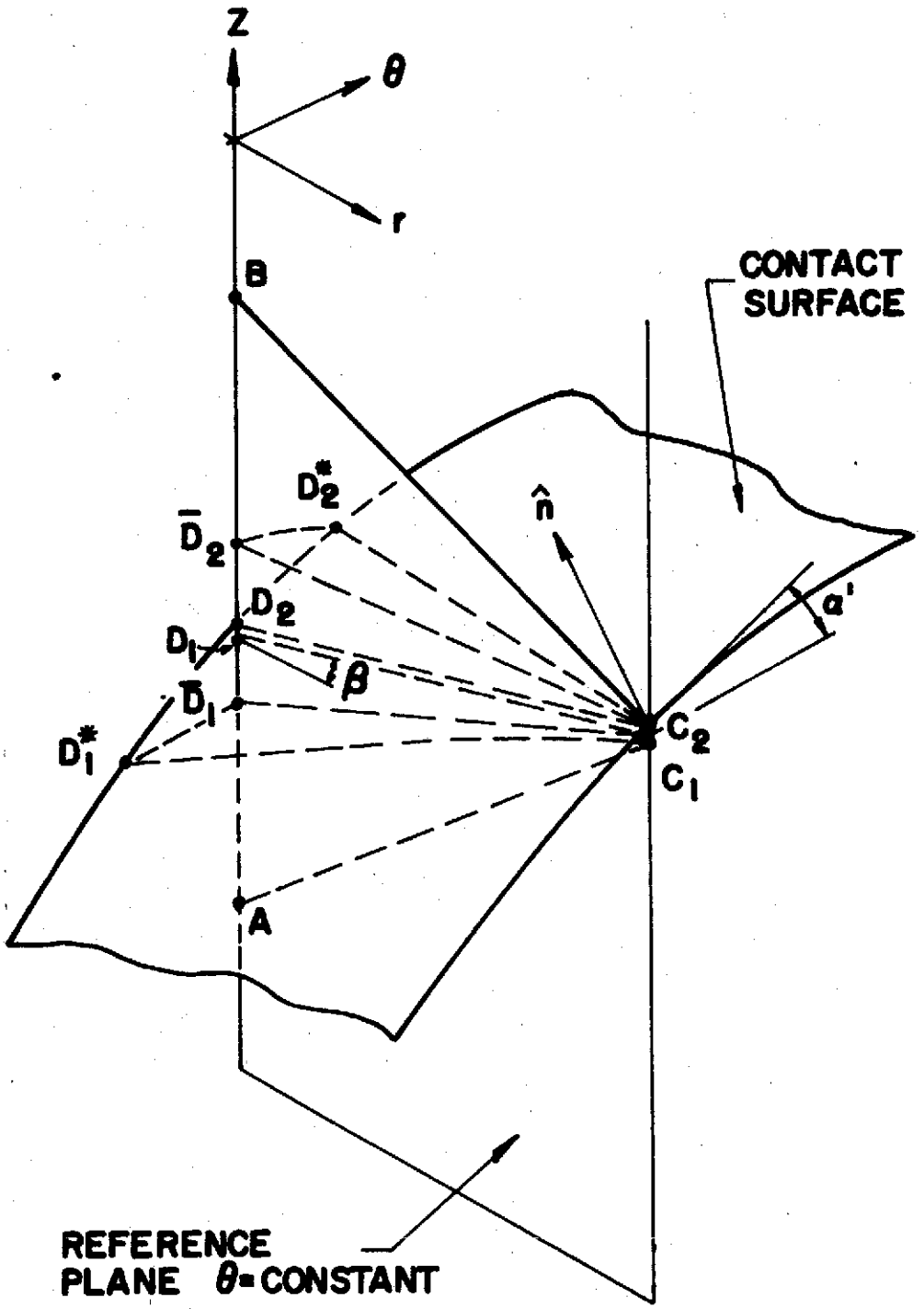

FIGURE 22. TYPICAL CONTACT SURFACE CALCULATION

The local geometry of the contact surface is identical to that of the shock surface as depicted in Figure (20).

There are two streamlines passing through the point C: $C_1D_1^*$ on the lower surface and $C_2D_2^*$ on the upper surface. These streamlines project onto the reference plane as $C_1\bar{D}_1$ and $C_2\bar{D}_2$ respectively.

The appropriate boundary conditions at point C are:

$$\bar{V}_{C_1} \cdot \hat{n} = 0 \tag{144}$$

$$\bar{V}_{C_2} \cdot \hat{n} = 0 \tag{145}$$

where

$$\hat{n} = - \cos \alpha \sin \beta \, \hat{i}_r - \sin \alpha \, \hat{i}_\theta + \cos \alpha \cos \beta \, \hat{i}_z \tag{146}$$

$$\tan \alpha = \tan \alpha' \cos \beta \tag{147}$$

and

$$P_{C_1} = P_{C_2} \tag{148}$$

The numerical solution proceeds as follows:

(a) In each reference plane θ=constant assume a value for β_c, for example $\beta_c = \beta_D$. The point C can then be located and values of α_c can be computed using the geometric location of the C points in all reference planes to compute α', and Equation (147) to determine α.

(b) A local iteration loop is required on either side of the contact to satisfy the following system of equations for the assumed value of β Equations (144) or (145) take the form

$$\sin (\beta - \phi_{c_{\frac{1}{2}}}) + \tan \alpha_c \tan \psi_{\frac{1}{2}} = 0 \qquad (149)$$

The compatibility relations along AC or BC take the form

$$\pm \rho q^2 (\phi_{c_{\frac{1}{2}}} - \phi_{\substack{A \\ B}}) + (P_{c_{\frac{1}{2}}} - P_{\substack{A \\ B}}) = \left|F \pm\right| \Delta r \qquad (150)$$

The Bernoulii relation (Equation 36) applied along $C_1D_1^*$ and $C_2D_2^*$ yields V_{c_1} and V_{c_2}.

The normal momentum equation applied along $C_1\bar{D}_1$ and $C_2\bar{D}_2$ yields v_{c_1} and v_{c_2}.

The cross flow angle ψ is obtained from the relation $\psi = \sin^{-1}(v/V)$ (151)

(c) The iteration proceeds as follows: A value of Beta (B_{c_2}) at C_2 is assumed and a pressure ($P_{c_1} = P_{c_2}$) is guessed. For this pressure and Beta, Equations (150), (151), and (36) yield all properties on either side of the contact. The boundary condition (149) on side 2 then is iterated until a consistent set of values B_{c_2}, ρ_{c_2}, ϕ_{c_2}, ψ_{c_2} and α are obtained.

The boundary condition (149) on side 1 then yields a value for B_{c_1} If this does not agree with B_{c_2} to within a specified tolerance a new value of pressure is guessed. From a linear error test a new value of Beta is obtained and the process repeated until Equations (144) through (149) are satisfied.

I. External Flow Interaction

As a result of the cowl length being considerably foreshortened a substantial amount of nozzle under-expansion can be expected. The resulting wave patterns can at certain flight conditions influence the pressure distribution on the vehicle undersurface and hence the thrust, lift and pitching moment. Figure (23) illustrates the nature of the waves produced in a typical reference plane. In some cases, as with end module configurations, significant sidewise under-expansion may also occur. The resulting waves are no longer quasi two dimensional but fully three dimensional in nature.

(1) Cowl Under-expansion Conditions At the cowl edge the flow phenomena in planes normal to the edge is locally two dimensional. Thus, in these planes the cowl under expansion shock and Prandtl-Meyer expansion can be computed from two dimensional considerations. It is assumed in these calculations that the chemistry is in equilibrium. Figure (24) depicts this locally oriented system. For a given cowl shape, data from the reference system may be transformed to the local coordinate plane. The calculations are performed in the local system and then transformed back to the original reference system.

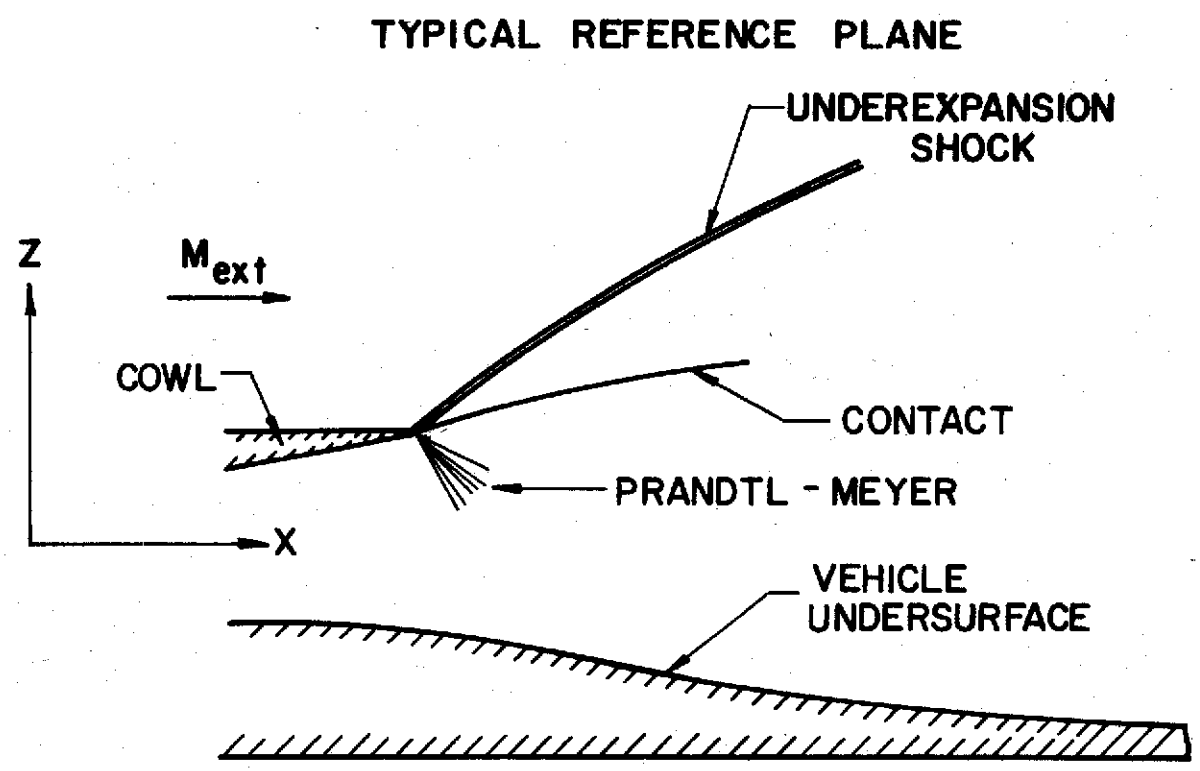

FIGURE 23. UNDER-EXPANSION INTERACTION

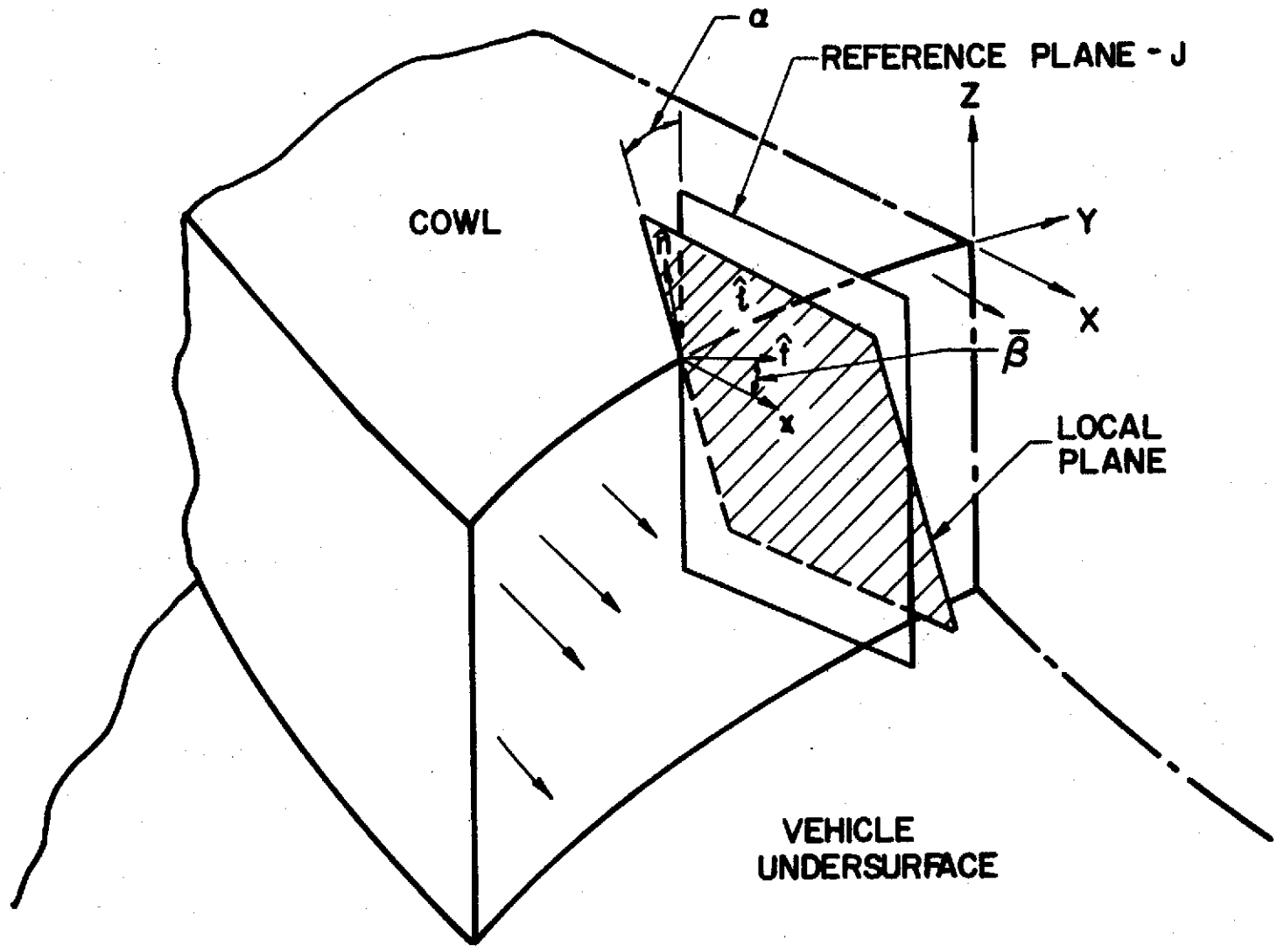

FIGURE 24. EXTERNAL FLOW INTERACTION LOCALLY ORIENTED SYSTEM

In Figure (25) let $\hat{\ell}$ be defined as the local unit tangent vector to the cowl edge. Then for a Cartesian (x,y,z) or cylindrical reference system (x,θ,r):

$$\hat{\ell} = \cos\alpha\ \hat{i}_{y,\theta} + \sin\alpha\ \hat{i}_{z,r} \tag{152a}$$

$$\hat{n} = \sin\bar{\beta}\ \hat{i}_{x} - \cos\bar{\beta}\ \sin\alpha\ \hat{i}_{y,\theta} + \cos\bar{\beta}\ \cos\alpha\ \hat{i}_{z,r} \tag{152b}$$

$$\hat{t} = \cos\bar{\beta}\ \hat{i}_{x} - \sin\bar{\beta}\ \sin\alpha\ \hat{i}_{y,\theta} + \sin\bar{\beta}\ \cos\alpha\ \hat{i}_{z,r} \tag{152c}$$

where $\hat{n}$ is the unit normal to the wave and $\hat{t}$ is the second tangent to the wave surface. Now:

$$\alpha|_{x} = \text{Arctan}\left(\frac{dz}{dy} \text{ or } \frac{1}{r}\frac{dr}{d\theta}\right) \tag{153a}$$

$$\beta|_{y,\theta} = \text{Arctan}\left(\frac{dz}{dx} \text{ or } \frac{dr}{dx}\right) \tag{153b}$$

and

$$\tan\bar{\beta} = \cos\alpha\ \tan\beta \tag{154}$$

The total velocity is defined as

$$\vec{V} = q(\cos\phi\hat{i}_{x} + \tan\psi\hat{i}_{y,\theta} + \sin\phi\hat{i}_{z,r}) = \tilde{u}\ \hat{n} + \tilde{v}\ \hat{\ell} + \tilde{w}\ \hat{t}. \tag{155}$$

Then:

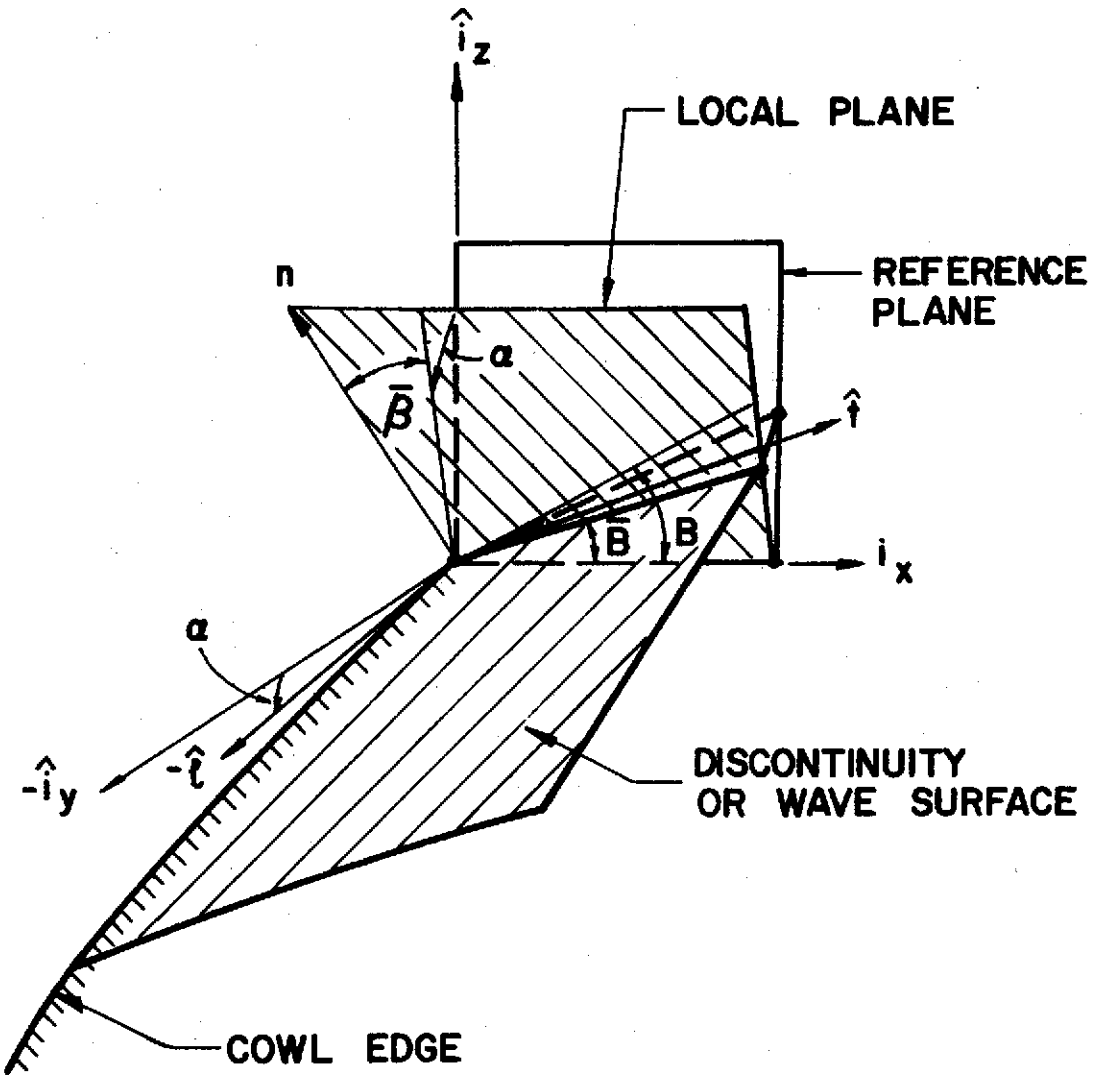

FIGURE 25. EXTERNAL FLOW INTERACTION-LOCAL AND REFERENCE PLANE ORIENTATION

$$\tilde{u} = - q(-\sin\bar{\beta}\cos\phi - \cos\bar{\beta}\sin\alpha\tan\psi + \cos\bar{\beta}\cos\alpha\sin\phi) \quad (156a)$$

$$\tilde{v} = q(\tan\psi\cos\alpha + \sin\phi\sin\alpha) \quad (156b)$$

$$\tilde{w} = q(\cos\bar{\beta}\cos\phi - \sin\bar{\beta}\sin\alpha\tan\psi + \sin\bar{\beta}\sin\phi\cos\alpha) \quad (156c)$$

For locally two dimensional flow $\tilde{v}$ = constant. Then for the expansion region the equations to be solved are:

$$\frac{dp}{\rho} + \frac{1}{2}\bar{q}^2 = 0 \quad (157a)$$

$$\frac{dp}{p} = \Gamma\frac{d\rho}{\rho} \quad (157b)$$

$$\frac{d\tilde{w}}{d\bar{\beta}} = - \tilde{u} \quad (157c)$$

$$h + \frac{\bar{q}^2}{2} = \text{constant} \quad (157d)$$

where: $\tilde{u}^2 = (\bar{q}^2 - \tilde{w}^2) = (\Gamma\frac{p}{\rho})$, $\bar{q}^2 = V^2 - \tilde{v}^2$ and Γ is the equilibrium isentropic exponent.

For small steps Δp in pressure the solution for Γ constant over the integration step

$$\bar{\beta}_2 = - \sqrt{\frac{\Gamma+1}{\Gamma-1}}(k_2 - k_1) + \bar{\beta}_1 \quad (158)$$

where

$$k = \text{Arctan}\left(\frac{\tilde{w}/c}{\sqrt{1-(\tilde{w}/c)^2}}\right)$$

and

$$c^2 = \frac{\Gamma+1}{\Gamma-1}\tilde{u}_1^2 + \tilde{w}^2$$

Thus the expansion region may be solved in a step by step manner using the above solution. The numerical iteration scheme is as follows.

Assume a shock strength Beta(β). Using the local Hugoniot solution previously described compute all flow properties downstream of the shock using the cowl external data. From the pressure downstream of the shock and the cowl internal data compute the Prandtl-Meyer turn using the solution described above. If the deflection angles from the shock and Prandtl-Meyer turns do not agree to within a specified tolerance a new shock strength is assumed and the process repeated.

After the above solution is obtained the local properties are transformed back to the original reference systems. That is:

$$q\cos\phi = u = \tilde{u}\sin\bar{\beta} + \tilde{w}\cos\bar{\beta} \qquad (159a)$$

$$q\tan\psi = v = \tilde{u}\cos\bar{\beta}\sin\alpha - \tilde{v}\cos\alpha - \tilde{w}\sin\bar{\beta}\sin\alpha \quad (159b)$$

$$q\sin\phi = w = \tilde{u}\cos\bar{\beta}\cos\alpha + \tilde{v}\sin\alpha + \tilde{w}\sin\bar{\beta}\cos\alpha \quad (159c)$$

$$q^2 = u^2+w^2 \quad (159d)$$

$$\tan\beta = \tan\bar{\beta}/\cos\alpha \quad (159e)$$

(2) External Corner-End Module As long as the cross flow in the vicinity of the external corner region remains continuous a local r,θ system can be used to represent the angular property variation at a given marching step Figures (26a) and (26b) depict the geometry of the reference system for an end module configuration.

For any property the crosswise solution may be represented as a polynomial

$$f = a + bs + \cdots + s^n$$

and (160)

$$r = cn(\theta) + g(\theta)$$

where "s" is a distance along a constant n surface. Since only the existence of the first derivative is required f and r may be approximated by

$$f = a + bs$$

and (161)

$$r = c(n_0 + n_1\theta) + g(\theta)$$

In region I we define (see Figure 26c)

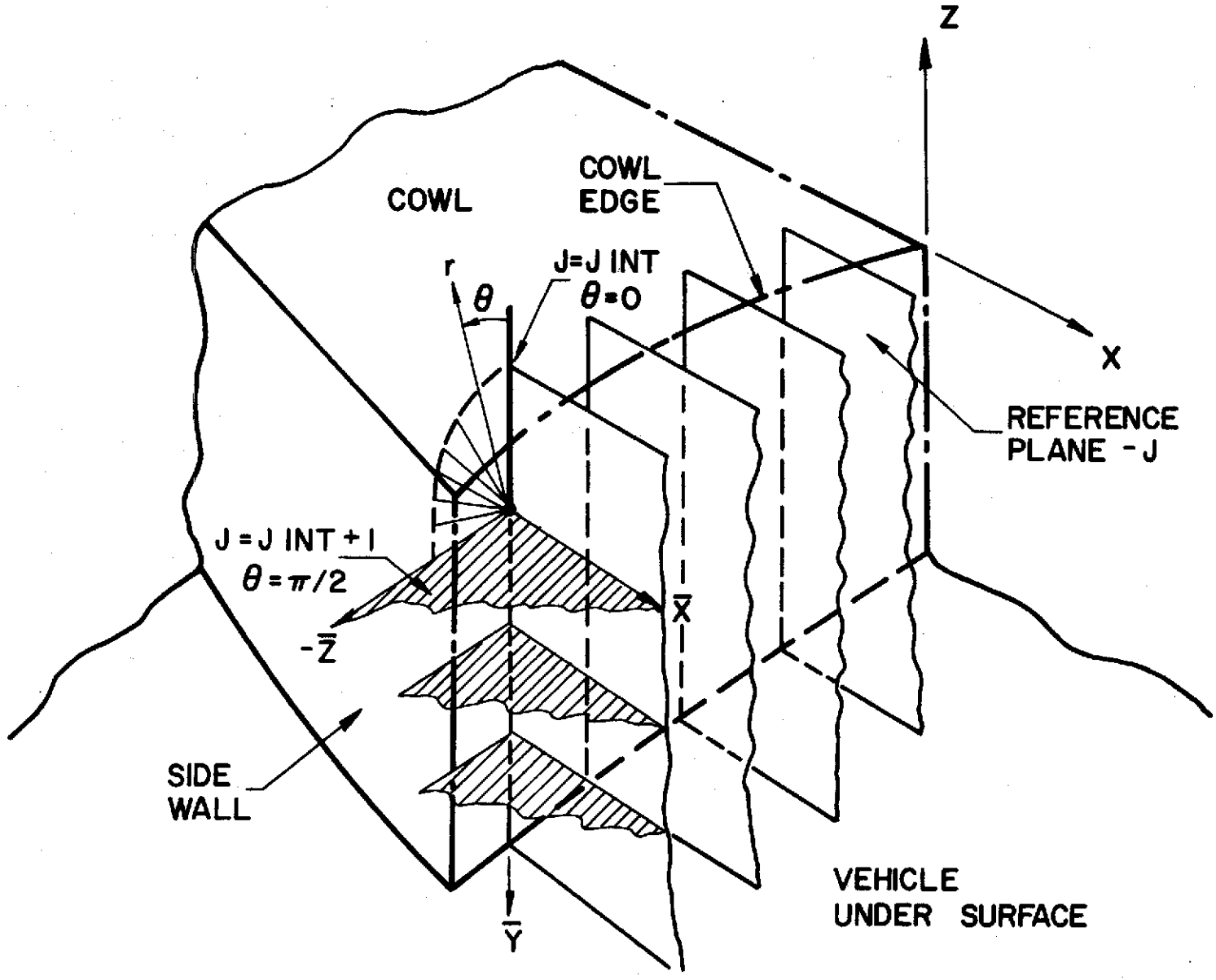

FIGURE 26a. EXTERNAL CORNER

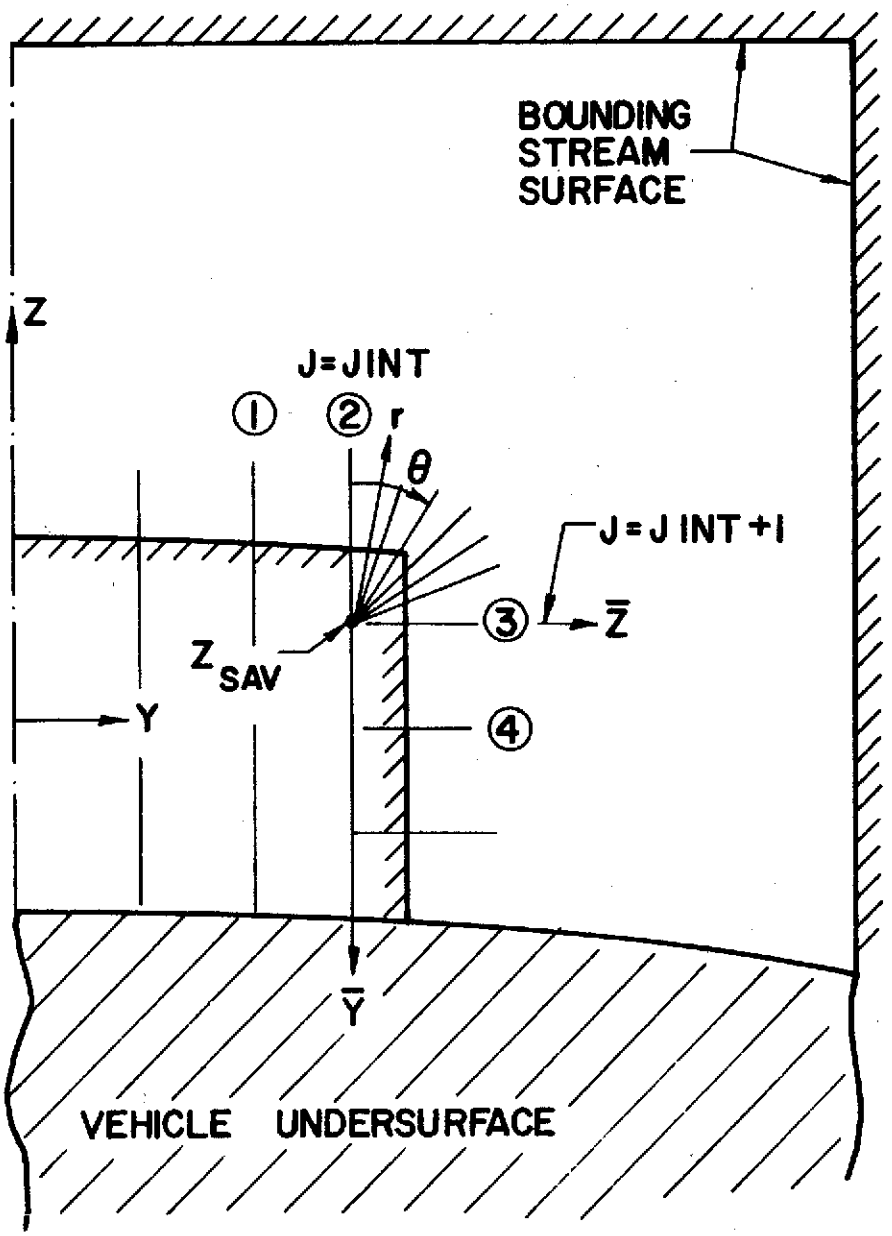

FIGURE 26b. EXTERNAL CORNER

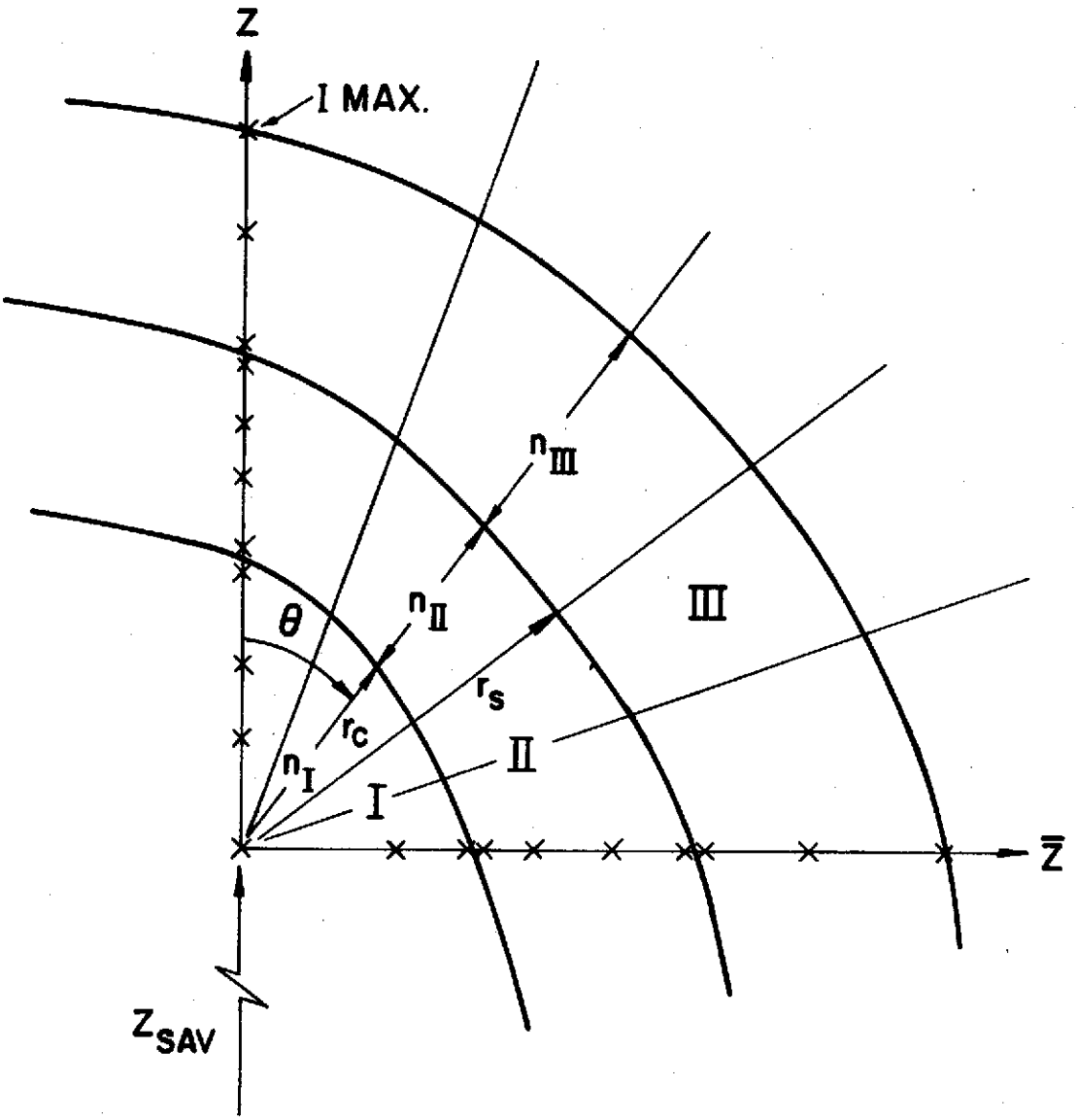

FIGURE 26c. EXTERNAL FLOW

$$n_I = (z_{contact} - z_{sav}) \qquad (162a)$$

$$g(\theta) = 0$$

For region II we define

$$n_{II} = (z_{contact} - z_{shock}) \qquad (162b)$$

$$g(\theta) = r_{contact}$$

and for region III we define

$$n_{III} = (z_{max} - z_{shock}) \qquad (162c)$$

$$g(\theta) = r_{shock}$$

The above technique allows the external corner region to be scaled in a manner consistent with the growth of the shock and contact surfaces, and analytically represented at each marching step.

J. Swept Throat

Due to vehicle aerodynamic and combustor design considerations it may be advantageous to introduce sweepback into the flow field upstream of the nozzle throat. The program described in this report is capable of accepting initial data along a swept initial surface. The following limitations apply to the sweepback option.

(1) The flow normal to the sweepback is supersonic.

(2) The sweepback is linear; that is, the crosswise location (y or θ) of the sweepback line on the upper or lower surfaces is a linear function of the marching distance.

(3) The sweepback lines lie on cylindrical or Cartesian surfaces.

(4) The sweep of the upper and lower surfaces is identical.

Figure (27) illustrates the geometry associated with a typical swept throat as defined in this program.

The numerical procedure is as follows: all data along the initial swept surface is stored in locations J = 1, 3, 4, ----. Initially calculations are carried out only in the J=1 plane with the necessary data for derivatives being interpolated between the first and second (stored as third) plane on the initial surface. This procedure is carried out until the marching step has reached the second reference plane. The marching continues with both the first and second planes being calculated. the data necessary for calculating derivatives on the second plane are interpolated between the second and third (stored as fourth) planes. Thus as the marching proceeds each subsequent reference plane is added to the calculation at the proper location. This continues until the swept region has been completed, whereupon the calculation automatically reverts to a normal marching procedure.

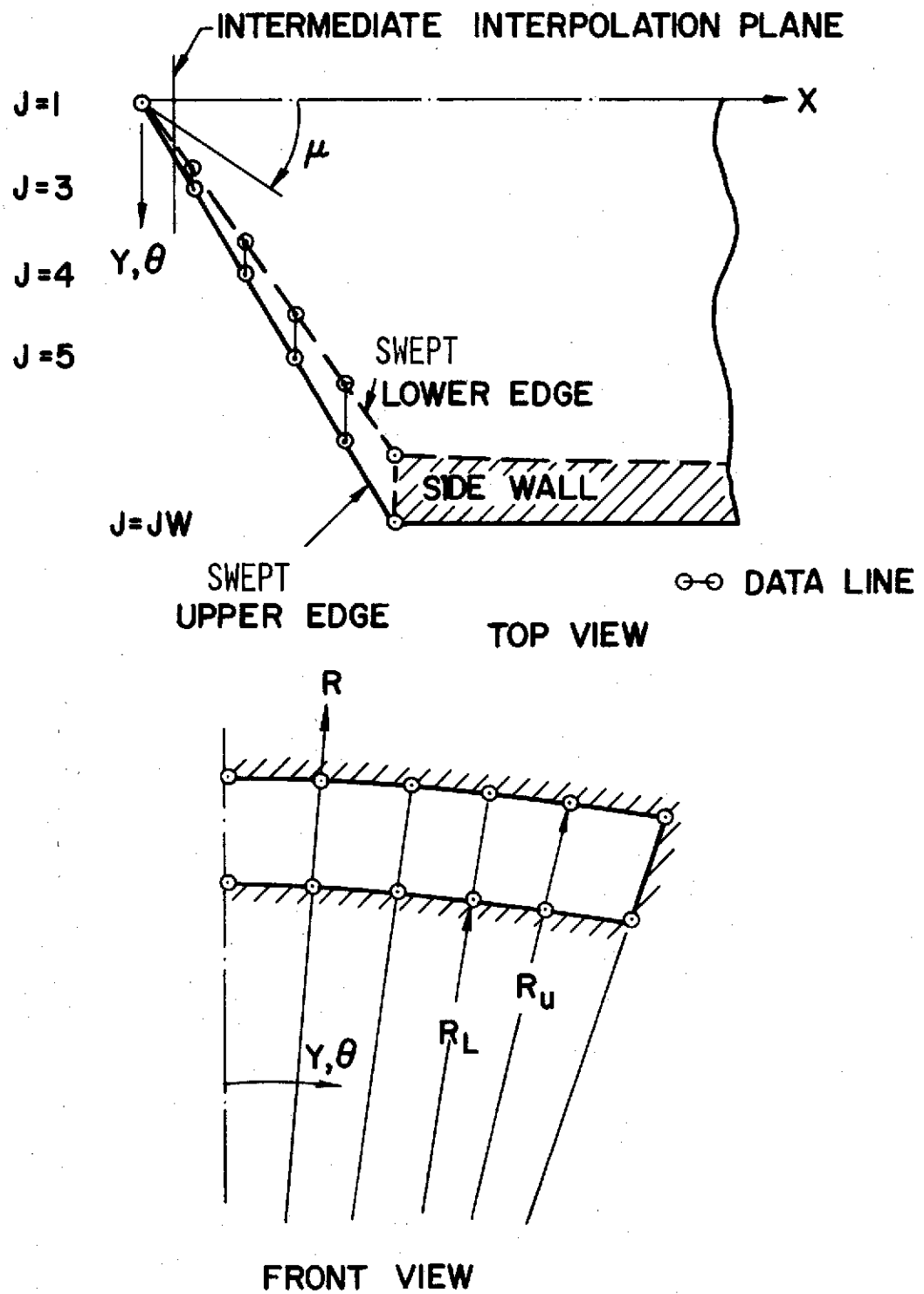

FIGURE 27. SWEPT THROAT

K. Discontinuities at Sidewalls

Implicit in the use of the reference plane technique is the assumption of a continuous crosswise flow; thus discontinuities formed at sidewalls or by large cross flow gradients cannot be analyzed. Only discontinuities which primarily propagate in the reference planes are considered. Consistent with this assumption no reflections of discontinuities at sidewalls are permitted. This is expressed geometrically as $\hat{n}_s \cdot \hat{n}_w = 0$. Where $\hat{n}_s$ is the normal to the discontinuity and $\hat{n}_w$ is the normal to the sidewall. Figure (28) illustrates the geometry of the sidewall and discontinuity intersection.

Assume that the discontinuity may be described by an equation of the form

$$z = f(x,y) \tag{163a}$$

$$\hat{n}_s = \hat{i}_z - f_x \hat{i}_x - f_y \hat{i}_y \tag{163b}$$

and the sidewall by an equation of the form

$$y = g(x,z) \tag{164a}$$

$$\hat{n}_w = \hat{i}_y - g_x \hat{i}_x - g_z \hat{i}_z \tag{164b}$$

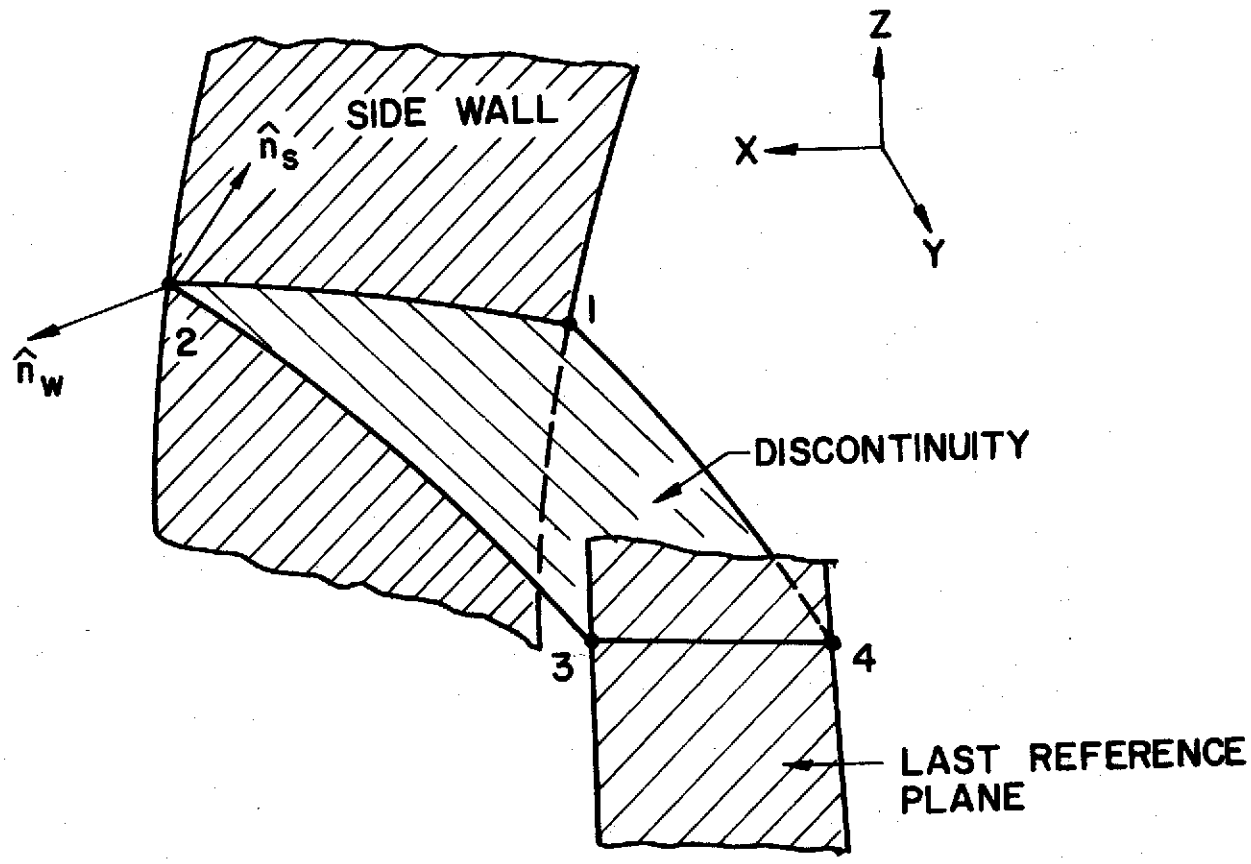

FIGURE 28. DISCONTINUITY AT SIDEWALL

Then $\hat{n}_s \cdot \hat{n}_w = 0$ yields

$$f_x g_x - f_y - g_z = 0 \tag{165}$$

From Figure (28) along (1-2) we may write

$$z_2 = z_1 + \frac{f_{x_1}+f_{x_2}}{2} \cdot (x_2-x_1) + \frac{f_{y_1}+f_{y_2}}{2} \cdot (y_2-y_1) \tag{166}$$

and along (3-2) we may write

$$z_2 = z_3 + \frac{f_{y_3}+f_{y_2}}{2} \cdot (y_2-y_3) \tag{167}$$

Equations (164a), (165), (166) and (167) are four equations in four unknowns y_2, z_2, f_{x_2}, f_{y_2}.

The numerical solution proceeds as follows:

(1) Assume z_2.

(2) Using Equation (164a) compute y_2, g_{x_2} and g_{z_2}.

(3) From Equation (167) compute f_{y_2} and from Equation (166) compute f_{x_2}.

(4) Equation (165) is checked for consistency.

If Equation (165) is not satisfied to within a given tolerance then a new value of z_2 is guessed and the process repeated until convergence is achieved.

L. Thrust, Lift, Pitching Moment

The following definitions are used in this report for thrust, lift, pitching moment

$$T = \iint_A (p-p_\infty)\, \hat{i}_x \cdot d\vec{A}_n \tag{168}$$

$$L = \iint_A (p-p_\infty)\, \hat{i}_z \cdot d\vec{A}_n \tag{169}$$

$$M_y = -\iint_A (p-p_\infty)\, \hat{i}_z \cdot x\, d\vec{A}_n + \iint_A (p-p_\infty)\, \hat{i}_x \cdot z\, d\vec{A}_n \tag{170}$$

Figure (29) gives the orientation of the vectors with respect to the vehicle. Internally the integrals range over all the vehicle surface areas. Externally they range over the complete vehicle undersurface as defined by the bounding stream surface. For external flow with wraparound, values of these parameters are computed upto the contact surface and shock surface, in addition to the values at the bounding stream surface.

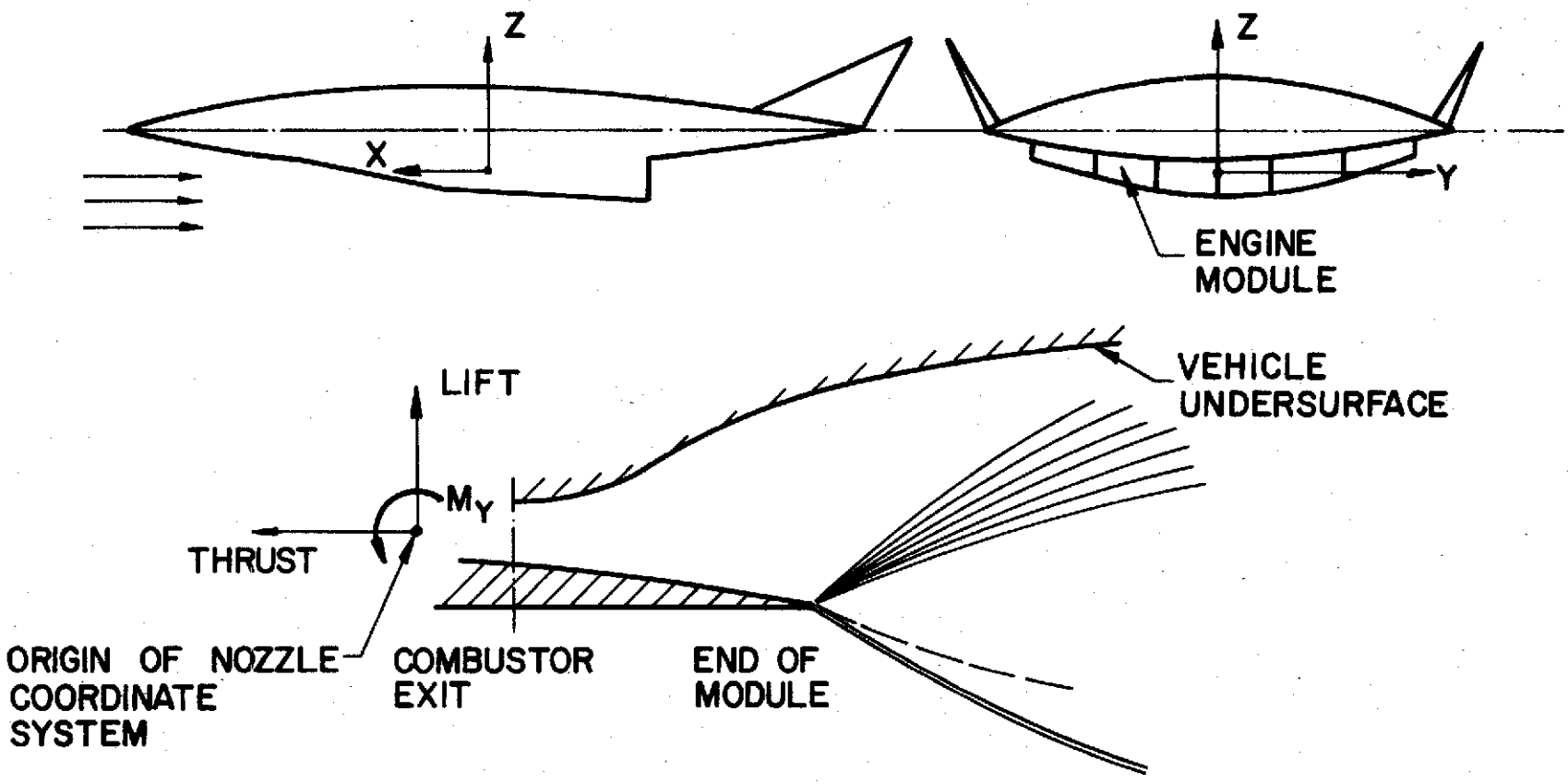

FIGURE 29. THRUST, LIFT, MOMENT

Based on throat data the program computes at the throat station values for the stream thrust in both the z and x directions. These quantities are defined as

$$T_{sx} = \iint_A \vec{V}\cdot\hat{i}_x \, (\rho\vec{V}\cdot\hat{n}) \, d\vec{A}_n + \iint_A (p-p_\infty) \, \hat{i}_x \cdot d\vec{A}_n \qquad (171)$$

$$T_{sz} = \iint_A \vec{V}\cdot i_z \, (\rho V\cdot\hat{n}) \, d\vec{A}_n + \iint_A (p-p_\infty) \, \hat{i}_z \cdot d\vec{A}_n \qquad (172)$$

M. Integral Correction Factors

Numerical solutions of the differential equations of motion generate errors associated with machine round-off procedures and truncation errors corresponding to the numerical algorithm employed. These errors result in global conservation of mass and energy not being satisfied exactly. The subject computer program can as a user option limit the propagation of these errors by providing at arbitrary calculation steps integral corrections for mass flow and energy. These correction procedures are described below.

Conservation of mass and total energy require that

$$M = \iint_A (\rho\vec{V}\cdot\hat{n}) \, d\vec{A}_n = \text{constant} \qquad (173)$$

$$H = \iint_A (h + \frac{1}{2} V^2) (\rho \vec{V} \cdot \hat{n}) \, d\vec{A}_n = \text{constant} \tag{174}$$

Referring to Figure (30) the integrals may be represented by the summations

$$M = \sum_{i,j} \overline{\rho u} \, \Delta A_x \tag{175}$$

and

$$H = \sum_{i,j} \overline{(h + \frac{1}{2} V^2) (\rho u)} \, \Delta A_x \tag{176}$$

where the barred quantities refer to averages over a numerical mesh. The average of any property f over a mesh interval can be defined as

$$\bar{f} = \frac{\int f \, ds}{\int ds}$$

where s is the line distance surrounding an elemental area dA.

The integral correction factors for mass and energy can be defined by noting that

$$\begin{aligned} \iint (\rho \vec{V} \cdot \hat{n}) \, d\vec{A}_n &= M + \varepsilon_1 \\ C_1 \iint (h + \frac{1}{2} V^2) (\rho \vec{V} \cdot \hat{n}) \, d\vec{A}_n &= H + \varepsilon_2 \end{aligned} \tag{177}$$

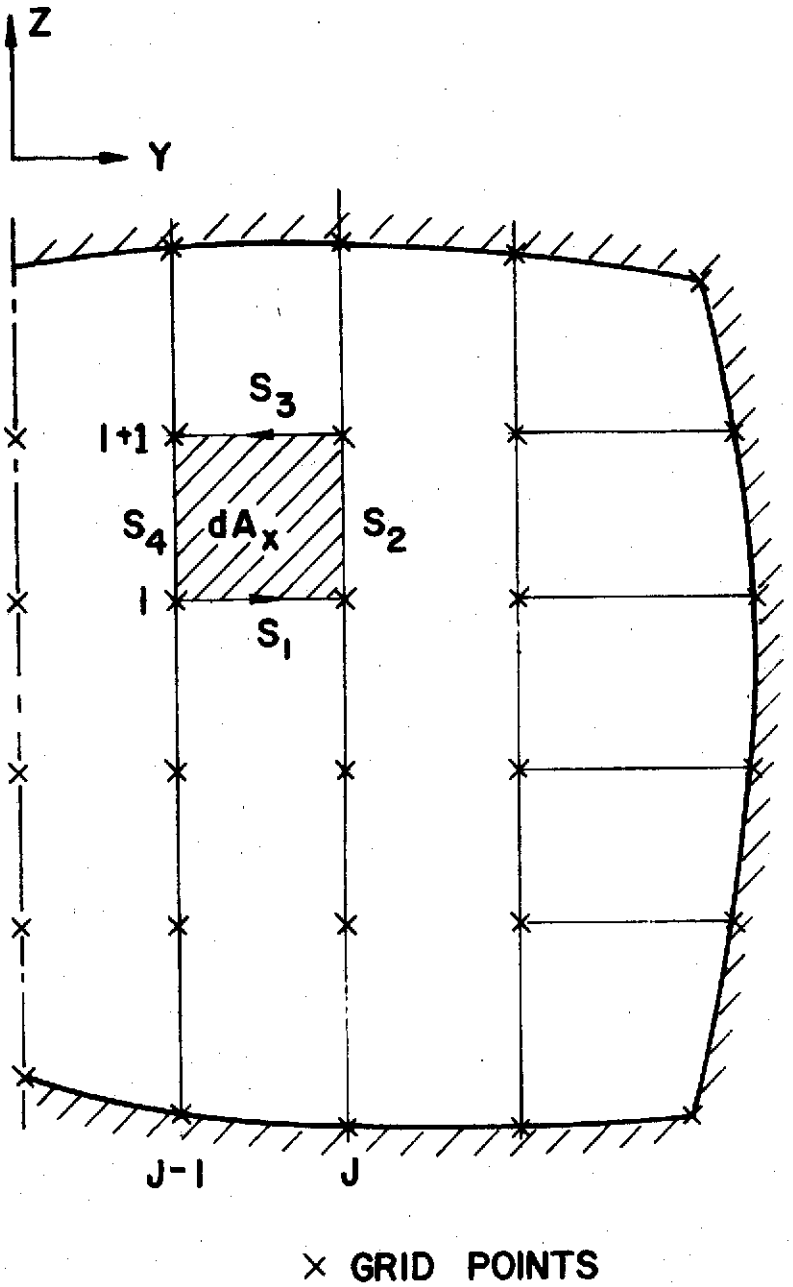

FIGURE 30. ELEMENTAL AREA ASSOCIATED WITH GRID SIZE

where ε_1 and ε_2 are errors in mass and energy. Then

$$C_1 = \frac{M}{M+\varepsilon_1}, \qquad C_2 = \frac{M}{M+\varepsilon_2} \tag{178}$$

With C_1 and C_2 defined the following system of equations are solved for the corrected properties

$$p^*/\rho^{*\Gamma} = \text{constant} \tag{179a}$$

$$p^*/\rho^* = RT^* \tag{179b}$$

$$h^* = h(p^*, \Phi, T^*) \tag{179c}$$

$$\rho^* V^* = C_1 \rho V \tag{179d}$$

$$(h + \tfrac{1}{2} V^2)^* = C_2 (h + \tfrac{1}{2} V^2) \tag{179e}$$

Thus, properties of each point in the flow field are corrected uniformly for the integral correction factors for mass (C_1) and energy (C_2).

N. Second Order Procedures

The numerical methods and analytic techniques presented in the previous sections were for the purposes of clarity and simplicity assumed to be first order in mesh size(Δx, Δy). However, the program is capable of second order computational accuracy with respect to both local and global calculations. Local refers to the computation of a single mesh point in a given reference plane using a fixed value of the cross derivative. Global refers to the computation of all the mesh points in the flow field with updated values for the cross derivatives.

1. Interior Point Calculations

Local Iterations - The basis for establishing a local second order numerical characteristic type calculation is well known (see Reference 2) and will briefly be described below.

Referring to Figure (12a) a typical interior point calculation for the line source system is performed as follows. The point C is located by projecting the quasi-streamline a distance Δr downstream. That is, in difference form Equation (22) is

$$z_C = z_D + (\tilde{\alpha} \tan \phi_D + \tilde{\beta} \tan \phi_C) \Delta r \qquad (180)$$

where $\tilde{\alpha}$ and $\tilde{\beta}$ are the local averaging coefficients with values ($\tilde{\alpha} = 1$, $\tilde{\beta} = 0$) or ($\tilde{\alpha} = \frac{1}{2}$, $\tilde{\beta} = \frac{1}{2}$). The initial computation (first order) is made with $\tilde{\alpha} = 1, \tilde{\beta} = 0$. Points A and B are located by shooting back, characteristic

projections from point C, and locating these between points I-1,I and I+1,I respectively, by an iteration procedure. Using Equation (21) in difference form:

$$z_{A,B} = z_C - (\tilde{\alpha}\, \lambda^{\pm}_{\substack{A \\ B}} + \tilde{\beta}\, \lambda^{\pm}_C)\, \Delta r. \tag{181}$$

All required properties can be obtained at A and B including cross derivatives by a linear interpolation procedure.

The pressure p_C and flow deflection angle ϕ_C in the reference plane can be determined by solving the compatibility relations along AC and BC.

$$(\tilde{\alpha}\, (\rho q^2)_A + \tilde{\beta}\, (\rho q^2)_C)\, (\phi_C - \phi_A) + (\tilde{\alpha}\, \beta_A + \tilde{\beta} \beta_C)\, (p_C - p_A) = F^+_A\, \Delta r \tag{182a}$$

$$(\tilde{\alpha}\, (\rho q^2)_B + \tilde{\beta}\, (\rho q^2)_C)\, (\phi_C - \phi_B) - (\tilde{\alpha}\, \beta_B + \tilde{\beta}\, B_C)\, (p_C - p_B) = F^-_B\, \Delta r \tag{182b}$$

where for a purely local iteration $F^{\pm}_{\substack{A \\ B}}$ are evaluated on the initial value surface. The cross velocity v_C may be obtained from Equation (59):

$$v_C = v_D - \left[\left(\frac{\tilde{\alpha}}{r \cos \phi}\right) + \left(\frac{\tilde{\beta}}{r \cos \phi}\right) \right] F^{(s)}\, \Delta r \tag{183}$$

where $F^{(s)}$ is evaluated only on the initial plane for a purely local itera-

tion. Properties at $\bar{D}^*$ may be obtained from the relation

$$f_{\bar{D}^*} = f_D - \left(\frac{f_{\theta_D} + f_{\theta_{\bar{D}^*}}}{2}\right) \Delta\theta \tag{184a}$$

which from geometry becomes

$$f_{\bar{D}^*} = f_D - \left[\left(f_\theta \frac{\tan\psi}{r\cos\phi}\right)_D + \left(f_\theta \frac{\tan\psi}{r\cos\phi}\right)_{\bar{D}^*}\right] \frac{\Delta r}{2} \tag{184b}$$

The pressure density relation (13) may be integrated along $\bar{D}^*C$ holding Γ constant for a small integration step, yielding as in Equation (62)

$$\rho_C = \rho_{\bar{D}^*} \left(\frac{p_C}{p_{\bar{D}^*}}\right)^{1/\Gamma_{\bar{D}^*}}$$

The Bernoulli relation, Eqution (64), then yields the total velocity v_C. Conservation of total enthalpy, Equation (65), yields h_C and for inviscid flows from Equation (66)

$$\Phi_C = \Phi_{\bar{D}^*}$$

The isentropic exponent Γ_C may be obtained from a polynomial curve fit

$$\Gamma_C = \Gamma\,(h_C, p_C, \Phi_C)$$

and the sound speed from Equation (68)

$$a_C = \left[\frac{\Gamma_C\, p_C}{\rho_C}\right]^{\frac{1}{2}}$$

For a purely first order calculation ($\tilde{\alpha} = 1$, $\tilde{\beta} = 0$) the computation would now be complete. However, for a local second order calculation, the above process would be repeated with ($\tilde{\alpha} = \frac{1}{2}$, $\tilde{\beta} = \frac{1}{2}$) until the newly calculated pressure $p^{(\nu)}$, converged to the previously calculated pressure $p^{(\nu-1)}$ to within a given tolerance. Note that in a purely local iteration $F^{\pm}$, $F^{(s)}$ are held constant at their initial values.

Global Iteration - After completing all calculations if overall second order accuracy is required the above process is repeated with updated values of the cross derivative functions. That is we may write:

$$F^{\pm}_{\substack{AC \\ BC}} = a \cdot F^{\pm}_{\substack{A \\ B}} + b \cdot F^{\pm}_{C} \tag{185}$$

$$F^{(s)}_{DC} = a \cdot F^{(s)}_{D} + b \cdot F^{(s)}_{C} \tag{186}$$

where a and b are the global averaging coefficients with values, a = 1, b = 0, for a first order global and, a = ½, b = ½, for a second order global calculation. The cross derivative functions $F^{\pm}_{C}$, $F^{(s)}_{C}$ are evaluated on the new data surface ($r_1 + \Delta r$) using the converged properties previously computed from local iterations. These functions are held constant while new local iterations are performed with $\tilde{\alpha} = \frac{1}{2}$, $\tilde{\beta} = \frac{1}{2}$. This process requires storing the cross derivatives at the new data surface in addition to the flow field properties.

The program thus provides the user with a choice of computational accuracy which can be tailored to the complexity of the flow field. That is, in some instances it may not be necessary to go beyond the local iteration procedure with consequent savings in computational time. Thus, computational accuracy from first order to fully second order may be chosen at the users discretion.

2. Boundary Point Calculations

All wall boundary calculations are formally identically to those described in the earlier sections of this report. Second order procedures are applied to characteristic coefficients and cross derivative functions, as described above for an interior point calculation. The local iterate is the pressure $p^{(\nu)}$.

A fully second order (global) shock and contact discontinuity calculation requires updating of both the cross derivative functions and the discontinuity surface cross anglesupon completion of all the local calculations. All local discontinuity computations remain formally identical to those described earlier in this report. However, the characteristic relations are modified as described above for locally a second order interior point calculation. For shock wave and contact calculations the local iterate is the surface discontinuity angle, Beta, in the reference plane. That is locally converged properties are obtained when $\text{Beta}^{(\nu)}$ and $\text{Beta}^{(\nu-1)}$ agree to within a specified tolerance.

O. Embedded Shock Waves

The presence of compression waves in a supersonic flow field may, depending on the numerical scheme employed, lead to computational problems if these waves are not treated as finite discontinuities. The Hartree type grid employed in the numerical scheme does not follow characteristics. This property of the scheme renders it relatively insensitive to numerical difficulties if moderately weak compressions are encountered.

In each reference plane a two dimensional type of procedure is employed to detect characteristic crossings. In each plane (J) using the initial data at points (I) and (I+1) the following equations are solved for a downstream crossing (if any) of waves of the same family (see Figure 31a).

$$z_c = z_a + \tan(\phi \pm \mu)_a \, (x_c - x_a)$$

$$z_c = z_b + \tan(\phi \pm \mu)_b \, (x_c - x_d)$$

The minimum downstream location of these crossings is determined and stored for later use. This procedure is repeated in each reference plane and an overall minimum crossing (i.e., strongest wave) is determined. The initial data associated with this crossing will determine whether a strong compression wave is present at this point. Figure (31b) indicates the isentropic two

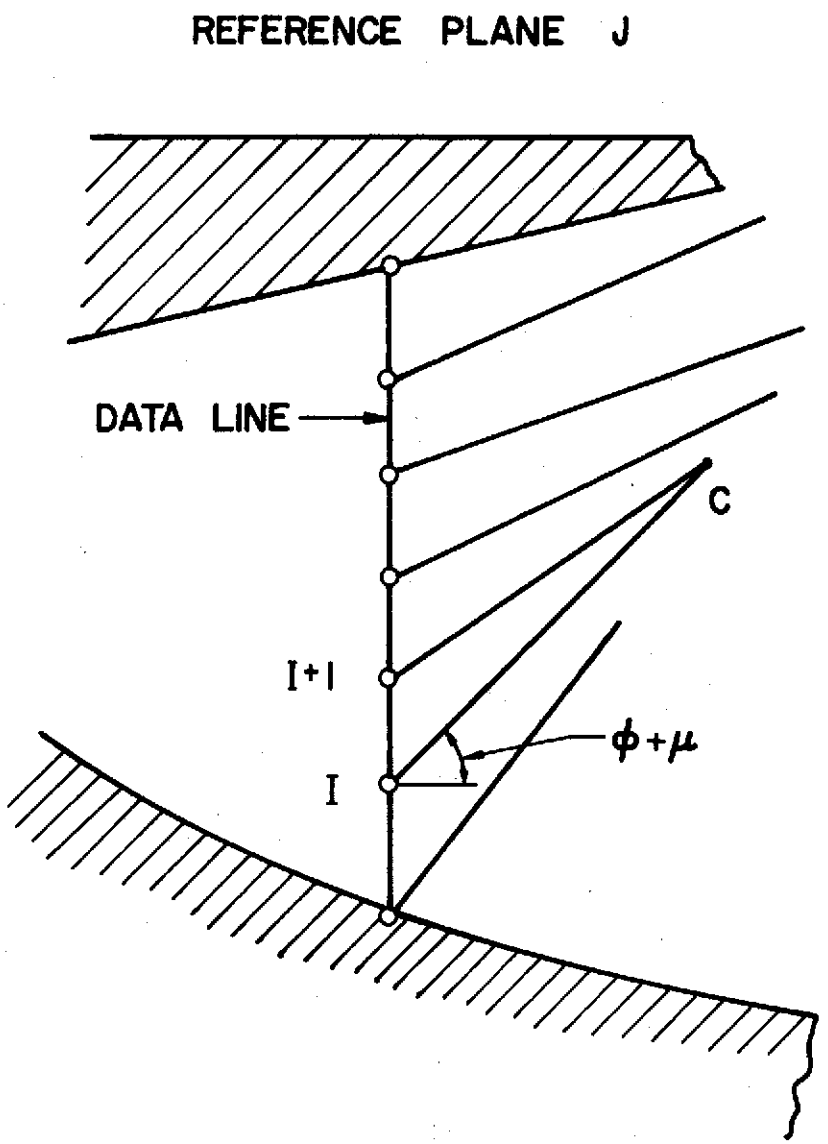

FIGURE 31a. CROSSING OF CHARACTERISTICS

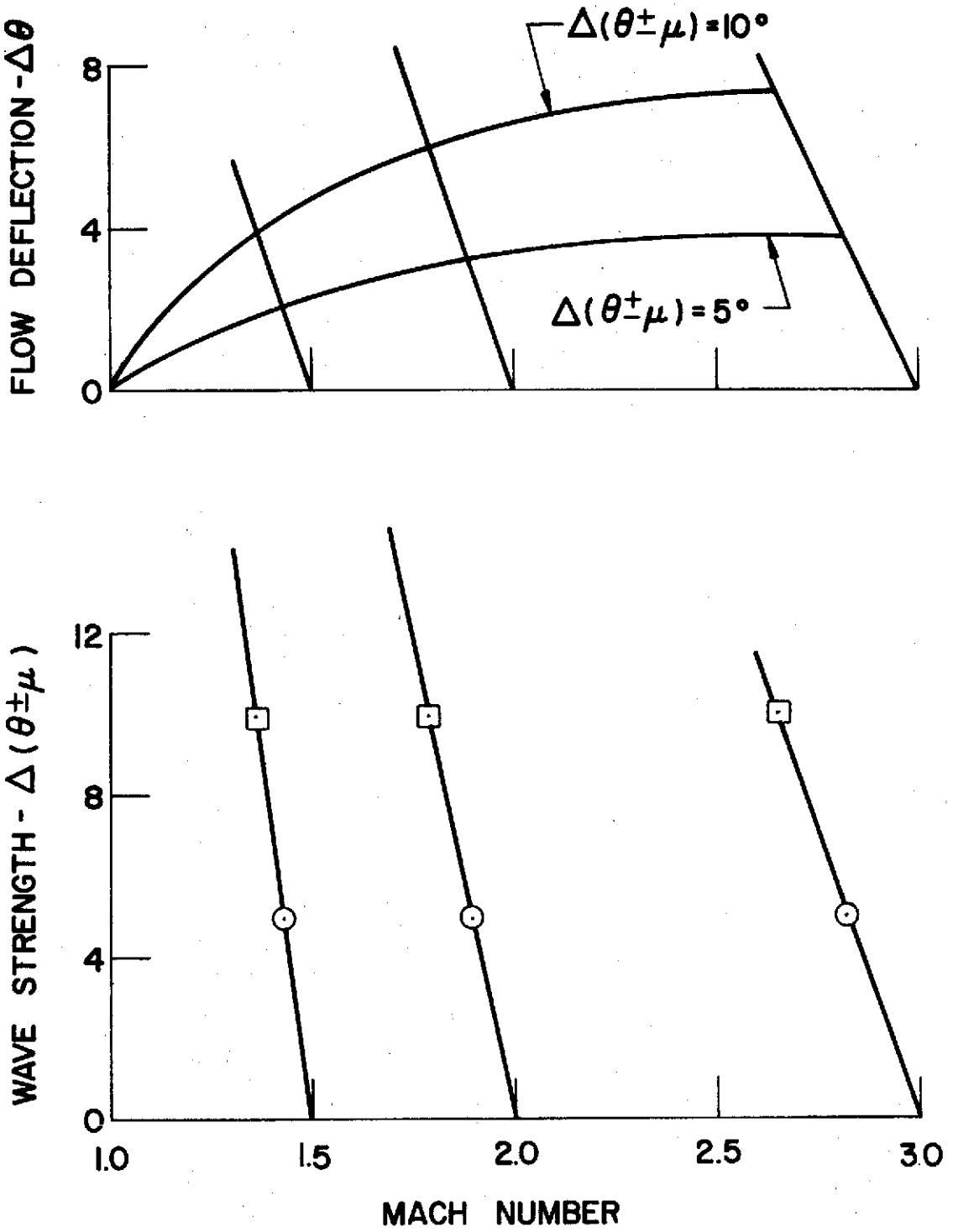

FIGURE 31b. TWO DIMENSIONAL WAVE STRENGTH

dimensional flow deflections associated with waves, $\Delta(\phi \pm \mu)$, propagating at various Mach numbers.

A test is now made of the strength of the strongest wave detected with respect to a specified tolerance. If the wave strength, $\Delta(\phi \pm \mu)$ exceeds this tolerance a shock wave strength is assumed to be of the average $(\phi \pm \mu)_I$ and $(\phi \pm \mu)_{I+1}$. That is, $\beta_{shock} = ((\phi \pm \mu)_I + (\phi \pm \mu)_{I+1})/2$ between points (I) and (I+1). It should be noted that both grid spacing and wave strength tolerance determine the location of the shock formation. Once detected the program does not carry the shock wave as part of the internal calculation but does specify its location.

P. Simulator Fluids

The computer program described in this report contains provisions for the use of two gases other than equilibrium mixtures of Hydrogen-Air. As discussed in Volume IV of this report CH_4 (Methane) and C_2H_4 (Ethylene) can be used in cold flow exhaust nozzle tests to accurately simulate various equilibrium Hydrogen-Air thermodynamic and nozzle flow parameters. Curve fits of the thermodynamic properties of CH_4 and C_2H_4 have been taken from data given in Reference (2) of Volume IV.

The computer program will accept CH_4 or C_2H_4 as the nozzle simulation fluid by simply specifying hypothetical fuel-air equivalence

ratios $\Phi = -1$ (CH_4) or $\Phi = -2$ (C_2H_4) for the internal flow. For the external medium $\Phi = 0$ specifies air inequilibrium. All subsequent logical and numerical operations of the program remain unchanged.

IV. SAMPLE CALCULATIONS

In order to demonstrate the program's capabilities, three sample calculations have been performed.

For Case I, the flow field in a Vehicle I central module was computed. For the internal portion of the flow field, a line source reference plane system was employed as shown in Figures (32) and (33). Five reference planes (J=1, --5) were employed in this calculation with eleven data points on each reference plane. The radius of the initial station was equal to 27.5127. The external flow was taken as representative of that on the surface of a 10 degree cone at an altitude of 165,000 ft. and Mach number of M=10.

The streamline pattern and shock and contact shape are shown in Figure (34) for reference plane J=1, while axial surface pressure distributions in this reference plane are plotted in Figure (35).

An analysis of the pressure distribution on the vehicle undersurface in Figure (35) indicates that the first expansion wave from the initial turning, reaches the undersurface somewhat downstream of the cowl exit. In addition, some reflected waves from the internal portion of the cowl appear to be cap-

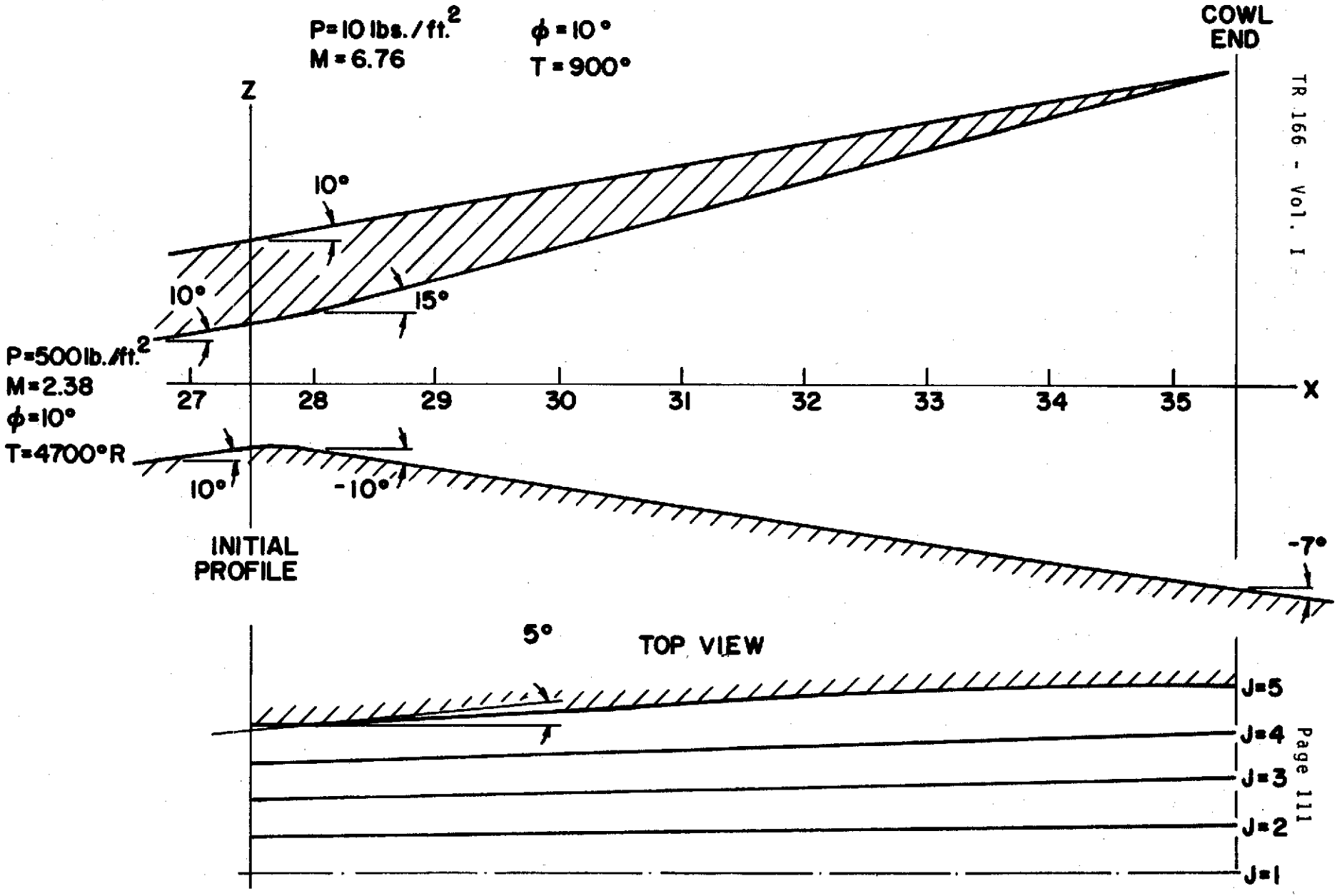

FIGURE 32. CASE I VEHICLE SIDE AND TOP VIEW

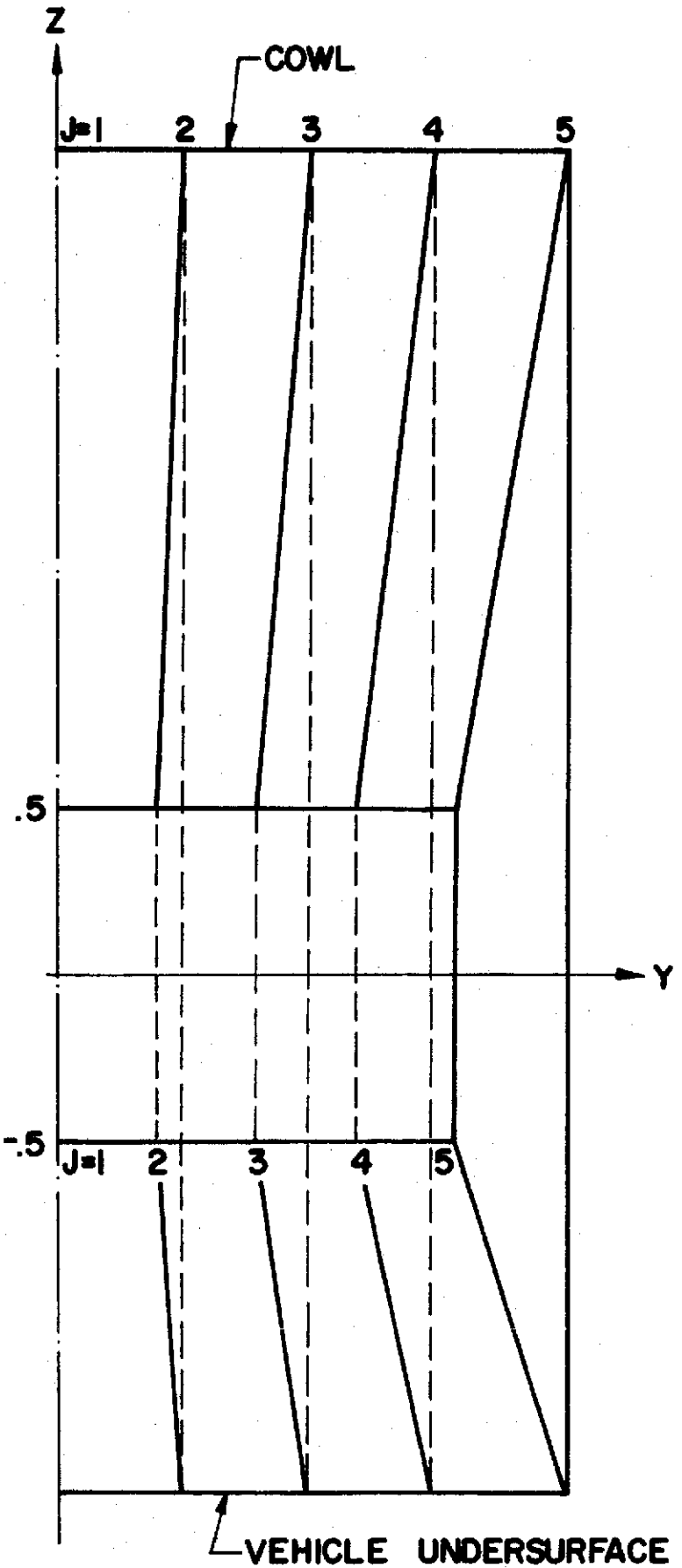

FIGURE 33. CASE I VEHICLE REAR VIEW

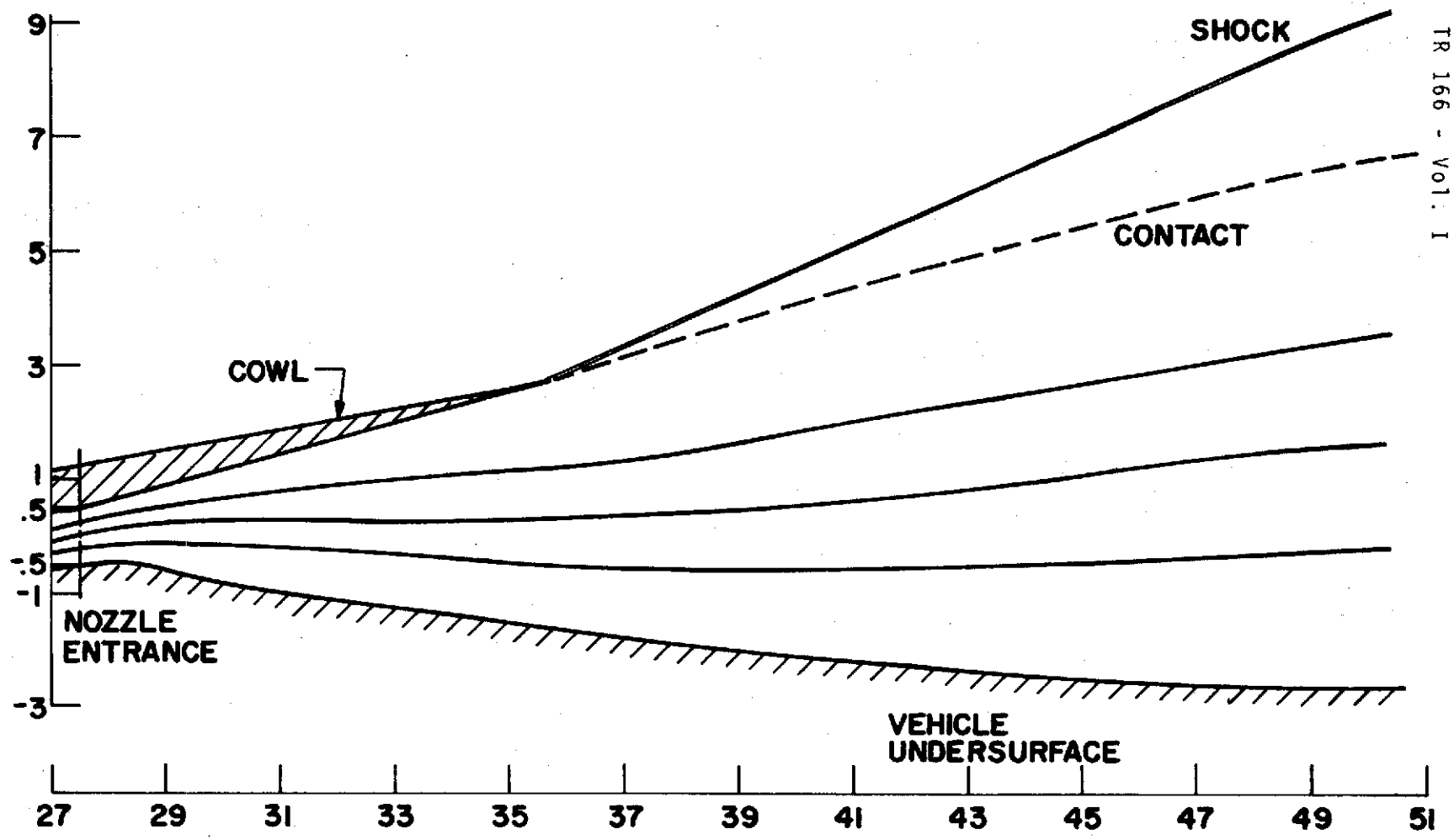

FIGURE 34. CASE I OVERALL SHOCK, CONTACT AND STREAMLINE PATTERN-PLANE 1

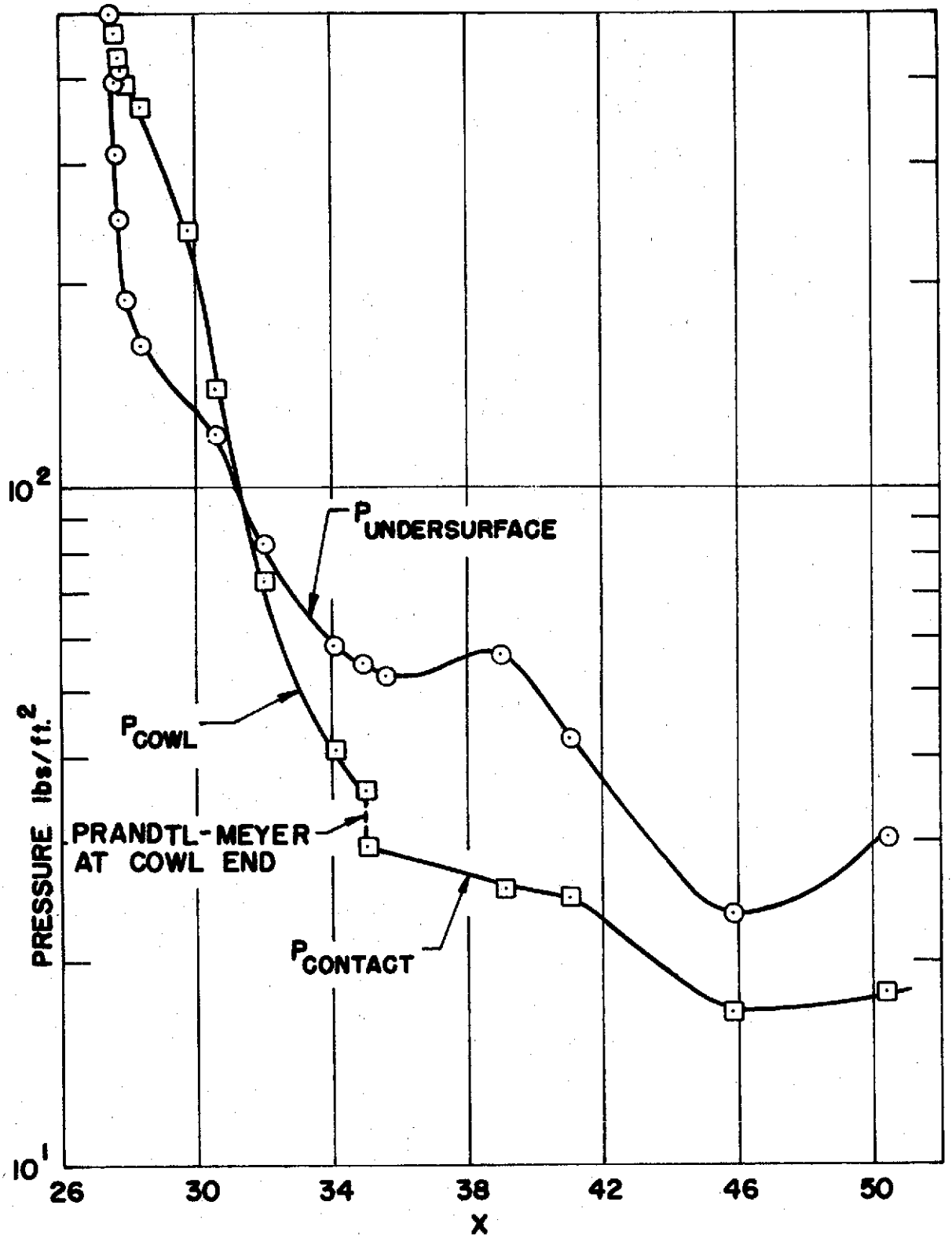

FIGURE 35. CASE I AXIAL SURFACE PRESSURE DISTRIBUTION

tured by the vehicle undersurface. The last waves appear to reach the undersurface at x=46, just short of the vehicle end. It should be noted that no waves from the external flow interaction reach the vehicle undersurface. In Figure (36), the Mach number and pressure profiles are depicted at the cowl end.

The flow variables at the initial station (KOUNT=0), a station just downstream of the cowl end (KOUNT=55) and at the vehicle end (KOUNT=114) are tabulated in Tables Ia, Ib and Ic respectively. The reference planes are denoted by J=1, 2 etc., and the grid points in each reference plane by the index I: the reference planes in the internal flow are in a line source system and hence each reference plane has a constant θ, while for the external portion of the flow a Cartesian system is employed and each reference plane has a constant value of Y as indicated.

The value of the Z coordinate in each reference plane is tabulated under Z, the pressure under P, the velocity component in the reference plane under Q, the flow angle ϕ in the reference plane under PHE, the cross flow angle ψ under SI, the Mach number under M, the static enthalpy under H, the fuel to air equivalence ratio Φ under PHI, the density ρ under RHO,

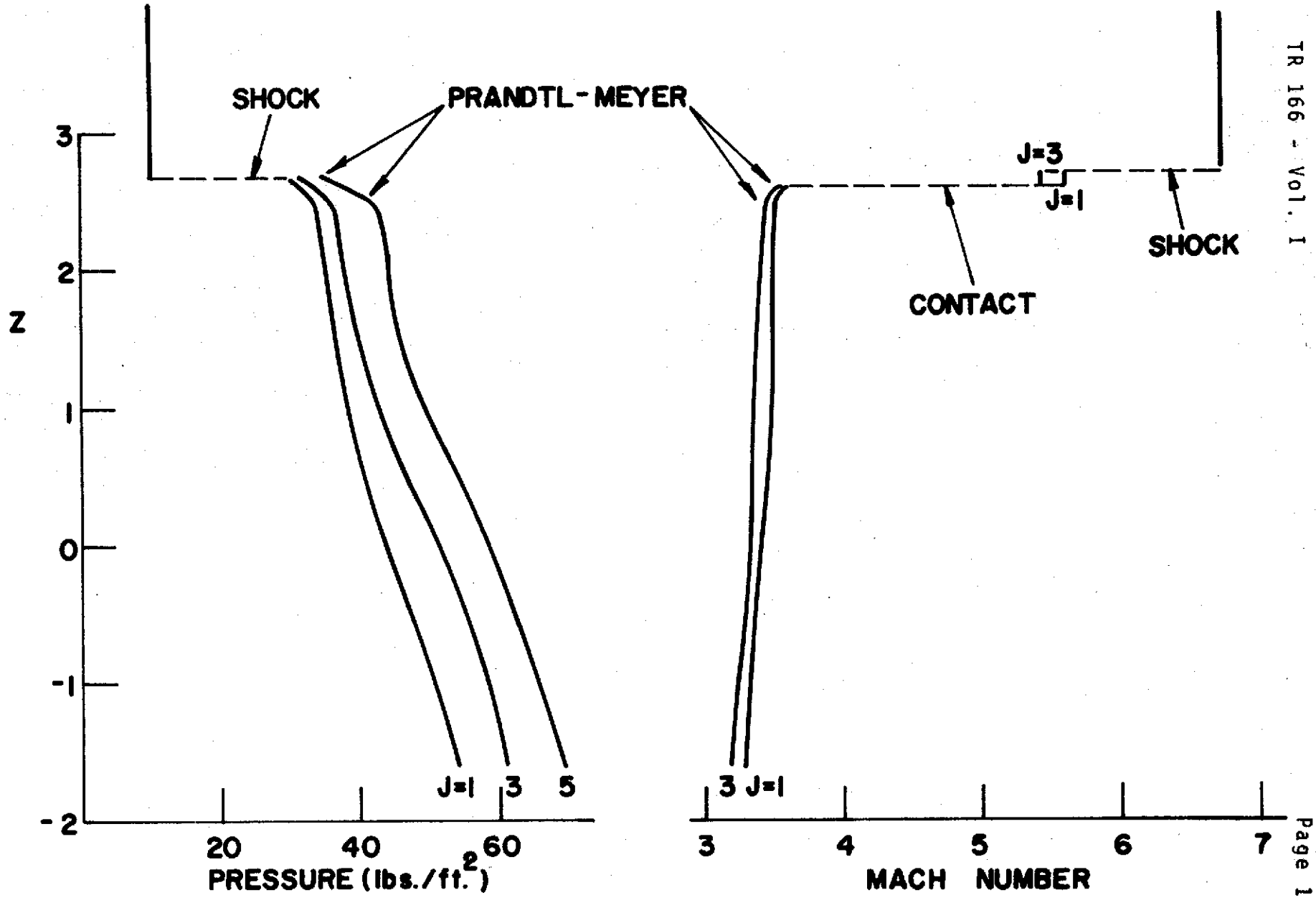

FIGURE 36. CASE I PRESSURE AND MACH NUMBER PROFILES AT COWL STATION

the equilibrium isentropic exponent Γ under GAM and the temperature under T. In the external flow data, the shock and contact are identified as points where two successive I indices have the same value of Z: the shock has a jump in pressure for these indices while the contact has the same value of pressure.

Case II demonstrates a fully second order calculation of an end module flow field. A simple two dimensional expansion of the internal cowl surface was chosen, with a uniform external flow. This generated mild lateral pressure gradients at the cowl edge but significant corner gradients externally.

The initial pressure was assumed to be 500 lb/ft^2 at a Mach number of 2.21 and an equivalence ratio of 0.8. The external flow conditions were those of Case I. The lower surface and sidewalls are flat surfaces, while the upper wall has an initial small radius turn of 10^o followed by a flat 10^o surface to the cowl edge. The flow variables at the initial station (KOUNT=0), a station at the cowl end (KOUNT=70) and the last calculated station (KOUNT=120) are tabulated in Tables IIa, IIb and IIc. For the external wraparound flow the tabulated values of Y on the rotated planes are measured from the last internal reference plane (J=JINT). That is $Y = \bar{Z}$.

As shown in Figures (37) and (38), significant pressure gradients are induced in the external corner interaction region. Contract surface pressures equilibrate more quickly than those downstream of the shock surface. This is the result of the contract surface being a stream surface of the flow field.

Case III demonstrates the programs' sweepback capability. The initial conditions are similar to those of Case I but are given along a swept initial surface. A cylindrical type of configuration was chosen having geometry similar to Case I with the initial surface swept back approximately 30 degrees. The flow variables at the initial station (KOUNT=1) and at a station downstream in the recompression region (KOUNT=110) just downstream of the end of the sweepback region are given in Tables IIIa and IIIb. All surfaces are identical along lines ($X-X_{swp}$) equal to a constant. The sidewalls are assumed flat along a surface theta (θ) equal to a constant, thus the expansions should be two dimensional along lines ($X-X_{swp}$). Figure (39) indicates that the program is calculating correctly. Variations in pressure between reference planes that occur downstream of the expansion region are due to reflections of waves off the internal symmetry plane. The flow in this region has become fully three dimensional.

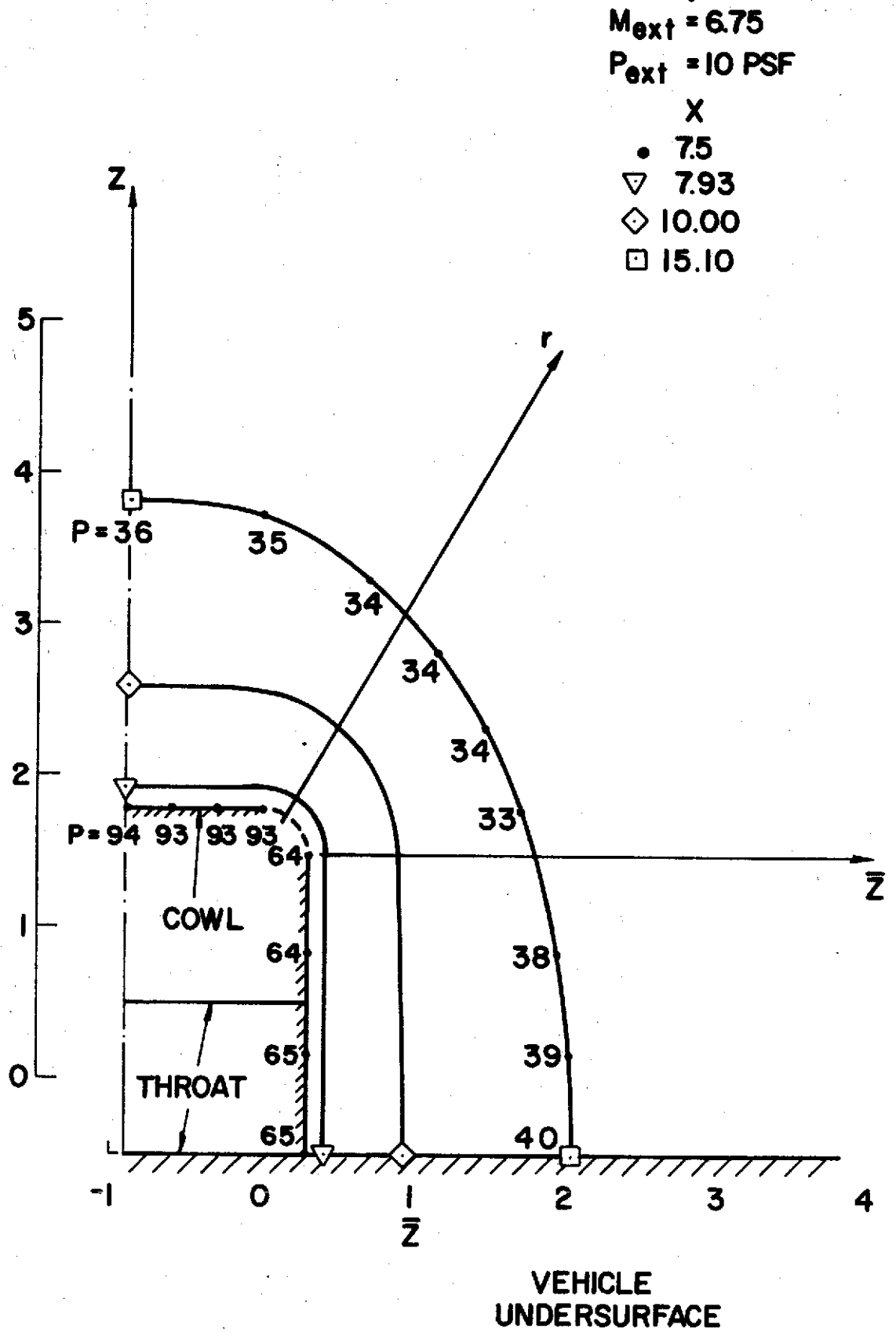

FIGURE 37. CASE II CONTACT SHAPES AND PRESSURE DISTRIBUTIONS AT VARIOUS AXIAL LOCATIONS

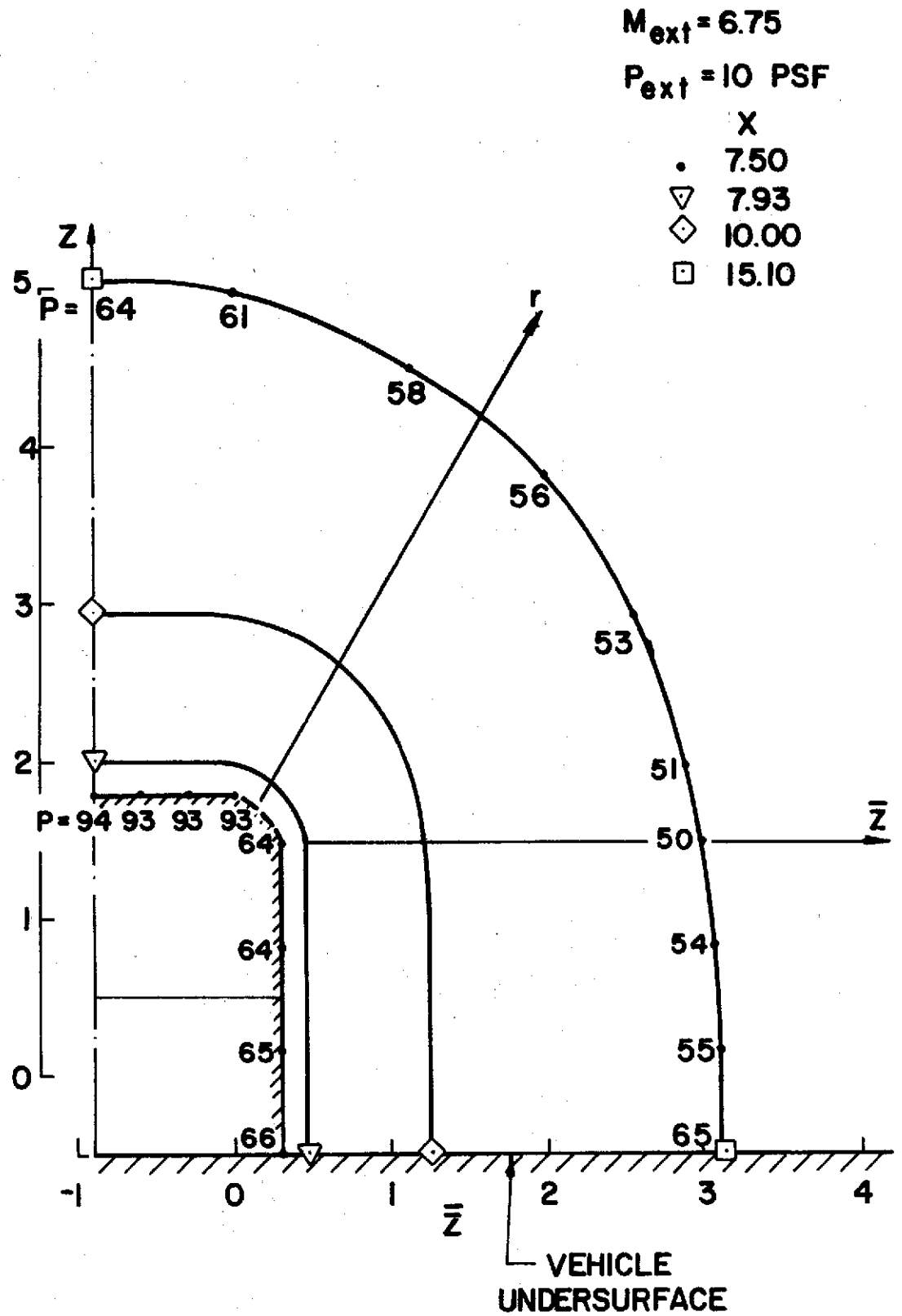

FIGURE 38. CASE II SHOCK SHAPES AND PRESSURE DISTRIBUTIONS AT VARIOUS AXIAL LOCATIONS

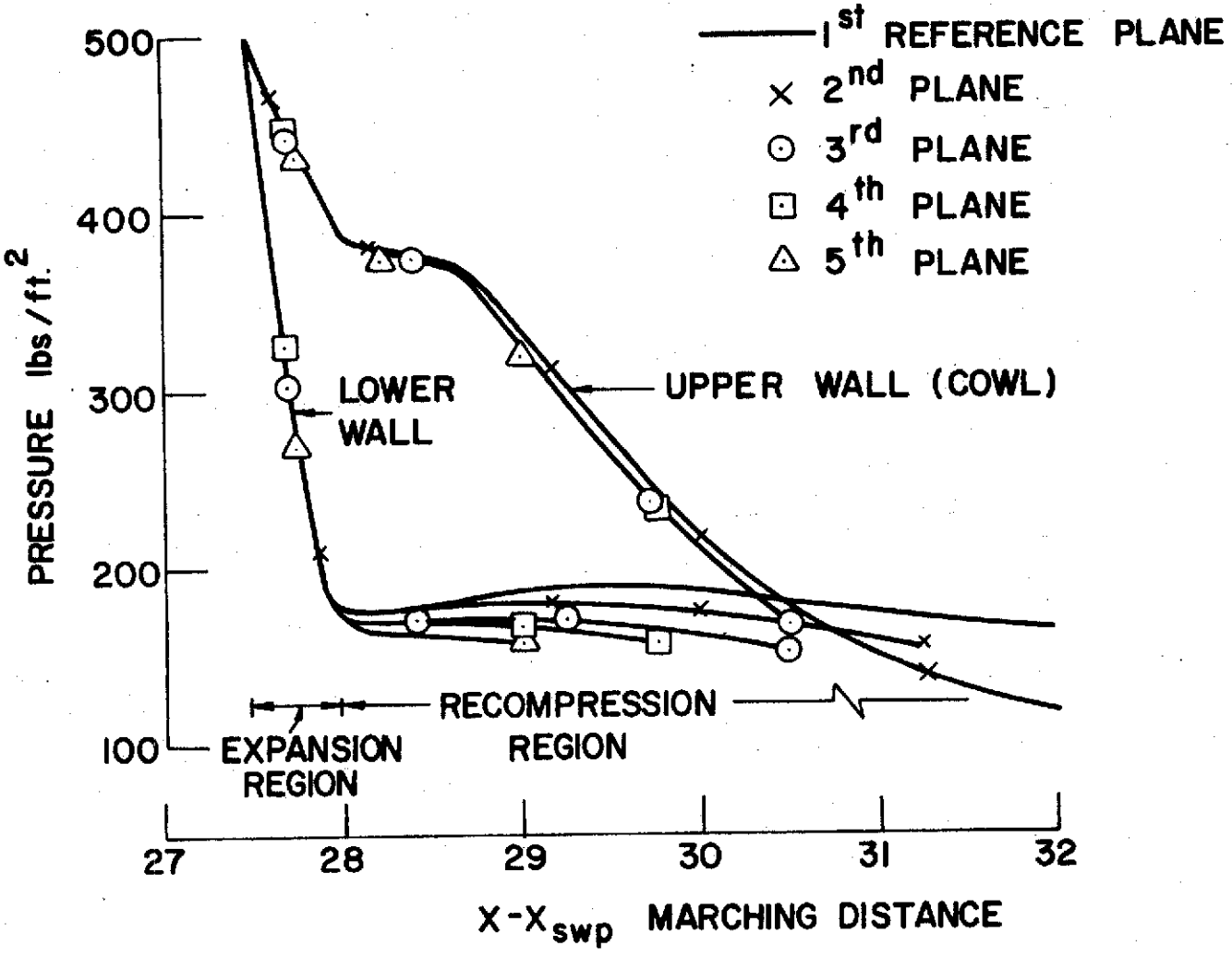

FIGURE 39. CASE III AXIAL SURFACE PRESSURE DISTRIBUTIONS CORRELATED WITH $X-X_{swp}$

TABLE Ia

J = 1 THETA = 0.

I	Z	P	Q	P_{HE}	S_I
1	-4.956E-01	5.000E+02	7.420E+03	1.566E-01	0.
2	-4.000E-01	5.000E+02	7.420E+03	1.745E-01	0.
3	-3.000E-01	5.000E+02	7.420E+03	1.745E-01	0.
4	-2.000E-01	5.000E+02	7.420E+03	1.745E-01	0.
5	-1.000E-01	5.000E+02	7.420E+03	1.745E-01	0.
6	0.	5.000E+02	7.420E+03	1.745E-01	0.
7	1.000E-01	5.000E+02	7.420E+03	1.745E-01	0.
8	2.000E-01	5.000E+02	7.420E+03	1.745E-01	0.
9	3.000E-01	5.000E+02	7.420E+03	1.745E-01	0.
10	4.000E-01	5.000E+02	7.420E+03	1.745E-01	0.
11	5.047E-01	5.000E+02	7.420E+03	1.792E-01	0.

J = 2 THETA = 1.09075E-02

I	Z	P	Q	P_{HE}	S_I
1	-4.959E-01	5.000E+02	7.420E+03	1.577E-01	0.
2	-4.000E-01	5.000E+02	7.420E+03	1.745E-01	0.
3	-3.000E-01	5.000E+02	7.420E+03	1.745E-01	0.
4	-2.000E-01	5.000E+02	7.420E+03	1.745E-01	0.
5	-1.000E-01	5.000E+02	7.420E+03	1.745E-01	0.
6	0.	5.000E+02	7.420E+03	1.745E-01	0.
7	1.000E-01	5.000E+02	7.420E+03	1.745E-01	0.
8	2.000E-01	5.000E+02	7.420E+03	1.745E-01	0.
9	3.000E-01	5.000E+02	7.420E+03	1.745E-01	0.
10	4.000E-01	5.000E+02	7.420E+03	1.745E-01	0.
11	5.044E-01	5.000E+02	7.420E+03	1.789E-01	0.

J = 3 THETA = 2.18150E-02

I	Z	P	Q	P_{HE}	S_I
1	-4.967E-01	5.000E+02	7.420E+03	1.611E-01	0.
2	-4.000E-01	5.000E+02	7.420E+03	1.745E-01	0.
3	-3.000E-01	5.000E+02	7.420E+03	1.745E-01	0.
4	-2.000E-01	5.000E+02	7.420E+03	1.745E-01	0.
5	-1.000E-01	5.000E+02	7.420E+03	1.745E-01	0.
6	0.	5.000E+02	7.420E+03	1.745E-01	0.
7	1.000E-01	5.000E+02	7.420E+03	1.745E-01	0.
8	2.000E-01	5.000E+02	7.420E+03	1.745E-01	0.
9	3.000E-01	5.000E+02	7.420E+03	1.745E-01	0.
10	4.000E-01	5.000E+02	7.420E+03	1.745E-01	0.
11	5.035E-01	5.000E+02	7.420E+03	1.780E-01	0.

J = 4 THETA = 3.27225E-02

I	Z	P	Q	P_{HE}	S_I
1	-4.980E-01	5.000E+02	7.420E+03	1.647E-01	0.
2	-4.000E-01	5.000E+02	7.420E+03	1.745E-01	0.
3	-3.000E-01	5.000E+02	7.420E+03	1.745E-01	0.
4	-2.000E-01	5.000E+02	7.420E+03	1.745E-01	0.
5	-1.000E-01	5.000E+02	7.420E+03	1.745E-01	0.
6	0.	5.000E+02	7.420E+03	1.745E-01	0.
7	1.000E-01	5.000E+02	7.420E+03	1.745E-01	0.
8	2.000E-01	5.000E+02	7.420E+03	1.745E-01	0.
9	3.000E-01	5.000E+02	7.420E+03	1.745E-01	0.
10	4.000E-01	5.000E+02	7.420E+03	1.745E-01	0.
11	5.020E-01	5.000E+02	7.420E+03	1.766E-01	0.

M	H	PHI	RHO	GAM	T
2.383E+00	4.270E+07	0.	6.100E-05	1.183E+00	4.698E+03
2.383E+00	4.270E+07	0.	6.100E-05	1.183E+00	4.698E+03
2.383E+00	4.270E+07	0.	6.100E-05	1.183E+00	4.698E+03
2.383E+00	4.270E+07	0.	6.100E-05	1.183E+00	4.698E+03
2.383E+00	4.270E+07	0.	6.100E-05	1.183E+00	4.698E+03
2.383E+00	4.270E+07	0.	6.100E-05	1.183E+00	4.698E+03
2.383E+00	4.270E+07	0.	6.100E-05	1.183E+00	4.698E+03
2.383E+00	4.270E+07	0.	6.100E-05	1.183E+00	4.698E+03
2.383E+00	4.270E+07	0.	6.100E-05	1.183E+00	4.698E+03
2.383E+00	4.270E+07	0.	6.100E-05	1.183E+00	4.698E+03
2.383E+00	4.270E+07	0.	6.100E-05	1.183E+00	4.698E+03

M	H	PHI	RHO	GAM	T
2.383E+00	4.270E+07	0.	6.100E-05	1.183E+00	4.698E+03
2.383E+00	4.270E+07	0.	6.100E-05	1.183E+00	4.698E+03
2.383E+00	4.270E+07	0.	6.100E-05	1.183E+00	4.698E+03
2.383E+00	4.270E+07	0.	6.100E-05	1.183E+00	4.698E+03
2.383E+00	4.270E+07	0.	6.100E-05	1.183E+00	4.698E+03
2.383E+00	4.270E+07	0.	6.100E-05	1.183E+00	4.698E+03
2.383E+00	4.270E+07	0.	6.100E-05	1.183E+00	4.698E+03
2.383E+00	4.270E+07	0.	6.100E-05	1.183E+00	4.698E+03
2.383E+00	4.270E+07	0.	6.100E-05	1.183E+00	4.698E+03
2.383E+00	4.270E+07	0.	6.100E-05	1.183E+00	4.698E+03
2.383E+00	4.270E+07	0.	6.100E-05	1.183E+00	4.698E+03

M	H	PHI	RHO	GAM	T
2.383E+00	4.270E+07	0.	6.100E-05	1.183E+00	4.698E+03
2.383E+00	4.270E+07	0.	6.100E-05	1.183E+00	4.698E+03
2.383E+00	4.270E+07	0.	6.100E-05	1.183E+00	4.698E+03
2.383E+00	4.270E+07	0.	6.100E-05	1.183E+00	4.698E+03
2.383E+00	4.270E+07	0.	6.100E-05	1.183E+00	4.698E+03
2.383E+00	4.270E+07	0.	6.100E-05	1.183E+00	4.698E+03
2.383E+00	4.270E+07	0.	6.100E-05	1.183E+00	4.698E+03
2.383E+00	4.270E+07	0.	6.100E-05	1.183E+00	4.698E+03
2.383E+00	4.270E+07	0.	6.100E-05	1.183E+00	4.698E+03
2.383E+00	4.270E+07	0.	6.100E-05	1.183E+00	4.698E+03
2.383E+00	4.270E+07	0.	6.100E-05	1.183E+00	4.698E+03

M	H	PHI	RHO	GAM	T
2.383E+00	4.270E+07	0.	6.100E-05	1.183E+00	4.698E+03
2.383E+00	4.270E+07	0.	6.100E-05	1.183E+00	4.698E+03
2.383E+00	4.270E+07	0.	6.100E-05	1.183E+00	4.698E+03
2.383E+00	4.270E+07	0.	6.100E-05	1.183E+00	4.698E+03
2.383E+00	4.270E+07	0.	6.100E-05	1.183E+00	4.698E+03
2.383E+00	4.270E+07	0.	6.100E-05	1.183E+00	4.698E+03
2.383E+00	4.270E+07	0.	6.100E-05	1.183E+00	4.698E+03
2.383E+00	4.270E+07	0.	6.100E-05	1.183E+00	4.698E+03
2.383E+00	4.270E+07	0.	6.100E-05	1.183E+00	4.698E+03
2.383E+00	4.270E+07	0.	6.100E-05	1.183E+00	4.698E+03
2.383E+00	4.270E+07	0.	6.100E-05	1.183E+00	4.698E+03

SIDEWALL

J = 5

I	X Z	Y P	U Q	W PHE	V SI
	2.749E+01	1.200E+00	7.420E+03	1.290E+03	-1.273E-01
1	-5.000E-01	5.000E+02	7.420E+03	1.723E-01	-4.360E-02
	2.749E+01	1.200E+00	7.420E+03	1.290E+03	-1.273E-01
2	-4.000E-01	5.000E+02	7.420E+03	1.723E-01	-4.360E-02
	2.749E+01	1.200E+00	7.420E+03	1.290E+03	-1.273E-01
3	-3.000E-01	5.000E+02	7.420E+03	1.723E-01	-4.360E-02
	2.749E+01	1.200E+00	7.420E+03	1.290E+03	-1.273E-01
4	-2.000E-01	5.000E+02	7.420E+03	1.723E-01	-4.360E-02
	2.749E+01	1.200E+00	7.420E+03	1.290E+03	-1.273E-01
5	-1.000E-01	5.000E+02	7.420E+03	1.723E-01	-4.360E-02
	2.749E+01	1.200E+00	7.420E+03	1.290E+03	-1.273E-01
6	0.	5.000E+02	7.420E+03	1.723E-01	-4.360E-02
	2.749E+01	1.200E+00	7.420E+03	1.290E+03	-1.273E-01
7	1.000E-01	5.000E+02	7.420E+03	1.723E-01	-4.360E-02
	2.749E+01	1.200E+00	7.420E+03	1.290E+03	-1.273E-01
8	2.000E-01	5.000E+02	7.420E+03	1.723E-01	-4.360E-02
	2.749E+01	1.200E+00	7.420E+03	1.290E+03	-1.273E-01
9	3.000E-01	5.000E+02	7.420E+03	1.723E-01	-4.360E-02
	2.749E+01	1.200E+00	7.420E+03	1.290E+03	-1.273E-01
10	4.000E-01	5.000E+02	7.420E+03	1.723E-01	-4.360E-02
	2.749E+01	1.200E+00	7.420E+03	1.290E+03	-1.273E-01
11	5.000E-01	5.000E+02	7.420E+03	1.723E-01	-4.360E-02

M	H	PHI	RHO	GAM	T
2.419E+00	4.270E+07	0.	6.100E-05	1.183E+00	4.698E+03
2.419E+00	4.270E+07	0.	6.100E-05	1.183E+00	4.698E+03
2.419E+00	4.270E+07	0.	6.100E-05	1.183E+00	4.698E+03
2.419E+00	4.270E+07	0.	6.100E-05	1.183E+00	4.698E+03
2.419E+00	4.270E+07	0.	6.100E-05	1.183E+00	4.698E+03
2.419E+00	4.270E+07	0.	6.100E-05	1.183E+00	4.698E+03
2.419E+00	4.270E+07	0.	6.100E-05	1.183E+00	4.698E+03
2.419E+00	4.270E+07	0.	6.100E-05	1.183E+00	4.698E+03
2.419E+00	4.270E+07	0.	6.100E-05	1.183E+00	4.698E+03
2.419E+00	4.270E+07	0.	6.100E-05	1.183E+00	4.698E+03
2.419E+00	4.270E+07	0.	6.100E-05	1.183E+00	4.698E+03

TABLE Ib

J = 1 Y = 0.

I	Z	P	Q	PHE	SI
1	-1.619E+00	4.763E+01	9.326E+03	-1.218E-01	0.
2	-1.222E+00	4.551E+01	9.352E+03	-9.746E-02	0.
3	-8.392E-01	4.337E+01	9.380E+03	-7.266E-02	0.
4	-4.550E-01	4.119E+01	9.409E+03	-4.642E-02	0.
5	-6.298E-02	3.904E+01	9.439E+03	-1.744E-02	0.
6	3.413E-01	3.704E+01	9.468E+03	1.573E-02	0.
7	7.595E-01	3.531E+01	9.495E+03	5.429E-02	0.
8	1.192E+00	3.391E+01	9.516E+03	9.866E-02	0.
9	1.638E+00	3.280E+01	9.534E+03	1.483E-01	0.
10	2.100E+00	3.185E+01	9.550E+03	2.024E-01	0.
11	2.491E+00	3.116E+01	9.561E+03	2.744E-01	0.
12	2.497E+00	2.968E+01	9.587E+03	2.849E-01	0.
13	2.503E+00	2.861E+01	9.606E+03	2.928E-01	0.
14	2.510E+00	2.822E+01	9.613E+03	2.958E-01	0.
15	2.626E+00	2.823E+01	9.613E+03	2.959E-01	0.
16	2.626E+00	2.823E+01	9.686E+03	2.959E-01	0.
17	2.687E+00	2.824E+01	9.686E+03	2.959E-01	0.
18	2.687E+00	1.000E+01	9.900E+03	1.745E-01	0.
19	2.509E+01	9.998E+00	9.900E+03	1.745E-01	0.
20	5.009E+01	1.000E+01	9.900E+03	1.745E-01	0.

J = 2 Y = 3.81631E-01

I	Z	P	Q	PHE	SI
1	-1.619E+00	4.978E+01	9.298E+03	-1.218E-01	-1.949E-02
2	-1.223E+00	4.776E+01	9.323E+03	-9.897E-02	-1.686E-02
3	-8.398E-01	4.580E+01	9.347E+03	-7.403E-02	-1.447E-02
4	-4.542E-01	4.375E+01	9.374E+03	-4.621E-02	-1.207E-02
5	-6.088E-02	4.157E+01	9.403E+03	-1.517E-02	-1.000E-02
6	3.442E-01	3.936E+01	9.434E+03	1.963E-02	-8.359E-03
7	7.630E-01	3.729E+01	9.464E+03	5.890E-02	-7.137E-03
8	1.196E+00	3.553E+01	9.491E+03	1.031E-01	-6.266E-03
9	1.643E+00	3.415E+01	9.512E+03	1.519E-01	-5.793E-03
10	2.104E+00	3.303E+01	9.530E+03	2.046E-01	-5.717E-03
11	2.491E+00	3.202E+01	9.547E+03	2.745E-01	2.842E-03
12	2.497E+00	3.040E+01	9.574E+03	2.857E-01	2.844E-03
13	2.504E+00	2.917E+01	9.596E+03	2.945E-01	2.841E-03
14	2.510E+00	2.869E+01	9.604E+03	2.981E-01	2.857E-03
15	2.627E+00	2.871E+01	9.604E+03	2.981E-01	2.880E-03
16	2.627E+00	2.871E+01	9.681E+03	2.981E-01	-4.595E-05
17	2.688E+00	2.872E+01	9.681E+03	2.981E-01	-5.346E-04
18	2.688E+00	1.000E+01	9.900E+03	1.745E-01	-1.285E-11
19	2.509E+01	9.998E+00	9.900E+03	1.745E-01	-7.979E-09
20	5.009E+01	1.000E+01	9.900E+03	1.745E-01	0.

J = 3 Y = 7.63352E-01

I	Z	P	Q	PHE	SI
1	-1.619E+00	5.710E+01	9.216E+03	-1.218E-01	-2.021E-02
2	-1.210E+00	5.503E+01	9.238E+03	-9.519E-02	-1.999E-02
3	-8.283E-01	5.318E+01	9.259E+03	-6.934E-02	-1.893E-02
4	-4.491E-01	5.088E+01	9.285E+03	-4.224E-02	-1.758E-02
5	-6.258E-02	4.794E+01	9.321E+03	-1.271E-02	-1.663E-02
6	3.379E-01	4.458E+01	9.363E+03	2.045E-02	-1.636E-02
7	7.548E-01	4.133E+01	9.406E+03	5.843E-02	-1.672E-02
8	1.187E+00	3.865E+01	9.444E+03	1.019E-01	-1.760E-02

	M	H	PHI	RHO	GAM	T
	3.588E+00	2.674E+07	0.	8.730E-06	1.238E+00	3.305E+03
	3.613E+00	2.650E+07	0.	8.415E-06	1.239E+00	3.274E+03
	3.639E+00	2.624E+07	0.	8.094E-06	1.240E+00	3.240E+03
	3.667E+00	2.596E+07	0.	7.764E-06	1.241E+00	3.205E+03
	3.695E+00	2.568E+07	0.	7.434E-06	1.242E+00	3.168E+03
	3.724E+00	2.540E+07	0.	7.125E-06	1.244E+00	3.132E+03
	3.750E+00	2.516E+07	0.	6.855E-06	1.245E+00	3.099E+03
	3.771E+00	2.495E+07	0.	6.635E-06	1.246E+00	3.072E+03
	3.789E+00	2.478E+07	0.	6.460E-06	1.247E+00	3.050E+03
	3.805E+00	2.463E+07	0.	6.308E-06	1.247E+00	3.030E+03
	3.817E+00	2.452E+07	0.	6.198E-06	1.248E+00	3.016E+03
	3.844E+00	2.428E+07	0.	5.962E-06	1.249E+00	2.984E+03
	3.864E+00	2.409E+07	0.	5.790E-06	1.250E+00	2.960E+03
	3.872E+00	2.403E+07	0.	5.726E-06	1.251E+00	2.951E+03
	3.871E+00	2.403E+07	0.	5.728E-06	1.251E+00	2.951E+03
	5.687E+00	1.205E+07	0.	1.332E-05	1.369E+00	1.235E+03
	5.687E+00	1.205E+07	0.	1.333E-05	1.369E+00	1.235E+03
	6.755E+00	9.950E+06	0.	6.456E-06	1.387E+00	9.024E+02
	6.755E+00	9.950E+06	0.	6.455E-06	1.387E+00	9.024E+02
	6.755E+00	9.950E+06	0.	6.456E-06	1.387E+00	9.024E+02

-01

	M	H	PHI	RHO	GAM	T
02	3.564E+00	2.699E+07	0.	9.047E-06	1.237E+00	3.337E+03
02	3.587E+00	2.676E+07	0.	8.750E-06	1.238E+00	3.308E+03
02	3.609E+00	2.653E+07	0.	8.459E-06	1.239E+00	3.278E+03
02	3.634E+00	2.628E+07	0.	8.151E-06	1.240E+00	3.246E+03
02	3.661E+00	2.601E+07	0.	7.821E-06	1.241E+00	3.211E+03
03	3.691E+00	2.572E+07	0.	7.482E-06	1.242E+00	3.173E+03
03	3.720E+00	2.544E+07	0.	7.163E-06	1.243E+00	3.136E+03
03	3.746E+00	2.519E+07	0.	6.890E-06	1.245E+00	3.104E+03
03	3.767E+00	2.498E+07	0.	6.673E-06	1.246E+00	3.077E+03
03	3.785E+00	2.481E+07	0.	6.496E-06	1.246E+00	3.055E+03
03	3.802E+00	2.466E+07	0.	6.336E-06	1.247E+00	3.034E+03
03	3.831E+00	2.440E+07	0.	6.077E-06	1.249E+00	2.999E+03
03	3.854E+00	2.419E+07	0.	5.880E-06	1.250E+00	2.972E+03
03	3.863E+00	2.411E+07	0.	5.802E-06	1.250E+00	2.961E+03
03	3.862E+00	2.411E+07	0.	5.805E-06	1.250E+00	2.962E+03
05	5.669E+00	1.209E+07	0.	1.347E-05	1.368E+00	1.242E+03
04	5.668E+00	1.209E+07	0.	1.347E-05	1.368E+00	1.242E+03
11	6.755E+00	9.950E+06	0.	6.456E-06	1.387E+00	9.024E+02
09	6.755E+00	9.950E+06	0.	6.455E-06	1.387E+00	9.024E+02
	6.755E+00	9.950E+06	0.	6.456E-06	1.387E+00	9.024E+02

-01

	M	H	PHI	RHO	GAM	T
02	3.491E+00	2.775E+07	0.	1.011E-05	1.235E+00	3.434E+03
02	3.511E+00	2.754E+07	0.	9.814E-06	1.235E+00	3.408E+03
02	3.529E+00	2.735E+07	0.	9.545E-06	1.236E+00	3.383E+03
02	3.552E+00	2.711E+07	0.	9.209E-06	1.237E+00	3.352E+03
02	3.584E+00	2.678E+07	0.	8.774E-06	1.238E+00	3.310E+03
02	3.624E+00	2.638E+07	0.	8.273E-06	1.239E+00	3.259E+03
02	3.664E+00	2.598E+07	0.	7.783E-06	1.241E+00	3.207E+03
02	3.701E+00	2.562E+07	0.	7.372E-06	1.243E+00	3.161E+03

9	1.635E+00	3.662E+01	9.474E+03	1.507E-01	-1.878E-02
10	2.100E+00	3.512E+01	9.496E+03	2.039E-01	-2.027E-02
11	2.490E+00	3.412E+01	9.513E+03	2.744E-01	1.409E-02
12	2.497E+00	3.215E+01	9.544E+03	2.874E-01	1.406E-02
13	2.504E+00	3.055E+01	9.571E+03	2.982E-01	1.403E-02
14	2.512E+00	2.984E+01	9.584E+03	3.032E-01	1.405E-02
15	2.630E+00	2.983E+01	9.584E+03	3.033E-01	1.412E-02
16	2.630E+00	2.983E+01	9.670E+03	3.032E-01	-1.134E-04
17	2.691E+00	2.985E+01	9.669E+03	3.032E-01	-1.366E-03
18	2.691E+00	1.000E+01	9.900E+03	1.745E-01	-3.355E-11
19	2.509E+01	9.998E+00	9.900E+03	1.745E-01	-4.100E-08
20	5.009E+01	1.000E+01	9.900E+03	1.745E-01	0.

J = 4 Y = 1.14525E+00

I	Z	P	Q	PHE	SI
1	-1.619E+00	6.571E+01	9.124E+03	-1.218E-01	-1.874E-02
2	-1.204E+00	6.341E+01	9.148E+03	-9.553E-02	-1.750E-02
3	-8.241E-01	6.119E+01	9.172E+03	-6.953E-02	-1.758E-02
4	-4.447E-01	5.848E+01	9.201E+03	-4.185E-02	-1.744E-02
5	-5.817E-02	5.512E+01	9.237E+03	-1.174E-02	-1.600E-02
6	3.417E-01	5.136E+01	9.279E+03	2.178E-02	-1.312E-02
7	7.579E-01	4.773E+01	9.321E+03	5.995E-02	-1.059E-02
8	1.191E+00	4.463E+01	9.359E+03	1.035E-01	-9.441E-03
9	1.640E+00	4.219E+01	9.390E+03	1.522E-01	-9.781E-03
10	2.104E+00	4.044E+01	9.413E+03	2.045E-01	-1.123E-02
11	2.487E+00	3.967E+01	9.424E+03	2.745E-01	2.953E-03
12	2.496E+00	3.676E+01	9.466E+03	2.914E-01	2.989E-03
13	2.506E+00	3.417E+01	9.506E+03	3.070E-01	2.988E-03
14	2.516E+00	3.277E+01	9.528E+03	3.159E-01	3.051E-03
15	2.636E+00	3.276E+01	9.529E+03	3.159E-01	3.092E-03
16	2.636E+00	3.276E+01	9.640E+03	3.158E-01	-1.102E-04
17	2.697E+00	3.274E+01	9.640E+03	3.158E-01	-1.502E-03
18	2.697E+00	1.000E+01	9.900E+03	1.745E-01	-1.864E-11
19	2.509E+01	9.999E+00	9.900E+03	1.745E-01	-1.014E-08
20	5.009E+01	1.000E+01	9.900E+03	1.745E-01	0.

J = 5 Y = 1.52806E+00

I	Z	P	Q	PHE	SI
1	-1.619E+00	6.593E+01	9.193E+03	-1.218E-01	5.318E-07
2	-1.211E+00	6.488E+01	9.203E+03	-1.040E-01	5.484E-07
3	-8.293E-01	6.374E+01	9.202E+03	-7.943E-02	5.482E-07
4	-4.499E-01	6.146E+01	9.201E+03	-5.185E-02	5.494E-07
5	-6.339E-02	5.793E+01	9.222E+03	-2.220E-02	5.509E-07
6	3.368E-01	5.381E+01	9.288E+03	1.087E-02	5.528E-07
7	7.542E-01	5.021E+01	9.359E+03	4.963E-02	5.539E-07
8	1.188E+00	4.729E+01	9.405E+03	9.459E-02	5.527E-07
9	1.639E+00	4.483E+01	9.439E+03	1.458E-01	5.490E-07
10	2.108E+00	4.292E+01	9.463E+03	2.014E-01	5.800E-07
11	2.487E+00	4.214E+01	9.469E+03	2.742E-01	5.752E-07
12	2.497E+00	3.876E+01	9.516E+03	2.928E-01	5.724E-07
13	2.507E+00	3.572E+01	9.561E+03	3.103E-01	5.697E-07
14	2.519E+00	3.396E+01	9.588E+03	3.209E-01	5.681E-07
15	2.638E+00	3.395E+01	9.588E+03	3.208E-01	5.681E-07
16	2.638E+00	3.395E+01	9.628E+03	3.208E-01	0.
17	2.699E+00	3.394E+01	9.628E+03	3.208E-01	0.
18	2.699E+00	1.000E+01	9.900E+03	1.745E-01	0.
19	2.509E+01	9.999E+00	9.900E+03	1.745E-01	0.
20	5.009E+01	1.000E+01	9.900E+03	1.745E-01	0.

3.730E+00	2.534E+07	0.	7.058E-06	1.244E+00	3.124E+03
3.753E+00	2.513E+07	0.	6.824E-06	1.245E+00	3.096E+03
3.768E+00	2.498E+07	0.	6.669E-06	1.246E+00	3.076E+03
3.801E+00	2.468E+07	0.	6.357E-06	1.247E+00	3.036E+03
3.829E+00	2.442E+07	0.	6.102E-06	1.249E+00	3.003E+03
3.842E+00	2.430E+07	0.	5.988E-06	1.249E+00	2.987E+03
3.842E+00	2.430E+07	0.	5.987E-06	1.249E+00	2.987E+03
5.625E+00	1.220E+07	0.	1.380E-05	1.367E+00	1.259E+03
5.624E+00	1.221E+07	0.	1.381E-05	1.367E+00	1.259E+03
6.755E+00	9.950E+06	0.	6.456E-06	1.387E+00	9.024E+02
6.755E+00	9.950E+06	0.	6.455E-06	1.387E+00	9.024E+02
6.755E+00	9.950E+06	0.	6.456E-06	1.387E+00	9.024E+02

M	H	PHI	RHO	GAM	T
3.413E+00	2.857E+07	0.	1.133E-05	1.232E+00	3.537E+03
3.434E+00	2.836E+07	0.	1.101E-05	1.233E+00	3.512E+03
3.453E+00	2.815E+07	0.	1.070E-05	1.234E+00	3.485E+03
3.477E+00	2.789E+07	0.	1.031E-05	1.234E+00	3.452E+03
3.509E+00	2.755E+07	0.	9.824E-06	1.235E+00	3.409E+03
3.547E+00	2.716E+07	0.	9.279E-06	1.237E+00	3.359E+03
3.586E+00	2.676E+07	0.	8.744E-06	1.238E+00	3.307E+03
3.621E+00	2.640E+07	0.	8.282E-06	1.239E+00	3.261E+03
3.651E+00	2.610E+07	0.	7.914E-06	1.241E+00	3.222E+03
3.674E+00	2.587E+07	0.	7.648E-06	1.242E+00	3.192E+03
3.684E+00	2.577E+07	0.	7.531E-06	1.242E+00	3.179E+03
3.726E+00	2.537E+07	0.	7.083E-06	1.244E+00	3.127E+03
3.766E+00	2.499E+07	0.	6.679E-06	1.246E+00	3.078E+03
3.788E+00	2.478E+07	0.	6.458E-06	1.247E+00	3.050E+03
3.786E+00	2.478E+07	0.	6.456E-06	1.247E+00	3.050E+03
5.517E+00	1.249E+07	0.	1.464E-05	1.365E+00	1.303E+03
5.517E+00	1.249E+07	0.	1.464E-05	1.365E+00	1.303E+03
6.755E+00	9.950E+06	0.	6.456E-06	1.387E+00	9.024E+02
6.755E+00	9.950E+06	0.	6.456E-06	1.387E+00	9.024E+02
6.755E+00	9.950E+06	0.	6.456E-06	1.387E+00	9.024E+02

M	H	PHI	RHO	GAM	T
3.437E+00	2.859E+07	0.	1.136E-05	1.232E+00	3.541E+03
3.445E+00	2.849E+07	0.	1.121E-05	1.233E+00	3.527E+03
3.449E+00	2.835E+07	0.	1.104E-05	1.233E+00	3.511E+03
3.460E+00	2.813E+07	0.	1.072E-05	1.234E+00	3.482E+03
3.487E+00	2.781E+07	0.	1.023E-05	1.235E+00	3.441E+03
3.534E+00	2.737E+07	0.	9.629E-06	1.236E+00	3.386E+03
3.583E+00	2.700E+07	0.	9.104E-06	1.237E+00	3.338E+03
3.620E+00	2.670E+07	0.	8.676E-06	1.238E+00	3.300E+03
3.650E+00	2.643E+07	0.	8.310E-06	1.239E+00	3.265E+03
3.674E+00	2.620E+07	0.	8.022E-06	1.240E+00	3.235E+03
3.682E+00	2.610E+07	0.	7.905E-06	1.241E+00	3.222E+03
3.727E+00	2.566E+07	0.	7.393E-06	1.242E+00	3.165E+03
3.772E+00	2.523E+07	0.	6.920E-06	1.244E+00	3.109E+03
3.800E+00	2.497E+07	0.	6.644E-06	1.246E+00	3.075E+03
3.800E+00	2.497E+07	0.	6.643E-06	1.246E+00	3.075E+03
5.474E+00	1.260E+07	0.	1.497E-05	1.364E+00	1.321E+03
5.475E+00	1.260E+07	0.	1.497E-05	1.364E+00	1.321E+03
6.755E+00	9.950E+06	0.	6.456E-06	1.387E+00	9.024E+02
6.756E+00	9.950E+06	0.	6.456E-06	1.387E+00	9.024E+02
6.755E+00	9.950E+06	0.	6.456E-06	1.387E+00	9.024E+02

13	2.507E+00	3.576E+01	9.561E+03	3.103E-01	5.697E-07
14	2.519E+00	3.396E+01	9.588E+03	3.209E-01	5.681E-07
15	2.638E+00	3.395E+01	9.588E+03	3.208E-01	5.681E-07
16	2.638E+00	3.395E+01	9.628E+03	3.208E-01	0.
17	2.699E+00	3.394E+01	9.628E+03	3.208E-01	0.
18	2.699E+00	1.000E+01	9.900E+03	1.745E-01	0.
19	2.509E+01	9.999E+00	9.900E+03	1.745E-01	0.
20	5.009E+01	1.000E+01	9.900E+03	1.745E-01	0.

ALP

J					
1	0.	0.	0.	0.	0.
2	4.603E-03	0.	4.717E-03	0.	0.
3	1.131E-02	0.	1.197E-02	0.	0.
4	1.136E-02	0.	1.061E-02	0.	0.
5	0.	0.	0.	0.	0.

ALPHA

J					
1	0.	0.	0.	0.	0.
2	4.212E-03	0.	4.509E-03	0.	0.
3	1.033E-02	0.	1.142E-02	0.	0.
4	1.032E-02	0.	1.008E-02	0.	0.
5	0.	0.	0.	0.	0.

BETA

J					
1	4.133E-01	0.	2.959E-01	0.	0.
2	4.152E-01	0.	2.991E-01	0.	0.
3	4.197E-01	0.	3.032E-01	0.	0.
4	4.309E-01	0.	3.158E-01	0.	0.
5	4.354E-01	0.	3.208E-01	0.	0.

IS

J					
1	18	0	16	0	0
2	18	0	16	0	0
3	18	0	16	0	0
4	18	0	16	0	0
5	18	0	16	0	0

TABLE Ic

J = 1 Y = 0.

I	Z	P	Q	PHE	S_I
1	-2.644E+00	2.585E+01	9.657E+03	-1.507E-02	0.
2	-1.892E+00	2.337E+01	9.707E+03	7.575E-03	0.
3	-1.107E+00	2.109E+01	9.756E+03	3.221E-02	0.
4	-2.917E-01	1.900E+01	9.805E+03	5.892E-02	0.
5	5.636E-01	1.705E+01	9.855E+03	8.717E-02	0.
6	1.462E+00	1.530E+01	9.903E+03	1.153E-01	0.
7	2.403E+00	1.393E+01	9.944E+03	1.414E-01	0.
8	3.380E+00	1.314E+01	9.969E+03	1.636E-01	0.
9	4.380E+00	1.297E+01	9.974E+03	1.813E-01	0.
10	5.388E+00	1.321E+01	9.967E+03	1.957E-01	0.
11	6.434E+00	1.342E+01	9.960E+03	2.107E-01	0.
12	6.434E+00	1.342E+01	9.832E+03	2.107E-01	0.
13	7.382E+00	1.627E+01	9.802E+03	2.303E-01	0.
14	9.10RE+00	2.531E+01	9.716E+03	2.817E-01	0.
15	9.10RE+00	1.000E+01	9.900E+03	1.745E-01	0.
16	2.772E+01	9.999E+00	9.900E+03	1.745E-01	0.
17	5.272E+01	1.000E+01	9.900E+03	1.745E-01	0.

J = 2 Y = 3.81631E-01

I	Z	P	Q	PHE	SI
1	-2.644E+00	2.693E+01	9.628E+03	-1.507E-02	-3.614E-02
2	-1.917E+00	2.430E+01	9.679E+03	6.834E-03	-3.640E-02
3	-1.145E+00	2.167E+01	9.735E+03	3.016E-02	-3.723E-02
4	-3.351E-01	1.925E+01	9.790E+03	5.512E-02	-3.890E-02
5	5.186E-01	1.717E+01	9.842E+03	8.164E-02	-4.143E-02
6	1.421E+00	1.549E+01	9.887E+03	1.089E-01	-4.450E-02
7	2.373E+00	1.431E+01	9.920E+03	1.355E-01	-4.738E-02
8	3.367E+00	1.373E+01	9.938E+03	1.593E-01	-4.864E-02
9	4.384E+00	1.371E+01	9.940E+03	1.793E-01	-4.802E-02
10	5.408E+00	1.401E+01	9.934E+03	1.958E-01	-3.751E-02
11	6.431E+00	1.430E+01	9.930E+03	2.109E-01	-2.442E-02
12	6.431E+00	1.430E+01	9.820E+03	2.113E-01	-9.274E-03
13	7.351E+00	1.683E+01	9.795E+03	2.305E-01	-8.395E-04
14	9.125E+00	2.497E+01	9.720E+03	2.800E-01	5.569E-04
15	9.125E+00	1.000E+01	9.900E+03	1.745E-01	-1.049E-07
16	2.772E+01	9.999E+00	9.900E+03	1.745E-01	1.270E-06
17	5.272E+01	1.000E+01	9.900E+03	1.745E-01	0.

J = 3 Y = 7.63352E-01

I	Z	P	Q	PHE	SI
1	-2.644E+00	2.448E+01	9.631E+03	-1.507E-02	-1.117E-01
2	-1.872E+00	2.199E+01	9.682E+03	7.639E-03	-1.119E-01
3	-1.091E+00	1.975E+01	9.733E+03	3.142E-02	-1.116E-01
4	-2.859E-01	1.777E+01	9.784E+03	5.657E-02	-1.098E-01
5	5.605E-01	1.613E+01	9.830E+03	8.311E-02	-1.058E-01
6	1.453E+00	1.488E+01	9.870E+03	1.104E-01	-9.977E-02
7	2.391E+00	1.410E+01	9.899E+03	1.372E-01	-9.177E-02
8	3.366E+00	1.379E+01	9.916E+03	1.619E-01	-8.180E-02
9	4.361E+00	1.394E+01	9.920E+03	1.831E-01	-6.942E-02
10	5.361E+00	1.450E+01	9.913E+03	2.009E-01	-5.360E-02
11	6.455E+00	1.564E+01	9.890E+03	2.181E-01	-3.316E-02
12	6.455E+00	1.564E+01	9.800E+03	2.207E-01	-1.578E-02
13	7.352E+00	1.776E+01	9.784E+03	2.364E-01	-4.439E-03
14	9.104E+00	2.352E+01	9.735E+03	2.724E-01	1.852E-04

M	H	PHI	RHO	GAM	T
3.921E+00	2.360E+07	0.	5.338E-06	1.253E+00	2.894E+03
3.976E+00	2.312E+07	0.	4.926E-06	1.256E+00	2.830E+03
4.033E+00	2.264E+07	0.	4.540E-06	1.260E+00	2.765E+03
4.091E+00	2.216E+07	0.	4.178E-06	1.263E+00	2.700E+03
4.152E+00	2.167E+07	0.	3.834E-06	1.267E+00	2.634E+03
4.214E+00	2.119E+07	0.	3.520E-06	1.271E+00	2.568E+03
4.267E+00	2.079E+07	0.	3.270E-06	1.274E+00	2.513E+03
4.301E+00	2.054E+07	0.	3.123E-06	1.277E+00	2.479E+03
4.309E+00	2.049E+07	0.	3.093E-06	1.277E+00	2.471E+03
4.299E+00	2.056E+07	0.	3.137E-06	1.277E+00	2.482E+03
4.290E+00	2.063E+07	0.	3.176E-06	1.276E+00	2.491E+03
6.361E+00	1.062E+07	0.	7.753E-06	1.381E+00	1.010E+03
6.179E+00	1.091E+07	0.	8.908E-06	1.378E+00	1.056E+03
5.805E+00	1.175E+07	0.	1.240E-05	1.371E+00	1.189E+03
6.755E+00	9.950E+06	0.	6.456E-06	1.387E+00	9.024E+02
6.755E+00	9.950E+06	0.	6.455E-06	1.387E+00	9.024E+02
6.755E+00	9.950E+06	0.	6.456E-06	1.387E+00	9.024E+02

M	H	PHI	RHO	GAM	T
3.897E+00	2.380E+07	0.	5.518E-06	1.252E+00	2.921E+03
3.954E+00	2.330E+07	0.	5.083E-06	1.255E+00	2.855E+03
4.018E+00	2.276E+07	0.	4.640E-06	1.259E+00	2.782E+03
4.084E+00	2.222E+07	0.	4.224E-06	1.263E+00	2.708E+03
4.149E+00	2.170E+07	0.	3.857E-06	1.267E+00	2.638E+03
4.207E+00	2.124E+07	0.	3.556E-06	1.270E+00	2.576E+03
4.252E+00	2.090E+07	0.	3.342E-06	1.273E+00	2.529E+03
4.276E+00	2.073E+07	0.	3.235E-06	1.275E+00	2.505E+03
4.277E+00	2.072E+07	0.	3.231E-06	1.275E+00	2.504E+03
4.265E+00	2.081E+07	0.	3.286E-06	1.274E+00	2.516E+03
4.254E+00	2.090E+07	0.	3.340E-06	1.273E+00	2.528E+03
6.296E+00	1.074E+07	0.	8.110E-06	1.380E+00	1.029E+03
6.146E+00	1.098E+07	0.	9.128E-06	1.378E+00	1.068E+03
5.824E+00	1.172E+07	0.	1.229E-05	1.371E+00	1.183E+03
6.755E+00	9.950E+06	0.	6.456E-06	1.387E+00	9.024E+02
6.755E+00	9.950E+06	0.	6.456E-06	1.387E+00	9.024E+02
6.755E+00	9.950E+06	0.	6.456E-06	1.387E+00	9.024E+02

M	H	PHI	RHO	GAM	T
3.951E+00	2.329E+07	0.	5.107E-06	1.255E+00	2.853E+03
4.010E+00	2.279E+07	0.	4.690E-06	1.259E+00	2.785E+03
4.070E+00	2.228E+07	0.	4.304E-06	1.262E+00	2.717E+03
4.129E+00	2.181E+07	0.	3.958E-06	1.266E+00	2.652E+03
4.184E+00	2.138E+07	0.	3.666E-06	1.269E+00	2.594E+03
4.229E+00	2.103E+07	0.	3.443E-06	1.272E+00	2.547E+03
4.261E+00	2.081E+07	0.	3.301E-06	1.274E+00	2.516E+03
4.274E+00	2.073E+07	0.	3.246E-06	1.275E+00	2.505E+03
4.268E+00	2.078E+07	0.	3.274E-06	1.275E+00	2.512E+03
4.246E+00	2.095E+07	0.	3.376E-06	1.273E+00	2.536E+03
4.203E+00	2.128E+07	0.	3.583E-06	1.270E+00	2.581E+03
6.199E+00	1.092E+07	0.	8.620E-06	1.378E+00	1.058E+03
6.097E+00	1.109E+07	0.	9.495E-06	1.377E+00	1.084E+03
5.889E+00	1.157E+07	0.	1.181E-05	1.373E+00	1.160E+03

15	9.104E+00	1.000E+01	9.900E+03	1.745E-01	-5.266E-07
16	2.772E+01	9.998E+00	9.900E+03	1.745E-01	5.958E-06
17	5.272E+01	1.000E+01	9.900E+03	1.745E-01	0.

J = 4 Y = 1.14525E+00

I	Z	P	Q	PHE	SI
1	-2.644E+00	2.136E+01	9.717E+03	-1.507E-02	-8.193E-02
2	-1.863E+00	1.947E+01	9.762E+03	5.263E-03	-8.238E-02
3	-1.083E+00	1.817E+01	9.793E+03	2.901E-02	-8.293E-02
4	-2.781E-01	1.716E+01	9.819E+03	5.559E-02	-8.167E-02
5	5.665E-01	1.630E+01	9.845E+03	8.416E-02	-7.757E-02
6	1.458E+00	1.556E+01	9.870E+03	1.135E-01	-7.035E-02
7	2.397E+00	1.499E+01	9.891E+03	1.419E-01	-6.056E-02
8	3.372E+00	1.467E+01	9.905E+03	1.675E-01	-4.931E-02
9	4.368E+00	1.473E+01	9.908E+03	1.884E-01	-3.770E-02
10	5.358E+00	1.530E+01	9.895E+03	2.080E-01	-2.635E-02
11	6.543E+00	1.678E+01	9.853E+03	2.298E-01	-1.394E-02
12	6.543E+00	1.678E+01	9.781E+03	2.300E-01	-5.727E-03
13	7.410E+00	1.895E+01	9.768E+03	2.444E-01	1.265E-04
14	9.123E+00	2.295E+01	9.741E+03	2.693E-01	5.581E-04
15	9.123E+00	1.000E+01	9.900E+03	1.745E-01	-1.319E-07
16	2.772E+01	9.998E+00	9.900E+03	1.745E-01	1.367E-06
17	5.272E+01	1.000E+01	9.900E+03	1.745E-01	0.

J = 5 Y = 1.52806E+00

I	Z	P	Q	PHE	SI
1	-2.644E+00	2.166E+01	9.806E+03	-1.507E-02	3.861E-07
2	-1.933E+00	2.004E+01	9.842E+03	1.623E-03	4.130E-07
3	-1.186E+00	1.914E+01	9.852E+03	2.394E-02	4.300E-07
4	-4.032E-01	1.862E+01	9.843E+03	5.011E-02	4.501E-07
5	4.212E-01	1.822E+01	9.838E+03	7.877E-02	4.756E-07
6	1.300E+00	1.777E+01	9.869E+03	1.088E-01	5.062E-07
7	2.245E+00	1.719E+01	9.913E+03	1.388E-01	5.261E-07
8	3.243E+00	1.657E+01	9.939E+03	1.664E-01	5.272E-07
9	4.276E+00	1.617E+01	9.953E+03	1.896E-01	5.178E-07
10	5.310E+00	1.628E+01	9.949E+03	2.086E-01	5.330E-07
11	6.491E+00	1.727E+01	9.919E+03	2.279E-01	5.903E-07
12	6.491E+00	1.727E+01	9.773E+03	2.279E-01	0.
13	7.332E+00	1.894E+01	9.768E+03	2.407E-01	0.
14	9.099E+00	2.246E+01	9.746E+03	2.667E-01	0.
15	9.099E+00	1.000E+01	9.900E+03	1.745E-01	0.
16	2.772E+01	9.998E+00	9.900E+03	1.745E-01	0.
17	5.272E+01	1.000E+01	9.900E+03	1.745E-01	0.

ALP

J					
1	0.	0.	0.	0.	0.
2	-5.484E-03	0.	3.145E-02	0.	0.
3	-1.873E-03	0.	1.504E-01	0.	0.
4	-6.141E-03	0.	2.164E-02	0.	0.
5	0.	0.	0.	0.	0.

ALPHA

J					
1	0.	0.	0.	0.	0.
2	-5.052E-03	0.	3.074E-02	0.	0.
3	-1.730E-03	0.	1.467E-01	0.	0.
4	-5.678E-03	0.	2.107E-02	0.	0.
5	0.	0.	0.	0.	0.

6.755E+00	9.950E+06	0.	6.456E-06	1.387E+00	9.024E+02
6.755E+00	9.950E+06	0.	6.455E-06	1.387E+00	9.024E+02
6.755E+00	9.950E+06	0.	6.456E-06	1.387E+00	9.024E+02

M	H	PHI	RHO	GAM	T
4.027E+00	2.270E+07	0.	4.587E-06	1.259E+00	2.774E+03
4.079E+00	2.228E+07	0.	4.262E-06	1.262E+00	2.716E+03
4.118E+00	2.195E+07	0.	4.035E-06	1.265E+00	2.673E+03
4.150E+00	2.169E+07	0.	3.855E-06	1.267E+00	2.637E+03
4.178E+00	2.146E+07	0.	3.702E-06	1.269E+00	2.606E+03
4.205E+00	2.126E+07	0.	3.569E-06	1.270E+00	2.578E+03
4.226E+00	2.110E+07	0.	3.465E-06	1.272E+00	2.556E+03
4.237E+00	2.102E+07	0.	3.409E-06	1.272E+00	2.544E+03
4.235E+00	2.103E+07	0.	3.420E-06	1.272E+00	2.547E+03
4.213E+00	2.120E+07	0.	3.524E-06	1.271E+00	2.570E+03
4.159E+00	2.160E+07	0.	3.790E-06	1.267E+00	2.625E+03
6.102E+00	1.112E+07	0.	8.990E-06	1.376E+00	1.089E+03
6.030E+00	1.124E+07	0.	9.532E-06	1.375E+00	1.109E+03
5.915E+00	1.151E+07	0.	1.162E-05	1.373E+00	1.151E+03
6.755E+00	9.950E+06	0.	6.456E-06	1.387E+00	9.024E+02
6.755E+00	9.950E+06	0.	6.455E-06	1.387E+00	9.024E+02
6.755E+00	9.950E+06	0.	6.456E-06	1.387E+00	9.024E+02

M	H	PHI	RHO	GAM	T
4.043E+00	2.277E+07	0.	4.634E-06	1.259E+00	2.783E+03
4.086E+00	2.240E+07	0.	4.356E-06	1.261E+00	2.733E+03
4.106E+00	2.216E+07	0.	4.200E-06	1.263E+00	2.700E+03
4.113E+00	2.202E+07	0.	4.109E-06	1.264E+00	2.682E+03
4.120E+00	2.194E+07	0.	4.041E-06	1.265E+00	2.671E+03
4.142E+00	2.181E+07	0.	3.962E-06	1.266E+00	2.653E+03
4.173E+00	2.167E+07	0.	3.859E-06	1.267E+00	2.634E+03
4.199E+00	2.154E+07	0.	3.750E-06	1.268E+00	2.616E+03
4.214E+00	2.145E+07	0.	3.678E-06	1.269E+00	2.603E+03
4.211E+00	2.148E+07	0.	3.698E-06	1.268E+00	2.608E+03
4.176E+00	2.174E+07	0.	3.877E-06	1.266E+00	2.644E+03
6.061E+00	1.120E+07	0.	9.141E-06	1.376E+00	1.102E+03
6.026E+00	1.125E+07	0.	9.914E-06	1.375E+00	1.110E+03
5.938E+00	1.146E+07	0.	1.145E-05	1.374E+00	1.143E+03
6.755E+00	9.950E+06	0.	6.456E-06	1.387E+00	9.024E+02
6.755E+00	9.950E+06	0.	6.455E-06	1.387E+00	9.024E+02
6.755E+00	9.950E+06	0.	6.456E-06	1.387E+00	9.024E+02

0.	0.
0.	0.
0.	0.
0.	0.
0.	0.

0.	0.
0.	0.
0.	0.
0.	0.
0.	0.

7	[illegible]	[illegible]	[illegible]	[illegible]	[illegible]
8	3.243E+00	1.657E+01	9.939E+03	1.664E-01	5.272E-07
9	4.276E+00	1.617E+01	9.953E+03	1.896E-01	5.178E-07
10	5.310E+00	1.628E+01	9.949E+03	2.086E-01	5.330E-07
11	6.491E+00	1.727E+01	9.919E+03	2.279E-01	5.903E-07
12	6.491E+00	1.727E+01	9.773E+03	2.279E-01	0.
13	7.332E+00	1.894E+01	9.768E+03	2.407E-01	0.
14	9.099E+00	2.246E+01	9.746E+03	2.667E-01	0.
15	9.099E+00	1.000E+01	9.900E+03	1.745E-01	0.
16	2.772E+01	9.998E+00	9.900E+03	1.745E-01	0.
17	5.272E+01	1.000E+01	9.900E+03	1.745E-01	0.

ALP

J					
1	0.	0.	0.	0.	0.
2	-5.484E-03	0.	3.145E-02	0.	0.
3	-1.873E-03	0.	1.504E-01	0.	0.
4	-6.141E-03	0.	2.164E-02	0.	0.
5	0.	0.	0.	0.	0.

ALPHA

J					
1	0.	0.	0.	0.	0.
2	-5.052E-03	0.	3.074E-02	0.	0.
3	-1.730E-03	0.	1.467E-01	0.	0.
4	-5.678E-03	0.	2.107E-02	0.	0.
5	0.	0.	0.	0.	0.

BETA

J					
1	4.011E-01	0.	2.107E-01	0.	0.
2	3.996E-01	0.	2.116E-01	0.	0.
3	3.933E-01	0.	2.230E-01	0.	0.
4	3.908E-01	0.	2.301E-01	0.	0.
5	3.886E-01	0.	2.279E-01	0.	0.

IS

J					
1	15	0	12	0	0
2	15	0	12	0	0
3	15	0	12	0	0
4	15	0	12	0	0
5	15	0	12	0	0

TABLE IIa

J = 1 Y = 0.

I	Z	P	Q	PHE	SI
1	-5.000E-01	5.000E+02	7.420E+03	0.	0.
2	-4.000E-01	5.000E+02	7.420E+03	0.	0.
3	-3.000E-01	5.000E+02	7.420E+03	0.	0.
4	-2.000E-01	5.000E+02	7.420E+03	0.	0.
5	-1.000E-01	5.000E+02	7.420E+03	0.	0.
6	0.	5.000E+02	7.420E+03	0.	0.
7	1.000E-01	5.000E+02	7.420E+03	0.	0.
8	2.000E-01	5.000E+02	7.420E+03	0.	0.
9	3.000E-01	5.000E+02	7.420E+03	0.	0.
10	4.000E-01	5.000E+02	7.420E+03	0.	0.
11	5.000E-01	5.000E+02	7.420E+03	0.	0.

J = 2 Y = 3.00000E-01

I	Z	P	Q	PHE	SI
1	-5.000E-01	5.000E+02	7.420E+03	0.	0.
2	-4.000E-01	5.000E+02	7.420E+03	0.	0.
3	-3.000E-01	5.000E+02	7.420E+03	0.	0.
4	-2.000E-01	5.000E+02	7.420E+03	0.	0.
5	-1.000E-01	5.000E+02	7.420E+03	0.	0.
6	0.	5.000E+02	7.420E+03	0.	0.
7	1.000E-01	5.000E+02	7.420E+03	0.	0.
8	2.000E-01	5.000E+02	7.420E+03	0.	0.
9	3.000E-01	5.000E+02	7.420E+03	0.	0.
10	4.000E-01	5.000E+02	7.420E+03	0.	0.
11	5.000E-01	5.000E+02	7.420E+03	0.	0.

J = 3 Y = 6.00000E-01

I	Z	P	Q	PHE	SI
1	-5.000E-01	5.000E+02	7.420E+03	0.	0.
2	-4.000E-01	5.000E+02	7.420E+03	0.	0.
3	-3.000E-01	5.000E+02	7.420E+03	0.	0.
4	-2.000E-01	5.000E+02	7.420E+03	0.	0.
5	-1.000E-01	5.000E+02	7.420E+03	0.	0.
6	0.	5.000E+02	7.420E+03	0.	0.
7	1.000E-01	5.000E+02	7.420E+03	0.	0.
8	2.000E-01	5.000E+02	7.420E+03	0.	0.
9	3.000E-01	5.000E+02	7.420E+03	0.	0.
10	4.000E-01	5.000E+02	7.420E+03	0.	0.
11	5.000E-01	5.000E+02	7.420E+03	0.	0.

J = 4 Y = 9.00000E-01

I	Z	P	Q	PHE	SI
1	-5.000E-01	5.000E+02	7.420E+03	0.	0.
2	-4.000E-01	5.000E+02	7.420E+03	0.	0.
3	-3.000E-01	5.000E+02	7.420E+03	0.	0.
4	-2.000E-01	5.000E+02	7.420E+03	0.	0.
5	-1.000E-01	5.000E+02	7.420E+03	0.	0.
6	0.	5.000E+02	7.420E+03	0.	0.
7	1.000E-01	5.000E+02	7.420E+03	0.	0.
8	2.000E-01	5.000E+02	7.420E+03	0.	0.
9	3.000E-01	5.000E+02	7.420E+03	0.	0.
10	4.000E-01	5.000E+02	7.420E+03	0.	0.
11	5.000E-01	5.000E+02	7.420E+03	0.	0.

M	H	PHI	RHO	GAM	T
2.211E+00	6.450E+07	8.000E-01	5.089E-05	1.147E+00	4.728E+03
2.211E+00	6.450E+07	8.000E-01	5.089E-05	1.147E+00	4.728E+03
2.211E+00	6.450E+07	8.000E-01	5.089E-05	1.147E+00	4.728E+03
2.211E+00	6.450E+07	8.000E-01	5.089E-05	1.147E+00	4.728E+03
2.211E+00	6.450E+07	8.000E-01	5.089E-05	1.147E+00	4.728E+03
2.211E+00	6.450E+07	8.000E-01	5.089E-05	1.147E+00	4.728E+03
2.211E+00	6.450E+07	8.000E-01	5.089E-05	1.147E+00	4.728E+03
2.211E+00	6.450E+07	8.000E-01	5.089E-05	1.147E+00	4.728E+03
2.211E+00	6.450E+07	8.000E-01	5.089E-05	1.147E+00	4.728E+03
2.211E+00	6.450E+07	8.000E-01	5.089E-05	1.147E+00	4.728E+03
2.211E+00	6.450E+07	8.000E-01	5.089E-05	1.147E+00	4.728E+03

M	H	PHI	RHO	GAM	T
2.211E+00	6.450E+07	8.000E-01	5.089E-05	1.147E+00	4.728E+03
2.211E+00	6.450E+07	8.000E-01	5.089E-05	1.147E+00	4.728E+03
2.211E+00	6.450E+07	8.000E-01	5.089E-05	1.147E+00	4.728E+03
2.211E+00	6.450E+07	8.000E-01	5.089E-05	1.147E+00	4.728E+03
2.211E+00	6.450E+07	8.000E-01	5.089E-05	1.147E+00	4.728E+03
2.211E+00	6.450E+07	8.000E-01	5.089E-05	1.147E+00	4.728E+03
2.211E+00	6.450E+07	8.000E-01	5.089E-05	1.147E+00	4.728E+03
2.211E+00	6.450E+07	8.000E-01	5.089E-05	1.147E+00	4.728E+03
2.211E+00	6.450E+07	8.000E-01	5.089E-05	1.147E+00	4.728E+03
2.211E+00	6.450E+07	8.000E-01	5.089E-05	1.147E+00	4.728E+03
2.211E+00	6.450E+07	8.000E-01	5.089E-05	1.147E+00	4.728E+03

M	H	PHI	RHO	GAM	T
2.211E+00	6.450E+07	8.000E-01	5.089E-05	1.147E+00	4.728E+03
2.211E+00	6.450E+07	8.000E-01	5.089E-05	1.147E+00	4.728E+03
2.211E+00	6.450E+07	8.000E-01	5.089E-05	1.147E+00	4.728E+03
2.211E+00	6.450E+07	8.000E-01	5.089E-05	1.147E+00	4.728E+03
2.211E+00	6.450E+07	8.000E-01	5.089E-05	1.147E+00	4.728E+03
2.211E+00	6.450E+07	8.000E-01	5.089E-05	1.147E+00	4.728E+03
2.211E+00	6.450E+07	8.000E-01	5.089E-05	1.147E+00	4.728E+03
2.211E+00	6.450E+07	8.000E-01	5.089E-05	1.147E+00	4.728E+03
2.211E+00	6.450E+07	8.000E-01	5.089E-05	1.147E+00	4.728E+03
2.211E+00	6.450E+07	8.000E-01	5.089E-05	1.147E+00	4.728E+03
2.211E+00	6.450E+07	8.000E-01	5.089E-05	1.147E+00	4.728E+03

M	H	PHI	RHO	GAM	T
2.211E+00	6.450E+07	8.000E-01	5.089E-05	1.147E+00	4.728E+03
2.211E+00	6.450E+07	8.000E-01	5.089E-05	1.147E+00	4.728E+03
2.211E+00	6.450E+07	8.000E-01	5.089E-05	1.147E+00	4.728E+03
2.211E+00	6.450E+07	8.000E-01	5.089E-05	1.147E+00	4.728E+03
2.211E+00	6.450E+07	8.000E-01	5.089E-05	1.147E+00	4.728E+03
2.211E+00	6.450E+07	8.000E-01	5.089E-05	1.147E+00	4.728E+03
2.211E+00	6.450E+07	8.000E-01	5.089E-05	1.147E+00	4.728E+03
2.211E+00	6.450E+07	8.000E-01	5.089E-05	1.147E+00	4.728E+03
2.211E+00	6.450E+07	8.000E-01	5.089E-05	1.147E+00	4.728E+03
2.211E+00	6.450E+07	8.000E-01	5.089E-05	1.147E+00	4.728E+03
2.211E+00	6.450E+07	8.000E-01	5.089E-05	1.147E+00	4.728E+03

J = 5

SIDEWALL

I	X Z	Y P	U Q	W PHE	V SI
	0.	1.200E+00	7.420E+03	0.	0.
1	-5.000E-01	5.000E+02	7.420E+03	0.	0.
	0.	1.200E+00	7.420E+03	0.	0.
2	-4.000E-01	5.000E+02	7.420E+03	0.	0.
	0.	1.200E+00	7.420E+03	0.	0.
3	-3.000E-01	5.000E+02	7.420E+03	0.	0.
	0.	1.200E+00	7.420E+03	0.	0.
4	-2.000E-01	5.000E+02	7.420E+03	0.	0.
	0.	1.200E+00	7.420E+03	0.	0.
5	-1.000E-01	5.000E+02	7.420E+03	0.	0.
	0.	1.200E+00	7.420E+03	0.	0.
6	0.	5.000E+02	7.420E+03	0.	0.
	0.	1.200E+00	7.420E+03	0.	0.
7	1.000E-01	5.000E+02	7.420E+03	0.	0.
	0.	1.200E+00	7.420E+03	0.	0.
8	2.000E-01	5.000E+02	7.420E+03	0.	0.
	0.	1.200E+00	7.420E+03	0.	0.
9	3.000E-01	5.000E+02	7.420E+03	0.	0.
	0.	1.200E+00	7.420E+03	0.	0.
10	4.000E-01	5.000E+02	7.420E+03	0.	0.
	0.	1.200E+00	7.420E+03	0.	0.
11	5.000E-01	5.000E+02	7.420E+03	0.	0.

M	H	PHI	RHO	GAM	T
2.211E+00	6.450E+07	8.000E-01	5.089E-05	1.147E+00	4.728E+03
2.211E+00	6.450E+07	8.000E-01	5.089E-05	1.147E+00	4.728E+03
2.211E+00	6.450E+07	8.000E-01	5.089E-05	1.147E+00	4.728E+03
2.211E+00	6.450E+07	8.000E-01	5.089E-05	1.147E+00	4.728E+03
2.211E+00	6.450E+07	8.000E-01	5.089E-05	1.147E+00	4.728E+03
2.211E+00	6.450E+07	8.000E-01	5.089E-05	1.147E+00	4.728E+03
2.211E+00	6.450E+07	8.000E-01	5.089E-05	1.147E+00	4.728E+03
2.211E+00	6.450E+07	8.000E-01	5.089E-05	1.147E+00	4.728E+03
2.211E+00	6.450E+07	8.000E-01	5.089E-05	1.147E+00	4.728E+03
2.211E+00	6.450E+07	8.000E-01	5.089E-05	1.147E+00	4.728E+03
2.211E+00	6.450E+07	8.000E-01	5.089E-05	1.147E+00	4.728E+03

COWL AND FREE STREAM DATA AT KOUNT = 70

TABLE IIb

J = 1

I	Z	P	Q	PHE	SI	M
1	-5.000E-01	1.639E+02	8.680E+03	0.	0.	2.771E+00
2	-2.816E-01	1.637E+02	8.681E+03	4.241E-03	0.	2.772E+00
3	-5.989E-02	1.630E+02	8.684E+03	1.029E-02	0.	2.773E+00
4	1.638E-01	1.623E+02	8.688E+03	1.953E-02	0.	2.775E+00
5	3.886E-01	1.616E+02	8.693E+03	3.264E-02	0.	2.778E+00
6	6.173E-01	1.610E+02	8.697E+03	4.977E-02	0.	2.780E+00
7	8.484E-01	1.605E+02	8.699E+03	7.057E-02	0.	2.781E+00
8	1.083E+00	1.600E+02	8.703E+03	9.441E-02	0.	2.783E+00
9	1.313E+00	1.594E+02	8.707E+03	1.198E-01	0.	2.784E+00
10	1.778E+00	1.578E+02	8.717E+03	1.745E-01	0.	2.787E+00
11	1.778E+00	1.365E+02	8.854E+03	2.159E-01	0.	2.857E+00
12	1.778E+00	1.153E+02	9.009E+03	2.631E-01	0.	2.939E+00
13	1.778E+00	9.399E+01	9.188E+03	3.184E-01	0.	3.037E+00
14	1.778E+00	9.399E+01	9.188E+03	3.184E-01	0.	3.037E+00
15	1.778E+00	9.399E+01	9.040E+03	3.184E-01	0.	4.120E+00
16	1.778E+00	9.399E+01	9.040E+03	3.184E-01	0.	4.120E+00
17	1.778E+00	1.000E+01	9.900E+03	0.	0.	6.755E+00
18	2.500E+01	1.000E+01	9.900E+03	0.	0.	6.755E+00
19	5.000E+01	1.000E+01	9.900E+03	0.	0.	6.755E+00

J = 2

I	Z	P	Q	PHE	SI	M
1	-5.000E-01	1.676E+02	8.657E+03	0.	-4.870E-05	2.760E+00
2	-2.776E-01	1.673E+02	8.659E+03	6.561E-03	-3.357E-04	2.760E+00
3	-5.412E-02	1.664E+02	8.664E+03	1.453E-02	-2.142E-04	2.764E+00
4	1.696E-01	1.651E+02	8.672E+03	2.503E-02	-3.061E-04	2.767E+00
5	3.955E-01	1.637E+02	8.680E+03	3.873E-02	-1.958E-04	2.771E+00
6	6.242E-01	1.623E+02	8.689E+03	5.584E-02	-3.506E-04	2.776E+00
7	8.522E-01	1.609E+02	8.697E+03	7.590E-02	-2.288E-04	2.780E+00
8	1.083E+00	1.596E+02	8.705E+03	9.861E-02	-1.214E-04	2.784E+00
9	1.315E+00	1.584E+02	8.713E+03	1.232E-01	-3.654E-04	2.787E+00
10	1.778E+00	1.562E+02	8.726E+03	1.745E-01	-1.101E-03	2.792E+00
11	1.778E+00	1.353E+02	8.862E+03	2.156E-01	-1.084E-03	2.862E+00
12	1.778E+00	1.143E+02	9.016E+03	2.624E-01	-1.065E-03	2.943E+00
13	1.778E+00	9.341E+01	9.193E+03	3.171E-01	-1.045E-03	3.040E+00
14	1.778E+00	9.341E+01	9.193E+03	3.171E-01	-1.045E-03	3.040E+00
15	1.778E+00	9.341E+01	9.046E+03	3.171E-01	0.	4.129E+00
16	1.778E+00	9.341E+01	9.046E+03	3.171E-01	0.	4.129E+00
17	1.778E+00	1.000E+01	9.900E+03	0.	0.	6.755E+00
18	2.500E+01	1.000E+01	9.900E+03	0.	0.	6.755E+00
19	5.000E+01	1.000E+01	9.900E+03	0.	0.	6.755E+00

H	PHI	RHO	GAM	T
5.435E+07	8.000E-01	1.933E-05	1.159E+00	4.218E+03
5.435E+07	8.000E-01	1.931E-05	1.159E+00	4.217E+03
5.432E+07	8.000E-01	1.924E-05	1.159E+00	4.216E+03
5.427E+07	8.000E-01	1.917E-05	1.159E+00	4.214E+03
5.423E+07	8.000E-01	1.909E-05	1.159E+00	4.212E+03
5.421E+07	8.000E-01	1.904E-05	1.159E+00	4.211E+03
5.418E+07	8.000E-01	1.897E-05	1.159E+00	4.209E+03
5.415E+07	8.000E-01	1.893E-05	1.159E+00	4.208E+03
5.412E+07	8.000E-01	1.886E-05	1.159E+00	4.206E+03
5.404E+07	8.000E-01	1.870E-05	1.159E+00	4.202E+03
5.283E+07	8.000E-01	1.651E-05	1.161E+00	4.145E+03
5.144E+07	8.000E-01	1.427E-05	1.163E+00	4.079E+03
4.982E+07	8.000E-01	1.197E-05	1.166E+00	4.004E+03
4.982E+07	8.000E-01	1.197E-05	1.166E+00	4.004E+03
1.809E+07	0.	2.565E-05	1.314E+00	2.135E+03
1.809E+07	0.	2.565E-05	1.314E+00	2.135E+03
9.950E+06	0.	6.456E-06	1.387E+00	9.024E+02
9.950E+06	0.	6.456E-06	1.387E+00	9.024E+02
9.950E+06	0.	6.456E-06	1.387E+00	9.024E+02

H	PHI	RHO	GAM	T
5.455E+07	8.000E-01	1.971E-05	1.159E+00	4.227E+03
5.453E+07	8.000E-01	1.967E-05	1.159E+00	4.226E+03
5.449E+07	8.000E-01	1.959E-05	1.159E+00	4.224E+03
5.442E+07	8.000E-01	1.945E-05	1.159E+00	4.221E+03
5.435E+07	8.000E-01	1.931E-05	1.159E+00	4.217E+03
5.427E+07	8.000E-01	1.917E-05	1.159E+00	4.214E+03
5.420E+07	8.000E-01	1.903E-05	1.159E+00	4.210E+03
5.413E+07	8.000E-01	1.890E-05	1.159E+00	4.207E+03
5.407E+07	8.000E-01	1.877E-05	1.159E+00	4.204E+03
5.395E+07	8.000E-01	1.854E-05	1.159E+00	4.198E+03
5.275E+07	8.000E-01	1.638E-05	1.161E+00	4.141E+03
5.138E+07	8.000E-01	1.417E-05	1.163E+00	4.076E+03
4.977E+07	8.000E-01	1.191E-05	1.166E+00	4.002E+03
4.977E+07	8.000E-01	1.191E-05	1.166E+00	4.002E+03
1.804E+07	0.	2.558E-05	1.314E+00	2.128E+03
1.804E+07	0.	2.558E-05	1.314E+00	2.128E+03
9.950E+06	0.	6.456E-06	1.387E+00	9.024E+02
9.950E+06	0.	6.456E-06	1.387E+00	9.024E+02
9.950E+06	0.	6.456E-06	1.387E+00	9.024E+02

J = 3

I	Z	P	Q	PHE	SI	M
1	-5.000E-01	1.667E+02	8.663E+03	0.	-1.329E-04	2.762E+00
2	-2.827E-01	1.664E+02	8.664E+03	4.426E-03	-8.644E-05	2.764E+00
3	-6.349E-02	1.655E+02	8.670E+03	1.059E-02	-2.453E-05	2.766E+00
4	1.615E-01	1.643E+02	8.677E+03	1.985E-02	5.974E-05	2.770E+00
5	3.811E-01	1.630E+02	8.684E+03	3.245E-02	1.260E-04	2.774E+00
6	6.117E-01	1.618E+02	8.691E+03	4.943E-02	9.871E-05	2.777E+00
7	8.403E-01	1.607E+02	8.698E+03	6.960E-02	6.624E-05	2.781E+00
8	1.071E+00	1.599E+02	8.703E+03	9.278E-02	5.129E-05	2.782E+00
9	1.306E+00	1.591E+02	8.707E+03	1.186E-01	1.639E-05	2.785E+00
10	1.778E+00	1.576E+02	8.717E+03	1.745E-01	-4.141E-05	2.788E+00
11	1.778E+00	1.364E+02	8.854E+03	2.158E-01	-4.077E-05	2.858E+00
12	1.778E+00	1.152E+02	9.009E+03	2.630E-01	-4.007E-05	2.940E+00
13	1.778E+00	9.393E+01	9.187E+03	3.182E-01	-3.929E-05	3.037E+00

H	PHI	RHO	GAM	T
5.450E+07	8.000E-01	1.961E-05	1.159E+00	4.225E+03
5.448E+07	8.000E-01	1.959E-05	1.159E+00	4.224E+03
5.444E+07	8.000E-01	1.949E-05	1.159E+00	4.222E+03
5.438E+07	8.000E-01	1.937E-05	1.159E+00	4.219E+03
5.431E+07	8.000E-01	1.924E-05	1.159E+00	4.216E+03
5.425E+07	8.000E-01	1.912E-05	1.159E+00	4.213E+03
5.420E+07	8.000E-01	1.901E-05	1.159E+00	4.210E+03
5.415E+07	8.000E-01	1.891E-05	1.159E+00	4.208E+03
5.410E+07	8.000E-01	1.884E-05	1.159E+00	4.206E+03
5.403E+07	8.000E-01	1.870E-05	1.159E+00	4.202E+03
5.283E+07	8.000E-01	1.650E-05	1.161E+00	4.144E+03
5.144E+07	8.000E-01	1.426E-05	1.163E+00	4.079E+03
4.982E+07	8.000E-01	1.197E-05	1.166E+00	4.004E+03

14	1.778E+00	9.393E+01	9.187E+03	3.182E-01	-3.929E-05	3.037E+00
15	1.778E+00	9.393E+01	9.041E+03	3.182E-01	0.	4.121E+00
16	1.778E+00	9.393E+01	9.041E+03	3.182E-01	0.	4.121E+00
17	1.778E+00	1.000E+01	9.900E+03	0.	0.	6.755E+00
18	2.500E+01	1.000E+01	9.900E+03	0.	0.	6.755E+00
19	5.000E+01	1.000E+01	9.900E+03	0.	0.	6.755E+00

J = 4

I	Z	P	Q	PHE	SI	M
1	-5.000E-01	1.676E+02	8.657E+03	0.	5.768E-03	2.760E+00
2	-2.782E-01	1.673E+02	8.659E+03	6.443E-03	4.502E-03	2.761E+00
3	-5.487E-02	1.664E+02	8.664E+03	1.433E-02	4.099E-03	2.764E+00
4	1.696E-01	1.651E+02	8.672E+03	2.484E-02	2.745E-03	2.768E+00
5	3.950E-01	1.637E+02	8.680E+03	3.853E-02	1.798E-03	2.772E+00
6	6.243E-01	1.623E+02	8.690E+03	5.578E-02	9.103E-04	2.775E+00
7	8.530E-01	1.609E+02	8.697E+03	7.597E-02	1.995E-04	2.779E+00
8	1.083E+00	1.596E+02	8.705E+03	9.863E-02	-7.681E-04	2.784E+00
9	1.315E+00	1.584E+02	8.713E+03	1.232E-01	-2.479E-03	2.787E+00
10	1.778E+00	1.562E+02	8.725E+03	1.745E-01	-8.864E-03	2.792E+00
11	1.778E+00	1.353E+02	8.861E+03	2.156E-01	-8.728E-03	2.862E+00
12	1.778E+00	1.143E+02	9.015E+03	2.624E-01	-8.579E-03	2.942E+00
13	1.778E+00	9.342E+01	9.192E+03	3.171E-01	-8.414E-03	3.039E+00
14	1.778E+00	9.342E+01	9.192E+03	3.171E-01	-8.414E-03	3.039E+00
15	1.778E+00	9.342E+01	9.046E+03	3.171E-01	0.	4.129E+00
16	1.778E+00	9.342E+01	9.046E+03	3.171E-01	0.	4.129E+00
17	1.778E+00	1.000E+01	9.900E+03	0.	0.	6.755E+00
18	2.500E+01	1.000E+01	9.900E+03	0.	0.	6.755E+00
19	5.000E+01	1.000E+01	9.900E+03	0.	0.	6.755E+00

J = 5

I	Z	P	Q	PHE	SI	M
1	0.	1.559E+02	8.649E+03	-3.654E-03	-1.412E-01	2.795E+00
2	3.000E-01	1.574E+02	8.638E+03	1.516E-14	-1.525E-01	2.796E+00
3	3.000E-01	1.262E+02	8.847E+03	6.311E-02	-1.490E-01	2.902E+00
4	3.000E-01	9.507E+01	9.100E+03	1.411E-01	-1.449E-01	3.038E+00
5	3.000E-01	6.393E+01	9.428E+03	2.449E-01	-1.399E-01	3.227E+00
6	3.000E-01	6.393E+01	9.428E+03	2.449E-01	-1.399E-01	3.227E+00
7	3.000E-01	6.393E+01	9.335E+03	2.448E-01	0.	4.659E+00
8	3.000E-01	6.393E+01	9.335E+03	2.448E-01	0.	4.659E+00
9	3.000E-01	1.000E+01	9.900E+03	0.	0.	6.755E+00
10	2.500E+01	1.000E+01	9.900E+03	0.	0.	6.755E+00
11	5.000E+01	1.000E+01	9.900E+03	0.	0.	6.755E+00

J = 6

I	Z	P	Q	PHE	SI	M
1	0.	1.593E+02	8.691E+03	3.049E-04	-7.300E-02	2.785E+00
2	3.000E-01	1.592E+02	8.683E+03	-1.006E-14	-8.974E-02	2.786E+00
3	3.000E-01	1.276E+02	8.893E+03	6.321E-02	-8.763E-02	2.893E+00
4	3.000E-01	9.591E+01	9.147E+03	1.414E-01	-8.521E-02	3.030E+00
5	3.000E-01	6.426E+01	9.476E+03	2.458E-01	-8.226E-02	3.221E+00
6	3.000E-01	6.426E+01	9.476E+03	2.458E-01	-8.226E-02	3.221E+00
7	3.000E-01	6.426E+01	9.331E+03	2.457E-01	0.	4.651E+00
8	3.000E-01	6.426E+01	9.331E+03	2.457E-01	0.	4.651E+00
9	3.000E-01	1.000E+01	9.900E+03	0.	0.	6.755E+00
10	2.500E+01	1.000E+01	9.900E+03	0.	0.	6.755E+00
11	5.000E+01	1.000E+01	9.900E+03	0.	0.	6.755E+00

4.982E+07	8.000E-01	1.197E-05	1.160E+00	4.004E+03
1.809E+07	0.	2.564E-05	1.314E+00	2.134E+03
1.809E+07	0.	2.564E-05	1.314E+00	2.134E+03
9.950E+06	0.	6.456E-06	1.387E+00	9.024E+02
9.950E+06	0.	6.456E-06	1.387E+00	9.024E+02
9.950E+06	0.	6.456E-06	1.387E+00	9.024E+02

H	PHI	RHO	GAM	T
5.454E+07	8.000E-01	1.970E-05	1.159E+00	4.227E+03
5.453E+07	8.000E-01	1.967E-05	1.159E+00	4.226E+03
5.449E+07	8.000E-01	1.958E-05	1.159E+00	4.224E+03
5.442E+07	8.000E-01	1.945E-05	1.159E+00	4.221E+03
5.435E+07	8.000E-01	1.931E-05	1.159E+00	4.217E+03
5.427E+07	8.000E-01	1.916E-05	1.159E+00	4.214E+03
5.419E+07	8.000E-01	1.902E-05	1.159E+00	4.210E+03
5.413E+07	8.000E-01	1.890E-05	1.159E+00	4.207E+03
5.407E+07	8.000E-01	1.877E-05	1.159E+00	4.204E+03
5.395E+07	8.000E-01	1.854E-05	1.159E+00	4.198E+03
5.275E+07	8.000E-01	1.638E-05	1.161E+00	4.141E+03
5.138E+07	8.000E-01	1.417E-05	1.163E+00	4.076E+03
4.977E+07	8.000E-01	1.191E-05	1.166E+00	4.002E+03
4.977E+07	8.000E-01	1.191E-05	1.166E+00	4.002E+03
1.804E+07	0.	2.558E-05	1.314E+00	2.128E+03
1.804E+07	0.	2.558E-05	1.314E+00	2.128E+03
9.950E+06	0.	6.456E-06	1.387E+00	9.024E+02
9.950E+06	0.	6.456E-06	1.387E+00	9.024E+02
9.950E+06	0.	6.456E-06	1.387E+00	9.024E+02

H	PHI	RHO	GAM	T
5.388E+07	8.000E-01	1.851E-05	1.159E+00	4.196E+03
5.395E+07	8.000E-01	1.867E-05	1.159E+00	4.199E+03
5.212E+07	8.000E-01	1.543E-05	1.162E+00	4.112E+03
4.985E+07	8.000E-01	1.209E-05	1.166E+00	4.006E+03
4.682E+07	8.000E-01	8.606E-06	1.172E+00	3.871E+03
4.682E+07	8.000E-01	8.606E-06	1.172E+00	3.871E+03
1.539E+07	0.	2.138E-05	1.343E+00	1.742E+03
1.539E+07	0.	2.138E-05	1.343E+00	1.742E+03
9.950E+06	0.	6.456E-06	1.387E+00	9.024E+02
9.950E+06	0.	6.456E-06	1.387E+00	9.024E+02
9.950E+06	0.	6.456E-06	1.387E+00	9.024E+02

H	PHI	RHO	GAM	T
5.406E+07	8.000E-01	1.886E-05	1.159E+00	4.204E+03
5.406E+07	8.000E-01	1.885E-05	1.159E+00	4.204E+03
5.222E+07	8.000E-01	1.557E-05	1.162E+00	4.116E+03
4.993E+07	8.000E-01	1.218E-05	1.166E+00	4.010E+03
4.686E+07	8.000E-01	8.638E-06	1.171E+00	3.873E+03
4.686E+07	8.000E-01	8.638E-06	1.171E+00	3.873E+03
1.542E+07	0.	2.144E-05	1.343E+00	1.746E+03
1.542E+07	0.	2.144E-05	1.343E+00	1.746E+03
9.950E+06	0.	6.456E-06	1.387E+00	9.024E+02
9.950E+06	0.	6.456E-06	1.387E+00	9.024E+02
9.950E+06	0.	6.456E-06	1.387E+00	9.024E+02

J = 7

I	Z	P	Q	PHE	SI	M
1	0.	1.633E+02	8.687E+03	2.805E-03	-2.438E-02	2.773E+00
2	3.000E-01	1.632E+02	8.692E+03	2.177E-14	-3.471E-02	2.776E+00
3	3.000E-01	1.305E+02	8.903E+03	6.371E-02	-3.388E-02	2.883E+00

H	PHI	RHO	GAM	T
5.427E+07	8.000E-01	1.927E-05	1.159E+00	4.214E+03
5.427E+07	8.000E-01	1.926E-05	1.159E+00	4.214E+03
5.241E+07	8.000E-01	1.589E-05	1.162E+00	4.125E+03

4	3.000E-01	9.788E+01	9.160E+03	1.427E-01	-3.293E-02	3.021E+00
5	3.000E-01	6.522E+01	9.494E+03	2.484E-01	-3.178E-02	3.215E+00
6	3.000E-01	6.522E+01	9.494E+03	2.484E-01	-3.178E-02	3.215E+00
7	3.000E-01	6.522E+01	9.322E+03	2.483E-01	0.	4.631E+00
8	3.000E-01	6.522E+01	9.322E+03	2.483E-01	0.	4.631E+00
9	3.000E-01	1.000E+01	9.900E+03	0.	0.	6.755E+00
10	2.500E+01	1.000E+01	9.900E+03	0.	0.	6.755E+00
11	5.000E+01	1.000E+01	9.900E+03	0.	0.	6.755E+00

J = 8

I	Z	P	Q	PHE	SI	M
1	0.	1.657E+02	8.676E+03	5.768E-03	0.	2.765E+00
2	3.000E-01	1.663E+02	8.672E+03	8.390E-15	0.	2.764E+00
3	3.000E-01	1.329E+02	8.886E+03	6.420E-02	0.	2.872E+00
4	3.000E-01	9.948E+01	9.145E+03	1.439E-01	0.	3.011E+00
5	3.000E-01	6.607E+01	9.483E+03	2.507E-01	0.	3.206E+00
6	3.000E-01	6.607E+01	9.483E+03	2.507E-01	0.	3.206E+00
7	3.000E-01	6.607E+01	9.314E+03	2.506E-01	0.	4.613E+00
8	3.000E-01	6.607E+01	9.314E+03	2.506E-01	0.	4.613E+00
9	3.000E-01	1.000E+01	9.900E+03	0.	0.	6.755E+00
10	2.500E+01	1.000E+01	9.900E+03	0.	0.	6.755E+00
11	5.000E+01	1.000E+01	9.900E+03	0.	0.	6.755E+00

5.009E+07	8.000E-01	1.240E-05	1.166E+00	4.017E+03
4.697E+07	8.000E-01	8.753E-06	1.171E+00	3.878E+03
4.697E+07	8.000E-01	8.753E-06	1.171E+00	3.878E+03
1.551E+07	0.	2.160E-05	1.342E+00	1.759E+03
1.551E+07	0.	2.160E-05	1.342E+00	1.759E+03
9.950E+06	0.	6.456E-06	1.387E+00	9.024E+02
9.950E+06	0.	6.456E-06	1.387E+00	9.024E+02
9.950E+06	0.	6.456E-06	1.387E+00	9.024E+02

H	PHI	RHO	GAM	T
5.439E+07	8.000E-01	1.951E-05	1.159E+00	4.220E+03
5.443E+07	8.000E-01	1.957E-05	1.159E+00	4.222E+03
5.255E+07	8.000E-01	1.612E-05	1.162E+00	4.132E+03
5.021E+07	8.000E-01	1.257E-05	1.165E+00	4.023E+03
4.706E+07	8.000E-01	8.845E-06	1.171E+00	3.882E+03
4.706E+07	8.000E-01	8.845E-06	1.171E+00	3.882E+03
1.558E+07	0.	2.174E-05	1.341E+00	1.771E+03
1.558E+07	0.	2.174E-05	1.341E+00	1.771E+03
9.950E+06	0.	6.456E-06	1.387E+00	9.024E+02
9.950E+06	0.	6.456E-06	1.387E+00	9.024E+02
9.950E+06	0.	6.456E-06	1.387E+00	9.024E+02

ALPHA

J							
1	0.	0.	0.	0.	0.	0.	0.
2	0.	0.	0.	0.	0.	0.	0.
3	0.	0.	0.	0.	0.	0.	0.
4	0.	0.	0.	0.	0.	0.	0.
5	0.	0.	0.	0.	0.	0.	0.
6	0.	0.	0.	0.	0.	0.	0.
7	0.	0.	0.	0.	0.	0.	0.
8	0.	0.	0.	0.	0.	0.	0.

BETA

J							
1	4.347E-01	0.	3.184E-01	0.	0.	0.	0.
2	4.334E-01	0.	3.171E-01	0.	0.	0.	0.
3	4.346E-01	0.	3.182E-01	0.	0.	0.	0.
4	4.334E-01	0.	3.171E-01	0.	0.	0.	0.
5	3.570E-01	0.	2.449E-01	0.	0.	0.	0.
6	3.579E-01	0.	2.458E-01	0.	0.	0.	0.
7	3.606E-01	0.	2.484E-01	0.	0.	0.	0.
8	3.629E-01	0.	2.507E-01	0.	0.	0.	0.

IS

J							
1	17	0	15	0	0	0	0
2	17	0	15	0	0	0	0
3	17	0	15	0	0	0	0
4	17	0	15	0	0	0	0
5	9	0	7	0	0	0	0
6	9	0	7	0	0	0	0
7	9	0	7	0	0	0	0
8	9	0	7	0	0	0	0

KOUNT = 120 X = 1.50989E+01

TABLE IIc

Z MOMENT AXIS = -0. X MOMENT AXIS = -0.

THRUST =	3.810E+02	LIFT =	1.346E+03	PITCHING MOMENT =	1.124E+04
THRUST =	3.810E+02	LIFT =	1.333E+03	PITCHING MOMENT =	1.105E+04
THRUST =	3.810E+02	LIFT =	1.346E+03	PITCHING MOMENT =	1.124E+04

J = 1 Y = 0.

I	Z	P	Q	PHE	SI	M
1	-5.000E-01	2.240E+01	1.020E+04	0.	0.	3.724E+00
2	-1.381E-01	2.232E+01	1.021E+04	2.918E-02	0.	3.725E+00
3	2.359E-01	2.217E+01	1.021E+04	5.846E-02	0.	3.728E+00
4	6.247E-01	2.195E+01	1.022E+04	8.703E-02	0.	3.733E+00
5	1.029E+00	2.179E+01	1.022E+04	1.130E-01	0.	3.737E+00
6	1.453E+00	2.190E+01	1.022E+04	1.345E-01	0.	3.735E+00
7	1.894E+00	2.253E+01	1.020E+04	1.495E-01	0.	3.721E+00
8	2.345E+00	2.397E+01	1.016E+04	1.561E-01	0.	3.691E+00
9	2.783E+00	2.630E+01	1.010E+04	1.558E-01	0.	3.644E+00
10	3.181E+00	2.945E+01	1.003E+04	1.574E-01	0.	3.587E+00
11	3.597E+00	3.336E+01	9.939E+03	1.675E-01	0.	3.526E+00
12	3.814E+00	3.550E+01	9.897E+03	1.762E-01	0.	3.495E+00
13	3.814E+00	3.550E+01	9.385E+03	1.762E-01	0.	4.769E+00
14	4.251E+00	4.473E+01	9.347E+03	2.056E-01	0.	4.680E+00
15	5.054E+00	6.421E+01	9.332E+03	2.456E-01	0.	4.653E+00
16	5.054E+00	1.000E+01	9.900E+03	4.767E-14	0.	6.755E+00
17	2.500E+01	1.000E+01	9.900E+03	0.	0.	6.755E+00
18	5.000E+01	1.000E+01	9.900E+03	0.	0.	6.755E+00

J = 2 Y = 3.00000E-01

I	Z	P	Q	PHE	SI	M
1	-5.000E-01	2.311E+01	1.017E+04	0.	3.760E-02	3.713E+00
2	-1.156E-01	2.304E+01	1.017E+04	3.216E-02	3.782E-02	3.714E+00
3	2.737E-01	2.277E+01	1.018E+04	6.339E-02	3.673E-02	3.721E+00
4	6.690E-01	2.246E+01	1.019E+04	9.215E-02	3.587E-02	3.728E+00
5	1.077E+00	2.226E+01	1.020E+04	1.178E-01	3.519E-02	3.732E+00
6	1.499E+00	2.235E+01	1.020E+04	1.385E-01	3.466E-02	3.732E+00
7	1.924E+00	2.291E+01	1.018E+04	1.514E-01	3.492E-02	3.719E+00
8	2.352E+00	2.422E+01	1.015E+04	1.557E-01	3.570E-02	3.688E+00
9	2.779E+00	2.646E+01	1.009E+04	1.543E-01	3.586E-02	3.640E+00
10	3.165E+00	2.945E+01	1.002E+04	1.554E-01	3.086E-02	3.587E+00
11	3.569E+00	3.315E+01	9.940E+03	1.647E-01	2.574E-02	3.529E+00
12	3.787E+00	3.526E+01	9.899E+03	1.730E-01	2.071E-02	3.498E+00
13	3.787E+00	3.526E+01	9.389E+03	1.735E-01	1.045E-02	4.780E+00
14	4.223E+00	4.426E+01	9.355E+03	2.027E-01	1.304E-02	4.698E+00
15	5.032E+00	6.347E+01	9.338E+03	2.431E-01	1.496E-02	4.669E+00
16	5.032E+00	1.000E+01	9.900E+03	4.602E-14	-1.439E-15	6.755E+00
17	2.500E+01	1.000E+01	9.900E+03	0.	0.	6.755E+00
18	5.000E+01	1.000E+01	9.900E+03	0.	0.	6.755E+00

M	H	PHI	RHO	GAM	T
3.724E+00	3.996E+07	8.000E-01	3.529E-06	1.184E+00	3.599E+03
3.725E+00	3.994E+07	8.000E-01	3.519E-06	1.184E+00	3.598E+03
3.728E+00	3.990E+07	8.000E-01	3.500E-06	1.184E+00	3.594E+03
3.733E+00	3.983E+07	8.000E-01	3.470E-06	1.184E+00	3.587E+03
3.737E+00	3.978E+07	8.000E-01	3.448E-06	1.184E+00	3.582E+03
3.735E+00	3.983E+07	8.000E-01	3.464E-06	1.184E+00	3.587E+03
3.721E+00	4.001E+07	8.000E-01	3.546E-06	1.183E+00	3.603E+03
3.691E+00	4.041E+07	8.000E-01	3.739E-06	1.182E+00	3.617E+03
3.644E+00	4.101E+07	8.000E-01	4.043E-06	1.181E+00	3.639E+03
3.587E+00	4.175E+07	8.000E-01	4.449E-06	1.180E+00	3.665E+03
3.526E+00	4.263E+07	8.000E-01	4.948E-06	1.179E+00	3.698E+03
3.495E+00	4.305E+07	8.000E-01	5.214E-06	1.178E+00	3.714E+03
4.769E+00	1.491E+07	0.	1.234E-05	1.346E+00	1.672E+03
4.680E+00	1.527E+07	0.	1.506E-05	1.344E+00	1.724E+03
4.653E+00	1.541E+07	0.	2.143E-05	1.343E+00	1.746E+03
6.755E+00	9.950E+06	0.	6.456E-06	1.387E+00	9.024E+02
6.755E+00	9.950E+06	0.	6.456E-06	1.387E+00	9.024E+02
6.755E+00	9.950E+06	0.	6.456E-06	1.387E+00	9.024E+02

M	H	PHI	RHO	GAM	T
3.713E+00	4.020E+07	8.000E-01	3.638E-06	1.183E+00	3.610E+03
3.714E+00	4.017E+07	8.000E-01	3.627E-06	1.183E+00	3.609E+03
3.721E+00	4.010E+07	8.000E-01	3.592E-06	1.183E+00	3.607E+03
3.728E+00	4.000E+07	8.000E-01	3.550E-06	1.183E+00	3.603E+03
3.732E+00	3.994E+07	8.000E-01	3.524E-06	1.184E+00	3.598E+03
3.732E+00	3.997E+07	8.000E-01	3.537E-06	1.183E+00	3.602E+03
3.719E+00	4.012E+07	8.000E-01	3.609E-06	1.183E+00	3.608E+03
3.688E+00	4.048E+07	8.000E-01	3.777E-06	1.182E+00	3.620E+03
3.640E+00	4.104E+07	8.000E-01	4.064E-06	1.181E+00	3.640E+03
3.587E+00	4.174E+07	8.000E-01	4.448E-06	1.180E+00	3.665E+03
3.529E+00	4.259E+07	8.000E-01	4.921E-06	1.179E+00	3.697E+03
3.498E+00	4.300E+07	8.000E-01	5.184E-06	1.178E+00	3.712E+03
4.780E+00	1.487E+07	0.	1.230E-05	1.347E+00	1.665E+03
4.698E+00	1.519E+07	0.	1.500E-05	1.344E+00	1.713E+03
4.669E+00	1.535E+07	0.	2.130E-05	1.343E+00	1.736E+03
6.755E+00	9.950E+06	0.	6.456E-06	1.387E+00	9.024E+02
6.755E+00	9.950E+06	0.	6.456E-06	1.387E+00	9.024E+02
6.755E+00	9.950E+06	0.	6.456E-06	1.387E+00	9.024E+02

J = 3 Y = 6.00000E-01

I	Z	P	Q	PHE	SI	M
1	-5.000E-01	2.408E+01	1.016E+04	0.	6.785E-02	3.653E+00
2	-1.444E-01	2.396E+01	1.016E+04	2.918E-02	6.661E-02	3.654E+00
3	2.218E-01	2.379E+01	1.016E+04	5.812E-02	6.655E-02	3.655E+00
4	6.125E-01	2.352E+01	1.016E+04	8.720E-02	6.548E-02	3.658E+00
5	1.007E+00	2.330E+01	1.017E+04	1.131E-01	6.449E-02	3.662E+00
6	1.432E+00	2.315E+01	1.017E+04	1.354E-01	6.424E-02	3.662E+00
7	1.863E+00	2.353E+01	1.015E+04	1.501E-01	6.868E-02	3.671E+00
8	2.293E+00	2.462E+01	1.012E+04	1.554E-01	7.221E-02	3.672E+00
9	2.712E+00	2.661E+01	1.007E+04	1.533E-01	7.220E-02	3.641E+00

H	PHI	RHO	GAM	T
4.026E+07	8.000E-01	3.665E-06	1.183E+00	3.612E+03
4.022E+07	8.000E-01	3.648E-06	1.183E+00	3.611E+03
4.020E+07	8.000E-01	3.627E-06	1.183E+00	3.610E+03
4.014E+07	8.000E-01	3.589E-06	1.183E+00	3.608E+03
4.009E+07	8.000E-01	3.560E-06	1.183E+00	3.606E+03
4.006E+07	8.000E-01	3.537E-06	1.183E+00	3.605E+03
4.021E+07	8.000E-01	3.621E-06	1.183E+00	3.611E+03
4.058E+07	8.000E-01	3.813E-06	1.182E+00	3.623E+03
4.113E+07	8.000E-01	4.086E-06	1.181E+00	3.643E+03

10	3.106E+00	2.953E+01	1.001E+04	1.532E-01	6.279E-02	3.587E+00
11	3.520E+00	3.321E+01	9.926E+03	1.621E-01	5.305E-02	3.528E+00
12	3.779E+00	3.565E+01	9.883E+03	1.715E-01	4.344E-02	3.493E+00
13	3.779E+00	3.565E+01	9.382E+03	1.749E-01	2.041E-02	4.767E+00
14	4.204E+00	4.419E+01	9.355E+03	2.018E-01	2.519E-02	4.705E+00
15	5.017E+00	6.288E+01	9.341E+03	2.404E-01	2.765E-02	4.682E+00
16	5.017E+00	1.000E+01	9.900E+03	4.727E-14	1.615E-17	6.755E+00
17	2.500E+01	1.000E+01	9.900E+03	0.	0.	6.755E+00
18	5.000E+01	1.000E+01	9.900E+03	0.	0.	6.755E+00

J = 4 Y = 9.00000E-01

I	Z	P	Q	PHE	SI	M
1	-5.000E-01	2.485E+01	1.006E+04	0.	9.131E-02	3.775E+00
2	-1.277E-01	2.482E+01	1.006E+04	3.021E-02	9.331E-02	3.778E+00
3	2.525E-01	2.472E+01	1.007E+04	6.026E-02	9.038E-02	3.780E+00
4	6.406E-01	2.451E+01	1.008E+04	8.938E-02	8.930E-02	3.787E+00
5	1.040E+00	2.423E+01	1.009E+04	1.161E-01	8.864E-02	3.797E+00
6	1.458E+00	2.570E+01	1.002E+04	1.422E-01	1.222E-01	3.773E+00
7	1.875E+00	2.408E+01	1.009E+04	1.553E-01	1.017E-01	3.693E+00
8	2.270E+00	2.482E+01	1.007E+04	1.569E-01	1.082E-01	3.667E+00
9	2.632E+00	2.630E+01	1.003E+04	1.515E-01	1.117E-01	3.642E+00
10	3.002E+00	2.880E+01	9.985E+03	1.483E-01	9.855E-02	3.596E+00
11	3.401E+00	3.204E+01	9.928E+03	1.553E-01	8.377E-02	3.545E+00
12	3.704E+00	3.462E+01	9.887E+03	1.656E-01	7.057E-02	3.507E+00
13	3.704E+00	3.462E+01	9.388E+03	1.712E-01	3.336E-02	4.788E+00
14	4.130E+00	4.244E+01	9.370E+03	1.950E-01	3.922E-02	4.751E+00
15	4.962E+00	6.061E+01	9.359E+03	2.318E-01	4.217E-02	4.732E+00
16	4.962E+00	1.000E+01	9.900E+03	4.650E-14	-5.065E-15	6.755E+00
17	2.500E+01	1.000E+01	9.900E+03	0.	0.	6.755E+00
18	5.000E+01	1.000E+01	9.900E+03	0.	0.	6.755E+00

J = 5 Z = 1.47900E+00

I	Y	P	Q	PHE	SI	M
1	0.	2.562E+01	9.996E+03	1.224E-01	-1.418E-01	3.769E+00
2	6.264E-01	2.794E+01	9.940E+03	1.313E-01	-1.433E-01	3.652E+00
3	1.026E+00	2.978E+01	9.902E+03	1.467E-01	-1.444E-01	3.604E+00
4	1.428E+00	3.156E+01	9.866E+03	1.578E-01	-1.463E-01	3.563E+00
5	1.799E+00	3.309E+01	9.836E+03	1.645E-01	-1.473E-01	3.529E+00
6	1.799E+00	3.309E+01	9.520E+03	1.469E-01	-3.200E-02	5.146E+00
7	2.258E+00	3.958E+01	9.497E+03	1.708E-01	-2.881E-02	5.071E+00
8	2.968E+00	5.008E+01	9.467E+03	2.026E-01	-2.411E-02	4.989E+00
9	2.968E+00	1.000E+01	9.900E+03	6.056E-14	-1.534E-14	6.755E+00
10	2.500E+01	1.000E+01	9.900E+03	0.	-1.998E-15	6.755E+00
11	5.000E+01	1.000E+01	9.900E+03	0.	0.	6.755E+00

3.567E+00	4.180E+07	8.000E-01	4.461E-06	1.180E+00	3.667E+03
3.528E+00	4.262E+07	8.000E-01	4.932E-06	1.179E+00	3.698E+03
3.493E+00	4.310E+07	8.000E-01	5.236E-06	1.178E+00	3.716E+03
4.767E+00	1.492E+07	0.	1.239E-05	1.346E+00	1.673E+03
4.705E+00	1.517E+07	0.	1.502E-05	1.344E+00	1.710E+03
4.682E+00	1.529E+07	0.	2.120E-05	1.343E+00	1.728E+03
6.755E+00	9.950E+06	0.	6.456E-06	1.387E+00	9.024E+02
6.755E+00	9.950E+06	0.	6.456E-06	1.387E+00	9.024E+02
6.755E+00	9.950E+06	0.	6.456E-06	1.387E+00	9.024E+02

M	H	PHI	RHO	GAM	T
3.775E+00	4.082E+07	8.000E-01	4.094E-06	1.181E+00	3.632E+03
3.778E+00	4.083E+07	8.000E-01	4.094E-06	1.181E+00	3.632E+03
3.780E+00	4.080E+07	8.000E-01	4.079E-06	1.181E+00	3.631E+03
3.787E+00	4.074E+07	8.000E-01	4.053E-06	1.181E+00	3.629E+03
3.797E+00	4.068E+07	8.000E-01	4.024E-06	1.182E+00	3.627E+03
3.773E+00	4.102E+07	8.000E-01	4.239E-06	1.181E+00	3.639E+03
3.693E+00	4.048E+07	8.000E-01	3.771E-06	1.182E+00	3.620E+03
3.667E+00	4.064E+07	8.000E-01	3.846E-06	1.182E+00	3.625E+03
3.642E+00	4.104E+07	8.000E-01	4.046E-06	1.181E+00	3.640E+03
3.596E+00	4.161E+07	8.000E-01	4.367E-06	1.180E+00	3.660E+03
3.545E+00	4.236E+07	8.000E-01	4.782E-06	1.179E+00	3.688E+03
3.507E+00	4.288E+07	8.000E-01	5.106E-06	1.178E+00	3.708E+03
4.788E+00	1.483E+07	0.	1.212E-05	1.347E+00	1.660E+03
4.751E+00	1.499E+07	0.	1.466E-05	1.346E+00	1.683E+03
4.732E+00	1.509E+07	0.	2.081E-05	1.345E+00	1.697E+03
6.755E+00	9.950E+06	0.	6.456E-06	1.387E+00	9.024E+02
6.755E+00	9.950E+06	0.	6.456E-06	1.387E+00	9.024E+02
6.755E+00	9.950E+06	0.	6.456E-06	1.387E+00	9.024E+02

M	H	PHI	RHO	GAM	T
3.769E+00	4.099E+07	8.000E-01	4.216E-06	1.181E+00	3.638E+03
3.652E+00	4.153E+07	8.000E-01	4.361E-06	1.180E+00	3.657E+03
3.604E+00	4.191E+07	8.000E-01	4.557E-06	1.180E+00	3.671E+03
3.563E+00	4.225E+07	8.000E-01	4.749E-06	1.179E+00	3.684E+03
3.529E+00	4.254E+07	8.000E-01	4.913E-06	1.179E+00	3.695E+03
5.146E+00	1.359E+07	0.	1.310E-05	1.356E+00	1.473E+03
5.071E+00	1.382E+07	0.	1.527E-05	1.354E+00	1.507E+03
4.989E+00	1.412E+07	0.	1.879E-05	1.352E+00	1.553E+03
6.755E+00	9.950E+06	0.	6.456E-06	1.387E+00	9.024E+02
6.755E+00	9.950E+06	0.	6.456E-06	1.387E+00	9.024E+02
6.755E+00	9.950E+06	0.	6.456E-06	1.387E+00	9.024E+02

J = 6 Z = 8.19333E-01

I	Y	P	Q	PHE	SI	M
1	0.	2.439E+01	1.007E+04	8.946E-02	-1.009E-01	3.791E+00
2	6.376E-01	2.910E+01	9.967E+03	1.251E-01	-1.001E-01	3.640E+00
3	1.053E+00	3.202E+01	9.914E+03	1.418E-01	-9.837E-02	3.571E+00
4	1.501E+00	3.515E+01	9.860E+03	1.519E-01	-9.571E-02	3.512E+00
5	1.964E+00	3.831E+01	9.809E+03	1.581E-01	-9.176E-02	3.459E+00
6	1.964E+00	3.831E+01	9.483E+03	1.701E-01	-2.199E-02	5.034E+00
7	2.374E+00	4.426E+01	9.458E+03	1.897E-01	-2.135E-02	4.962E+00
8	3.047E+00	5.389E+01	9.430E+03	2.150E-01	-1.974E-02	4.891E+00
9	3.047E+00	1.000E+01	9.900E+03	4.779E-14	3.616E-17	6.755E+00
10	2.500E+01	1.000E+01	9.900E+03	0.	-4.823E-16	6.755E+00
11	5.000E+01	1.000E+01	9.900E+03	0.	0.	6.755E+00

J = 7 Z = 1.59667E-01

I	Y	P	Q	PHE	SI	M
1	0.	2.474E+01	1.010E+04	9.123E-02	-5.270E-02	3.779E+00

H	PHI	RHO	GAM	T
4.071E+07	8.000E-01	4.040E-06	1.181E+00	3.628E+03
4.183E+07	8.000E-01	4.532E-06	1.180E+00	3.668E+03
4.242E+07	8.000E-01	4.851E-06	1.179E+00	3.690E+03
4.301E+07	8.000E-01	5.206E-06	1.178E+00	3.713E+03
4.359E+07	8.000E-01	5.560E-06	1.177E+00	3.735E+03
1.397E+07	0.	1.460E-05	1.353E+00	1.530E+03
1.421E+07	0.	1.645E-05	1.351E+00	1.566E+03
1.447E+07	0.	1.956E-05	1.349E+00	1.605E+03
9.950E+06	0.	6.456E-06	1.387E+00	9.024E+02
9.950E+06	0.	6.456E-06	1.387E+00	9.024E+02
9.950E+06	0.	6.456E-06	1.387E+00	9.024E+02

H	PHI	RHO	GAM	T
4.081E+07	8.000E-01	4.083E-06	1.181E+00	3.631E+03

2	6.732E-01	2.984E+01	9.990E+03	1.327E-01	-4.944E-02	3.623E+00
3	1.117E+00	3.299E+01	9.936E+03	1.534E-01	-4.576E-02	3.556E+00
4	1.571E+00	3.617E+01	9.877E+03	1.665E-01	-4.685E-02	3.498E+00
5	2.025E+00	3.932E+01	9.820E+03	1.745E-01	-4.797E-02	3.446E+00
6	2.025E+00	3.932E+01	9.473E+03	1.768E-01	-1.438E-02	5.003E+00
7	2.430E+00	4.573E+01	9.444E+03	1.965E-01	-1.007E-02	4.921E+00
8	3.090E+00	5.550E+01	9.416E+03	2.205E-01	-9.498E-03	4.852E+00
9	3.090E+00	1.000E+01	9.900E+03	5.893E-14	-2.737E-14	6.755E+00
10	2.500E+01	1.000E+01	9.900E+03	0.	2.570E-17	6.755E+00
11	5.000E+01	1.000E+01	9.900E+03	0.	0.	6.755E+00

4.198E+07	8.000E-01	4.618E-06	1.180E+00	3.674E+03
4.261E+07	8.000E-01	4.970E-06	1.179E+00	3.697E+03
4.319E+07	8.000E-01	5.331E-06	1.178E+00	3.719E+03
4.374E+07	8.000E-01	5.685E-06	1.177E+00	3.741E+03
1.408E+07	0.	1.483E-05	1.352E+00	1.546E+03
1.436E+07	0.	1.676E-05	1.350E+00	1.588E+03
1.462E+07	0.	1.987E-05	1.348E+00	1.628E+03
9.950E+06	0.	6.456E-06	1.387E+00	9.024E+02
9.950E+06	0.	6.456E-06	1.387E+00	9.024E+02
9.950E+06	0.	6.456E-06	1.387E+00	9.024E+02

SIDEWALL

J = 8

I	X / Y	Z / P	U / Q	W / PHE	V / SI	M
	1.510E+01	-5.000E-01	1.006E+04	9.216E+02	-0.	
1	0.	2.485E+01	1.011E+04	9.131E-02	0.	3.775E+00
	1.510E+01	-5.000E-01	9.906E+03	1.402E+03	0.	
2	6.732E-01	3.005E+01	1.000E+04	1.406E-01	0.	3.622E+00
	1.510E+01	-5.000E-01	9.830E+03	1.599E+03	0.	
3	1.117E+00	3.314E+01	9.960E+03	1.612E-01	0.	3.560E+00
	1.510E+01	-5.000E-01	9.736E+03	1.729E+03	0.	
4	1.571E+00	3.653E+01	9.889E+03	1.758E-01	0.	3.496E+00
	1.510E+01	-5.000E-01	9.612E+03	1.961E+03	0.	
5	2.047E+00	4.032E+01	9.810E+03	2.012E-01	0.	3.432E+00
	1.510E+01	-5.000E-01	9.273E+03	1.891E+03	0.	
6	2.047E+00	4.032E+01	9.464E+03	2.012E-01	0.	4.975E+00
	1.510E+01	-5.000E-01	9.287E+03	1.827E+03	0.	
7	2.430E+00	4.541E+01	9.465E+03	1.942E-01	0.	4.967E+00
	1.510E+01	-5.000E-01	9.038E+03	2.289E+03	0.	
8	3.105E+00	6.511E+01	9.323E+03	2.480E-01	0.	4.633E+00
	1.510E+01	-5.000E-01	9.900E+03	0.	0.	
9	3.105E+00	1.000E+01	9.900E+03	0.	0.	6.755E+00
	1.510E+01	-5.000E-01	9.900E+03	0.	0.	
10	2.500E+01	1.000E+01	9.900E+03	0.	0.	6.755E+00
	1.510E+01	-5.000E-01	9.900E+03	0.	0.	
11	5.000E+01	1.000E+01	9.900E+03	0.	0.	6.755E+00

H	PHI	RHO	GAM	T
4.082E+07	8.000E-01	4.094E-06	1.181E+00	3.632E+03
4.204E+07	8.000E-01	4.646E-06	1.179E+00	3.676E+03
4.265E+07	8.000E-01	4.990E-06	1.178E+00	3.699E+03
4.326E+07	8.000E-01	5.376E-06	1.177E+00	3.722E+03
4.391E+07	8.000E-01	5.806E-06	1.176E+00	3.748E+03
1.417E+07	0.	1.506E-05	1.352E+00	1.561E+03
1.421E+07	0.	1.690E-05	1.351E+00	1.567E+03
1.549E+07	0.	2.158E-05	1.342E+00	1.758E+03
9.950E+06	0.	6.456E-06	1.387E+00	9.024E+02
9.950E+06	0.	6.456E-06	1.387E+00	9.024E+02
9.950E+06	0.	6.456E-06	1.387E+00	9.024E+02

ALP

J							
1	0.	0.	0.	0.	0.	0.	0.
2	-6.207E-02	0.	-5.905E-02	0.	0.	0.	0.
3	-1.157E-01	0.	-1.373E-01	0.	0.	0.	0.
4	-1.816E-01	0.	-2.435E-01	0.	0.	0.	0.
5	1.193E-01	0.	2.440E-01	0.	0.	0.	0.
6	9.229E-02	0.	1.693E-01	0.	0.	0.	0.
7	4.346E-02	0.	6.343E-02	0.	0.	0.	0.
8	0.	0.	0.	0.	0.	0.	0.

ALPHA

J							
1	0.	0.	0.	0.	0.	0.	0.
2	-5.818E-02	0.	-5.816E-02	0.	0.	0.	0.
3	-1.085E-01	0.	-1.351E-01	0.	0.	0.	0.
4	-1.707E-01	0.	-2.399E-01	0.	0.	0.	0.
5	1.133E-01	0.	2.416E-01	0.	0.	0.	0.
6	8.737E-02	0.	1.668E-01	0.	0.	0.	0.
7	4.108E-02	0.	6.243E-02	0.	0.	0.	0.
8	0.	0.	0.	0.	0.	0.	0.

BETA

J							
1	3.577E-01	0.	1.762E-01	0.	0.	0.	0.
2	3.563E-01	0.	1.740E-01	0.	0.	0.	0.
3	3.562E-01	0.	1.780E-01	0.	0.	0.	0.
4	3.528E-01	0.	1.762E-01	0.	0.	0.	0.
5	3.180E-01	0.	1.421E-01	0.	0.	0.	0.
6	3.289E-01	0.	1.739E-01	0.	0.	0.	0.
7	3.328E-01	0.	1.777E-01	0.	0.	0.	0.
8	3.603E-01	0.	2.012E-01	0.	0.	0.	0.

IS

J							
1	16	0	13	0	0	0	0
2	16	0	13	0	0	0	0
3	16	0	13	0	0	0	0
4	16	0	13	0	0	0	0
5	9	0	6	0	0	0	0
6	9	0	6	0	0	0	0
7	9	0	6	0	0	0	0
8	9	0	6	0	0	0	0

3.483E+00	IIIII	2.225E+00	IIIII	IIIII	IIIII	IIIII
-6.397E-01	IIIII	-5.528E-01	IIIII	IIIII	IIIII	IIIII
-3.782E-02	IIIII	-9.898E-02	IIIII	IIIII	IIIII	IIIII
1.505E-01	IIIII	1.772E-01	IIIII	IIIII	IIIII	IIIII

EXTERNAL WRAP AROUND REGION

I = 7

R	TH	P	Q	PHE	SI
3.956E-01	0.	2.408E+01	1.009E+04	1.553E-01	1.017E-01
3.872E-01	1.745E-01	2.441E+01	1.008E+04	1.519E-01	7.197E-02
3.787E-01	3.491E-01	2.473E+01	1.006E+04	1.485E-01	4.293E-02
3.703E-01	5.236E-01	2.505E+01	1.005E+04	1.452E-01	1.452E-02
3.619E-01	6.981E-01	2.536E+01	1.003E+04	1.420E-01	-1.325E-02
3.535E-01	8.727E-01	2.566E+01	1.002E+04	1.388E-01	-4.039E-02
3.451E-01	1.047E+00	2.596E+01	1.001E+04	1.357E-01	-6.688E-02
3.367E-01	1.222E+00	2.625E+01	9.993E+03	1.327E-01	-9.274E-02
3.283E-01	1.396E+00	2.653E+01	9.980E+03	1.298E-01	-1.180E-01
3.199E-01	1.571E+00	2.680E+01	9.968E+03	1.270E-01	-1.425E-01

I = 8

R	TH	P	Q	PHE	SI
7.909E-01	0.	2.482E+01	1.007E+04	1.569E-01	1.082E-01
7.741E-01	1.745E-01	2.521E+01	1.005E+04	1.538E-01	7.762E-02
7.573E-01	3.491E-01	2.559E+01	1.004E+04	1.508E-01	4.770E-02
7.404E-01	5.236E-01	2.596E+01	1.002E+04	1.479E-01	1.844E-02
7.236E-01	6.981E-01	2.632E+01	1.001E+04	1.451E-01	-1.016E-02
7.068E-01	8.727E-01	2.667E+01	9.994E+03	1.423E-01	-3.810E-02
6.900E-01	1.047E+00	2.702E+01	9.979E+03	1.396E-01	-6.539E-02
6.732E-01	1.222E+00	2.735E+01	9.966E+03	1.369E-01	-9.202E-02
6.564E-01	1.396E+00	2.768E+01	9.952E+03	1.344E-01	-1.180E-01
6.395E-01	1.571E+00	2.800E+01	9.939E+03	1.318E-01	-1.433E-01

I = 9

R	TH	P	Q	PHE	SI
1.153E+00	0.	2.630E+01	1.003E+04	1.515E-01	1.117E-01
1.129E+00	1.745E-01	2.667E+01	1.002E+04	1.505E-01	8.057E-02
1.104E+00	3.491E-01	2.704E+01	1.000E+04	1.495E-01	5.015E-02
1.080E+00	5.236E-01	2.739E+01	9.987E+03	1.485E-01	2.040E-02
1.055E+00	6.981E-01	2.774E+01	9.974E+03	1.475E-01	-8.690E-03
1.031E+00	8.727E-01	2.808E+01	9.961E+03	1.466E-01	-3.711E-02
1.006E+00	1.047E+00	2.841E+01	9.948E+03	1.457E-01	-6.486E-02
9.816E-01	1.222E+00	2.873E+01	9.935E+03	1.448E-01	-9.194E-02
9.570E-01	1.396E+00	2.904E+01	9.923E+03	1.440E-01	-1.184E-01
9.325E-01	1.571E+00	2.935E+01	9.911E+03	1.431E-01	-1.441E-01

I = 10

R	TH	P	Q	PHE	SI
1.523E+00	0.	2.880E+01	9.985E+03	1.483E-01	9.855E-02
1.491E+00	1.745E-01	2.903E+01	9.972E+03	1.488E-01	6.890E-02
1.459E+00	3.491E-01	2.925E+01	9.960E+03	1.492E-01	3.989E-02
1.426E+00	5.236E-01	2.947E+01	9.949E+03	1.497E-01	1.151E-02
1.394E+00	6.981E-01	2.969E+01	9.937E+03	1.502E-01	-1.623E-02
1.361E+00	8.727E-01	2.990E+01	9.926E+03	1.507E-01	-4.333E-02
1.329E+00	1.047E+00	3.010E+01	9.915E+03	1.511E-01	-6.979E-02
1.297E+00	1.222E+00	3.030E+01	9.904E+03	1.515E-01	-9.562E-02
1.264E+00	1.396E+00	3.050E+01	9.894E+03	1.520E-01	-1.208E-01
1.232E+00	1.571E+00	3.069E+01	9.883E+03	1.524E-01	-1.454E-01

H	PHI	RHO	GAM
4.048E+07	8.000E-01	3.771E-06	1.182E+00
4.057E+07	8.000E-01	3.834E-06	1.182E+00
4.067E+07	8.000E-01	3.896E-06	1.182E+00
4.076E+07	8.000E-01	3.956E-06	1.182E+00
4.085E+07	8.000E-01	4.015E-06	1.181E+00
4.094E+07	8.000E-01	4.073E-06	1.181E+00
4.102E+07	8.000E-01	4.129E-06	1.181E+00
4.110E+07	8.000E-01	4.184E-06	1.181E+00
4.119E+07	8.000E-01	4.238E-06	1.181E+00
4.126E+07	8.000E-01	4.290E-06	1.181E+00

H	PHI	RHO	GAM
4.064E+07	8.000E-01	3.846E-06	1.182E+00
4.075E+07	8.000E-01	3.909E-06	1.182E+00
4.086E+07	8.000E-01	3.971E-06	1.182E+00
4.096E+07	8.000E-01	4.032E-06	1.181E+00
4.106E+07	8.000E-01	4.092E-06	1.181E+00
4.116E+07	8.000E-01	4.150E-06	1.181E+00
4.126E+07	8.000E-01	4.206E-06	1.181E+00
4.136E+07	8.000E-01	4.261E-06	1.181E+00
4.145E+07	8.000E-01	4.315E-06	1.180E+00
4.154E+07	8.000E-01	4.368E-06	1.180E+00

H	PHI	RHO	GAM
4.104E+07	8.000E-01	4.046E-06	1.181E+00
4.114E+07	8.000E-01	4.103E-06	1.181E+00
4.123E+07	8.000E-01	4.158E-06	1.181E+00
4.132E+07	8.000E-01	4.212E-06	1.181E+00
4.141E+07	8.000E-01	4.265E-06	1.181E+00
4.149E+07	8.000E-01	4.317E-06	1.180E+00
4.158E+07	8.000E-01	4.367E-06	1.180E+00
4.166E+07	8.000E-01	4.417E-06	1.180E+00
4.174E+07	8.000E-01	4.465E-06	1.180E+00
4.182E+07	8.000E-01	4.511E-06	1.180E+00

H	PHI	RHO	GAM
4.161E+07	8.000E-01	4.367E-06	1.180E+00
4.167E+07	8.000E-01	4.402E-06	1.180E+00
4.172E+07	8.000E-01	4.436E-06	1.180E+00
4.178E+07	8.000E-01	4.470E-06	1.180E+00
4.183E+07	8.000E-01	4.503E-06	1.180E+00
4.189E+07	8.000E-01	4.535E-06	1.180E+00
4.194E+07	8.000E-01	4.566E-06	1.180E+00
4.199E+07	8.000E-01	4.597E-06	1.180E+00
4.204E+07	8.000E-01	4.626E-06	1.180E+00
4.208E+07	8.000E-01	4.656E-06	1.179E+00

R	TH	P	Q	PHE	SI
1.922E+00	0.	3.204E+01	9.928E+03	1.553E-01	8.377E-02
1.881E+00	1.745E-01	3.204E+01	9.919E+03	1.559E-01	5.576E-02
1.840E+00	3.491E-01	3.205E+01	9.910E+03	1.565E-01	2.835E-02
1.799E+00	5.236E-01	3.205E+01	9.902E+03	1.570E-01	1.546E-03
1.759E+00	6.981E-01	3.206E+01	9.894E+03	1.576E-01	-2.466E-02

H	PHI	RHO	GAM
4.236E+07	8.000E-01	4.782E-06	1.179E+00
4.236E+07	8.000E-01	4.785E-06	1.179E+00
4.236E+07	8.000E-01	4.788E-06	1.179E+00
4.236E+07	8.000E-01	4.790E-06	1.179E+00
4.235E+07	8.000E-01	4.793E-06	1.179E+00

1.718E+00	8.727E-01	3.206E+01	9.886E+03	1.581E-01	-5.026E-02
1.677E+00	1.047E+00	3.207E+01	9.878E+03	1.586E-01	-7.526E-02
1.636E+00	1.222E+00	3.207E+01	9.870E+03	1.591E-01	-9.966E-02
1.595E+00	1.396E+00	3.207E+01	9.863E+03	1.596E-01	-1.235E-01
1.554E+00	1.571E+00	3.208E+01	9.856E+03	1.601E-01	-1.467E-01

I = 12

R	TH	P	Q	PHE	SI
2.225E+00	0.	3.462E+01	9.887E+03	1.656E-01	7.057E-02
2.178E+00	1.745E-01	3.443E+01	9.881E+03	1.654E-01	4.408E-02
2.130E+00	3.491E-01	3.425E+01	9.875E+03	1.653E-01	1.817E-02
2.083E+00	5.236E-01	3.407E+01	9.869E+03	1.652E-01	-7.177E-03
2.036E+00	6.981E-01	3.390E+01	9.863E+03	1.650E-01	-3.195E-02
1.989E+00	8.727E-01	3.373E+01	9.857E+03	1.649E-01	-5.616E-02
1.941E+00	1.047E+00	3.357E+01	9.852E+03	1.648E-01	-7.980E-02
1.894E+00	1.222E+00	3.340E+01	9.846E+03	1.647E-01	-1.029E-01
1.847E+00	1.396E+00	3.325E+01	9.841E+03	1.646E-01	-1.254E-01
1.799E+00	1.571E+00	3.309E+01	9.836E+03	1.645E-01	-1.473E-01

4.235E+07	8.000E-01	4.795E-06	1.179E+00
4.235E+07	8.000E-01	4.798E-06	1.179E+00
4.235E+07	8.000E-01	4.800E-06	1.179E+00
4.235E+07	8.000E-01	4.803E-06	1.179E+00
4.235E+07	8.000E-01	4.805E-06	1.179E+00

H	PHI	RHO	GAM
4.288E+07	8.000E-01	5.106E-06	1.178E+00
4.284E+07	8.000E-01	5.083E-06	1.178E+00
4.280E+07	8.000E-01	5.060E-06	1.178E+00
4.276E+07	8.000E-01	5.037E-06	1.178E+00
4.272E+07	8.000E-01	5.015E-06	1.178E+00
4.269E+07	8.000E-01	4.994E-06	1.179E+00
4.265E+07	8.000E-01	4.973E-06	1.179E+00
4.261E+07	8.000E-01	4.953E-06	1.179E+00
4.258E+07	8.000E-01	4.933E-06	1.179E+00
4.254E+07	8.000E-01	4.913E-06	1.179E+00

I = 13

R	TH	P	Q	PHE	SI
2.225E+00	0.	3.462E+01	9.388E+03	1.712E-01	3.336E-02
2.178E+00	1.745E-01	3.443E+01	9.443E+03	1.703E-01	1.140E-02
2.130E+00	3.491E-01	3.425E+01	9.496E+03	1.695E-01	-1.009E-02
2.083E+00	5.236E-01	3.407E+01	9.548E+03	1.688E-01	-3.111E-02
2.036E+00	6.981E-01	3.390E+01	9.599E+03	1.680E-01	-5.165E-02
1.989E+00	8.727E-01	3.373E+01	9.649E+03	1.673E-01	-7.173E-02

I = 13

R	TH	P	Q	PHE	SI
2.225E+00	0.	3.462E+01	9.388E+03	1.712E-01	3.336E-02
2.178E+00	1.745E-01	3.443E+01	9.443E+03	1.703E-01	1.140E-02
2.130E+00	3.491E-01	3.425E+01	9.496E+03	1.695E-01	-1.009E-02
2.083E+00	5.236E-01	3.407E+01	9.548E+03	1.688E-01	-3.111E-02
2.036E+00	6.981E-01	3.390E+01	9.599E+03	1.680E-01	-5.165E-02
1.989E+00	8.727E-01	3.373E+01	9.649E+03	1.673E-01	-7.173E-02
1.941E+00	1.047E+00	3.357E+01	9.697E+03	1.665E-01	-9.133E-02
1.894E+00	1.222E+00	3.340E+01	9.745E+03	1.658E-01	-1.105E-01
1.847E+00	1.396E+00	3.325E+01	9.791E+03	1.651E-01	-1.291E-01
1.799E+00	1.571E+00	3.309E+01	9.836E+03	1.645E-01	-1.473E-01

I = 14

R	TH	P	Q	PHE	SI
2.651E+00	0.	4.244E+01	9.370E+03	1.950E-01	3.922E-02
2.601E+00	1.745E-01	4.199E+01	9.385E+03	1.917E-01	3.098E-02
2.550E+00	3.491E-01	4.155E+01	9.401E+03	1.885E-01	2.289E-02
2.499E+00	5.236E-01	4.112E+01	9.416E+03	1.853E-01	1.497E-02
2.449E+00	6.981E-01	4.069E+01	9.431E+03	1.822E-01	7.202E-03
2.398E+00	8.727E-01	4.028E+01	9.445E+03	1.791E-01	-4.052E-04
2.347E+00	1.047E+00	3.987E+01	9.459E+03	1.762E-01	-7.853E-03
2.297E+00	1.222E+00	3.947E+01	9.473E+03	1.732E-01	-1.514E-02
2.246E+00	1.396E+00	3.908E+01	9.487E+03	1.704E-01	-2.227E-02
2.195E+00	1.571E+00	3.870E+01	9.500E+03	1.676E-01	-2.924E-02

I = 15

R	TH	P	Q	PHE	SI
3.483E+00	0.	6.061E+01	9.359E+03	2.318E-01	4.217E-02
3.426E+00	1.745E-01	5.936E+01	9.371E+03	2.284E-01	3.428E-02
3.369E+00	3.491E-01	5.812E+01	9.384E+03	2.249E-01	2.653E-02
3.311E+00	5.236E-01	5.691E+01	9.397E+03	2.216E-01	1.890E-02
3.254E+00	6.981E-01	5.572E+01	9.409E+03	2.183E-01	1.141E-02

H	PHI	RHO	GAM
1.483E+07	0.	1.212E-05	1.347E+00
1.820E+07	9.725E-02	1.124E-05	1.326E+00
2.150E+07	1.924E-01	1.038E-05	1.306E+00
2.472E+07	2.855E-01	9.545E-06	1.287E+00
2.787E+07	3.765E-01	8.726E-06	1.268E+00
3.095E+07	4.653E-01	7.926E-06	1.249E+00

H	PHI	RHO	GAM
1.483E+07	0.	1.212E-05	1.347E+00
1.820E+07	9.725E-02	1.124E-05	1.326E+00
2.150E+07	1.924E-01	1.038E-05	1.306E+00
2.472E+07	2.855E-01	9.545E-06	1.287E+00
2.787E+07	3.765E-01	8.726E-06	1.268E+00
3.095E+07	4.653E-01	7.926E-06	1.249E+00
3.396E+07	5.521E-01	7.145E-06	1.231E+00
3.689E+07	6.368E-01	6.382E-06	1.213E+00
3.975E+07	7.195E-01	5.638E-06	1.196E+00
4.254E+07	8.000E-01	4.913E-06	1.179E+00

H	PHI	RHO	GAM
1.499E+07	0.	1.466E-05	1.346E+00
1.484E+07	0.	1.470E-05	1.347E+00
1.470E+07	0.	1.474E-05	1.348E+00
1.456E+07	0.	1.477E-05	1.349E+00
1.443E+07	0.	1.481E-05	1.350E+00
1.429E+07	0.	1.485E-05	1.351E+00
1.416E+07	0.	1.488E-05	1.352E+00
1.404E+07	0.	1.491E-05	1.353E+00
1.391E+07	0.	1.495E-05	1.354E+00
1.379E+07	0.	1.498E-05	1.355E+00

H	PHI	RHO	GAM
1.509E+07	0.	2.081E-05	1.345E+00
1.497E+07	0.	2.057E-05	1.346E+00
1.486E+07	0.	2.033E-05	1.347E+00
1.475E+07	0.	2.010E-05	1.347E+00
1.464E+07	0.	1.987E-05	1.348E+00

3.197E+00	8.727E-01	5.455E+01	9.421E+03	2.150E-01	4.040E-03
3.140E+00	1.047E+00	5.340E+01	9.433E+03	2.119E-01	-3.194E-03
3.083E+00	1.222E+00	5.227E+01	9.444E+03	2.087E-01	-1.030E-02
3.025E+00	1.396E+00	5.117E+01	9.455E+03	2.057E-01	-1.727E-02
2.968E+00	1.571E+00	5.008E+01	9.467E+03	2.026E-01	-2.411E-02

I = 16

R	TH	P	Q	PHE	SI
3.483E+00	0.	1.000E+01	9.900E+03	4.650E-14	-5.065E-15
3.426E+00	1.745E-01	1.477E+01	9.848E+03	2.411E-02	-2.869E-03
3.369E+00	3.491E-01	1.946E+01	9.798E+03	4.783E-02	-5.691E-03
3.311E+00	5.236E-01	2.407E+01	9.748E+03	7.114E-02	-8.466E-03
3.254E+00	6.981E-01	2.860E+01	9.699E+03	9.406E-02	-1.119E-02
3.197E+00	8.727E-01	3.306E+01	9.651E+03	1.166E-01	-1.387E-02
3.140E+00	1.047E+00	3.743E+01	9.603E+03	1.387E-01	-1.650E-02
3.083E+00	1.222E+00	4.173E+01	9.557E+03	1.604E-01	-1.909E-02
3.025E+00	1.396E+00	4.594E+01	9.511E+03	1.817E-01	-2.163E-02
2.968E+00	1.571E+00	5.008E+01	9.467E+03	2.026E-01	-2.411E-02

I = 17

R	TH	P	Q	PHE	SI
2.352E+01	0.	1.000E+01	9.900E+03	0.	0.
2.369E+01	1.745E-01	1.000E+01	9.900E+03	8.732E-29	-2.160E-16
2.385E+01	3.491E-01	1.000E+01	9.900E+03	1.753E-28	-4.335E-16
2.401E+01	5.236E-01	1.000E+01	9.900E+03	2.638E-28	-6.525E-16
2.418E+01	6.981E-01	1.000E+01	9.900E+03	3.529E-28	-8.730E-16
2.434E+01	8.727E-01	1.000E+01	9.900E+03	4.427E-28	-1.095E-15
2.451E+01	1.047E+00	1.000E+01	9.900E+03	5.331E-28	-1.319E-15
2.467E+01	1.222E+00	1.000E+01	9.900E+03	6.240E-28	-1.544E-15
2.484E+01	1.396E+00	1.000E+01	9.900E+03	7.156E-28	-1.770E-15
2.500E+01	1.571E+00	1.000E+01	9.900E+03	8.078E-28	-1.998E-15

1.453E+07	0.	1.965E-05	1.349E+00
1.443E+07	0.	1.943E-05	1.350E+00
1.432E+07	0.	1.921E-05	1.351E+00
1.422E+07	0.	1.900E-05	1.351E+00
1.412E+07	0.	1.879E-05	1.352E+00

H	PHI	RHO	GAM
9.950E+06	0.	6.456E-06	1.387E+00
1.045E+07	0.	7.924E-06	1.383E+00
1.093E+07	0.	9.368E-06	1.379E+00
1.141E+07	0.	1.079E-05	1.375E+00
1.189E+07	0.	1.218E-05	1.371E+00
1.235E+07	0.	1.355E-05	1.367E+00
1.280E+07	0.	1.490E-05	1.363E+00
1.325E+07	0.	1.622E-05	1.359E+00
1.369E+07	0.	1.752E-05	1.356E+00
1.412E+07	0.	1.879E-05	1.352E+00

H	PHI	RHO	GAM
9.950E+06	0.	6.456E-06	1.387E+00
9.950E+06	0.	6.456E-06	1.387E+00
9.950E+06	0.	6.456E-06	1.387E+00
9.950E+06	0.	6.456E-06	1.387E+00
9.950E+06	0.	6.456E-06	1.387E+00
9.950E+06	0.	6.456E-06	1.387E+00
9.950E+06	0.	6.456E-06	1.387E+00
9.950E+06	0.	6.456E-06	1.387E+00
9.950E+06	0.	6.456E-06	1.387E+00
9.950E+06	0.	6.456E-06	1.387E+00

KOUNT = 0 X = 2.74900E+01

TABLE IIIa

J = 1 THETA = 0.

I	R	P	Q	PHE	SI
1	1.500E+01	5.000E+02	7.420E+03	1.745E-01	0.
2	1.510E+01	5.000E+02	7.420E+03	1.745E-01	0.
3	1.520E+01	5.000E+02	7.420E+03	1.745E-01	0.
4	1.530E+01	5.000E+02	7.420E+03	1.745E-01	0.
5	1.540E+01	5.000E+02	7.420E+03	1.745E-01	0.
6	1.550E+01	5.000E+02	7.420E+03	1.745E-01	0.
7	1.560E+01	5.000E+02	7.420E+03	1.745E-01	0.
8	1.570E+01	5.000E+02	7.420E+03	1.745E-01	0.
9	1.580E+01	5.000E+02	7.420E+03	1.745E-01	0.
10	1.590E+01	5.000E+02	7.420E+03	1.745E-01	0.
11	1.600E+01	5.000E+02	7.420E+03	1.745E-01	0.

M	H	PHI	RHO	GAM	T
2.211E+00	6.450E+07	8.000E-01	5.089E-05	1.147E+00	4.728E+03
2.211E+00	6.450E+07	8.000E-01	5.089E-05	1.147E+00	4.728E+03
2.211E+00	6.450E+07	8.000E-01	5.089E-05	1.147E+00	4.728E+03
2.211E+00	6.450E+07	8.000E-01	5.089E-05	1.147E+00	4.728E+03
2.211E+00	6.450E+07	8.000E-01	5.089E-05	1.147E+00	4.728E+03
2.211E+00	6.450E+07	8.000E-01	5.089E-05	1.147E+00	4.728E+03
2.211E+00	6.450E+07	8.000E-01	5.089E-05	1.147E+00	4.728E+03
2.211E+00	6.450E+07	8.000E-01	5.089E-05	1.147E+00	4.728E+03
2.211E+00	6.450E+07	8.000E-01	5.089E-05	1.147E+00	4.728E+03
2.211E+00	6.450E+07	8.000E-01	5.089E-05	1.147E+00	4.728E+03
2.211E+00	6.450E+07	8.000E-01	5.089E-05	1.147E+00	4.728E+03

KOUNT = 110 X = 3.07600E+01

TABLE IIIb

J = 1 THETA = 0.

I	R	P	Q	PHE	SI
1	1.454E+01	1.770E+02	8.611E+03	-1.551E-01	0.
2	1.482E+01	1.700E+02	8.650E+03	-1.149E-01	0.
3	1.507E+01	1.640E+02	8.686E+03	-8.491E-02	0.
4	1.532E+01	1.604E+02	8.707E+03	-5.567E-02	0.
5	1.555E+01	1.597E+02	8.711E+03	-2.279E-02	0.
6	1.578E+01	1.613E+02	8.702E+03	1.493E-02	0.
7	1.600E+01	1.638E+02	8.687E+03	5.729E-02	0.
8	1.621E+01	1.658E+02	8.675E+03	1.037E-01	0.
9	1.642E+01	1.665E+02	8.671E+03	1.536E-01	0.
10	1.663E+01	1.657E+02	8.676E+03	2.064E-01	0.
11	1.685E+01	1.631E+02	8.691E+03	2.618E-01	0.

J = 2 THETA = 8.72600E-02

I	R	P	Q	PHE	SI
1	1.466E+01	1.746E+02	8.586E+03	-1.604E-01	-1.177E-01
2	1.491E+01	1.705E+02	8.627E+03	-1.330E-01	-7.593E-02
3	1.514E+01	1.685E+02	8.640E+03	-1.020E-01	-7.008E-02
4	1.536E+01	1.709E+02	8.625E+03	-6.293E-02	-7.150E-02
5	1.557E+01	1.777E+02	8.586E+03	-1.800E-02	-7.252E-02
6	1.577E+01	1.876E+02	8.532E+03	2.862E-02	-7.073E-02
7	1.596E+01	1.989E+02	8.474E+03	7.452E-02	-6.637E-02
8	1.614E+01	2.094E+02	8.424E+03	1.197E-01	-6.096E-02
9	1.631E+01	2.170E+02	8.389E+03	1.653E-01	-5.620E-02
10	1.648E+01	2.203E+02	8.373E+03	2.123E-01	-5.747E-02
11	1.665E+01	2.189E+02	8.378E+03	2.618E-01	-5.952E-02

J = 3 THETA = 1.74520E-01

I	R	P	Q	PHE	SI
1	1.479E+01	1.705E+02	8.609E+03	-1.656E-01	-1.113E-01
2	1.502E+01	1.744E+02	8.607E+03	-1.416E-01	-7.177E-02
3	1.522E+01	1.855E+02	8.548E+03	-1.012E-01	-6.276E-02
4	1.541E+01	2.014E+02	8.466E+03	-4.886E-02	-5.905E-02
5	1.558E+01	2.185E+02	8.383E+03	7.782E-03	-5.563E-02
6	1.573E+01	2.354E+02	8.306E+03	6.295E-02	-5.146E-02
7	1.589E+01	2.521E+02	8.234E+03	1.129E-01	-4.632E-02
8	1.603E+01	2.685E+02	8.166E+03	1.559E-01	-4.083E-02
9	1.617E+01	2.833E+02	8.107E+03	1.930E-01	-3.620E-02
10	1.631E+01	2.934E+02	8.068E+03	2.269E-01	-3.841E-02
11	1.645E+01	2.950E+02	8.061E+03	2.618E-01	-3.973E-02

J = 4 THETA = 2.61780E-01

I	R	P	Q	PHE	SI
1	1.491E+01	1.703E+02	8.601E+03	-1.709E-01	-1.217E-01
2	1.512E+01	2.031E+02	8.456E+03	-1.117E-01	-6.225E-02
3	1.529E+01	2.498E+02	8.246E+03	-4.354E-02	-4.109E-02
4	1.542E+01	2.988E+02	8.049E+03	1.967E-02	-3.086E-02
5	1.555E+01	3.410E+02	7.896E+03	7.456E-02	-2.531E-02
6	1.567E+01	3.706E+02	7.797E+03	1.227E-01	-2.197E-02
7	1.578E+01	3.853E+02	7.750E+03	1.656E-01	-1.997E-02
8	1.589E+01	3.860E+02	7.746E+03	2.031E-01	-1.908E-02
9	1.601E+01	3.805E+02	7.766E+03	2.332E-01	-1.925E-02
10	1.613E+01	3.740E+02	7.786E+03	2.526E-01	-2.263E-02
11	1.625E+01	3.700E+02	7.795E+03	2.618E-01	-2.508E-02

M	H	PHI	RHO	GAM	T
2.734E+00	5.496E+07	8.000E-01	2.065E-05	1.158E+00	4.248E+03
2.753E+00	5.461E+07	8.000E-01	1.995E-05	1.158E+00	4.231E+03
2.771E+00	5.431E+07	8.000E-01	1.934E-05	1.159E+00	4.216E+03
2.782E+00	5.412E+07	8.000E-01	1.898E-05	1.159E+00	4.207E+03
2.784E+00	5.408E+07	8.000E-01	1.890E-05	1.159E+00	4.205E+03
2.779E+00	5.417E+07	8.000E-01	1.907E-05	1.159E+00	4.209E+03
2.772E+00	5.430E+07	8.000E-01	1.932E-05	1.159E+00	4.216E+03
2.766E+00	5.440E+07	8.000E-01	1.952E-05	1.159E+00	4.221E+03
2.763E+00	5.444E+07	8.000E-01	1.960E-05	1.159E+00	4.223E+03
2.766E+00	5.439E+07	8.000E-01	1.951E-05	1.159E+00	4.220E+03
2.774E+00	5.426E+07	8.000E-01	1.925E-05	1.159E+00	4.214E+03

M	H	PHI	RHO	GAM	T
2.743E+00	5.467E+07	8.000E-01	2.035E-05	1.158E+00	4.236E+03
2.752E+00	5.460E+07	8.000E-01	1.999E-05	1.158E+00	4.231E+03
2.758E+00	5.452E+07	8.000E-01	1.980E-05	1.158E+00	4.227E+03
2.751E+00	5.465E+07	8.000E-01	2.004E-05	1.158E+00	4.233E+03
2.732E+00	5.498E+07	8.000E-01	2.072E-05	1.158E+00	4.249E+03
2.706E+00	5.545E+07	8.000E-01	2.172E-05	1.157E+00	4.272E+03
2.677E+00	5.596E+07	8.000E-01	2.285E-05	1.156E+00	4.297E+03
2.652E+00	5.642E+07	8.000E-01	2.389E-05	1.156E+00	4.319E+03
2.634E+00	5.673E+07	8.000E-01	2.464E-05	1.155E+00	4.335E+03
2.627E+00	5.686E+07	8.000E-01	2.496E-05	1.155E+00	4.341E+03
2.630E+00	5.681E+07	8.000E-01	2.483E-05	1.155E+00	4.338E+03

M	H	PHI	RHO	GAM	T
2.752E+00	5.449E+07	8.000E-01	1.995E-05	1.159E+00	4.227E+03
2.741E+00	5.479E+07	8.000E-01	2.038E-05	1.158E+00	4.240E+03
2.711E+00	5.534E+07	8.000E-01	2.151E-05	1.157E+00	4.267E+03
2.671E+00	5.606E+07	8.000E-01	2.309E-05	1.156E+00	4.302E+03
2.631E+00	5.678E+07	8.000E-01	2.479E-05	1.155E+00	4.337E+03
2.594E+00	5.745E+07	8.000E-01	2.644E-05	1.154E+00	4.370E+03
2.560E+00	5.806E+07	8.000E-01	2.805E-05	1.154E+00	4.401E+03
2.529E+00	5.863E+07	8.000E-01	2.963E-05	1.153E+00	4.429E+03
2.502E+00	5.912E+07	8.000E-01	3.105E-05	1.152E+00	4.454E+03
2.485E+00	5.943E+07	8.000E-01	3.199E-05	1.152E+00	4.469E+03
2.482E+00	5.949E+07	8.000E-01	3.215E-05	1.152E+00	4.472E+03

M	H	PHI	RHO	GAM	T
2.752E+00	5.445E+07	8.000E-01	1.992E-05	1.159E+00	4.226E+03
2.667E+00	5.612E+07	8.000E-01	2.325E-05	1.156E+00	4.305E+03
2.565E+00	5.797E+07	8.000E-01	2.783E-05	1.154E+00	4.396E+03
2.475E+00	5.961E+07	8.000E-01	3.251E-05	1.152E+00	4.478E+03
2.409E+00	6.083E+07	8.000E-01	3.647E-05	1.150E+00	4.540E+03
2.366E+00	6.162E+07	8.000E-01	3.921E-05	1.149E+00	4.580E+03
2.346E+00	6.198E+07	8.000E-01	4.056E-05	1.149E+00	4.599E+03
2.344E+00	6.202E+07	8.000E-01	4.069E-05	1.149E+00	4.600E+03
2.353E+00	6.186E+07	8.000E-01	4.012E-05	1.149E+00	4.592E+03
2.361E+00	6.170E+07	8.000E-01	3.952E-05	1.149E+00	4.584E+03

J = 5 THETA = 3.49040E-01

I	R	P	Q	PHE	SI
1	1.502E+01	2.670E+02	8.179E+03	-1.971E-02	0.
2	1.514E+01	3.912E+02	7.733E+03	9.771E-02	0.
3	1.525E+01	4.573E+02	7.537E+03	1.484E-01	0.
4	1.535E+01	4.849E+02	7.460E+03	1.677E-01	0.
5	1.545E+01	4.928E+02	7.439E+03	1.728E-01	0.
6	1.555E+01	4.945E+02	7.434E+03	1.738E-01	0.
7	1.565E+01	4.950E+02	7.433E+03	1.741E-01	0.
8	1.575E+01	4.942E+02	7.436E+03	1.750E-01	0.
9	1.585E+01	4.862E+02	7.452E+03	1.795E-01	0.
10	1.595E+01	4.690E+02	7.504E+03	1.935E-01	0.
11	1.605E+01	4.309E+02	7.613E+03	2.225E-01	0.

M	H	PHI	RHO	GAM	T
2.531E+00	5.858E+07	8.000E-01	2.948E-05	1.153E+00	4.426E+03
2.338E+00	6.213E+07	8.000E-01	4.110E-05	1.149E+00	4.606E+03
2.257E+00	6.365E+07	8.000E-01	4.708E-05	1.147E+00	4.683E+03
2.227E+00	6.420E+07	8.000E-01	4.955E-05	1.147E+00	4.712E+03
2.218E+00	6.436E+07	8.000E-01	5.025E-05	1.147E+00	4.721E+03
2.216E+00	6.439E+07	8.000E-01	5.041E-05	1.147E+00	4.722E+03
2.216E+00	6.440E+07	8.000E-01	5.045E-05	1.147E+00	4.723E+03
2.217E+00	6.438E+07	8.000E-01	5.037E-05	1.147E+00	4.722E+03
2.223E+00	6.427E+07	8.000E-01	4.984E-05	1.147E+00	4.716E+03
2.244E+00	6.387E+07	8.000E-01	4.813E-05	1.147E+00	4.696E+03
2.289E+00	6.305E+07	8.000E-01	4.470E-05	1.148E+00	4.653E+03

V. CONCLUSIONS

A numerical method based on reference plane characteristics has been developed for the calculation of steady three dimensional supersonic nozzle-exhaust flow fields. This reference plane technique by incorporating three separate coordinate systems, permits the calculation of geometrically complex flow fields using a relatively small amount of computer time.

The program developed has second order accuracy. The scheme used provides for convergence of reference plane properties prior to updating the cross derivatives. This is consistent with standard practice in computational schemes employing characteristic grids. Further improvements in computational accuracy are achieved through the use of integral correction factors for mass flow and total energy.

For end modules the external corner expansion is treated by a power series technique as described in this report. A further improvement in the program would be accomplished by replacing this expansion with a locally cylindrical reference plane system centered about the corner point.

The program developed computes the entire flow field given appropriate initial data, external flow data and the vehicle geometry. All required coordinate transformations are performed automatically. Shocks, contact surfaces and streamline pro-

jections are traced in individual reference planes to facilitate machine plotting. Additionally, initial data may be prescribed along a sweptback surface for a cylindrical or Cartesian coordinate system. Shock wave formation due to coalescence is detected, although these additional shock waves are not carried along as discontinuity surfaces.

The program developed can analyze a wider variety of problems than described in this report. This geometric flexibility is provided by incorporating three (3) separate coordinate reference systems and tha ability to compute discrete surfaces of discontinuity in these systems. A program of this size and complexity requires a thoughtful selection of the appropriate reference systems, initial and external flow data, and body geometry polynomials. However, it is felt that once the present program has been run and understood, modifications can be performed to yield program options encompassing a wide array of three dimensional supersonic flow problems.

REFERENCES

1. Ferrari, C., "Interference Between Wing and Body at Supersonic Speeds-Analysis by the Method of Characteristics," Journal of Aeronautical Sciences, Vol. 16, July 1949, pp. 411-434.

2. Ferri, A., "Methods of Characteristics," General Theory of High Speed Aerodynamics, Vol. VI, Section G, Princeton Press, (1954).

3. Moretti, G., "Three Dimensional Supersonic Flow Computations," AIAA Journal, Vol. 1, No. 9, September 1963.

4. Moretti, G., et al, "Supersonic Flow About General Three Dimensional Blunt Bodies," Technical Report No. ASD-TR-61-727, Volume III, General Applied Science Laboratory, October 1962, Contract No. AF33(616)-7721.

5. Rakich, J.V., "Three Dimensional Flow Calculation by The Method of Characteristics," AIAA Journal, Vol. 5, No. 10, October 1967, pp. 1906-1908.

6. Rakich, J.V., "A Method of Characteristics for Steady Three Dimensional Supersonic Flow with Application to Inclined Bodies of Revolution," TN D-5341, (1969), NASA.

7. Rakich, J.V. and Cleary, J.W., "Theoretical and Experimental Study of Supersonic Steady Flow Around Inclined Bodies of Revolution," AIAA Journal, Vol. 8, No. 3, March 1970, pp. 511-518.

8. Barnes, B., McIntyre, R.W. and Sims, J.A., "Properties of Air and Combustion Products with Kerosine and Hydrogen Fuels," Published by Bristol Siddley Engines Limited, P.O. Box 3, Filton, Bristol, England on behalf of the Propulsion and Energetics Panel of the Advisory Group for Aerospace Research and Development, (1967).

APPENDIX

CURVE FITS FOR Γ, h and ρ

APPENDIX

CURVE FITS FOR Γ, h and ρ

The variation of Γ (the equilibrium value of γ) as a function of temperature (T), pressure (P) and equivalence ratio (Φ) is presented graphically in Figures (A1), (A2) and (A3) from values tabulated in Reference (4). In Figure (A1) it can be seen that Γ is a strong function of T over the temperature range of interest, while the effect of varying composition is small by comparison. Moreover, Figure (A2) indicates that Γ is moderately sensitive to pressure and the degree of sensitivity increases substantially as the temperature level increases and dissociation effects become important.

As a result of these observations, temperature is the primary independent variable, while pressure is the secondary independent variable and composition acts as a perturbation variable. Thus, we can fit the function Γ (T,P,Φ) with a polynomial in T and add on a temperature dependent correction term for the effect of pressure and a temperature independent correction term for the effect of Φ.

An examination of Figure (A1) suggest that the function Γ (T) can best be curve fit by breaking up the temperature range into three intervals such that the function can be represent-

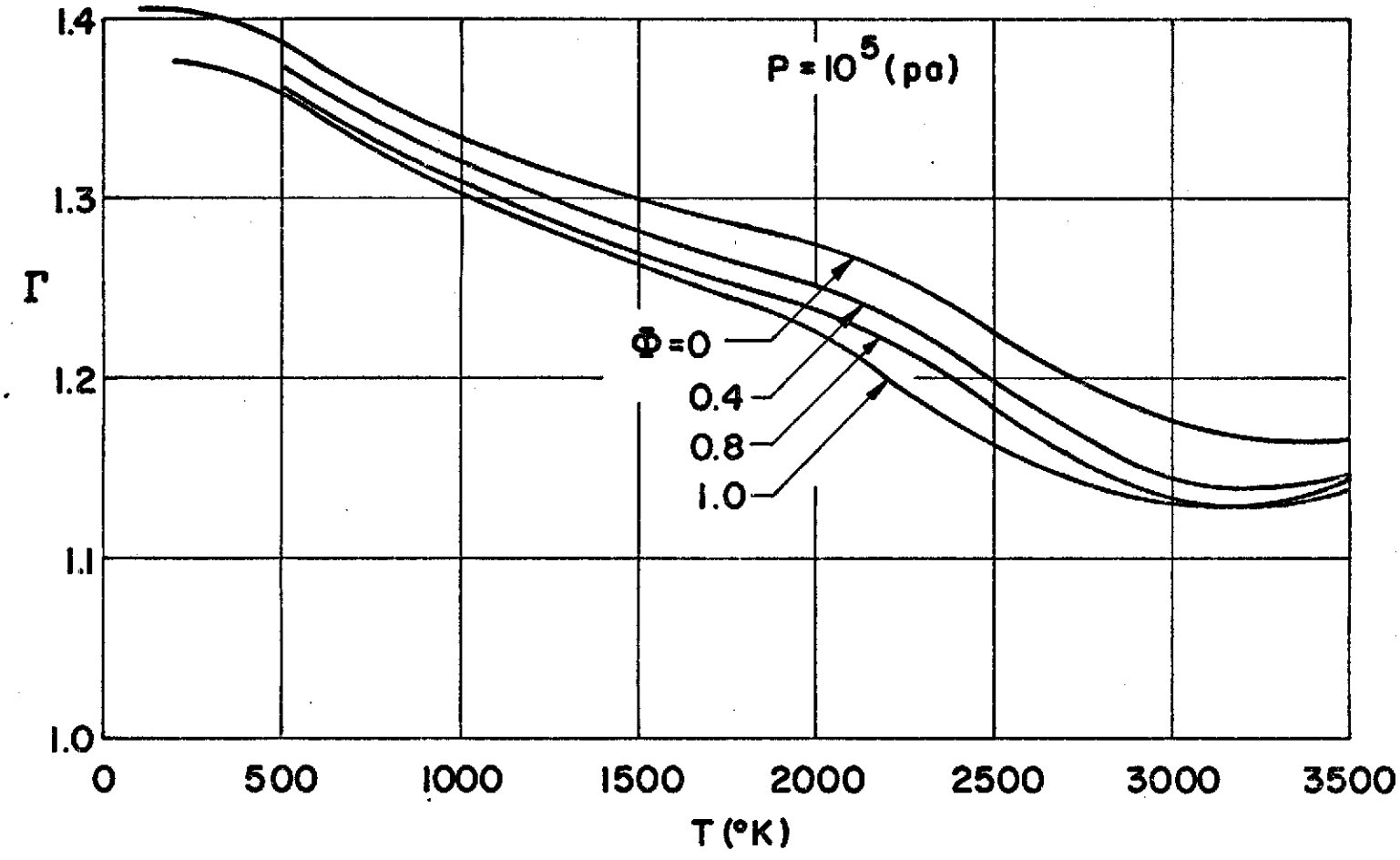

FIGURE A1. Γ VARIATION WITH TEMPERATURE

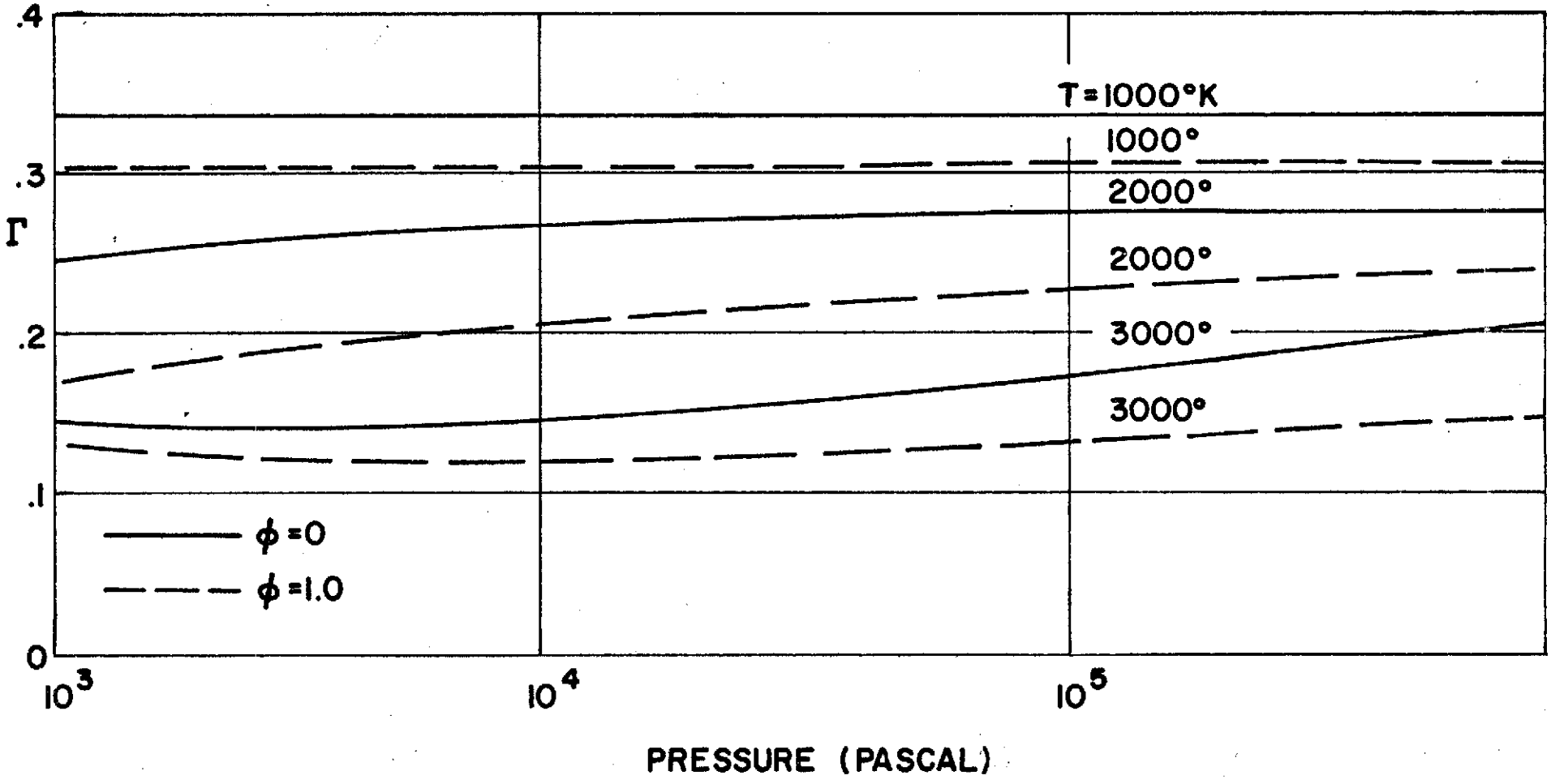

FIGURE A2. Γ VARIATION WITH PRESSURE

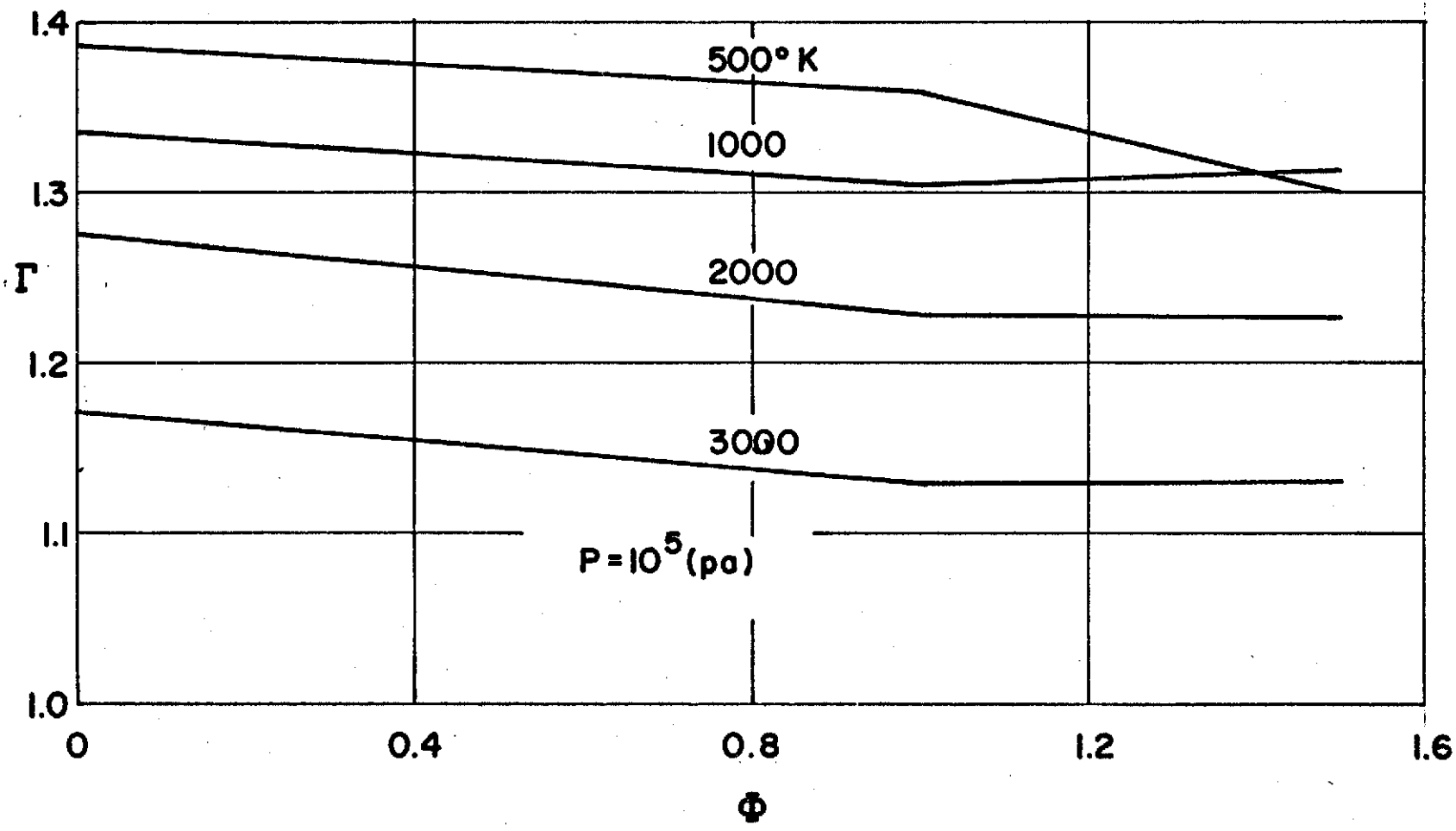

FIGURE A3. Γ VARIATION WITH Φ

ed by a parabola in each range. Choosing $p = 10^5$ pascal and $\phi=1$ as our base, we therefore find three functions

$$\Gamma_1(T,10^5,1) = - 1.833\times10^{-7}\ T^2 + 7.5\times10^{-5}\ T + 1.367 \qquad (1)$$

$$\Gamma_2(T,10^5,1) = 2.0\times10^{-8}\ T^2 - 1.38\times10^{-4}\ T + 1.423 \qquad (2)$$

$$\Gamma_3(T,10^5,1) = 7.27\times10^{-8}\ T^2 - 4.57\times10^{-4}\ T + 1.85 \qquad (3)$$

and define the basic temperature function as

$$\Gamma(T,10^5,1) = \begin{Bmatrix} \Gamma_1(T,10^5,1) \\ \Gamma_2(T,10^5,1) \\ \Gamma_3(T,10^5,1) \end{Bmatrix} \text{ for } \begin{Bmatrix} T\leq 500^oK \\ 500\leq T\leq 2000^oK \\ T\geq 2000^oK \end{Bmatrix} \qquad (4)$$

Figure (A3) indicates that $\frac{\partial\Gamma}{\partial\Phi}$ is constant in the two ranges $\Phi<1$ and $\Phi>1$, but is a function of T. Fitting the function $\frac{\partial\Gamma}{\partial\Phi}$ in each of the ranges of ϕ we obtain

$$\frac{\partial\Gamma}{\partial\Phi} = \begin{bmatrix} n_1(T) \\ n_2(T) \end{bmatrix} \text{ for } \begin{bmatrix} \Phi\leq 1 \\ \Phi\geq 1 \end{bmatrix} \qquad (5)$$

where

$$n_1(T) = 4\times10^{-9}\ T^2 - 2\times10^{-5}\ T - 0.019 \qquad (6)$$

$$n_2(T) = 3.39\times10^{-2}\ T^{0.5} - 3.91\times10^{-4}\ T - 0.681 \qquad (7)$$

This now defines Γ as a function of both temperature and Φ by means of the equation

$$\Gamma(T,10^5,\Phi) = \Gamma(T,10^5,1) + (\Phi-1)\frac{\partial\Gamma}{\partial\Phi} \tag{8}$$

Finally, the effect of pressure must be included. From Figure (18) we observe that Γ may be approximated as

$$\Gamma(T,P,\Phi) = \Gamma(T,10^5,\Phi) + m\,[\log_{10}(p\times10^5)-5] \tag{9}$$

where m is a function of T. Deriving m, we find

$$m = \left\{\begin{array}{l} 0 \\ -2.15\times10^{-8}T^2+0.91\times10^{-4}T-0.0695 \end{array}\right\} \text{ for } \left\{\begin{array}{l} T<1000^oK \\ T\geq1000^oK \end{array}\right\} \tag{10}$$

Summarizing, the final function obtained is

$$\Gamma(T,P,\Phi) = \Gamma(T,10^5,1) + m\left(\frac{\ln p}{2.3}-5\right) + \frac{\partial\Gamma}{\partial\Phi}(\Phi-1) \tag{11}$$

where the functions $\Gamma(T,10^5,1)$, $\frac{\partial\Gamma}{\partial\Phi}$ and m are given by Equations (4), (5) and (10) respectively.

The curve fit for enthalpy is derived in a similar way. Figures (A-4) and (A-5) present the variation of h with temperature, pressure and equivalence ratio. As was the case for Γ, the

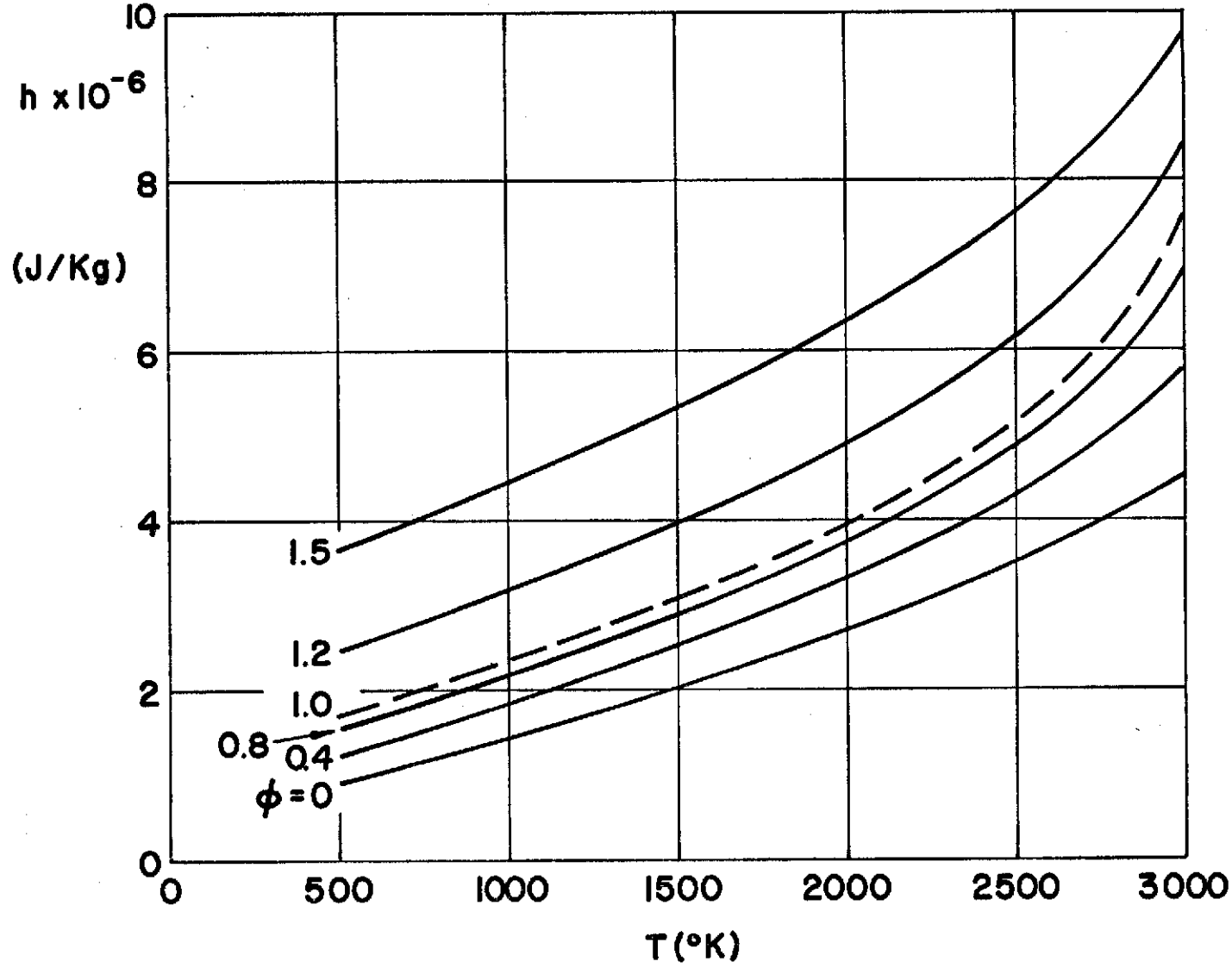

FIGURE A4. ENTHALPY AS A FUNCTION OF TEMPERATURE ($p=10^5$pa.)

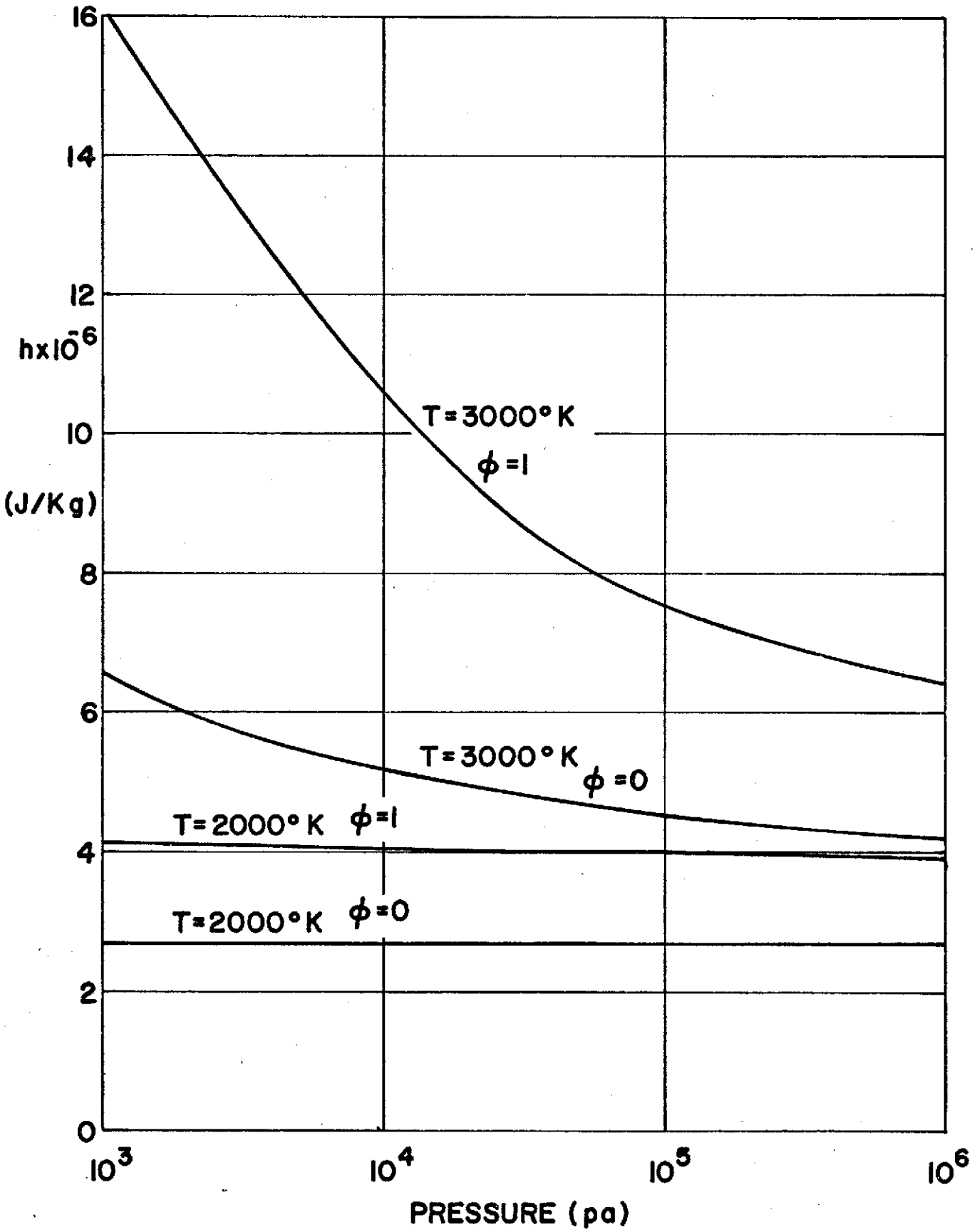

FIGURE A5. ENTHALPY AS A FUNCTION OF PRESSURE.

function $h(T, \phi, p)$ is fit by a quadratic function of T, the coefficients of which are functions of ϕ and an additive term for the effects of pressure. The resulting curve fit is summarized below.

$$h(T,\phi,p) = \begin{Bmatrix} h(T,\phi,10^5) \\ h(T,\phi,p) \end{Bmatrix} \quad \text{for} \quad \begin{Bmatrix} T \leq 2000^{\circ}K \\ T > 2000^{\circ}K \end{Bmatrix} \tag{12}$$

where $$h(T,\phi,p) = h(T,\phi,10^5) \left[1 + \frac{(1+\phi)(T-2000)}{2000} \left(.125\left(\frac{\ln p}{2.3} - 5\right)^2 - .275\left(\frac{\ln p}{2.3} - 5\right) \right) \right] \tag{13}$$

The basic function $h(T,\phi,10^5)$ is defined as

$$h(T,\phi,10^5) = 10^6 \, (a_1 T^2 + b_1 T + c_1) \tag{14}$$

with the coefficients a_1, b_1 and c_1 defined below:

For $T \leq 2000^{\circ}K$ and $\phi \leq 1$

$$\begin{aligned} a_1 &= 10^{-7} \, (-.1042\phi^2 + .8242\phi + .987) \\ b_1 &= 10^{-3} \, (.01167\phi^2 + .1503\phi + .938) \\ c_1 &= -.0284\phi^2 + .6731\,\phi + .4293 \end{aligned} \tag{15}$$

For $T \leq 2000^{o}K$ and $\phi > 1$

$$a_1 = 10^{-7} (1.787\phi^2 - 5.48\phi + 5.4)$$

$$b_1 = 10^{-3} (-.1867\phi^2 + 1.11\phi + .176) \quad (16)$$

$$c_1 = -.0933\phi^2 + 3.975\phi - 2.808$$

For $T > 2000^{o}K$ and $\phi \leq 1$

$$a_1 = 10^{-6} (1.792\phi^2 + .3983\phi + .310)$$

$$b_1 = 10^{-3} (-9.05\phi^2 - .07917\phi + .245) \quad (17)$$

$$c_1 = 10.86\phi^2 - .1183\phi + .970$$

For $T > 2000^{o}K$ and $\phi > 1$

$$a_1 = 10^{-6} (4.81\phi^2 - 13.9\phi + 11.59)$$

$$b_1 = 10^{-3} (-23.08\phi^2 + 66.82\phi - 52.61) \quad (18)$$

$$c_1 = 27.05\phi^2 - 73.73\phi + 58.39$$

When the inverse function $T(h,\phi,p)$ is required, it is obtained by an iterative solution of Equations (12) through (18)

The density is found by obtaining a curve fit for the mixture molecular weight and using the equation of state

$$\rho = \frac{pm}{\bar{R}T} \tag{19}$$

where $\bar{R}$ is the universal gas constant and m is the molecular weight.

The behavior of m with T,p and ϕ is illustrated in Figures (A6) and (A7). We see that for temperatures less than 2000°K, m is essentially independent of temperature. The discontinuity in slope of $m(\phi)$ shown in Figure (A7) requires that the equivalence ratio range be split in two. Thus,

for $T \leq 2000^{\circ}K$

$$m(\phi) = \left\{ \begin{array}{l} 1.53\phi^2 - 5.895\phi + 28.965 \\ 1.60\phi^2 - 10.6\phi + 33.6 \end{array} \right\} \text{ for } \left\{ \begin{array}{l} \phi \leq 1 \\ \phi > 1 \end{array} \right\} \tag{20}$$

For the higher temperature range, it is convenient to employ the form

$$m = m(\phi) - \delta(p,\phi,T) \tag{21}$$

where

$$\delta = d_2(p,\phi) \left(\frac{T-2000}{1000}\right)^{n_2(\phi)} \tag{22}$$

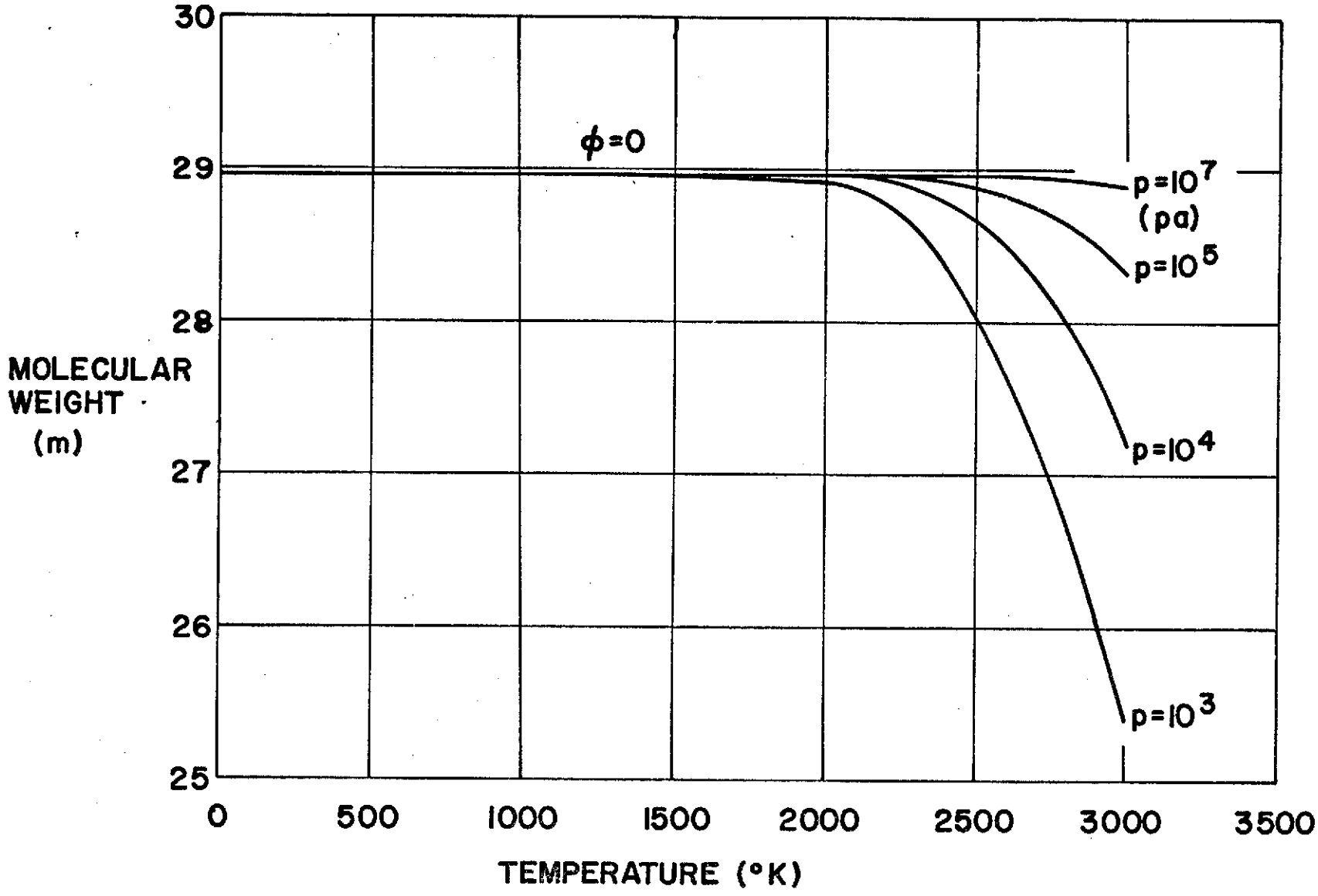

FIGURE A6. MOLECULAR WEIGHT AS A FUNCTION OF TEMPERATURE AND PRESSURE.

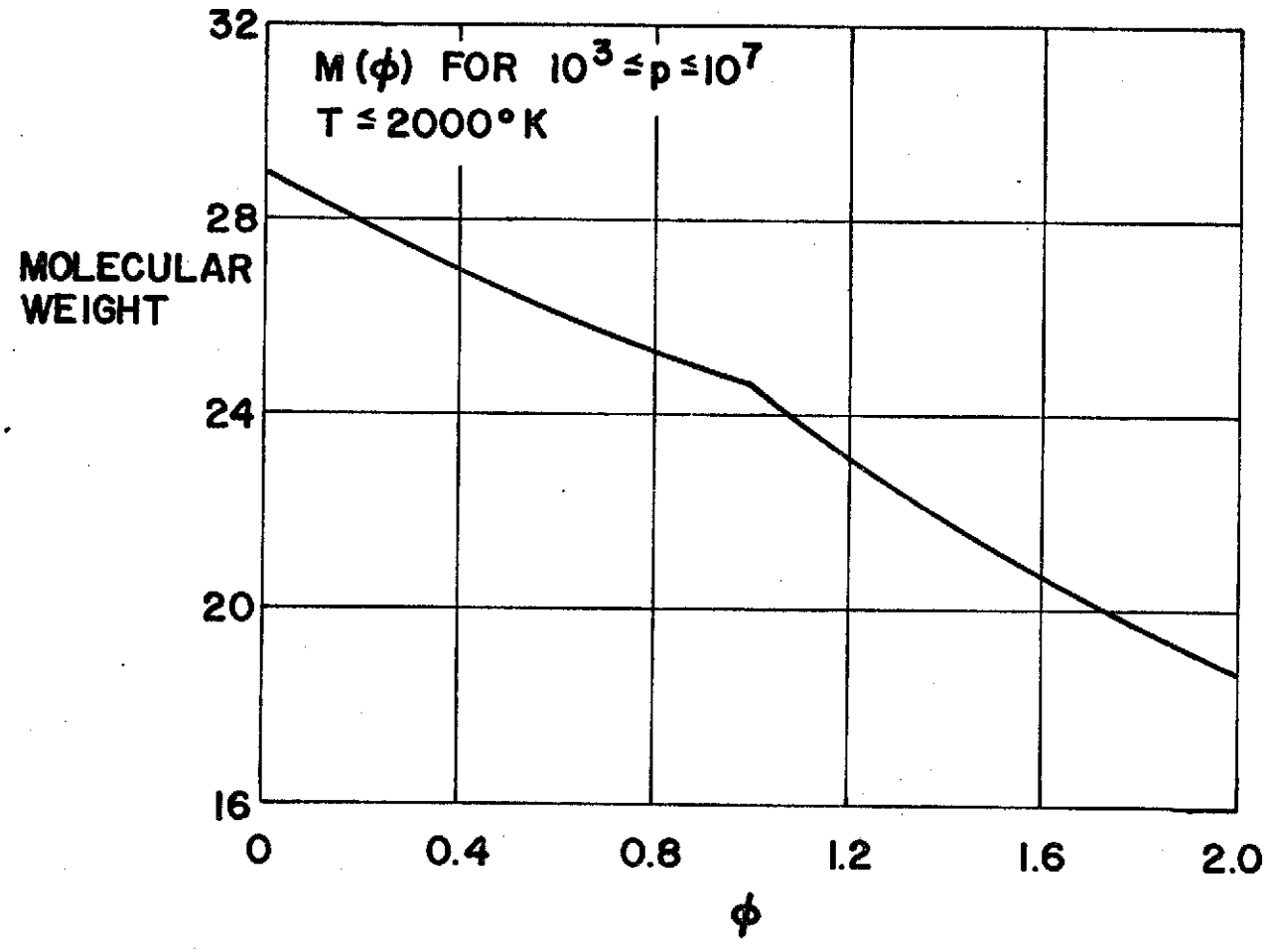

FIGURE A7. MOLECULAR WEIGHT AS A FUNCTION OF EQUIVALENCE RATIO FOR T≤2000°K.

and

$$d_2 = a_2 \left(\frac{\ln p}{2.3}\right)^{1.5} + b_2 \left(\frac{\ln p}{2.3}\right) + c_2 \qquad (23)$$

For $0 \le \phi \le 1$

$$\begin{aligned} a_2 &= -2.3\phi^2 + 4.01\phi + 1.736 \\ b_2 &= 8.61\phi^2 - 15.42\phi - 6.66 \\ c_2 &= -16.88\phi^2 + 33.21\phi + 14.58 \\ n_2 &= .4375\phi^2 + .0625\phi + 2.08 \end{aligned} \qquad (24)$$

and for $1 \le \phi < 2$

$$\begin{aligned} a_2 &= -.822\phi^2 + 2.363\phi + 1.905 \\ b_2 &= 2.76\phi^2 - 7.56\phi - 8.68 \\ c_2 &= 3.6\phi^2 + 7.36\phi + 27.15 \\ n_2 &= .47\phi^2 + 1.825\phi + .350 \end{aligned} \qquad (25)$$